Synthesis of Disila-Crown Ether Complexes and Heteroatomic Bridged Paracyclophanes

Kumulative Dissertation

zur Erlangung des Doktorgrades der Naturwissenschaften

(Dr. rer. nat.)

am Fachbereich Chemie

der Philipps-Universität Marburg

vorgelegt von

Kirsten Reuter

aus Oldenburg

Marburg (Lahn) 2017

Die vorliegende Arbeit wurde von Juni 2013 bis März 2017 unter der Leitung von Herrn Prof. Dr. Carsten von Hänisch am Fachbereich Chemie der Philipps-Universität Marburg angefertigt.

Vom Fachbereich Chemie der Philipps-Universität Marburg als Dissertation angenommen am:

Erstgutachter: Prof. Dr. Carsten von Hänisch

Zweitgutachter: Prof Dr. Bernhard Neumüller

Tag der mündlichen Prüfung:

Hochschulkennziffer: 1180

Erklärung

Ich erkläre, dass meine Promotion noch an keiner anderen Hochschule als der Philipps-Universität Marburg, Fachbereich Chemie, versucht wurde.

Ich versichere, dass ich meine vorgelegte Dissertation mit dem Titel

Synthesis of Disila-Crown Ether Complexes and Heteroatomic Bridged Paracyclophanes

selbst und ohne fremde Hilfe verfasst, nicht andere als die in ihr angegebenen Quellen oder Hilfsmittel benutzt, alle vollständig oder sinngemäß übernommenen Zitate als solche gekennzeichnet sowie die Dissertation in der vorliegenden oder einer ähnlichen Form noch bei keiner anderen in- oder ausländischen Hochschule anlässlich eines Promotionsgesuchs oder zu anderen Prüfungszwecken eingereicht habe.

Marburg, den 08.03.2017

Kirsten Reuter

Contents

1 Introduction

1.1 The Nature of the Si-O Bond

Owing to the wide abundance of silicon and oxygen in the earth crust and the affinity of silicon for oxygen, the Si-O bond is one of the most common chemical bonds.[1] Nevertheless, it was long-time poorly understood and has been issue of intensive discussion during the past 70 years. The chemical properties of siloxanes, such as their thermal and chemical stability, give rise to versatile applications in the material sciences.[2] Silicone based polymer materials are for instance highly hydrophobic, so they act as excellent water repellents.[3] These properties are in contrast to ethers, which show high reactivity, hydrophilicity and act as excellent *Lewis* bases.[4] Thereby, the described chemical properties are closely related to the structures of the two compound classes:[5] The bond angle widens along the series dimethyl ether (C-O-C: 112°)[6], alkoxysilane (Si-O-C: 120°)[7] and disiloxane (Si-O-Si: 144°)[8]. Similar trends were also found for the basicity of these compounds with decreasing basicity in the series C-O-C > Si-O-C > Si-O-Si.[9] Additionally, the Si-O bond in disiloxane is with a value of 163.4 pm[8] considerably shorter than the sum of the single bond covalent radii, which measure 191 – 193 pm.

For about 80 years, these characteristics are matter of ongoing discussion and especially recent theoretical and practical contributions yielded important clarification to this research issue. The development of the concerning discussion as well as the opposed points of view will be presented and associated in the following paragraphs.

1.1.1 Hyperconjugation in Siloxanes

In 1934, Brockway *et al.* related the short Si-O bond length to the presence of the double-bond character under involvement of 3d-orbitals of the silicon atom.[10] Originally based on silicon tetrahalides, this concept was later extended to siloxanes by assuming a donor-acceptor (p-d)π back-bonding between Si and O.[11] This approach was also in line with the inability of siloxanes to form stable adducts with *Lewis* acids due to the decreased availability of the lone pairs at the O atoms.[12] In the course of the implementation of theoretical studies, the involvement of d-orbitals was finally abandoned[13] and replaced by the concept of the negative hyperconjugation.[14] According to that, the electron density of n_O interacts with the σ* orbital of the Si-C or Si-H bond, respectively, which leads to a strengthening of the Si-O bond and simultaneously to a weakening of the Si-C or Si-H bond. A more in depth-analysis was performed very recently by *Weinhold* and *West*.[15] A*b initio* and density functional computational (DFT) methods revealed that negative hyperconjugation reduces the basicity of O in both, siloxanes and ethers, but with higher impact in siloxanes, especially in the case of the permethylated ones. This is closely related to larger angles in siloxanes, which again result from the weak force constant for the Si-O-Si bending.[15, 16] The *Lewis* acids thus competes with the intramolecular delocalisation $n_O \rightarrow \sigma^*_{(SiC)}$ for the same n_O oxygen lone-pairs (Scheme 1).

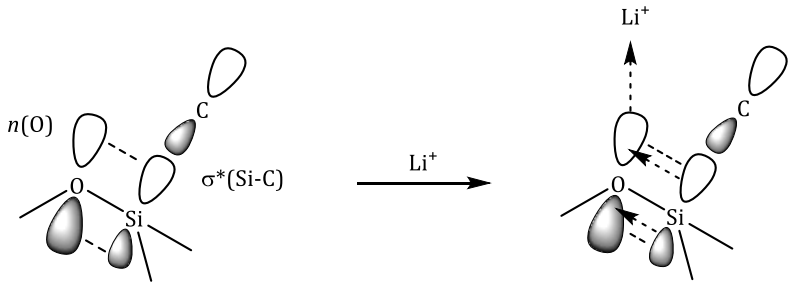

Scheme 1. Competitive interaction between intra- and intermolecular delocalisation of the O atom lone pairs in siloxanes.

1.1.2 Ionic Model of the Siloxane Linkage

The importance of the different nuclear charges of Si and O was first suggested in the 70s[17] and later emphasised by *ab initio* calculations. Accordingly, the short Si-O bond lengths were determined to be the consequence of the high ionic character of the bonding, while (p-d)π bonding, the prevalent model at that time, was considered to be of minor importance.[18] The O atom thus exhibits higher anionicity in Si-O-Si than in C-O-C, owing to the significant difference in electronegativity (χ_{AR} for Si: 1.8, C: 2.5 and O: 3.4).[19] Calculations of the electron density distribution and their Laplacian for the series of H_nXOXH_n (X = Li to F and Na to Cl; n = 0-2) revealed that the bond lengths (X-O) and angles (X-O-X) strongly depend on the difference in electronegativity between these elements (Table 1). In an isolated oxide ion O^{2-}, the overall electron density is spherical. The bonding to a ligand yields an attraction of the electron density towards the substituents and consequently to more localised electrons. In the presence of sufficiently electronegative moieties XH_n, such as NH_2, OH, SH, F and Cl the elec-

Table 1. Atomic charges q for $(H_nX)_2O$ and $(F_3X)_2O$, X-O-X bond angles (°) and X-O bond lengths (pm).[20]

molecule	q(O)	q(X)	X-O-X	X-O
Li_2O	−1.82	+0.91	180.0	159.6
$(HBe)_2O$	−1.79	+1.74	180.0	139.6
$(H_2B)_2O$	−1.68	+2.27	126.9	135.4
$(H_3C)_2O$	−1.29	+0.78	113.9	139.0
$(H_3Si)_2O$	−1.72	+3.05	148.3	162.1
$(H_2P)_2O$	−1.59	+1.97	129.8	163.6
$(F_3C)_2O$	−1.32	+2.84	118.9	135.4
$(F_3Si)_2O$	−1.68	+3.13	162.2	158.3

tron pair domains at the oxygen atom are relatively well localized and form a tetrahedral arrangement. However, with substituents X that are less electronegative than carbon, for instance BH_2, SiH_3 and PH_2, the electron pair domains become larger in extent and more diffuse, and consequently show higher overlap with X. The more the electronegativity of X decreases, the higher the diffuse character of the electrons. Thus, the X-O-X bond angle increases in the series H_2POPH_2 (129.8°), H_2BOBH_2 (135.4°) and $H_3Si-OSiH_3$ (144.1°), which is consistent with the increasing electronegativity from Si (1.8) and B (2.0) to P (2.1).[19] This approach was additionally amplified by substitution of the H atoms in $H_3SiOSiH_3$ by F atoms. The electron withdrawing effect of fluorine leads to larger charges on Si and O and indeed a further shortening of the bond length to 156.3 pm and an increase of the bond angle to 158.3° were found (Table 1).[20]

Moreover, *Passmore and Rautiainen* investigated recently the charge distribution of disiloxanes and ethers upon coordination of Li^+ and Ag^+.[21] By DFT calculation the complexation of Li^+ and Ag^+ was determined to be ~30 $kJ \cdot mol^{-1}$ less favourable for $O(SiH_2Me)_2$ than for OEt_2, which is in agreement with prior studies. Quantum theory of atoms in molecules (QTAIM) analysis also indicate that the charge of oxygen becomes more negative in the respective complex compared to that of $O(SiH_2Me)_2$ and OEt_2. Furthermore, the change of the charge is larger in diethylether, indicating that the electron density is easier to polarize further in comparison to that of the already polar bonds in $O(SiH_2Me)_2$. Despite the lower polarisation of disiloxane through complexation, the deformation energy, determined by energy decomposition analysis (EDA), is higher in disiloxane than in diethylether. The deformation energy relates to the "energetic penalty" for the bond formation upon complexation as well as changes in the charge distribution, e.g., polarisation. The authors of this theoretical study ascribe the unusual high deformation energy of disiloxane to the electrostatic repulsion between the positively polarised Si atom and the metal ion. This interaction counteracts the attraction of the negatively charged O atom and the cation. Furthermore, the significant weakening of the Si-O bonding upon complexation can be attributed to the repulsion between Si and metal ions.[21]

1.1.3 Bond Angles as an Indicator for Basicity

The association between the wide Si-O-Si angles, the ionic character of the Si-O bond and the localisation of the electron density gave rise to the question, whether the basicity of siloxanes can be modified by variation of the concerning angles.[22][23] According to the results of *Gillespie et al.*, the electron pair domains become more localised and less diffuse when the X-O-X angles are small, since the electron pair domains adopt the approximately tetrahedral arrangement.[20] This association can also be displayed by means of the electron localisation function (ELF). Relatively well-localised electron pair domains were determined for Si-O-Si angles of 110° with increasing delocalisation up to a completely spherical electron pair domain at 180°.[22] As can be derived from the bending potential energies shown in Figure 1, non-coordinating disiloxane (green curve) exhibits a broad range of adoptable angles: the bending potential remains relatively flat from 140° - 180°. Disiloxane that participates in hydrogen bonding with silanol (black curve) or water (red curve), shows a decrease in bending potential at smaller angles. The minimum angle is 137.8° for disiloxane···silanol and 140.1° for disiloxane···water. Moreover, an increase of the Si-O-Si angle becomes energetically unfavourable. *Ab initio* potential energy surface (PES) scans have shown that the basicity

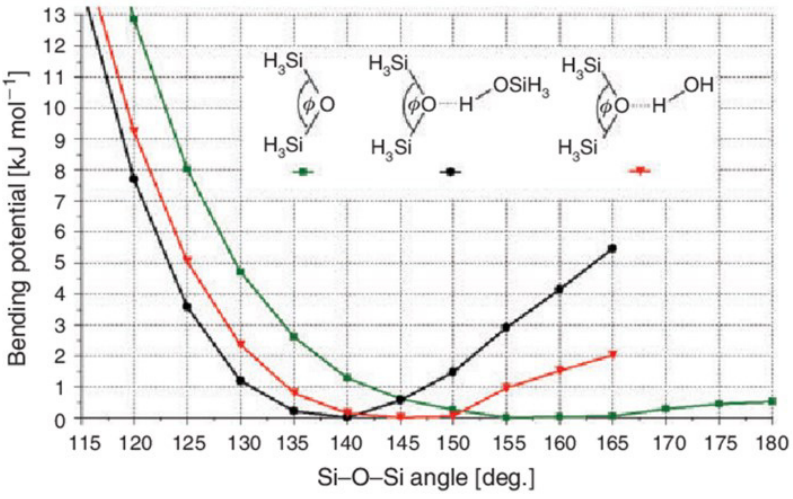

Figure 1. Bending-potential energies of disiloxane (green), disiloxane - silanol (black) and disiloxane - water (red). Reproduced from Grabowsky et al. (2012), with permission from CSIRO Publishing.[23]

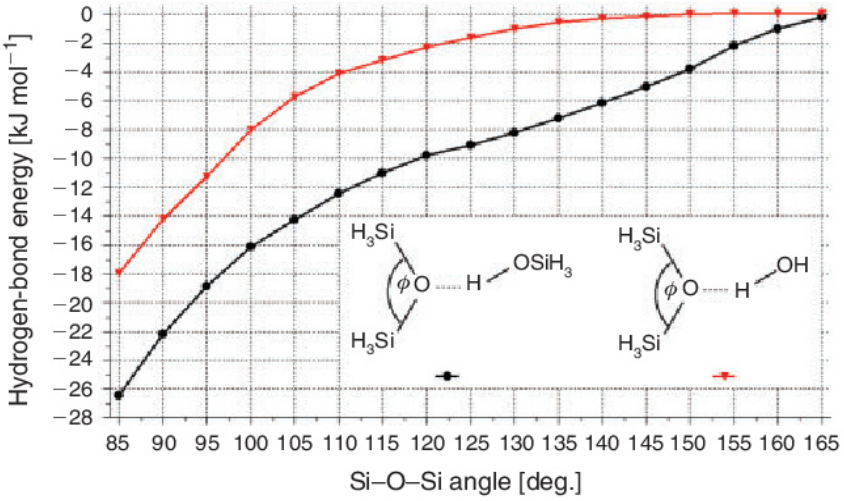

Figure 2. Hydrogen-bond energies in association with varying Si-O-Si angles. Reproduced from Grabowsky et al. (2012), with permission from CSIRO Publishing.[23]

of disiloxane increases with smaller Si-O-Si angles (Figure 2). Near 110°, approximately the tetrahedral angle, the hydrogen-bond energy of disiloxane···silanol has a value of −12.5 kJ·mol^{-1} and was determined to be twice as high as at 140° with −6.2 kJ·mol^{-1}.[23] These findings are in accordance with the low number of structures involving hydrogen bonding with disiloxanes. These have in common that the disiloxane fragment is incorporated into a small ring system, giving highly strained Si-O-Si angles of approximately 116°.[22, 24, 25]

1.2 Coordination Compounds Involving Siloxanes

1.2.1 Attempts with Open Chained Siloxanes

Although siloxanes are highly reluctant to form stable adducts with *Lewis* acids, a handful of coordination compounds have been reported. The first contemplation of cyclosiloxanes as ligands was published in the 70s. The authors accounted for the absence of a "crown" effect in D_7 and D_8 (D=Me_2SiO) towards Na^+, which was shown by the ineffectiveness of these compounds in the anionic ring-opening polymerisation of a cyclotrisiloxane. This was ascribed to the lower electron density of the O atoms in D_7 and D_8 compared to that in organic crown ethers.[26] Especially in the 80s, the synthesis of metallosiloxane polymers was an important issue for material scientists due to the valuable properties including their thermal stability and electrical conductivity. By twofold deprotonation to $[O(R_2SiO)_2]^{2-}$ (R = organic rest), the basicity of the terminal O atoms in disiloxanediol can be raised further in order to obtain bridging coordination patterns of the dianionic ligand with metal cations.[27, 28] For example, the reaction of $TiCl_4$ with 3 eq. of $[(Ph_2SiONa)_2O]$ in pyridine yields the titanate complex $[Ti\{O(SiPh_2O)_2\}_3]^{2-}$, which incorporates three six-membered $[O(SiPh_2O)_2Ti)]$-cycles (Scheme 2). Therein, the disiloxanediolate adopts the function of a bidentate ligand. Similar coordination compounds have been obtained by the use of $ZrCl_4$ and $HfCl_4$. In neither of these complexes, the twofold Si bonded O atoms participate in the coordination of the metal centre. Similar complexes were obtained in conjunction with incompletely condensed cage-type silesquioxanes. Deprotonation of the terminal Si-OH functional groups by bases such as triethylamine followed by reaction with main group[29] or transition metal halides[30] yielded coordination compounds, in which the metal binds exocyclic to the cage compound.[31, 32] Although this is the most common coordination pattern of siloxanediolates with *Lewis* acids,[33, 34] a few structures were found, wherein also the twofold Si bonded O atoms act as electron donor, as observed in $[Sr(NBN\text{-}SiMe_2OSiMe_2)]\cdot thf]_2$[35] (NBN = [(2,6-disopropylphenyl)N-B(H)-N(2,6-disopropylphenyl)]$^{2-}$ and $[(thf)_6Ba_6\text{-}(dmpz)_8\{(OSiMe_2)_2O\}_2]$.[36]

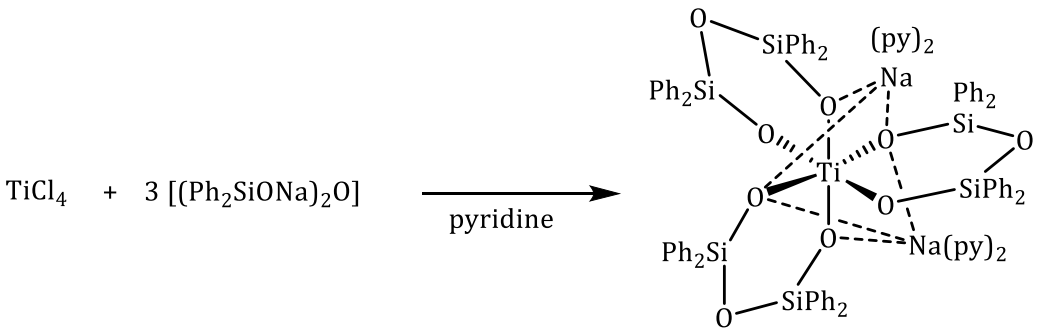

Scheme 2. Complex formation of $[(Ph_2SiONa)_2O]$ and $TiCl_4$.

However, the first structurally determined complex involving cyclosiloxanes was unexpectedly obtained in the 90s by *Churchill et al.* within the attempt to recrystallize $K[H\{In(CH_2CMe_3)_3\}_2]$ in the presence of silicone grease and heptane.[37] The obtained single crystals were determined to have the composition $[K^+]_3[KD_7^+][InH(CH_2CMe_3)_3]_4$. Shortly after, $[KD_7]^+$ was again obtained within the recrystallization of $K[C(SiMe_3)_2\{SiMe_2(CH{=}CH_2)\}]$ in the unintentional presence of small amounts of silicon grease.[38] Silicon grease is principally based on polymeric $(Me_2SiO)_x$-chains with terminal Si-OH groups, so the exclusive formation of D_7 was attributed to a template effect of potassium cations.[39] By contrast, in the reaction of Me_2GaCl and *t*$BuAsLi_2$ in THF, the linear polymeric structure of silicon grease was preserved. Instead of the expected product, a complex structure consisting of sixteen Li cations, whose coordination sphere was saturated by $O(SiMe_2O)_n$ (n = 2-3) chains, was determined by X-ray diffraction.[40]

1.2.2 Establishing Weakly Coordinating Anions

Most of the hitherto described complex structures, that involve siloxanes, were obtained unexpectedly in the presence of silicon grease. This gave rise to the aspiration to design reaction paths, which selectively yield complexes of siloxanes and *Lewis* acids. As was shown by *Passmore et al.* by calculation of binding enthalpies and free energies, stable complexes become favourable, if salts of weakly coordinating anions such as $[Al\{OC(CF_3)_3\}_4]^-$ ($[Al_F]$) are used. This was predicted accurately by means of the Born-Fajans-Haber cycle.[21] As is depicted in Scheme 3, the energy difference (ΔE) for the formation of LiD_6X is in the case of X = $[Al_F]$ with a value of −242 kJ·mol^{-1} significantly negative compared to X = I with ΔE = +66 kJ·mol^{-1}. The energy differences account for the smaller lattice energy changes ΔU_L for $LiAl_F$ to $[Li(D_6)][Al_F]$ compared to LiI to $[Li(D_6)]I$.[41, 42, 43] In 2006, *Decken et al.* reported the first successful incorporation of Li^+ in D_5 and D_6 directly from the components by using salts of weakly coordinating anions.[43] The anion of choice was beside $[Al_F]$ the phenylated derivative $[Al\{OC(CF_3)_2Ph\}_4]^-$ ($[Al_{PhF}]$). Shortly after, experiments involving $AgSbF_6$ and D_m (m = 3-6) in liquid SO_2 unexpectedly yielded complexes consisting of $[AgD_n][SbF_6]$ (n = 6-8). *Via* mass spectrometry, the proportion of $[AgD_6]^+/[AgD_7]^+/ [AgD_8]^+$ was determined to be 1:3.7:0.2, but only $[AgD_7][SbF_6]$ was characterised by single-crystal X-ray

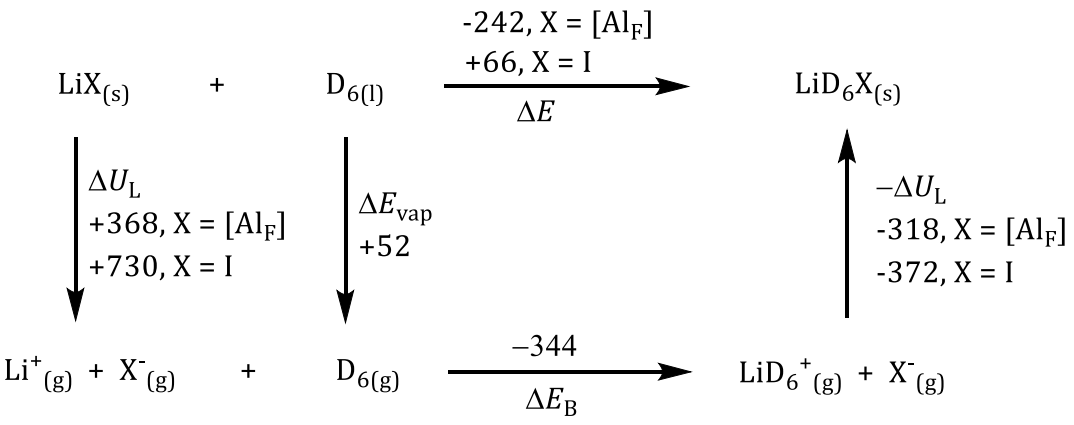

Scheme 3. Born-Fajans-Haber cycle for the reaction of D_6 with LiX with respect to lattice energies (ΔU_L), energy of vaporisation (ΔE_{vap}), binding energies (ΔE_B) and energies of formation (ΔE) in kJ·mol^{-1}.[43]

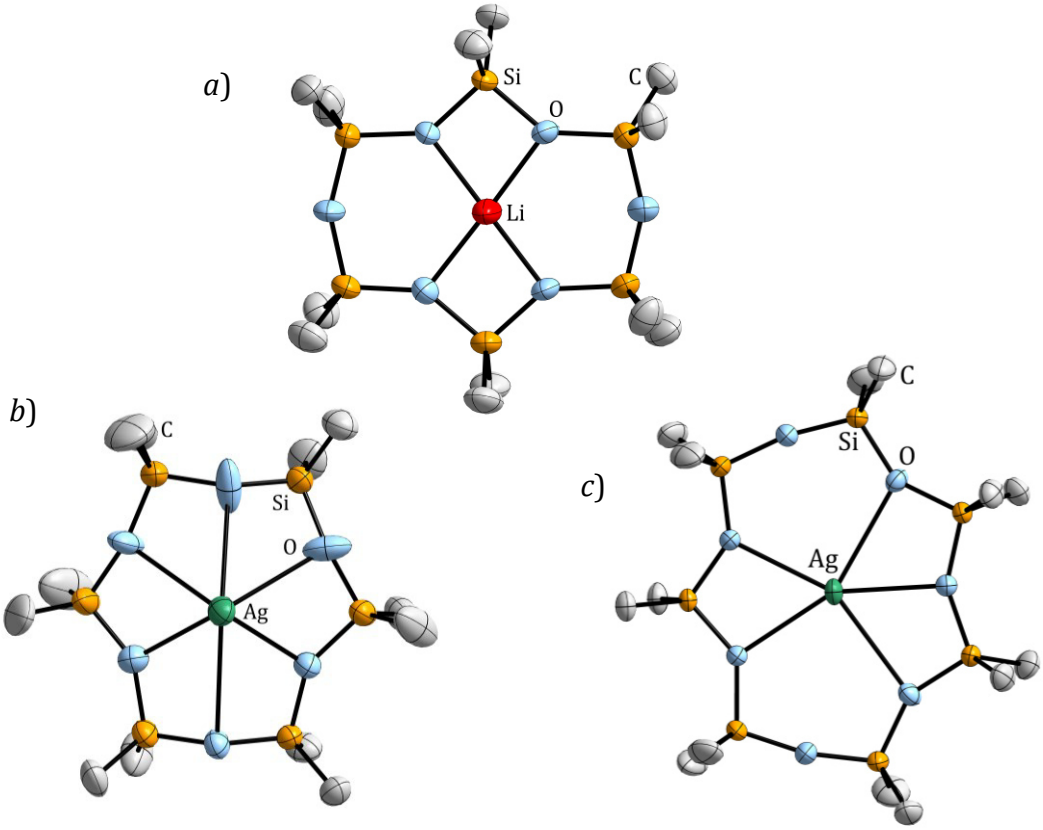

Figure 3. Binding modes of Li^+ in D_6 (*a*), Ag^+ in D_6 (*b*) and D_7 (*c*). The anions $[FAl\{OC(CF_3)_3\}_3]^-$ and $[SbF_6]^-$ as well as H atoms are not displayed.

diffraction (Figure 3c). To date, no verified mechanisms for the ring transformation have been published.[27, 33] By contrast, $[AgD_6][FAl\{OC(CF_3)_3\}_4]$ (Figure 3b) was synthesised without occurrence of ring transformation by the use of D_6 and the Ag^+ salt of the weakly coordinating anion $[FAl\{OC(CF_3)_3\}_3]^-$.[44] The molecular structures depicted in Figure 3 confirm the results of theoretical studies concerning the adopted Si-O-Si angles in coordinating and non-coordinating O atoms.[20, 21] In $[AgD_7]^+$ five of the overall seven O atoms participate in the coordination of the metal centre. Both non-coordinating O atoms show together with the adjacent Si atoms very large angles of 169.9°, while the coordinating O atoms have considerably smaller values from 138.7° to 148.4°. The cations are coplanar with the Si_6O_6 and Si_7O_7 cycles. Furthermore, the Me-groups of the Si atoms show an approximately ecliptic arrangement to each other. This conformation is common to cyclosiloxane complexes. By contrast, the O atoms in the analogous crown ether complexes remain coplanar to the metal centre, while the

C_2H_4 bridges are commonly located above or beneath the O atoms' mean plane. The H atoms thereby adopt the sterically preferred staggered conformation.[45, 46, 47, 48]

Cameron et al. were the first to give a substantial comparison on a theoretical and practical level between crown ether and cyclosiloxane complexes.[44] Quantum theory of atoms in molecules (QTAIM) analysis indicated that D_6 and 18-crown-6 provide a similar charge transfer to the cation (Ag^+/Li^+). Nevertheless, the cation shows an eminently weaker electrostatic attraction to the O atoms in cyclosiloxanes compared to crown ethers. By DFT calculations of the energy changes ΔE_{geom}, the authors of this study determined the required energy of the ligand for adopting the complex geometry as consistently higher in cyclosiloxanes than in crown ethers. For example, ΔE rises by 68.4 kJ·mol^{-1} in $[Li(18\text{-crown-6})]^+$ and 74.8 kJ·mol^{-1} in $[Li(D_6)]^+$. However, this "energy penalty" was not quoted as main impact on the lower overall stability of cyclosiloxane complexes. That was rather attributed to the repulsion between the positively charged Si atoms and the metal ion, which was also suggested for the lower complex stability of open chained disiloxane adducts.[21] The basis for the higher electrostatic repulsion can be deducted from several structural differences between cyclosiloxanes and crown ethers. First of all, Si atoms in siloxanes exhibit higher positive charges than C atoms in ethers as was already discussed in section 1.1.2. However, in these approaches, compounds of the type $X_3Si\text{-}O\text{-}SiX_3$ and $X_3C\text{-}O\text{-}CX_3$ (X = H, F) were matter of investigation.[20] Owing to the alternating sequence of Si and O in cyclosiloxanes, the charge of each Si atom is increased further, especially in comparison to that of the C atoms in crown ethers. Therein, the C atoms are each bonded to one C and one

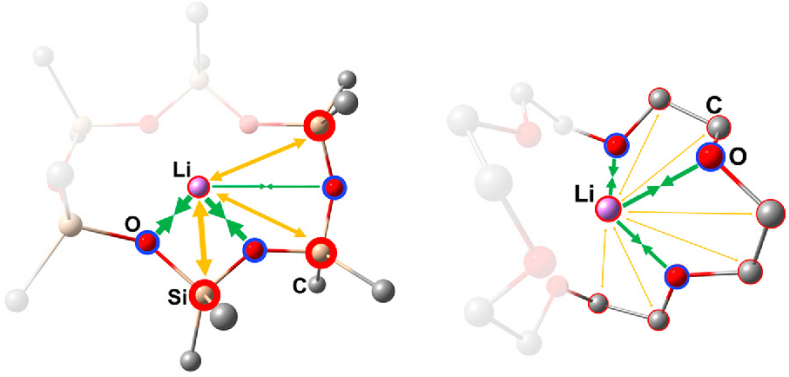

Figure 4. Attractive (*green*) and repulsive (*yellow*) electrostatic interactions between Li^+ and the ligand atoms in $[LiD_6]^+$ (*left*) and $[Li(18\text{-crown-6})]^+$.[44]

O atom, so they are far less positively charged. Another aspect consists of the reduced distance of the Si atoms to the metal centre in cyclosiloxane complexes. In $[LiD_6]^+$, the Si···Li distance is considerably short, especially when the adjacent O atoms are both participating in the coordination (ø 2.74 Å). In comparison, the C atoms in crown ether complexes establish larger distances to Li^+, owing to the flexible C_2H_4-bridge between the O atoms and the ability of the C-O-C fragments to adopt smaller angles (Figure 4).

The strategy to use salts including weakly coordinating anions gave rise to the establishment of cyclosiloxanes as ligands. Hitherto, a number of complexes has been synthesised with respect to this approach. According to this, another complex involving a cyclosiloxane and a salt of a weakly coordinating anion has been eventually published. Thereby, $[ZrD_6Br_2][Zr_2Br_9]_2$ occurred unintentionally in the presence of silicon grease, as reported for many other structures before.[49] In the course of the investigation of cyclosiloxanes, they were frequently denoted as "pseudo crown ethers",[43, 50] despite their eminent structural divergence to organic crown ethers.

1.2.3 Inorganic Cryptands

Additionally to cyclosiloxanes as equivalent to crown ethers, attempts have been made to obtain inorganic analogues of cryptands. This was accomplished by replacing the bridgehead N atoms by the heavier homologues from P to Bi, and the C_2H_4O-units by $SiMe_2O$. The smallest inorganic cryptands $E_2\{(SiMe_2)_2O\}_3$ (E = P - Bi) were obtained by treatment of $O(SiMe_2Cl)_2$ with $[Li(dme)EH_2]$ (E = P, As) or $[Na_3E']$(E' = Sb, Bi).[51, 52] However, they turned out to be instable to treatment with $Li[Al\{OC(CF_3)_3\}_4]$ as the P

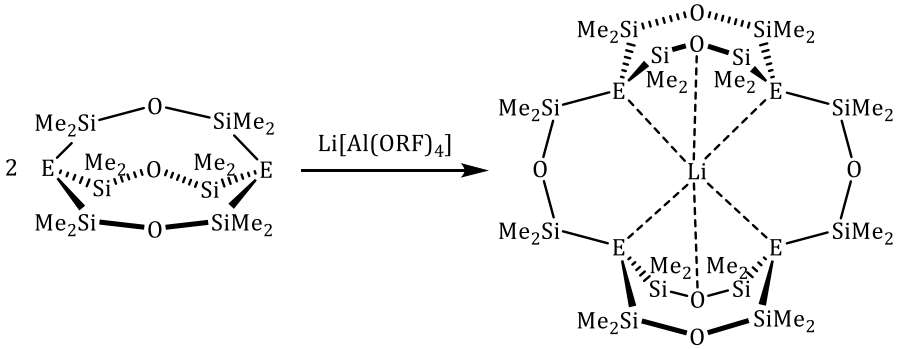

Scheme 4. Reaction of $E_2\{(SiMe_2)_2O\}_3$ (E = N, P) with $Li[Al(OR_F)_4]$ leads to the dimeric compound $[Li@E_4\{SiMe_2)_2O\}_6][Al(OR_F)_4]$.

and As incorporating ligands unexpectedly reacted to dimeric compounds (Scheme 4). As the resulting Li^+ incorporating dimer didn't turn out to be suitable for the growth of single-crystals, the cation was removed by addition of a small amount of tetrahydrofuran (THF), indicating the extremely weak coordination ability of the dimer. The existence of the dimeric complexes were eventually proven by mass spectrometric analysis and the structures determined by DFT calculations. According to that, Li^+ is coordinated by the four P or As atoms, respectively, and by two O atoms of the siloxane chain. However, decomposition was observed in the analogous reaction of $Li[Al\{OC(CF_3)_3\}_4]$ with the Sb and Bi bridged cryptands.

Another inorganic [2.1.1]cryptand was obtained by deprotonation of the eight membered heterocyclic compound $[O(Si\mathit{i}Pr_2)_2PH]_2$ with *n*-BuLi and subsequent reaction with $SiMe_2(OSiMe_2Cl)_2$ (Scheme 5).[52, 53] Treatment with $Li[Al(OR_F)_4]$ yielded the corresponding complex structure, which was determined by single-crystal X-ray diffraction (Figure 5). The molecular structure reveals a coordination of Li^+ by three of the four O atoms. The coordinating O atom located in the $SiMe_2(OSiMe_2)_2$-chain establishes the shortest binding to Li^+ (1.98 Å), which correlates with its small Si-O-Si angle of 135.6°. According to that, the Li-O contacts of the remaining coordinating O atoms are significantly longer (ø 2.08 Å) and the Si-O-Si angles larger (165.8°). By means of DFT calculations, *Hänisch et al.* determined the relative complex stability of the cationic structure to be 24 kJ·mol^{-1} higher than $[LiD_5]^+$ and 15 kJ·mol^{-1} lower than $[LiD_6]^+$.[53]

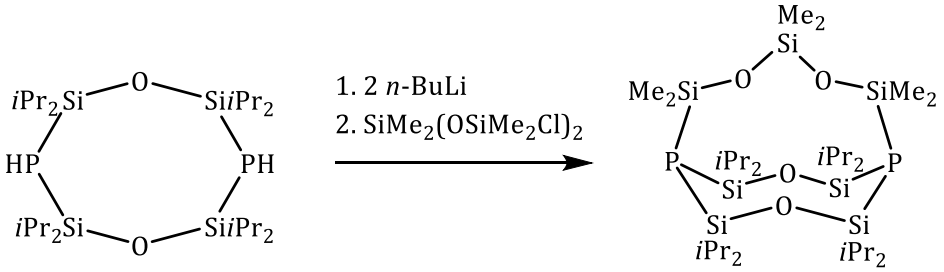

Scheme 5. Reaction path for $[P_2\{O(Si\mathit{i}Pr_2)_2\}_2\{SiMe_2(OSiMe_2)_2\}]$ (E = P, As).

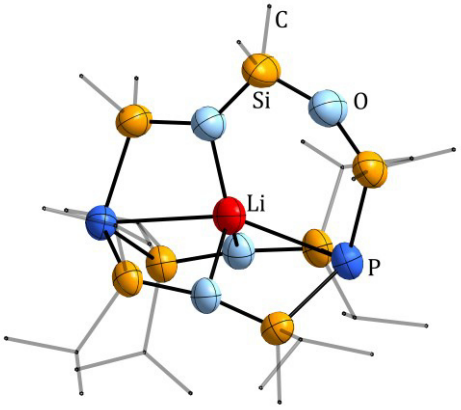

Figure 5. Molecular structure of the cation $[Li@P_2\{O(Si\textit{i}Pr_2)_2\}_2\{SiMe_2(OSiMe_2)_2\}]^+$.

1.2.4 Ring Strain as Inhibitor for Complex Formation

The most eye-catching difference between crown ethers and cyclosiloxanes or organic and inorganic cryptands represents the incorporation of C_2H_4O-groups rather than $SiMe_2O$. This structural divergence leads to a radical difference in binding affinity between these types of ligands. Upon coordination, the alternating series of Si and O in siloxanes give four-membered ring systems (Scheme 6, *left*), while crown ethers yield five-membered cycles (Scheme 6, *right*).

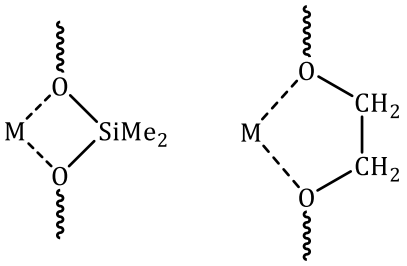

Scheme 6. Coordination pattern of a metal ion (M) in siloxanes (*left*) and crown ethers (*right*).

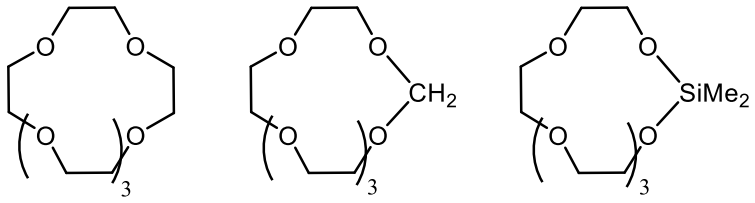

Scheme 7. Structures of [18]crown-6 (*left*), [17]crown-6 (*centre*) and sila[17]crown-6 (*right*).

The impact of ring strain on the coordination ability of ring contracted crown ethers was already shown in the 80s.[54] The authors of this study determined the extraction ability of crown ethers, ring contracted crown ethers and sila-crown ethers (Scheme 7). This was achieved by means of extraction experiments using aqueous alkali metal picrates and dichloromethane as a less polar phase including the respective crown compound. Subsequently, after the phase separation was completed, the picrate concentration in the organic phase was measured by its respective absorption. The extraction rate of [18]crown-6 is as expected at its maximum when K^+ is used.[45] 69.3% of potassium picrate were accordingly transferred from the aqueous into the organic solution. In the same row, [17]crown-6 and sila[17]crown-6 exhibit a drastically reduced extraction rate of 1.7% and 1.8% (Table 2). The authors explain these observations by the inability of the donor atoms to adopt the required planar alignment in order to form a complex, since CH_2 and $SiMe_2$ substituted cycles both show low extraction rates. However, within this study the sensitivity of sila-crown ethers

Table 2. Extraction ability (%) of [18]crown-6, [17]crown-6 and sila[17]crown-6 towards the cations Na^+, K^+, Rb^+ and Cs^+

	[18]crown-6	[17]crown-6	Sila-[17]crown-6
Na^+	6.3	0.8	0.3
K^+	69.3	1.7	1.8
Rb^+	57.6	1.0	1.8
Cs^+	36.7	0.7	0.7

towards water was not taken into account. According to results on the hydrolysis rate of sila-crown ethers, 63% of sila-14-crown-5 are decomposed after 66 minutes in an aqueous solution of NaCl, yielding polyethylene glycol and a not further identified silanol, possibly $Me_2Si(OH)(OCH_2CH_3)_4OH$.[55] Although polyethylene glycols and sila-crown ethers exhibit roughly similar extraction abilities,[54] it is still not definite whether the values shown in Table 2 are eventually meaningful.

However, this study indicates that higher complexation rates can be achieved by increasing the structural similarity between organic and sila-based crown ethers. Attempts have been made by the synthesis and characterisation of the cyclic compound $[O(Si_2Me_4)]_2$,[56] which is commonly abbreviated as $^2D_2$ (^2D = Me_4Si_2O). Larger cycles such as the nine-membered ring $^2D_3$ and traces of the twelve-membered ring $^2D_4$ were detected by gas-liquid chromatography after a cationic ring opening polymerisation of $^2D_2$ with trifluoromethanesulfonic acid.[57] The cationic ring opening polymerisation of $^2D_2$ was found to be faster compared to that of the cyclosiloxane D_4, which was attributed to the easier formation of the silyl oxonium ion in $^2D_2$.[58, 59] A*b initio* calculations revealed an increased basicity of $^2D_2$ compared to D_3 or D_4, owing to the less relevant negative hyperconjugation in systems of the type $n(O) \rightarrow \sigma^*(SiSi)$.[60] Despite the increased basicity, no stable complexes involving $^2D_2$ are available to date.

1.2.5 Coordination Chemistry of Sulfur Dioxide

Due to its physical properties, sulfur dioxide can be considered as a rather unusual solvent: The melting point is at −75.5 °C and the boiling point at −10.0 °C. As most proton free solvents, it has a low intrinsic conductivity ($1 \cdot 10^{-7}/(\Omega \cdot cm)$, which relates to the weak self-dissociation into a thionyl cation and a solvated oxygen anion[61, 62] (Scheme 8).

Scheme 8. Self-dissociation equilibrium of SO_2.

Depending on temperature (+20 to −70 °C), the permittivity ε of SO_2 varies from 14 to 25, which is in the range of NH_3 or H_2S. Sulfur dioxide is not an appropriate solvent for compounds, which crystallise in an ionic lattice such as LiCl, NaCl, KCl, $MgCl_2$ or $BaCl_2$. The solubility increases in the case of large anions, for example I^- or SCN^- [63] and especially with homopolar compounds, e.g. the halides of B, Al, Ge, Si, Sn, P, As, Sb and S.[64] For example, the solubility of $AlCl_3$ in SO_2 has been widely exploited for the synthesis of salts of the weakly coordinating anion $M^+[AlCl_4]^-\cdot nSO_2$. They were obtained after addition of MCl (M = Li, Na, K, NH_4) to a solution of $AlCl_3$ in SO_2. The amount of SO_2 in the complexes depends on the cation used as follows: M = Li, Na: n = 1.5 and 3; M = K: n = 1.5 and 5; M = NH_4: n = 5.[65] The structures of $Li[AlCl_4]\cdot 3SO_2$ and $Na[AlCl_4]\cdot 1.5SO_2$ were determined by single crystal X-ray diffraction. According to that, the Li cation is octahedrally coordinated by O,O'-bridging SO_2 molecules and forms $[Li(OSO)_{6/2}]_n^{n+}$ chains.[66] In $Na[AlCl_4]\cdot 1.5SO_2$, the sodium cation is additionally saturated by Cl atoms, giving NaO_2Cl_4 and NaO_3Cl_3 octahedra.[67] Analogous reaction paths also gave access to the weakly coordinating anions $[AsF_6]^-$ and $[SbF_6]^-$.[68] The use of transition metal fluorides such as NiF_2, MnF_2 or FeF_2 gave rise to complexes of the type $[M(SO_2)_x](AsF_6)_2$.[69, 70] Due to the barely interacting $[AsF_6]^-$ ions and the weakly coordinated SO_2 ligands, the transition metals are kept almost "naked" and are

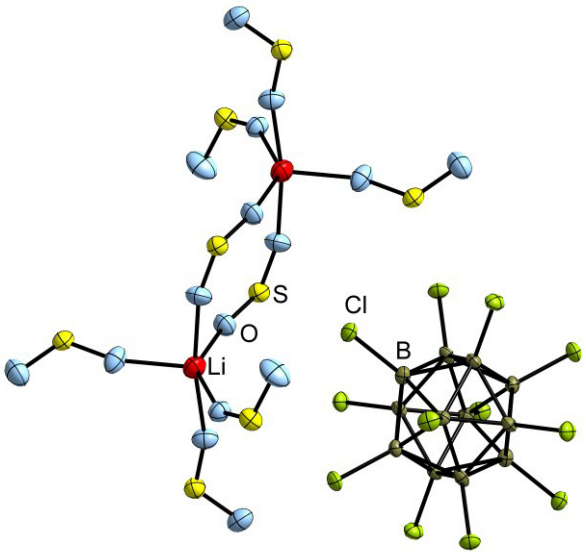

Figure 6. Molecular structure of the homoleptic complex $[Li_2(SO_2)_8][B_{12}Cl_{12}]$ in the crystal.[71]

thus highly reactive.[70] Indeed, the use of weakly coordinating anions turned out to be valuable for the participation of SO_2 in the coordination of metal ions. For example, the lithium salt of the perchlorinated *closo*-dodecaborate $[B_{12}Cl_{12}]^{2-}$ yielded a homoleptic SO_2 complex of Li^+ (Figure 6). In the cases of Na^+, K^+, Rb^+ and Cs^+, the coordination sphere was additionally to SO_2 saturated by interactions with Cl from $[B_{12}Cl_{12}]^{2-}$.[71] *O* and bridging μ-*O,O'* coordination is common for hard d-, f-block and main group metal centres.[72, 73] Towards soft metal centres such as in $[Mn(Cp)(CO_2)(SO_2)]$[74] and $[Mo(CO)_3(phen)(SO_2)]$[75] planar *S* and *S,O* interactions were observed (Figure 7).

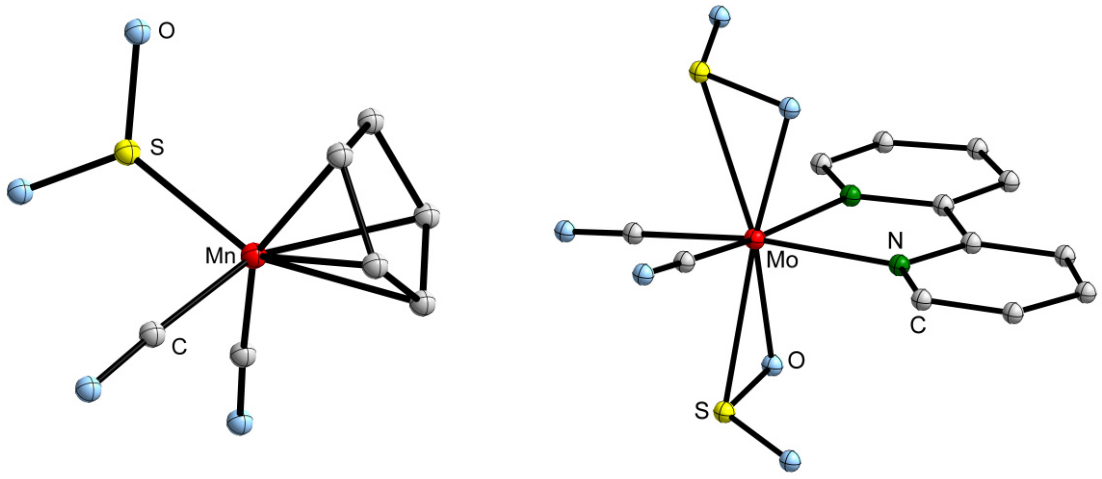

Figure 7. The molecular structures of $[Mn(C_5H_5)(CO)_2(SO_2)]$ (*left*) and $[Mo(CO)_3(phen)(SO_2)_2$ (*right*) display the versatile coordination modes of SO_2.[74] [75]

In contrast to aliphatic hydrocarbons, also polar organic compounds such as amines, aromatic hydrocarbons and alcohols are generally well soluble in sulfur dioxide. Therefore, SO_2 is broadly used for separation of aromatic and olefinic components within the purification process of fossil oil.[64] Although a number of organic solvates

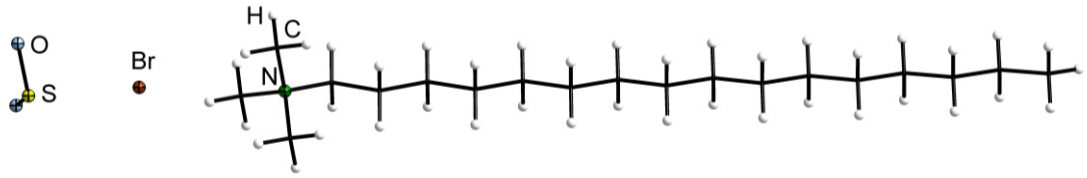

Figure 8. Expansion of the crystal structure of $C_{16}H_{33}NMe_3 \cdot Br \cdot SO_2$.[79]

of SO_2 is known to date,[76, 77] only few have been characterised by X-ray diffraction.[78] One example is the solvate of cetyltrimethylammonium bromide shown in Figure 8.[79] Therein, the bromide ion shows attractive interactions with both, the ammonium ion and sulfur. It is worth mentioning that the molecular structure remained stable at ambient temperature, release of SO_2 was not observed. Careful computational methods revealed that the solvation of halides in sulfur dioxide is a considerably exothermic process. For example the solvation of fluoride is favoured by 360 – 380 $kJ \cdot mol^{-1}$ and that of chloride by 200 $kJ \cdot mol^{-1}$. As a result F^- was found to be instable in liquid sulfur dioxide, since the formation of the fluorosulfite anion occurs without an activation barrier.[80] Very recently, even organic polymers such as poly(ethylene oxide) were found to exhibit high absorption capacities of SO_2.[81] Especially ionic liquids carrying functional groups such as amines thusly find application for the flue gas desulfurization.[82, 83, 84] The *Lewis* acidic character of SO_2 was furthermore shown by adduct formation with N-heterocyclic carbenes (NHC).[85, 86, 87]

For complexation reactions between cyclosiloxanes and salts of weakly coordinating anions, sulfur dioxide was occasionally used as the solvent of choice.[43] Unexpectedly, ring transformations were observed under these fairly mild conditions,[88] which is a typical phenomenon for siloxanes, but particularly in the presence *Lewis* acids.[39] The ring transformation of D_5 towards D_6 and D_7 in the presence of $AgSbF_6$ and SO_2 may be the result of an anionic ring opening polymerisation.[88] The authors suggest that in a first step, coordination of Ag^+ to D_5 weakens the Si-O bonds, followed by higher positive charges on silicon. This promotes the abstraction of an F^- ion from SbF_6^- and leads to a ring opening under formation of a Si-F bond. The resulting SbF_5 can be stabilised by adduct formation together with the weak base SO_2 (Scheme 9).[89] The open chained anion can attack other Si atoms to afford the thermodynamically favoured D_6 and D_7

species. Since ring transformations have not yet been observed in dichloromethane, SO_2 seems to be a highly efficient promotor for this type of reaction.

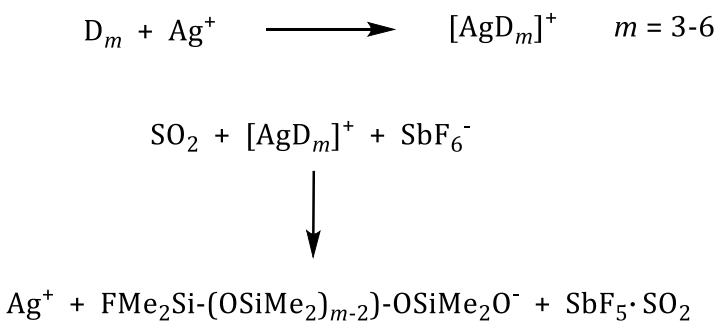

Scheme 9. SO_2 promoted ring opening of D_m (m = 3-6).

2.1. Synthesis and Application of Paracyclophanes

Besides cyclosiloxanes, other sila-bridged macrocycles such as silacyclophanes[90] and silacalixarenes[91] have attracted attention with respect to their application in the field of *host-guest* chemistry. The compound class of cyclophanes was discovered in 1949[92] and has been exploited in the field of organometallic chemistry[93], self-assembly[94] and as planar-chiral ligands[95] for example in the enantioselective catalysis.[96]

The main feature consists of π-interactions between two aromatic systems, which are in paracyclophanes anchored in 1,4- and in metacyclophanes in 1,3-position.[97] The

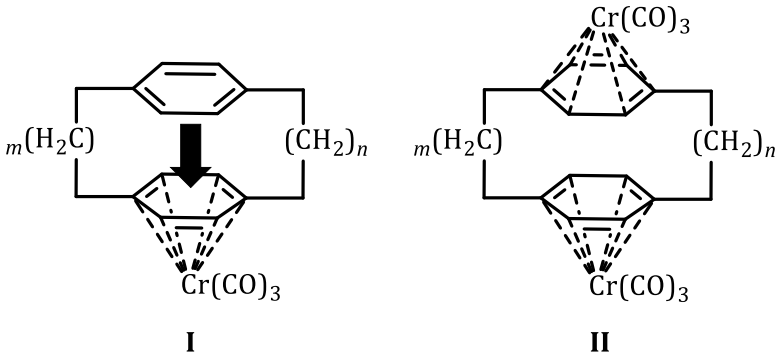

Scheme 10. Mono-complex (**I**) and bis-complex (**II**) of [m.n.]paracyclophanes (m, n = 2-6) with $Cr(CO)_3$.

length of the bridging moiety is defined by the numbers in square brackets, for example [2.2]paracyclophane is bridged on each side by two atoms such as an ethylene moiety. The distance between the aromatic rings in the ethylene bridged [2.2]paracyclophane is with values between 278 – 309 pm relatively short. The resulting significant strain within the molecule is presumably relieved by the two anchored C atoms in each benzene ring, which are displaced from the plane of the remaining four atoms by 0.13 Å.[92] Moreover, the inflexible ethylene bridges force the benzene rings in the energetically disfavoured sandwich configuration,[98, 99] which leads to significant transannular electronic interactions between the two aromatic rings.[100] This was shown by means of complexation of [m.n.]paracyclophane and $Cr(CO)_6$ under elimination of CO.[101] In the case of *m* and *n* smaller than four, exclusively the mono-complex was observed (Scheme 10 Type I). This was attributed to an electron withdrawing effect of Cr(0) on both aromatic rings. It follows that bis-complexes were formed with [4.5] and [6.6]paracyclophanes. The flexibility of these bridges enables the aromatic rings to act as independent π-electron systems (Scheme 10, Typ II).[100] The lower strain within the molecule leads to the common parallel displaced configuration of the aromatic rings,[102] which is for example typical in crystalline benzene.[99] To date, the incorporation of Cr(0) in the centre of the paracyclophane has not been successful by the use of $Cr(CO)_6$. (η^{12}-[2.2]paracyclophane)chromium(0) was rather synthesized by *Elschenbroich et al.* in 1978 by cocondensation of chromium and [2.2]paracyclophane.[103] That issue was later extended on the heteroatomic bridged tetrasila[2.2]paracyclophane, using a particular approach. The authors first cocondensed chromium together with the open chained 1,4-$C_6H_4(SiMe_2Cl)_2$ and obtained the corresponding complex [Cr{1,4-$C_6H_4(SiMe_2Cl)_2$}$_2$]. The required disilane bridge to form a tetrasila-[2.2]paracyclophane complex was only obtained after by a *Wurtz*-coupling using lithium.[104] Moreover, the complex was characterised by X-ray diffraction (Figure 9). Due to the presence of the Si_2Me_4-bridges and the metal atom between the aromatic rings, the inter-ring distance amounts to 335 – 346 pm.

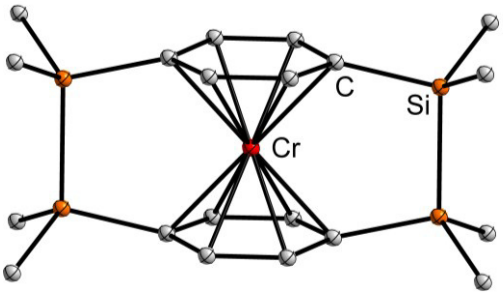

Figure 9. Molecular structure of (η^{12}-tetrasila[2.2]paracyclophane)chromium(0) in the crystal. H atoms are omitted.[104]

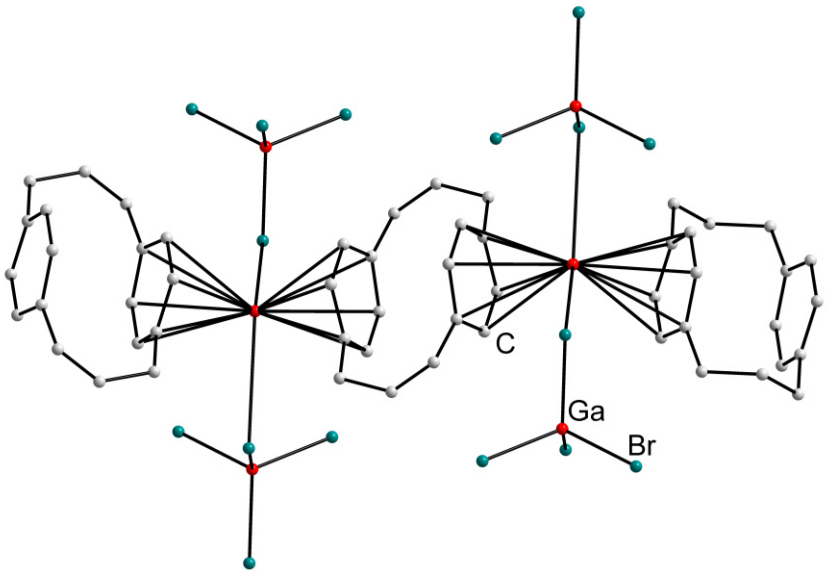

Figure 10. Expansion of the (paracyclophane-Ga(I)-paracyclophane)-coordination polymer. H atoms are not displayed.[105]

Beside transition metals, also main group compounds turned out to be suitable for the coordination by paracyclophanes. For example, the reaction of [3.3]paracyclophane with Ga[$GaBr_4$] yielded a strand-like coordination polymer with Ga(I) being exocyclic η^6-coordinated by the aryl rings of two paracyclophanes (Figure 10). The second aromatic ring is coordinating to another Ga(I) atom, respectively, giving a zigzag coordination pattern. The coordination sphere of Ga(I) is additionally saturated by two Br atoms. The $[GaBr_4]^-$ anions are each bonding to two Ga(I) atoms and thusly establish a 2D network.[105]

During the last decades, paracyclophanes have been vastly altered, as for example by the incorporation of heteroatoms such as S, N or P in the aromatic system.[106, 107, 108]

However, it must be noted that the bridges holding these molecules together have been largely neglected, only few paracyclophanes bridged by heteroatoms are known to date. One example represents the disiloxane bridged [3.3]paracyclophane,[97, 109] the first being obtained in 1964 as a by-product during the thermal cracking of poly(tetramethyl-*para*-silaphenylenesiloxane) in the presence of NaOH at 300 °C (Scheme 11, *left*). Also the corresponding metacyclophane (Scheme 11, *centre,* X = CH) was unintentionally synthesised within polymerisation attempts. Later, both silacyclophanes were directly obtained by hydrolytic polycondensation of the respective bis(chlorosilyl)arenes[110] in high dilution and were characterised among other by X-ray diffraction. Moreover, similar conditions using 1,3,5-tris(chlorodimethylsilyl)benzene yielded a threefold bridged silacyclophane.[109] Therein, the coplanar aromatic rings lie exactly above one another with an inter-ring distance of 3.503 Å. The structure shows many analogies to the in 1,3,5-position disilane-bridged cage compound,[111] which is known as superphane, due to the presence of three anchors between the aromatic rings.[112] Although a large number of disiloxane bridged paracyclophanes has been described, to date no coordination compounds have been synthesised yet.[113]

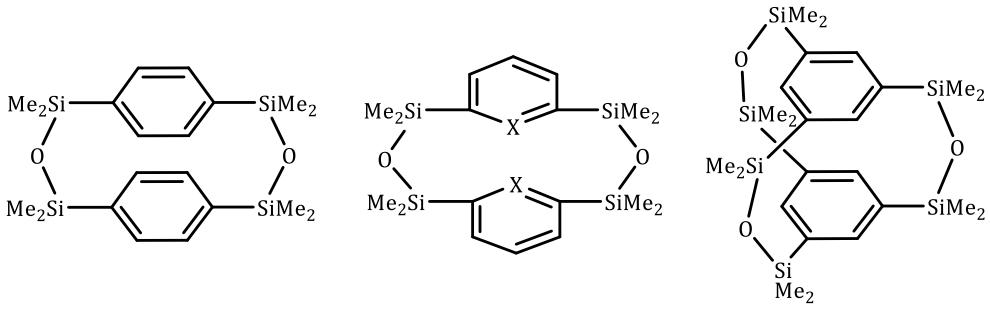

Scheme 11. Siloxane bridged [3.3]paracyclophane (*left*), [3.3]metacyclophane (X = CH, N, P) (*centre*) and the cage-type [3.3]silacyclophane (*right*).

2 Project Scope

Starting with the first unintended syntheses of cyclosiloxane complexes from silicon grease,[37] this compound class was most generally considered as pseudo crown ethers.[43][49] However, the structural analogy to organic crown ethers is poor, since the latter incorporate C_2H_4 units instead of $SiMe_2$ in between the O atoms. The alternating series of Si and O atoms in cyclosiloxane frameworks lead to an increased proximity and an electrostatic repulsion of the already positively polarised Si atoms and the *Lewis* acid. This is an effect that almost compensates the attraction between the cation and the O atoms.[44]

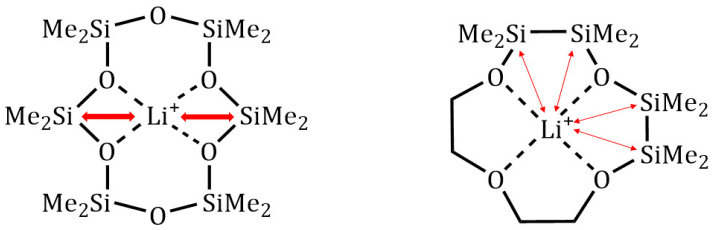

Scheme 12. Illustration of the repulsive interactions between Li^+ and the positively polarised Si atoms in cyclosiloxanes (*left*) and a hybrid sila-crown ether (*right*).

The first part of this project thusly targets to increase the comparability of crown ethers and Si-O based ligands. This can be achieved by crown ethers, which partially incorporate Si_2Me_4 linkers between the O atoms (Scheme 12). The resulting hybrid ligands provide larger interatomic distances between the coordinated *Lewis* acid and the Si atoms. The debut consists of the formal insertion of one disilane fragment into a residuary ethylene bridged framework. 1,2-Dichloro-1,1,2,2-tetramethyldisilane and a corresponding open chained glycol are taken into account as suitable starting reagents (Scheme 13). The stepwise growth of the disilane proportion within these hybrid crown ethers permits substantial insights into the coordination ability of the C, Si/C and Si bonded O atoms. Therefore, also disila-crown ethers with adjacent Si_2Me_4 moieties are part of this project. The required building block $O(Si_2Me_4Cl)_2$ cannot be purchased commercially and must be generated in a multistep synthesis. A conceivable

synthetic approach is depicted in Scheme 14. The long-term objective of this research project represents completely $(Si_2Me_4O)_n$ (n = 4 – 7) based crown ethers.

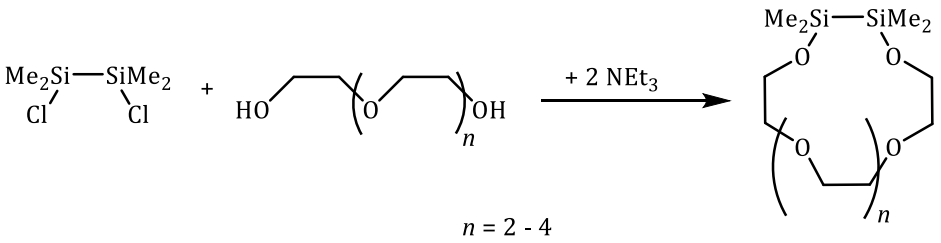

Scheme 13. Synthesis path of 1,2-disila-crown ethers with 12 to 18 ring atoms.

The synthesis of coordination compounds involving disila-crown ethers is one milestone of this project. Especially alkali metals salts are taken into account. Single crystal X-ray crystallography, mass spectrometry as well as NMR and IR spectroscopy are the methods of choice for the characterisation of the resulting complexes. To obtain insights into the coordination ability of these hybrid ligands in comparison to cyclosiloxanes and crown ethers, the reactivity towards salts of strongly coordinating anions such as Cl^- is matter of investigation. The complexation reactions are planned to be

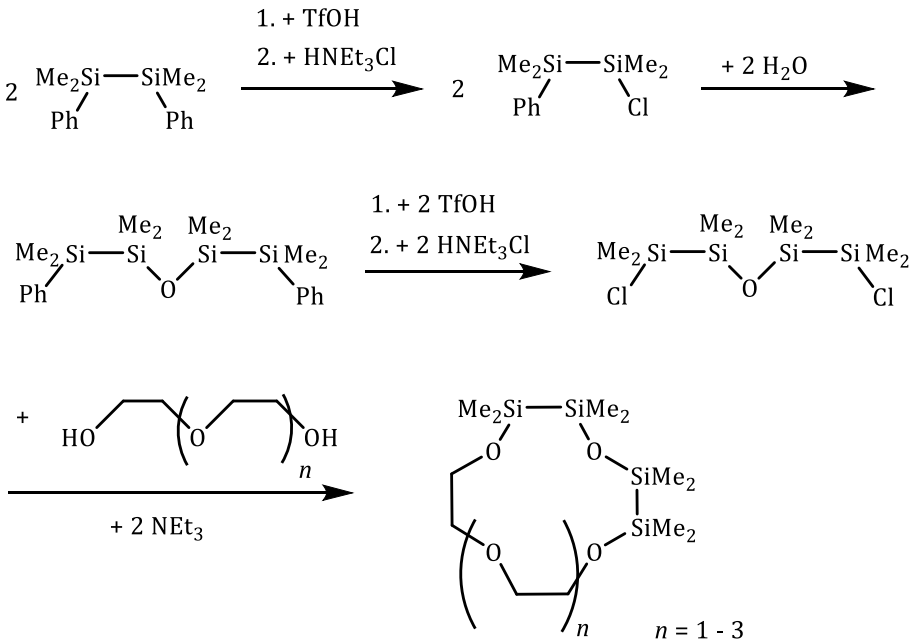

Scheme 14. Multistep synthesis of the inorganic building block $O(Si_2Me_4Cl)_2$ for hybrid sila-crown ethers with adjacent disilane moieties.

conducted in different solvents such as dichloromethane and liquid sulfur dioxide. Finally, the determination of the relative complex stability is the matter of essential interest. Theoretical and experimental methods such as mass spectrometry[114][115] as well as dynamic NMR spectroscopy[116] seem appropriate for the validation. This project thusly contributes to a better understanding if the Si-O bond and also to the ongoing discussion on the low basicity of siloxanes.

The second part of this work deals with the synthesis of heteroatomic bridged paracyclophanes. Despite the number of reported heteroatomic bridged paracyclophanes (see chapter 1.2.1), only few coordination compounds have been published to date. The incorporation of heteroatoms in the linking moieties as well as the resulting increased cavity diameter between the aromatic systems may give rise to improved coordinative properties. Conceivable are heteroatomic bridges with group 13 elements as for example -SiN(H)Si- and -SiP(H)Si-. After deprotonation of the secondary amine or phosphane by appropriate bases, also the linking groups can possibly participate in the coordination of *Lewis* acids. A conceivable synthetic approach for heteroatomic bridged paracyclophanes represents the reaction of 1,4- $C_6H_4(SiR_2Cl)_2$ (R = Me, *i*Pr) with NH_3 and $[LiPH_2(dme)]$, respectively. Subsequent deprotonation with an appropriate base such as *n*BuLi followed by salt metathesis with the corresponding 1,4-bis(chlorosilane)benzene gives access to [3.3]paracyclophanes (Scheme 15). Investigation of the exo- and endocyclic coordination ability of these compounds towards Brønsted bases such as $Li\{N(SiMe_3)_2\}$ and $Fe(\{N(SiMe_3)_2\})_2$ thusly represents the long-term objective.

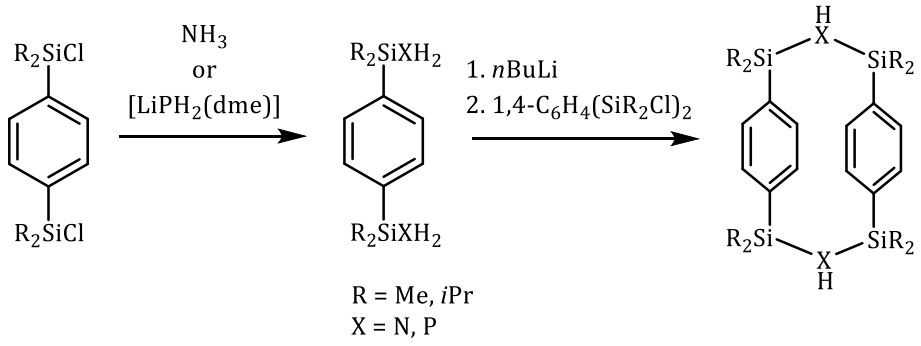

Scheme 15. Synthetic approach for heteroatomic bridged [3.3]paracyclophanes.

3 Summary

This work presents synthetic approaches towards Si_2Me_4 incorporating crown ethers. The derivatives with one disilane unit in a residuary organic framework were obtained by Williamson ether synthesis of 1,2-dichloro-1,1,2,2-tetramethyldisilane and the corresponding glycol in the presence of NEt_3. The products 1,2-disila[12]crown-4 (**1**), 1,2-disila[15]crown-5 (**2**) and 1,2-disila[18]crown-6 (**3**) are highly viscous oils. Reactions with alkali metal salts yielded colourless crystals, which were analysed by X-ray diffraction. The obtained structures exhibit contact ion pairs, the cation being furthermore coordinated by all O_{crown} atoms (Scheme 16).

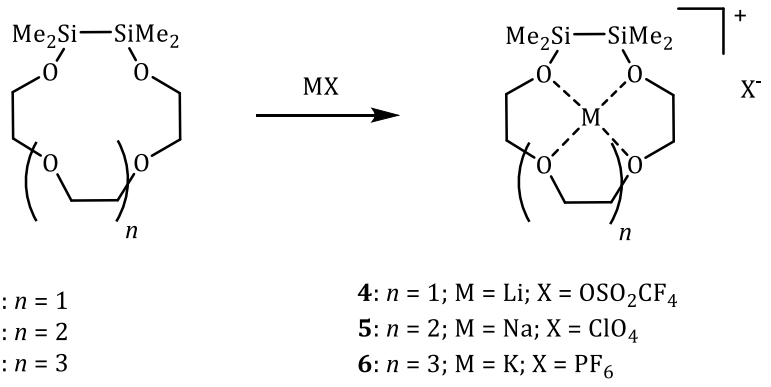

1: n = 1
2: n = 2
3: n = 3

4: n = 1; M = Li; X = OSO_2CF_4
5: n = 2; M = Na; X = ClO_4
6: n = 3; M = K; X = PF_6

Scheme 16. Complex formation of the disila-crown ethers **1**-**3** with alkali metal salts.

As was deducted from the molecular structures, the Si and C bonded O_{crown} atoms constantly establish shorter bond lengths to the cations compared to the fully C substituted O_{crown} atoms. The bond lengths are thereby indicative for the strength of the electrostatic attraction. As expected, the insertion of Si_2Me_4 groups leads to an increased distance of the Si atoms and the cation. In [Li(1,2-disila[12]crown-4)OSO_2CF_3] (**4**) (Figure 11*a*) it measures ø322.0(3) pm, compared to ø275.6(20) pm in $[LiD_6]^+$ (D = Me_2SiO).[43] The relative complex stability of compound **4** was determined by dynamic ^{1}H NMR spectroscopy. The reaction of [12]crown-4, **1** and Li(OSO_2CF_3) in a 1:1:1 ratio showed that the equilibrium is on the side of the Li-complex of **1**, while the large proportion of [12]crown-4 remains non-coordinated. A more precise interpretation of the dynamic NMR experiments was interfered by sandwich complex formation of the two

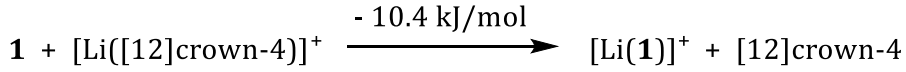

Scheme 17. Energy difference of the Li exchange from [12]crown-4 to **1** as obtained from DFT calculations.

ligands. DFT calculations (BP86 functional and def2-TZVP basis set) confirmed the slightly higher complexation ability of the hybrid crown ether as the exchange of Li^+ from [12]crown-4 to **1** is favoured by 10,4 $kJ \cdot mol^{-1}$ (Scheme 17). Moreover, single point calculations revealed that compound **1** requires significantly more energy to adopt the ligand structure found within the complex (+33.8 $kJ \cdot mol^{-1}$) compared to [12]crown-4 (+18.0 $kJ \cdot mol^{-1}$). Since the overall energy of the reaction shown in Scheme 17 is negative, the electrostatic attraction between the Si/C bonded O atoms and the cation must compensate for the increased energy effort for the rearrangement of the ligand in **4**.

To obtain further information about the complexation ability of completely Si bonded O atoms, hybrid crown ethers with adjacent Si_2Me_4 units were successfully implemented. The synthesis of the required building block $O(Si_2Me_4Cl)_2$ was realised by asymmetric chlorination of 1,1,2,2-tetramethyldisilane by the use of trichloroisocyanuric acid (TCCA) (Scheme 18). The chlorination appears not to occur statistically, since in the reaction solution 70% of the asymmetric chlorinated disilane was detected by means of $^{29}Si\{^1H\}$ NMR spectroscopy. Hydrolysis and chlorination of the terminal Si atoms afforded the required inorganic building block. However, the original approach, presented in the section *Project Scope*, turned out to be an impasse. The synthesis of $O(Si_2Me_4Ph)_2$ was successful, but the attempt to substitute the terminal Si atoms by the use of trifluoromethanesulfonic acid led to cleavage of the O bridged tetrasilane followed by decomposition.

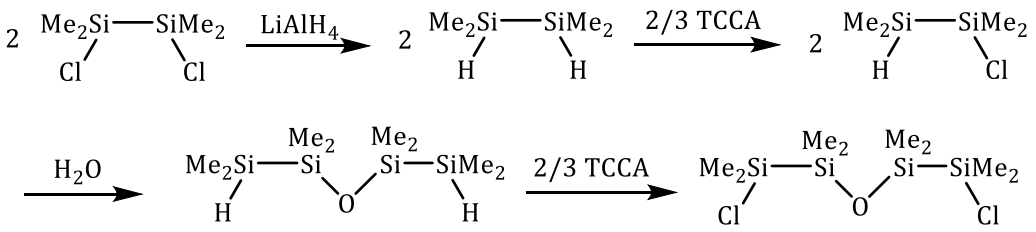

Scheme 18. Synthesis of the inorganic building block $O(Si_2Me_4Cl)_2$ for hybrid tetrasila-crown ethers.

Analogous reaction conditions as used for the synthesis of disila-crown ethers afforded in conjunction with $O(Si_2Me_4Cl)_2$ and diethylene glycol the required hybrid ligand 1,2,4,5-tetrasila[12]crown-4 (**7**) (Scheme 19). Complexation of $Li(SO_3CF_3)$ in dichloromethane yielded colourless crystalline material. The molecular structure, determined by X-ray diffraction, shows a contact ion pair of [Li(1,2,4,5-tetrasila[12]crown-4)OSO_2CF_3] (**8**) (Figure 11*b*). Due to the presence of two adjacent Si_2Me_4 groups, the ligand has an increased ring diameter, so the cation in **8** is located 56.8(4) pm above the calculated mean plane of the O_{crown} atoms compared to 83.6(9) pm in [Li([12]crown-4)(OSO_2CF_3)] (see Supplementary Information of publication n° 2).

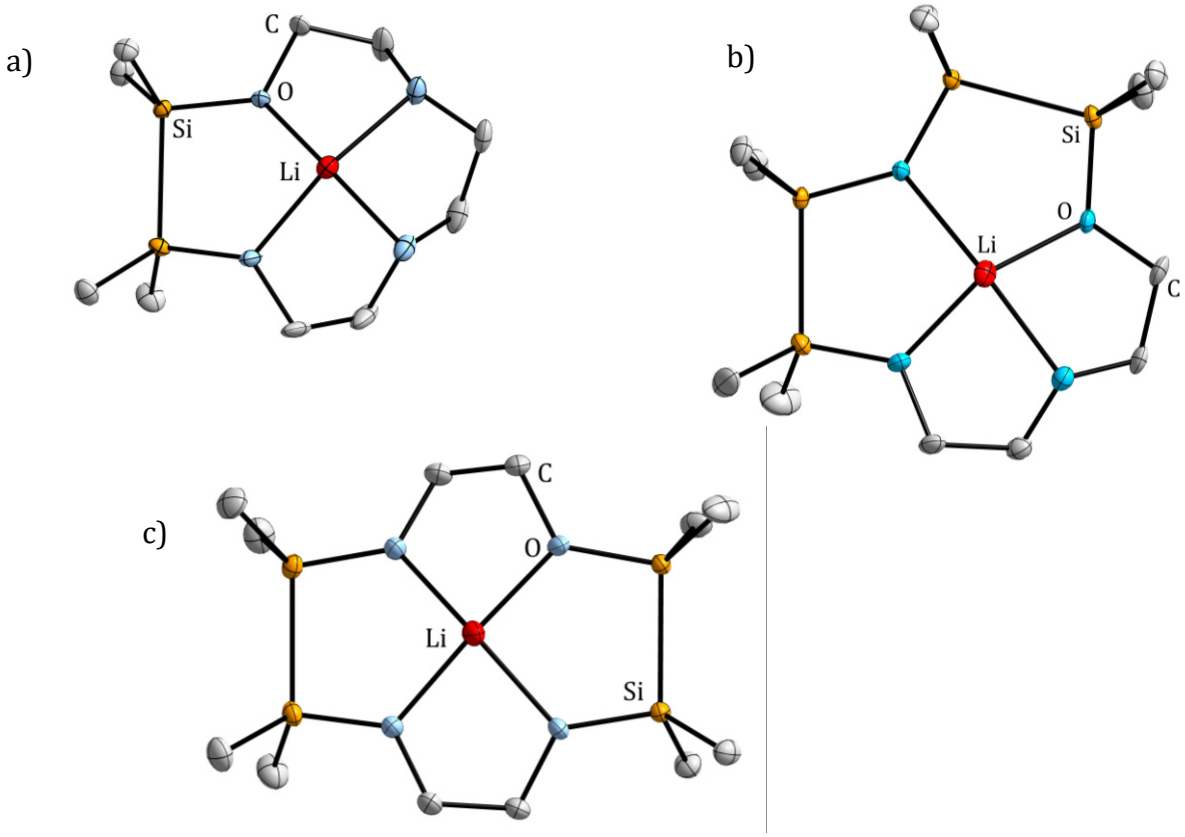

Figure 11. Top-views of the cationic complexes of *a*) [Li(1,2-disila[12]crown-4)]$^+$ (**4**), *b*) [Li(1,2,4,5-tetrasila[12]crown-4)]$^+$ (**8**) and *c*) [Li(1,2,7,8-tetrasila[12]crown-4)]$^+$ (**10**). The anions and H atoms are respectively omitted for clarity; the thermal ellipsoids represent the 50% probability level.

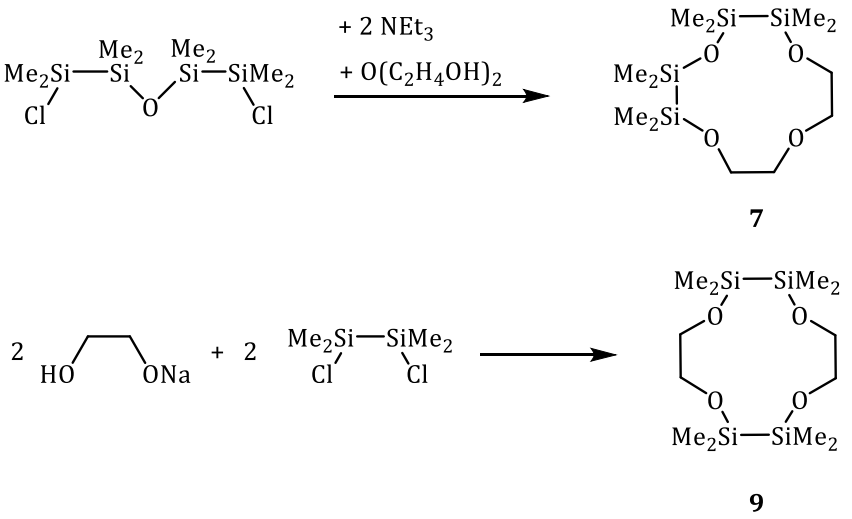

Scheme 19. Synthesis paths for the hybrid crown ethers **7** and **9**, which incorporate two Si_2Me_4 moieties.

Another method to increase the amount of Si in hybrid crown ethers consists of the asymmetric deprotonation of ethylene glycol by sodium hydride, followed by stoichiometric reaction with 1,2-dichloro-1,1,2,2-tetramethyldisilane (Scheme 19). Different to compound **7**, 1,2,7,8-tetrasila[12]crown-4 (**9**) incorporates two opposite positioned Si_2Me_4 moieties, so all O_{crown} atoms are equally Si and C substituted. Complexation and crystal growth was successful with $LiPF_6$. The crystal structure of [Li(1,2,7,8-tetrasila[12]crown-4)PF_6] (**10**) (Figure 11*c*) determined by X-ray diffraction shows the expected contact ion pair. The relative stability of the cationic Li-complexes of the tetrasila-crown ethers **7** and **9** was analysed by DFT calculations, using the BP86 functional and the def2-TZVP basis set. Thereby it was shown that the exchange of Li^+ from [Li([12]crown-4)]$^+$ to the ligand **7** is favoured by 29.5 kJ·mol^{-1}, while that to the ligand **9** is with +3.3 kJ·mol^{-1}almost isoenergetic. Additionally, single point calculations of the

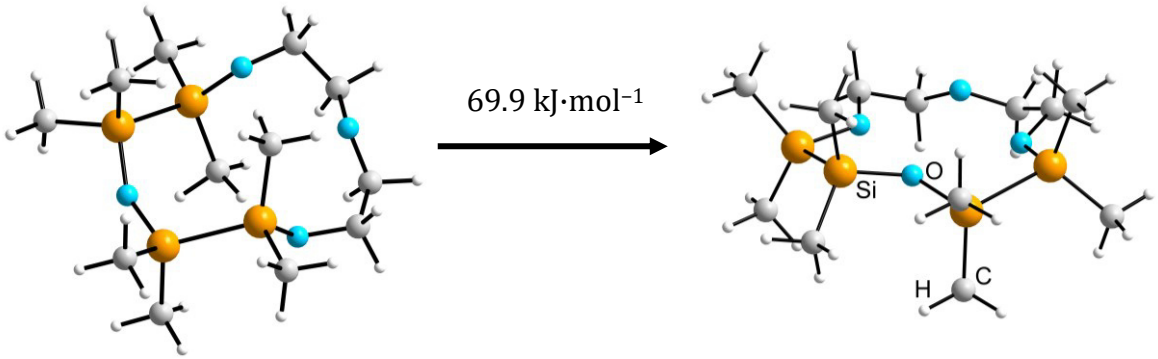

Scheme 20. Illustration of the transition from the calculated free ligand structure of compound **7** to the calculated structure within the complex and the specified energy

geometry optimised free ligands and the structures of the ligands within the complexes (see Scheme 20) revealed that both, **7** and **9**, require significantly more energy than 1,2-disila[12]crown-4 for adopting the complex geometry (Table 3). The energy effort of **7** was determined to be +69.9 kJ·mol^{-1} and that of compound **9** +60.4 kJ·mol^{-1}. Since the cationic Li-complex of **7** is, despite the increased value for ΔE_{geom}, considerably more stable than that of **9**, the Si bonded O_{crown} atoms must show stronger electrostatic attraction to the cation than the Si/C bonded O_{crown} atoms in **1** and **9**. The basicity of the C_2H_4 and/or Si_2Me_4 substituted O atoms thusly increases in the series $O_C < O_{Si/C} < O_{Si}$. These results underline the assumption that the low coordination ability of cyclosiloxanes is principally caused by the electrostatic repulsion of the positively polarised Si atoms and the cation. The insertion of Si_2Me_4 units leads to an increased interatomic distance between the Si atoms and the cation and additionally to a lower polarisation of the Si atoms.

Table 3. Comparison of the required energies for adopting the complex geometry (ΔE_{geom}) and relative complex stabilities ($\Delta E_{complex}$) of [12]crown-4 and the hybrid ligands **1**, **7** and **9** in kJ·mol^{-1}.difference ΔE_{geom}.

Ligand	ΔE_{geom}[a] (kJ·mol^{-1})	$\Delta E_{complex}$[b] (kJ·mol^{-1})
[12]crown-4	+18.0	
1,2-disila[12]crown-4 (**1**)	+33.8	−10.5
1,2,4,5-tetrasila[12]crown-4 (**7**)	+69.3	−29.5
1,2,7,8-tetrasila[12]crown-4 (**9**)	+60.4	+3.3

[a] energy effort for adopting the geometry within the complex. [b] complex stability of the cationic Li-complexes in comparison to [Li([12]crown-4)]$^+$

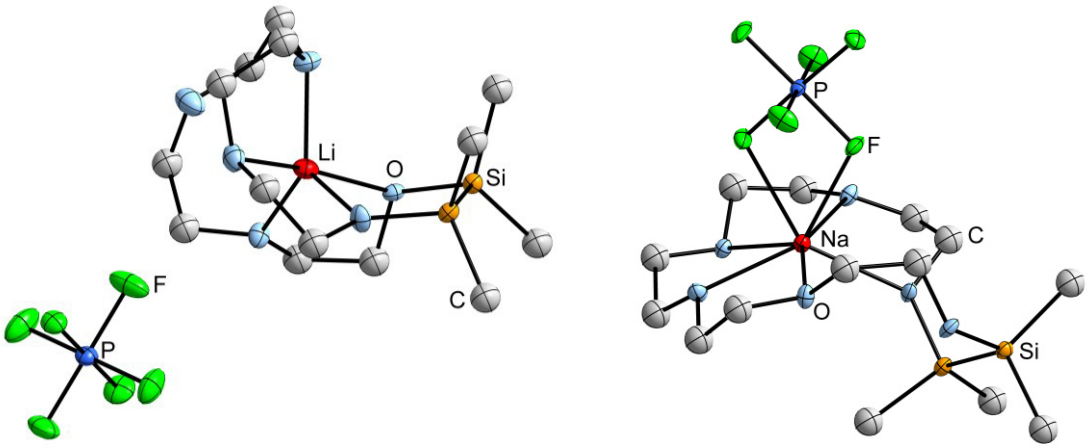

Figure 12. Molecular structures of [Li(1,2-disila[18]crown-6)]PF_6 (**11**) (*left*) and [Na(1,2-disila[18]crown-6)PF_6] (**12**) (*right*) in the crystal. Hydrogen atoms are not displayed, thermal ellipsoids represent the 50% probability level.

The complexation ability of hybrid crown ethers was characterised in more detail by the synthesis of mismatched complexes. For this issue, complexation reactions involving the relatively large ligand 1,2-disila[18]crown-6 (**3**) and the alkali metals salts $LiPF_6$ and $NaPF_6$ were performed. In [Li(1,2-disila[18]crown-6)]PF_6 (**11**), both Si/C bonded O_{crown} atoms participate in the coordination of the cation (Figure 12). It must be noted that the complex shows a discrete ion pair, since the coordination sphere of Li^+ is completely saturated by five of the six O_{crown} atoms. By contrast, the [Na(1,2-disila[18]crown-6)PF_6] (**12**) shows a contact ion pair and only one of the hybrid bonded O_{crown} atoms participates in the coordination. As a result, the Me groups of the Si atoms adopt the preferred staggered arrangement. DFT calculations confirm the lower energy amount for adopting the ligand geometry in the Na-complex **12** (ΔE_{geom} in **11**: 77.6 kJ·mol^{-1}; **12**: 29.2 kJ·mol^{-1}). This indicates that the ecliptic arranged Me groups account for increased values of ΔE_{geom}. The electrostatic attraction between Si/C bonded O_{crown} atoms and the Li^+ cation is apparently sufficient high for compensating ΔE_{geom}. Beside the ligand **3**, also 1,2,4,5-tetrasila[18]crown-6 (**13**), which incorporated two adjacent Si_2Me_4 moieties was matter of investigation. Unexpectedly, complexation of KPF_6 by the ligand **13** yielded a mismatched structure, as was confirmed by X-ray diffraction. In [K(1,2,4,5-tetrasila[18]crown-6)PF_6] (**14**) the fully Si bonded O atom does not participate in the coordination of the cation. The presence of two disilane

units leads to a significantly increased ring size, so presumably Rb^+ matches rather than K^+ with the ligand **13**.

Despite the superior complexation ability of 1,2-disila[12]crown-4 (**1**) and 1,2,4,5-tetrasila[12]crown-4 (**7**) in comparison to [12]crown-4, first attempts have failed to synthesise coordination compounds involving salts of strongly coordinating anions such as the halides: In dichloromethane as solvent, the salts remained non-complexed in conjunction with the hybrid sila-crown ethers. Since the ligands are sensitive towards moisture, water turned out to be an inappropriate solvent. However, complexation of LiCl by the ligand **1** was successful in liquid sulfur dioxide. This was initially observed by the chemical shift in the $^{29}Si\{^1H\}$ NMR spectrum from δ = 14.1 ppm of the free ligand **1** to δ = 17.1 ppm in the complex. Crystals were afforded from the saturated solutions and determined by X-ray diffraction as [Li(1,2-disila[12]crown-4)(SO_2Cl)] (**15**) (Figure 13, *left*). Apparently, the Cl^- anion reacted with the solvent to form the chlorosulfite anion, which coordinates Li^+ by one its O atoms. By contrast, the reaction of LiCl with [12]crown-4 afforded the contact ion pair [Li([12]crown-4)Cl]·$4SO_2$ (**16**) (Figure 13, *right*). Therein, the halide interacts with Li^+ and is furthermore solvated by four SO_2 molecules. Since **1** is reluctant to form sandwich complexes, no coordination compounds were obtained by the use of the heavier homologous chloride salts. However, solvates of RbCl and CsCl occurred in the presence of 1,2-disila[12]crown-4 with

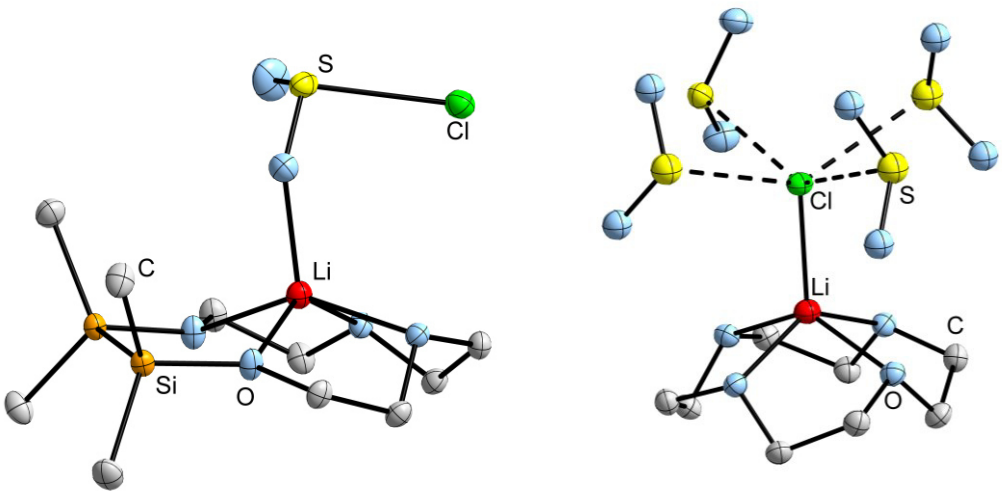

Figure 13. Molecular structures of [Li(1,2-disila[12]crown-4)SO_2Cl] (**15**) (*left*) and [Li([12]crown-4)Cl]·$4SO_2$ (**16**) (*right*) in the crystal. Hydrogen atoms are not displayed, thermal ellipsoids represent the 50% probability level.

the general formula MCl·3SO_2 (**17**: M = Rb; **18**: M = Cs). These represent the first examples of complexes with side on *O,O*' coordinated sulfur dioxide. By contrast, [12]crown-4 willingly forms sandwich complexes in conjunction with NaCl, KCl and RbCl. In the discrete ion pair of [Na([12]crown-4)$_2$]Cl·4SO_2,(**19**), the Na^+ cation has the coordination number eight. In [K([12]crown-4)$_2$(SO_2)]Cl·4SO_2 (**20**) and in [Rb([12]crown-4)$_2$(SO_2)]Cl·4SO_2 (**21**), the cations are additionally to the O_{crown} atoms saturated by side on *O,O'*-coordination of SO_2, giving the coordination number 10. In the case of CsCl, the presence of crystalline material of the known solvate CsCl·3SO_2 (**18**) as well as crystals of the type [12]crown-4·2SO_2 (**22**) indicate that the ionic radius of Cs^+ must be too large for any complex formation. These results underline the different coordination modes of the disila-crown ether **1** and [12]crown-4 (Scheme 21). The reluctance to form sandwich complexes is most notably based on the steric hindrance of the methyl groups, so **1** is highly selective in the coordination of cations.

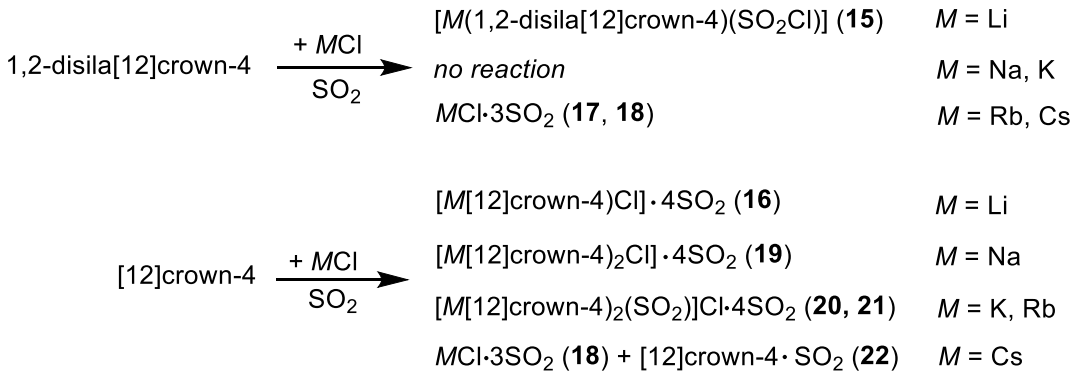

Scheme 21. Overview of the reactions involving **1** and [12]crown-4 with the alkali metal chlorides in liquid SO_2.

The second part of this work dealt with the synthesis of heteroatomic bridged paracyclophanes. The Si_2N bridged [3.3]paracyclophane [1,4-{$SiMe_2N(H)$}$_2C_6H_4$]$_2$ (**23**) was obtained by reaction of 1,4-$(SiMe_2Cl)_2C_6H_4$ with NH_3. Thereby, the small steric hindrance of the Me groups led directly to the condensation of the primary silyl amine under elimination of NH_3. By contrast, the structurally similar Si_2P bridged [3.3]paracyclophane [1,4-{Si*i*$Pr_2P(H)$}$_2C_6H_4$]$_2$ (**24**) was synthesised by twofold deprotonation of 1,4-(Si*i*$Pr_2PH_2)_2C_6H_4$ (**25**) by the use of *n*BuLi and subsequent reaction with 1,4-(Si*i*$Pr_2Cl)C_6H_4$, as was already depicted in the Project Scope (Scheme 13). In **23** and **24**, the aromatic rings are parallel displaced. The inter-aromatic distance is with 331.8 pm and 402.8 pm, respectively, sufficiently large for hosting metal ions, which is still matter of ongoing research. The presented heteroatomic bridged paracyclophanes thusly represent an appropriate basis for investigating their application in the field of the *host-guest* chemistry.

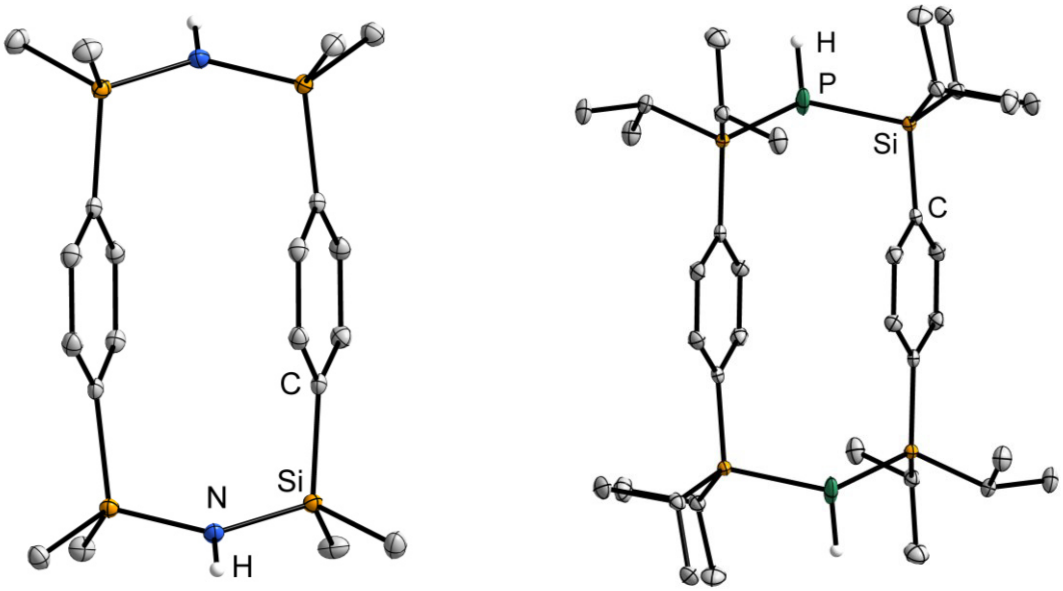

Figure 14. Molecular structures of [1,4-{$SiMe_2N(H)$}$_2C_6H_4$]$_2$ (**23**) (*left*) and [1,4-{Si*i*$Pr_2P(H)$}$_2C_6H_4$]$_2$ (**24**) (*right*). Carbon bonded hydrogen atoms are not displayed, thermal ellipsoids of the non-hydrogen atoms represent the 50% probability level.

Another approach to heteroatomic bridged paracyclophanes consists of the reaction of the primary silylphosphane **25** and the corresponding silylamine 1,4-(Si-*i*Pr$_2$NH)$_2$C$_6$H$_4$ (**26**) with stoichiometric amounts of the *Lewis* acid GaEt$_3$. Elimination of C$_2$H$_6$ leads to the formation of two (GaP)$_2$ and (GaN)$_2$ cycles, respectively, which act as linkers between the aromatic systems (Figure 15). The four membered rings thereby show σ-donor-σ-acceptor bonding interactions. The most eye-catching difference between these compounds represents the arrangement of the aromatic systems: In [1,4-(*i*Pr$_2$SiP(H)GaEt$_2$)$_2$C$_6$H$_4$]$_2$ (**27**), the aryl groups adopt the common parallel displaced conformation, while in the [1,4-(*i*Pr$_2$SiN(H)GaEt$_2$)$_2$C$_6$H$_4$]$_2$ (**28**)**,** they have the rare T-shaped orientation. Furthermore, the substituents of the (GaP)$_2$ and (GaN)$_2$ cycles show a *cis* configuration, which was shown stable in solid state and in solution, owing to the rigid structure of the aryl bridged framework.

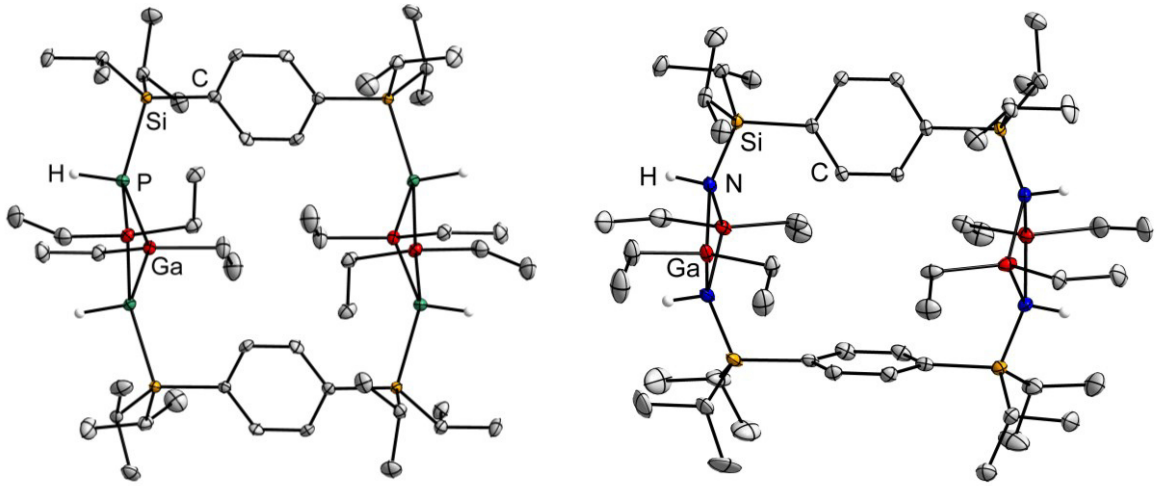

Figure 15. Molecular structures of the [1,4-C$_6$H$_4$(*i*Pr$_2$SiP(H)GaEt$_2$)$_2$]$_2$ (**27**) (*left*) and [1,4-C$_6$H$_4$(*i*Pr$_2$SiN(H)GaEt$_2$)$_2$]$_2$ (**28**) (*right*). Carbon bonded hydrogen atoms are not displayed, thermal ellipsoids of the non-hydrogen atoms represent the 50% probability level.

4 Zusammenfassung

In dieser Arbeit werden Synthesewege zu Si_2Me_4 verbrückten hybriden Kronenethern sowie ihren Komplexen vorgestellt. Die Einführung eines Si_2Me_4 Fragmentes gelang über die Williamsonsche Ethersynthese von 1,2-Dichloro-1,1,2,2-tetramethyldisilan mit dem entsprechenden Glykol unter Zusatz von Triethylamin bei ausreichend hoher Verdünnung. Die hybriden Liganden 1,2-Disila[12]Krone-4 (**1**), 1,2-Disila[15]Krone-5 (**2**) und 1,2-Disila[18]Krone-6 (**3**) wurden auf diese Weise erfolgreich synthetisiert. Komplexverbindungen wurden durch Umsetzungen mit den Alkalimetallsalzen $Li(OSO_2CF_3)$, $NaClO_4$ und KPF_6 in Dichlormethan erhalten (Schema 22) und unter anderem kristallographisch untersucht. In den Komplexen **4** – **6** werden die Kationen von allen Sauerstoffatomen des jeweiligen Kronenethers koordiniert und die Koordinationssphäre weiterhin durch Wechselwirkung mit dem jeweiligen Anion gesättigt. Wie anhand der Kristallstrukturen festgestellt werden konnte, führt die Einführung von Si_2Me_4 Einheiten anstelle von $SiMe_2$ wie erwartet zu einer Vergrößerung des Kation-Silicium Abstandes. So beträgt der Abstand in [Li(1,2-disila[12]Krone-4)(OSO_2CF_3)] (**4**) ø332.0(3) pm und im Vergleich dazu in $[LiD_6]^+$ (D = Me_2SiO) nur ø275.6(20) pm.[43] Anhand der Kristallstrukturen wurde auch festgestellt, dass Si und C gebundene Sauerstoffatome kürzere Bindungen zu den Kationen aufweisen als

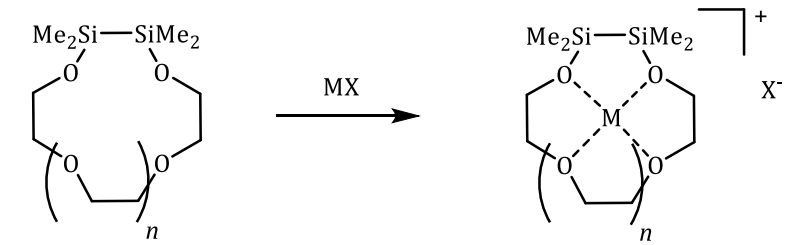

1: n = 1
2: n = 2
3: n = 3

4: n = 1; M = Li; X = OSO_2CF_4
5: n = 2; M = Na; X = ClO_4
6: n = 3; M = K; X = PF_6

Schema 22. Komplexierung von Alkalimetallkationen durch die hybriden Kronenether **1** – **3** führt zur Bildung der korrespondierenden Komplexe [Li(1,2-Disila[12]Krone-4)-(OSO_2CF_3)] (**4**), [Na(1,2-Disila[15]Krone-5)ClO_4] (**5**) und [K(1,2-Disila[18]Krone-6)PF_6] (**6**)

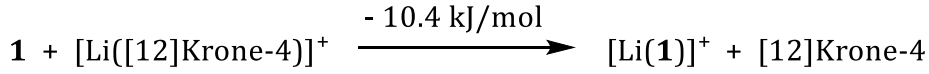

Schema 23. Energieänderung durch den Austausch eines Li-Kations von [12]Krone-4 in 1,2-Disila[12]Krone-4 (**1**).

vollständig C substituierte Sauerstoffatome. Dies könnte auf eine bevorzugte Wechselwirkung mit partiell Si gebundenen Donoratomen hinweisen. Die relative Komplexstabilität von Verbindung **4** wurde anschließend mittels dynamischer ^{1}H-NMR-Spektroskopie untersucht. Dabei konnte gezeigt werden, dass das Gleichgewicht der Reaktion von [12]Krone-4, Verbindung **1** und Li(OSO_2CF_3) unter Einhaltung eines 1:1:1 Verhältnisses auf der Seite des Li-Komplexes von **1** liegt, sodass [12]Krone-4 größtenteils frei vorliegt. Allerdings konnte das Gleichgewicht der Reaktion nicht präziser ermittelt werden, da aufgrund von Sandwichkomplexbildung der prozentuale Anteil an komplexierenden Liganden den des eingesetzten Salzes übersteigt. Mittels DFT Rechnungen (BP86 Funktional und def2-TZVP Basissatz) wurde die bevorzugte Komplexierung von Li^+ durch den Liganden **1** bestätigt. Die Komplexstabilität von $[Li(\mathbf{1})]^+$ ist um 10.4 kJ·mol^{-1} höher als die von $[Li([12]Krone\text{-}4)]^+$ (Schema 23). Dies ist aus dem Grunde erstaunlich, als das der Energieaufwand um von der Molekülstruktur des freien Liganden in die des Liganden im Komplex überzugehen für **1** mit 33.8 kJ·mol^{-1} deutlich höher ist als für [12]Krone-4 mit 18.0 kJ·mol^{-1}. Diese Differenz kann auf die unterschiedlichen Substituenten der beiden Kronenether zurückgeführt werden: **1** weist sterisch anspruchsvollere Methyl-Gruppen an den Si Atomen auf, die im freien Liganden gestaffelt zueinander stehen und im Komplex eine ekliptische Anordnung einnehmen. Hingegen trägt [12]Krone-4 ausschließlich H-Atome an den C_2-Brücken, die im freien Liganden wie im Komplex in einer gestaffelten Konformation vorliegen. Da $[Li(1,2\text{-}disila[12]Krone\text{-}4)]^+$ eine geringfügig höhere Komplexstabilität aufweist, ist davon auszugehen, dass die Si und C gebundenen O Atome eine höhere elektrostatische Wechselwirkung mit dem Kation eingehen als ausschließlich C gebundene O Atome.

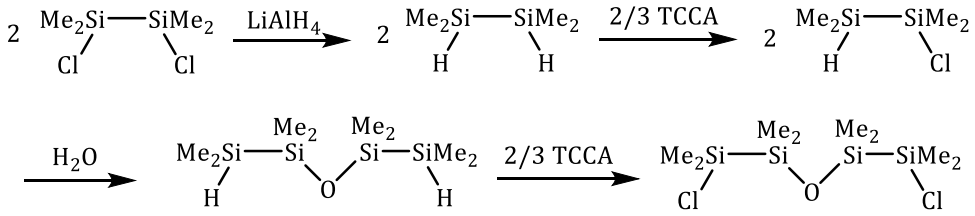

Schema 23. Syntheseweg zur Darstellung des anorganischen Bausteins $O(Si_2Me_4Cl)_2$ für hybride Kronenether mit benachbarten Si_2Me_4 Fragmenten.

Um weitere Informationen über das Koordinationsverhalten von siliciumbasierten Kronenethern zu erhalten, wurde der Si_2Me_4-Anteil sukzessiv erhöht. Hierbei stand die Synthese eines Liganden mit ausschließlich Si gebundenen O Atomen im Fokus. Das dazu notwendige Fragment $O(Si_2Me_4Cl)_2$ wurde im ersten Schritt über eine asymmetrische Chlorierung von 1,1,2,2-Tetramethyldisilan mittels Trichlorisocyanursäure (TCCA) erhalten. Anhand von $^{29}Si\{^1H\}$-NMR-Spektroskopie wurde nachgewiesen, dass diese Reaktion nicht statistisch, sondern selektiv abläuft, da in der Reaktionslösung 70% des asymmetrisch chlorierten Disilans enthalten waren. Nach Hydrolyse und anschließender Chlorierung der terminalen Si Atome, wurde das anorganische Fragment $O(Si_2Me_4Cl)_2$ für die Synthese des hybriden Kronenethers erhalten (Schema 23). Die ursprünglich geplante Darstellung von $O(Si_2Me_4Cl)_2$ ausgehend von 1,2-Diphenyl-1,1,2,2-tetramethyldisilan (siehe *Project Scope*, Schema 13) scheiterte an der Dephe-

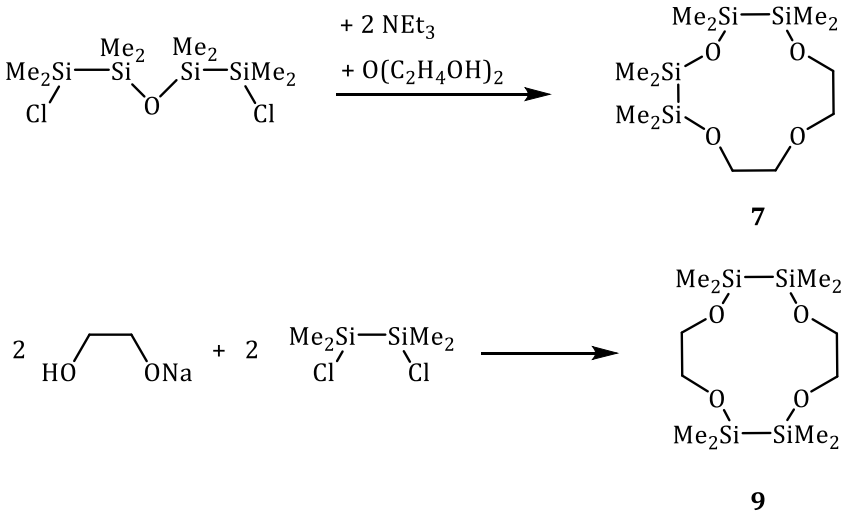

Schema 24. Darstellung von den hybriden Liganden **7** und **9** mit jeweils benachbarten bzw. gegenüberliegenden Si_2Me_4-Einheiten.

nylierung von $O(Si_2Me_4Ph)_2$ mittels Trifluormethansulfonsäure. Diese reagierte bevorzugt mit dem zentralen O Atom, sodass ausschließlich Zersetzungsprodukte nachgewiesen werden konnten.

Die Synthese von 1,2,4,5-Tetrasila[12]Krone-4 (**7**) erfolgte ausgehend von $O(Si_2Me_4Cl)_2$ und $O(C_2H_4OH)_2$ in analoger Weise zu der von **1** – **3** (Schema 24, *oben*). Nach der Komplexierung von $Li(OSO_2CF_3)$ durch **7** in Dichlormethan konnten farblose Kristalle erhalten werden, welche mittels Einkristalldiffraktometrie untersucht wurden. In [Li(1,2,4,5-Tetrasila[12]Krone-4)(OSO_2CF_3)] (**8**) wird das Kation analog zu Komplex **4** von den vier O Atomen des Kronenethers sowie dem Anion koordiniert (Abbildung 16). Die Si_2Me_4 Fragmente führen zu einer Vergrößerung des Ringsystems, sodass das Kation in **8** nur noch 56.8(4) pm oberhalb der koplanaren Sauerstoffatome liegt. Im Vergleich dazu beträgt dieser Wert 83.6(9) pm in [Li([12]crown-4)(OSO_2CF_3)].

Ein alternativer Synthesepfad zur Erhöhung des Sila-Anteils in hybriden Kronenethern stellte die asymmetrische Deprotonierung von Ethylenglykol mittels NaH und anschließende Umsetzung mit 1,2-Dichloro-1,1,2,2-tetramethyldisilan dar (Schema 24, *unten*). Hierbei wurde selektiv 1,2,7,8-Tetrasila[12]Krone-4 (**9**) erhalten. In diesem Liganden sind alle O Atome äquivalent Si und C substituiert, da die Si_2Me_4 Fragmente eine gegenüberliegende Position einnehmen. Nach einer Umsetzung mit $LiPF_6$ wurden Kristalle gezüchtet, die infolge einer Kristallstrukturanalyse als die zu

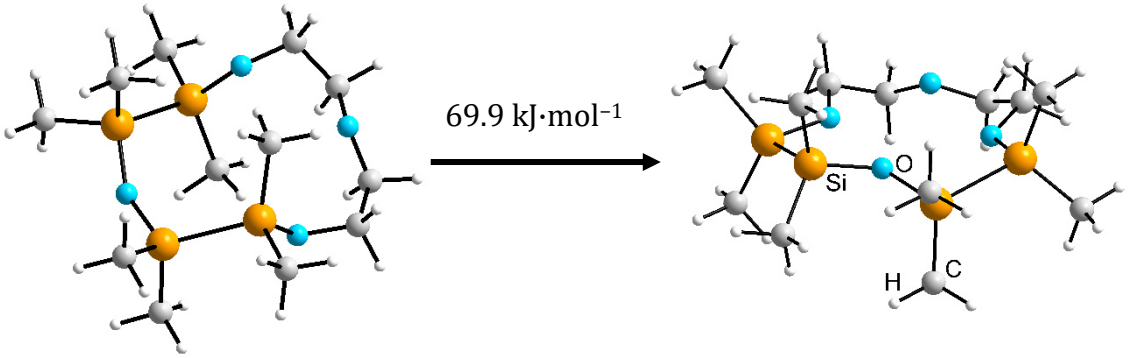

Schema 25. Darstellung der Konformationsänderung vom freien Liganden zum Liganden im Komplex sowie der damit verbundene Energieaufwand.

erwartende Komplexverbindung [Li(1,2,7,8-Tetrasila[12]Krone-4)PF_6] (**10**) identifiziert wurden (Abbildung 16*c*).

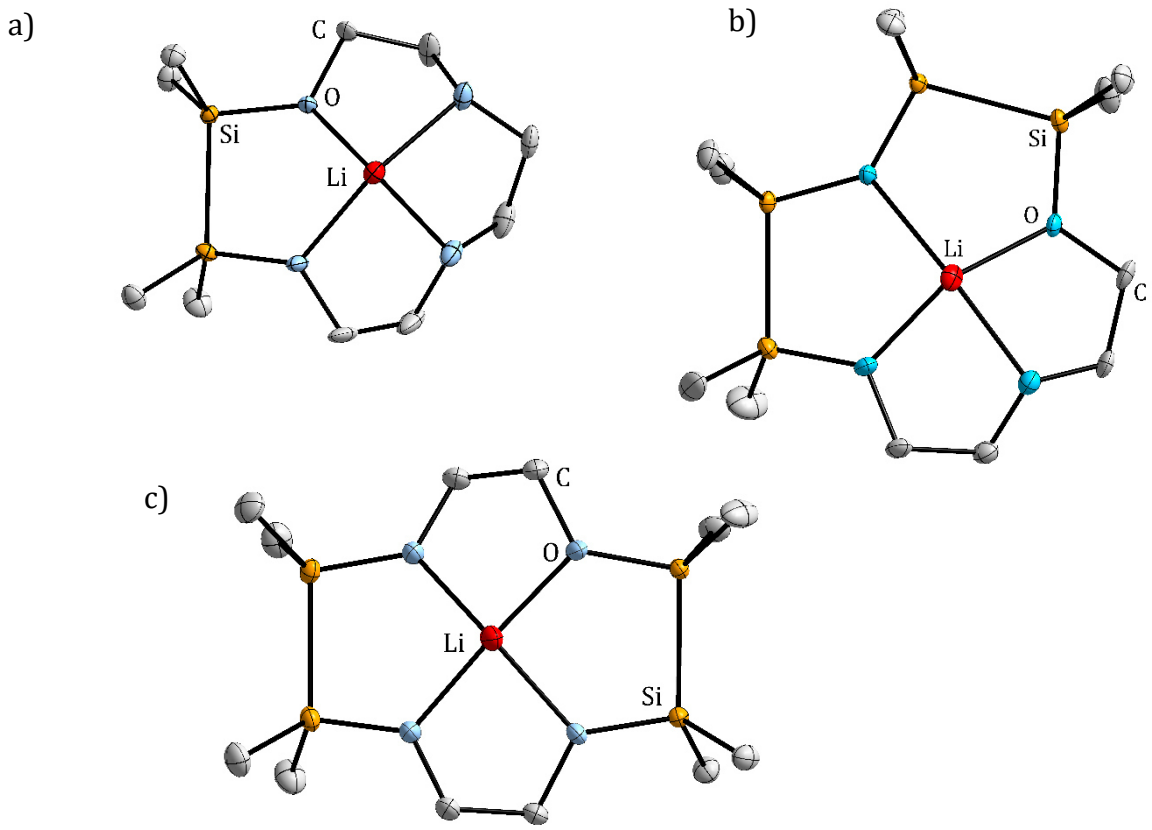

Abbildung 16: Kationische Lithium-Komplexe **4**, **8** und **10**. Die jeweiligen koordinierenden Anionen sowie H Atome wurden aus Gründen der Übersichtlichkeit nicht abgebildet. Die thermischen Ellipsoide entsprechen einer Aufenthaltswahrscheinlichkeit von 50%.

Wie bereits für [Li(1,2-Disila[12]Krone-4)]$^+$ wurde anhand von DFT Rechnungen die relative Stabilität der kationischen Komplexe von **8** und **10** bestimmt. Der Austausch eines Li^+ Kations von [12]Krone-4 zu Ligand **7** ist dabei um −29.5 kJ·mol^{-1} begünstigt, während der von [12]Krone-4 zu Verbindung **9** +3.3 kJ·mol^{-1} benötigt. Durch single-point Rechnungen konnte zudem festgestellt werden, dass **7** und **9** deutlich mehr Energie verbrauchen als Verbindung **1**, um von den Molekülstrukturen der freien Liganden in die Konformation der Komplexe zu gelangen (Schema 26). Der Energieaufwand beträgt 69.9 kJ·mol^{-1} (**7**) und 60.4 kJ·mol^{-1} (**9**) (Tabelle 4). Da der kationische Li-Komplex des Liganden **7** deutlich stabiler ist als der des Liganden **9**, muss die elektrostatische Wechselwirkung zwischen dem vollständig Si gebundenen O Atom in **9** und

Tabelle 4. Vergleich des Energieaufwandes, um von der Struktur des freien Liganden in die des Komplexes überzugehen (ΔE_{geom}) und die relative Komplexstabilität ($\Delta E_{complex}$) der kationischen Li-Komplexe von [12]Krone-4 und den hybriden Liganden **1**, **7** and **9** in kJ·mol^{-1}.

Ligand	ΔE_{geom}[a] (kJ·mol^{-1})	$\Delta E_{complex}$[b] (kJ·mol^{-1})
[12]Krone-4	+18.0	
1,2-Disila[12]Krone-4 (**1**)	+33.8	−10.5
1,2,4,5-Tetrasila[12]Krone-4 (**7**)	+69.3	−29.5
1,2,7,8-Tetrasila[12]Krone-4 (**9**)	+60.4	+3.3

[a] Energieaufwand um die Konformation im Komplex zu erreichen. [b] Komplexstabilität der kationischen Li-Komplexe in Relation zu [Li([12]Krone-4)]$^+$

dem Kation den hohen Energieaufwand der Konformationsänderung deutlich überkompensieren. Daraus resultiert, dass die Basizität der O Atome in der Reihe O_C < $O_{Si/C}$ < O_{Si} steigen muss, sofern die O Atome Si_2Me_4-verbrückt sind.

Um die Komplexierungseigenschaften der unterschiedlich gebundenen Donoratomen in hybriden Kronenethern weiter zu untersuchen wurden Mismatch-Strukturen synthetisiert. Dies gelang durch die Umsetzung von $LiPF_6$ und $NaPF_6$ mit den Liganden 1,2-Disila[18]Krone-4 (**3**). Die Einkristallstrukturanalyse zeigte, dass in [Li(1,2-Disila[18]Krone-6)]PF_6 (**11**) beide Si/C gebundenen O Atome an der Koordination des Kations teilnehmen, während in [Na(1,2-Disila[18]Krone-6)PF_6] (**12**) nur eines an der Koordination beteiligt ist (Abbildung 17). Daraus resultiert die ekliptische Konformation der Methyl-Gruppen in **11**, während sie in **12** gestaffelt vorliegen. Durch DFT Rechnungen wurde bestätigt, dass die Annahme der Ligandkonformation im Komplex **11** mit einer deutlich höheren Energieänderung einhergeht (+77.6 kJ·mol^{-1}) als in **12** (+29.2 kJ·mol^{-1}). Offensichtlich ist die elektrostatische Wechselwirkung zwischen dem harten Li^+ Kation und den hybrid substituierten Donoratomen ausreichend, um den hohen Energieaufwand für die Annahme der ekliptischen Konformation zu kompensieren. Ausgehend von 1,2,4,5-Tetrasila[18]Krone-6 (**13**), welcher zwei benachbarte

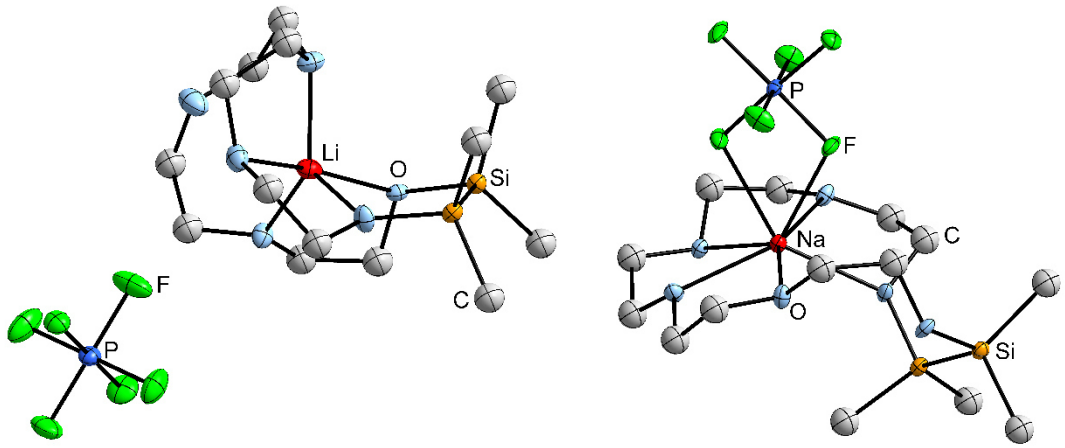

Abbildung 17. Molekülstrukturen von [Li(1,2-disila[18]crown-6)]PF_6 (**11**) (*links*) und [Na(1,2-disila[18]crown-6)PF_6] (**12**) (*rechts*) im Kristall. Wasserstoffatome sind nicht abgebildet. Die thermischen Ellipsoide entsprechen einer Aufenthaltswahrscheinlichkeit von 50%.

Si_2Me_4-Einheiten trägt, wurde überraschenderweise ebenfalls eine Mismatch-Struktur in Verbindung mit KPF_6 erhalten. In [K(1,2,4,5-Tetrasila[18]Krone-6)PF_6] (**14**) koordiniert das vollständig Si gebundene O Atom nicht an das Kation, sodass alle Methyl-Gruppen der Si Atome gestaffelt zueinander stehen. Durch die Anwesenheit von zwei Si_2Me_4-Fragmente scheint der Ligand anders als [18]Krone-6 zu groß zu sein, sodass der Ionenradius von K^+ nicht ausreicht, um mit allen O Atomen wechselwirken zu können.

Obwohl die Komplexierungseigenschaften von 1,2-Disila[12]Krone-4 und 1,2,4,5-Tetrasila[12]Krone-4 höher sind als die von [12]Krone-4, konnten aus Dichlormethan keine Komplexe mit Salzen stark koordinierender Anionen, wie beispielsweise in Alkalimetallchloriden vorhanden, synthetisiert werden. Da die Sila-Kronenether-Komplexe hydrolyseempfindlich waren, wurden Untersuchungen in wässriger Lösung ausgeschlossen. Dagegen war die Komplexierung von LiCl durch 1,2-Disila[12]Krone-4 (**1**) erstmals in flüssigem Schwefeldioxid erfolgreich, wie anhand von $^{29}Si\{^1H\}$-NMR-Experimenten nachgewiesen werden konnte: Die Spektren zeigten eine chemische Verschiebung von δ = 14.1 ppm für den freien Liganden nach δ = 17.1 ppm für den

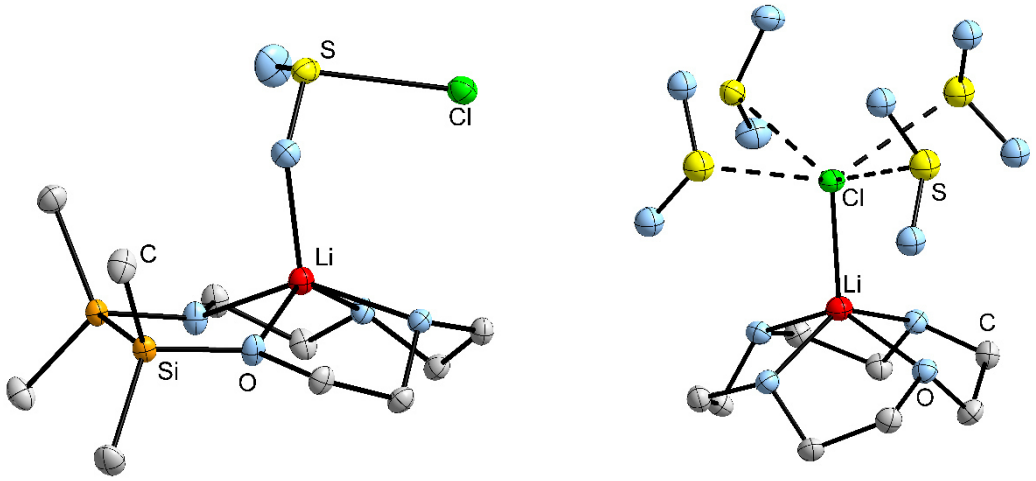

Abbildung 18. Molekülstrukturen von [Li(1,2-disila[12]crown-4)(SO_2Cl)] (**15**) (*links*) and [Li([12]crown-4)Cl]·4SO_2 (**16**) (*rechts*) im Kristall. Wasserstoffatome sind nicht abgebildet. Die thermischen Ellipsoide entsprechen einer Aufenthaltswahrscheinlichkeit von 50%.

Komplex. Die aus der gesättigten Lösung erhaltenen Kristalle konnten kristallographisch untersucht werden und wiesen die Struktur von [Li(1,2-Disila[12]Krone-4)(SO_2Cl)] (**15**) auf (Abbildung 18, *links*). Darin ist das Li^+ Kation von vier O_{Krone} Sauerstoffatomen koordiniert, sowie zusätzlich durch das Gegenion $[SO_2Cl]^-$. Das Chlorosulfit Anion ist aus einer Reaktion zwischen Cl^- und SO_2 hervorgegangen. Diese Reaktion ist bisher ausschließlich für F^--Anionen bekannt: Sie reagieren ohne Energiebarriere zu Fluorosulfit. Um den Einfluss von Si_2Me_4-Einheiten in hybriden Kronenethern beurteilen zu können, wurden die analoge Reaktion auch mit [12]Krone-4 durchgeführt. Gemeinsam mit LiCl und SO_2 konnten Kristalle gezüchtet werden: In [Li([12]Krone-4)Cl]·4SO_2 (**16**) weist das Li^+ Kation Wechselwirkungen mit Cl^- auf, welches selbst von vier SO_2-Molekülen solvatisiert wird. Mit den schwereren Homologen Alkalimetallchloriden NaCl und KCl bildeten sich in SO_2 keine Komplexe mit dem Liganden **1**, was auf seine fehlende Bereitschaft Sandwich-Komplexe auszubilden zurückgeführt werden kann. Überraschenderweise lieferte die gesättigte SO_2-Lösung aus RbCl bzw. CsCl mit **1** Kristalle, die nach einer Einkristallstrukturanalyse als die homoleptischen Solvate *M*Cl·3SO_2 identifiziert wurden (**17**: *M* = Rb; **18**: *M* = Cs). Sie sind trotz der Vielzahl an bekannten SO_2-Solvaten die ersten Beispiele einer *side on O,O'*-Koordination durch SO_2. Dagegen bildet [12]Krone-4 Sandwich-Komplexe mit den Sal-

zen NaCl, KCl und RbCl. In [Na([12]Krone-4)$_2$]Cl·4SO$_2$ (**19**) erhält Na$^+$ die Koordinationszahl acht, während die Kationen in den isotypen Verbindungen [K([12]Krone-4)$_2$(SO$_2$)]Cl·4SO$_2$ (**20**) und [Rb([12]Krone-4)$_2$(SO$_2$)]Cl·4SO$_2$ (**21**) aufgrund der *side on O,O'*-Koordination durch SO$_2$ jeweils die Koordinationszahl zehn aufweisen. Mit CsCl bildet [12]Krone-4 in SO$_2$ aufgrund des zu großen Ionenradius von Cs$^+$ keine Sandwich-Komplexe mehr. Stattdessen wurden ausschließlich Kristalle der bekannten Verbindung [CsCl]·3SO$_2$ (**18**)sowie des freien Kronenethersolvats [12]Krone-4·2SO$_2$ (**22**) identifiziert. Eine Übersicht wird in Schema 26 gewährleistet.

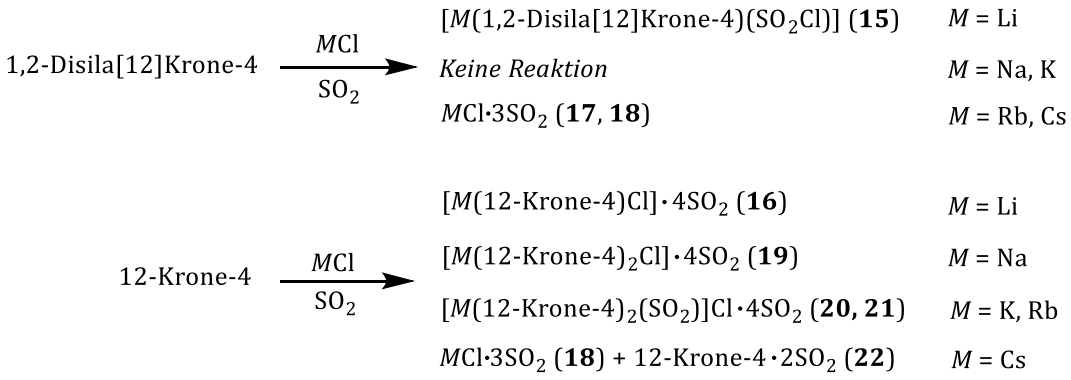

Schema 26. Übersicht der erhaltenen Strukturen aus den Reaktionen von **1** sowie [12]Krone-4 gegenüber den Alkalimetallchloriden LiCl – CsCl in flüssigem SO$_2$.

Der zweite Teil dieser Arbeit beschäftigte sich mit der Synthese heteroatomverbrückter Paracyclophane. Das Si_2N-verbrückte [3.3]Paracyclophan [1,4-C_6H_4{$SiMe_2N(H)$}$_2$]$_2$ (**23**) wurde durch Umsetzung von 1,4-$C_6H_4(SiMe_2Cl)_2$ mit NH_3 erhalten. Das primäre Amin wurde dabei nicht beobachtet, da der sterische Anspruch der Methyl-Gruppen an den Si-Atomen nicht ausreicht, um eine Kondensation zum verbrückenden sekundären Amin zu vermeiden. Dagegen wurde das strukturell ähnliche Si_2P-verbrückte [3.3]Paracyclophan [1,4-C_6H_4{Si*i*$Pr_2P(H)$}$_2$]$_2$ (**24**) mittels zweifacher Deprotonierung von 1,4-$C_6H_4(Si$*i*$Pr_2PH_2)_2$ (**25**) und anschließender Salzmetathese mit 1,4-$C_6H_4(Si$*i*$Pr_2Cl)_2$ synthetisiert. In **23** und **24** liegen die aromatischen Ringe parallel versetzt vor. Der Abstand zwischen ihnen beträgt 331.8 pm (**23**) und 402.8 pm (**24**), sodass ausreichend Platz für die Koordination eines Metalls im Zentrum der Liganden vorhanden ist. Zusätzlich dazu sind die koordinativen Eigenschaften der Brückenatome ein Thema aktueller Forschung.

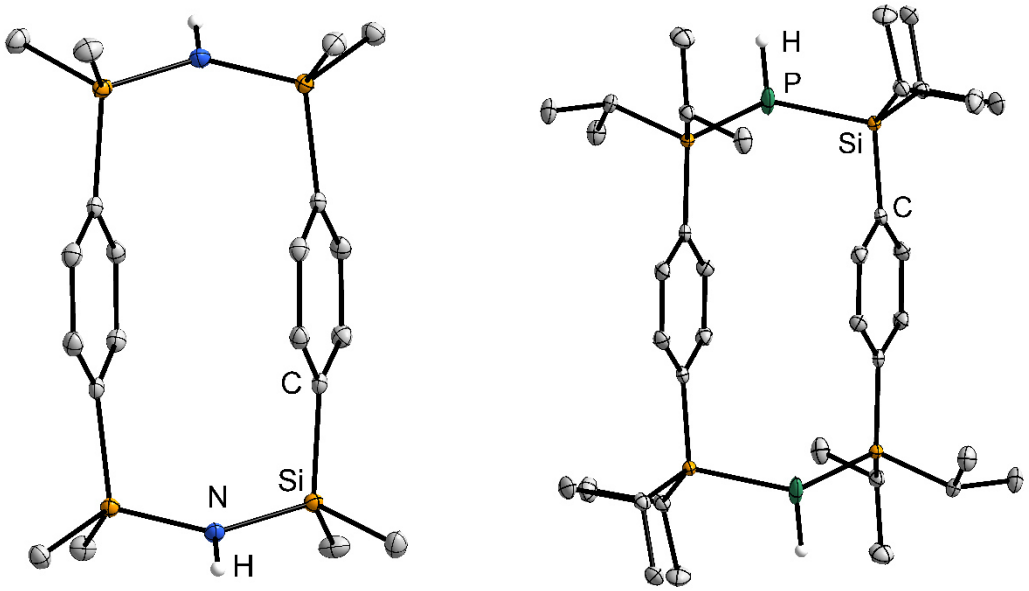

Abbildung 19. Molekülstrukturen von [1,4-C_6H_4{$SiMe_2N(H)$}$_2$]$_2$ (**23**) (*links*) und [1,4-C_6H_4{Si*i*$Pr_2P(H)$}$_2$]$_2$ (**24**) (*rechts*) im Kristall. C gebundene H Atome werden nicht gezeigt. Thermische Ellipsoide (außer H Atome) werden mit einer Aufenthaltswahrscheinlichkeit von 50% abgebildet.

Als zweite erfolgreiche Syntheseroute zu heteroatomverbrückten Paracyclophanen hat sich die Umsetzung des primären Silylphosphans **25** bzw. des primären Silylamins 1,4-$C_6H_4(SiiPr_2NH_2)_2$ (**26**) mit der *Lewis*-Säure $GaEt_3$ herausgestellt. Die Eliminierung von C_2H_6 führt zur Bildung von zwei $(GaP)_2$- sowie $(GaN)_2$-Cyclen, welche die aromatischen Ringe miteinander verknüpfen. Die viergliedrigen Cyclen weisen dabei σ-Donor-σ-Akkzeptor-Bindungen auf. Der auffälligste Unterschied zwischen den beiden Verbindungen stellt die Anordnung der Aromaten dar: Während sie in [1,4-$C_6H_4(iPr_2SiP(H)GaEt_2)_2]_2$ (**27**) parallel versetzt vorliegen, weisen sie in [1,4-$C_6H_4(iPr_2SiN(H)GaEt_2)_2]_2$ (**28**) eine T-Shape Orientierung auf (Abbildung 20). Diese wurde bisher noch nicht in Paracyclophanen beobachtet, obwohl der energetische Unterschied zwischen der T-Shape- und der parallel versetzten Konformation sehr gering ausfällt. Weiterhin weisen beide Verbindungen eine *cis*-Anordnung der Substituenten an den viergliedrigen Cyclen auf, die im Festkörper wie in Lösung aufgrund der starren Struktur des Moleküls stabil bleibt. Üblicherweise isomerisieren $(GaP)_2$ sowie $(GaN)_2$ Cyclen in Lösung, sodass Verbindungen **27** und **28** die ersten Verbindungen sind, die von diesem Trend abweichen.

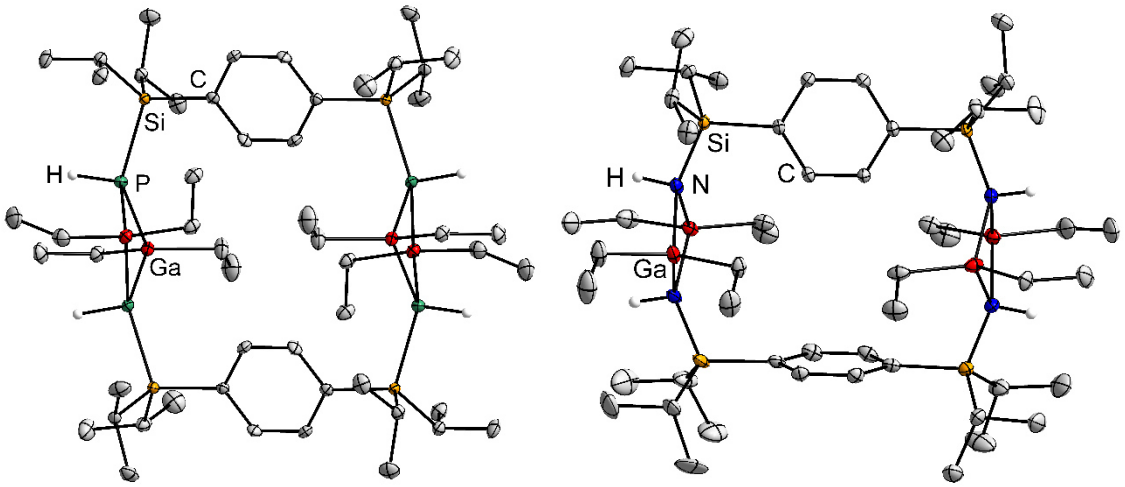

Abbildung 20. Molekülstrukturen von [1,4-$C_6H_4(iPr_2SiP(H)GaEt_2)_2]_2$ (**27**) (*links*) und [1,4-$C_6H_4(iPr_2SiN(H)GaEt_2)_2]_2$ (**28**) (*rechts*). C gebundene H Atome werden nicht gezeigt. Thermische Ellipsoide (außer H Atome) werden mit einer Aufenthaltswahrscheinlichkeit von 50% abgebildet.

5 Cumulative Part

Inorganic Chemistry **2016**, *55*, 4441–4447

Stable Alkali-Metal Complexes of Hybrid Disila-Crown Ethers

Kirsten Reuter, Magnus R. Buchner, Günther Thiele, Carsten von Hänisch

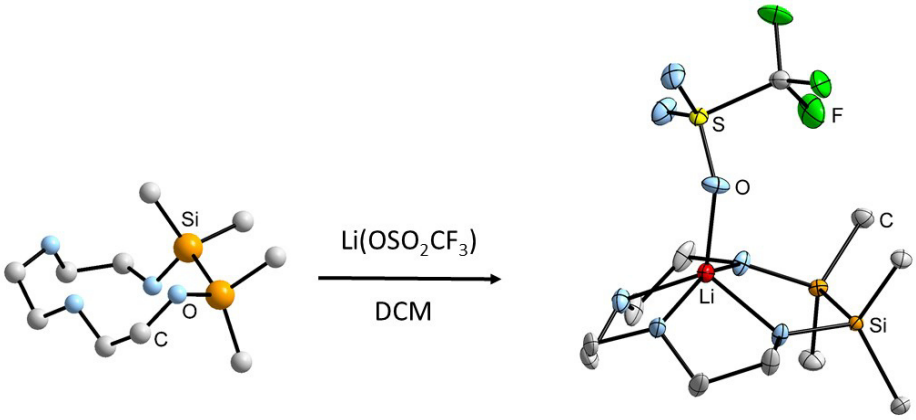

This report describes the synthesis paths of four hybrid sila-crown ethers. 1,2-Disila[12]crown-4, 1,2-disila[15]crown-5 and 1,2-disila[18]crown-6 were obtained by Williamson ether synthesis of 1,2-dichloro-1,1,2,2-tetramethyldisilane and the corresponding glycols. Furthermore, the amount of Si_2Me_4 was raised in 1,2,7,8-tetrasila[12]crown-4, which incorporates two opposite disilane units. The latter compound was obtained by asymmetric deprotonation of ethylene glycol by the use of NaH, followed by equimolar reaction with 1,2-dichloro-1,1,2,2-tetramethyldisilane. Complexation reactions with appropriate alkali metal salts in dichloromethane afforded the corresponding complexes, which were identified among others by single crystal X-ray diffraction. Thereby it was shown that the Si and C bonded O atoms establish consistently shorter bond lengths to the cations compared to the fully C bonded O atoms. The complexation ability of 1,2-disila[12]crown-4 and 1,2,7,8-tetrasila[12]crown-4 ethers

was shown to be similar to that of [12]crown-4 as was determined by dynamic ^{1}H NMR spectroscopy and DFT calculations. A more in-depth analysis of the bonding interaction within the cationic Li-complexes reveals a significant raise of relaxation energy with increasing amount of Si_2Me_4. The relaxation energy reflects the required energy of the respective free ligand to adopt the geometry found within the complex. Si_2Me_4 incorporating ligands require more energy than [12]crown-4, due to the sterically unfavourable ecliptic arrangement of the Me-groups. Since [12]crown-4, 1,2-disila[12]crown-4 and 1,2,7,8-tetrasila[12]crown-4 exhibit similar overall complex stabilities in conjunction with Li^+, independent of whether Si_2Me_4 is present or not, the electrostatic attraction between the O atoms and Li^+ in the sila-crown ethers must compensate for the increased relaxation energy.

Description of the Personal Contributions

Kirsten Reuter performed the syntheses, characterisations and interpretations and contributed to DFT calculations of the presented sila-crown ethers including their complexes. Dr. Günther Thiele crucially supported the DFT calculations and contributed to their interpretation and discussion. Kirsten Reuter wrote the manuscript except for the discussion of dynamic ^{1}H NMR experiments, which was done by Dr. Magnus R. Buchner. Prof. Dr. Carsten von Hänisch developed the research project, contributed to interpretations and gave valuable support.

Chemical Communications **2016**, *52*, 13265–13268

Synthesis and coordination ability of a partially silicon based crown ether

Kirsten Reuter, Günther Thiele, Thomas Hafner, Frank Uhlig, Carsten von Hänisch

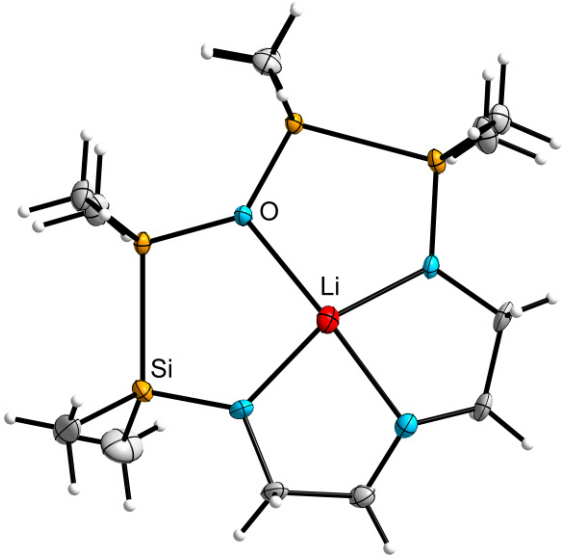

Hybrid crown ethers with two adjacent Si_2Me_4 linkers permit the comparison of C, C and Si as well as fully Si bonded O atoms. 1,2,4,5-Tetrasila[12]crown-4 was obtained by Williamson ether synthesis of $O(Si_2Me_4Cl)_2$ and diethylene glycol. The inorganic building block was accessed by a multistep synthesis involving the asymmetric chlorination of $H_2Si_2Me_4$ followed by hydrolysis and chlorination of the terminal Si-H functional groups. Equimolar reaction of the hybrid ligand with $LiOSO_2CF_3$ in dichloromethane yielded the corresponding complex. Single crystal X-ray diffraction confirm the presence of a contact ion pair. All four O_{crown} atoms participate in the coordination of Li^+. The fully Si bonded O atom thereby establishes the longest bond length to the cation. DFT calculation of the cationic complex do not confirm these observations, so possibly interactions of trifluoromethane sulfonate with the H atoms of the $SiMe_2$ groups manipulate the position of Li^+ in the crystal structure. The theoretical studies furthermore revealed a considerably increased complexation ability of 1,2,4,5-tetrasila[12]crown-4 towards Li^+ in comparison to [12]crown-4. Despite the steric hindrance of the $SiMe_2$ groups and the resulting higher energy effort for adopting the complex geometry of the ligand, the transfer of Li^+ from [12]crown-4 to the hybrid ligand

releases 29.5 kJ·mol^{-1}. The tetrasila-crown ether thusly shows the highest efficiency in comparison to the prior investigated hybrid ligands. This indicates a significantly and hitherto unprecedented increased basicity of fully Si bonded O atoms. These results amplify recent suggestions that electrostatic repulsion easily compensate for the attraction between donor atom and *Lewis* acid in cyclosiloxanes.

Description of the Personal Contributions

Kirsten Reuter performed the syntheses, characterisations and interpretations, contributed to DFT calculations of the presented sila-crown ethers including their complexes and wrote the manuscript. Thomas Hafner and Prof. Dr. Frank Uhlig gave valuable support for the synthesis of 1-chloro-2-hydrido-1,1,2,2-tetramethyldisilane, which is the indispensable precursor for the synthesis of 1,2,4,5-tetrasila[12]crown-4. Dr. Günther Thiele confirmed the theoretical geometry optimisation and performed single point calculations. Prof. Dr. Carsten von Hänisch afforded the collaboration with the research group of Prof. Dr. Frank Uhlig from TU Graz, crucially contributed to interpretations and led the overarching research project.

Inorganics **2017**, *5*, 11, DOI: 10.3390/inorganics5010011

Structural Study of Mismatched Disila-Crown Ether Complexes

Kirsten Reuter, Fabian Dankert, Carsten Donsbach, Carsten von Hänisch

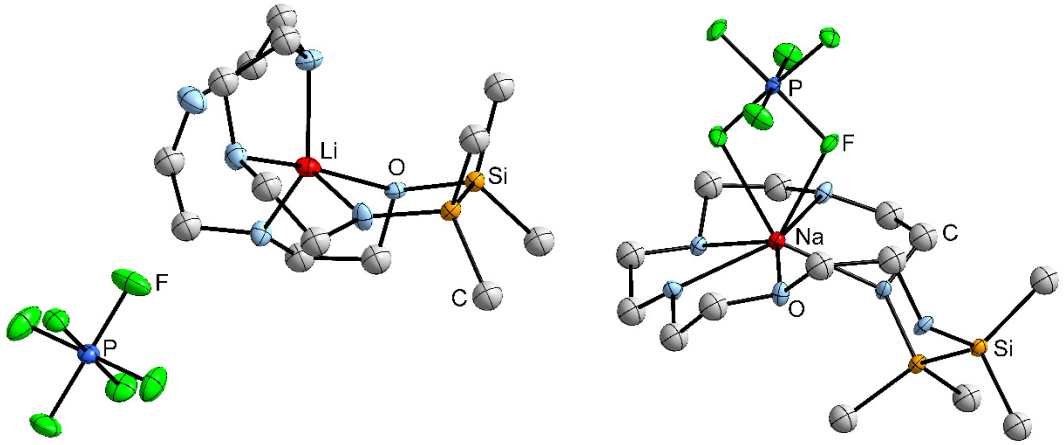

The present report considers the coordination of relatively small alkali metal cations by large hybrid ligands with the target to cause mismatch complexes. As was shown by recent experimental and theoretical studies, the coordination ability of crown ethers depends on whether silicon or carbon binds to the O atoms. Due to the mismatch, the O atoms are thusly competing for the interaction with the cation, which gives further information about the relative coordination ability of the differently substituted O atoms. This was achieved by the complexation of Li^+ and Na^+ by 1,2-disila[18]crown-6. The crystal structures show that Li^+ rather interacts with the Si/C bonded O atoms, while Na^+ prefers the interaction with the C substituted ones. DFT calculations reveal a significantly lower energy 'penalty' for the ligand to adopt the complexation mode within the Na^+ species, owing to the staggered arrangement of the adjacent $SiMe_2$ groups. This gives rise to the conclusion that Li^+ establishes stronger electrostatic interactions with the hybrid bonded O atoms, which compensate for the energy effort of the ligand to adopt the observed complex geometry.

The incorporation of $(OSi_2Me_4)_n$ into a residuary $(OC_2H_4)_n$ based crown ether leads to a significant ring size modification. K^+ ions, that commonly fit well into the cavity of [18]crown-6, give mismatch structures in conjunction with 1,2,4,5-tetrasila[18]crown-6. Hereby, the fully Si substituted O atom does not participate in the coordination, presumably because the electrostatic interaction between the cation and Si bonded O atoms does not compensate for adopting the common complex geometry. Furthermore, the inverse case, the coordination of the large Ba^{2+} ion by the relatively small ligand 1,2-disila[15]crown-5, was investigated. The resulting dinuclear complex gives a first outlook on sandwich complexes based on hybrid crown ethers.

Description of the Personal Contributions

Kirsten Reuter performed the syntheses, characterisations and interpretations of [Li(1,2-disila[18]crown-6)]PF_6, [Na(1,2-disila[18]crown-6)PF_6] as well as 1,2,4,5-tetrasila[18]crown-6 and its complex. She performed the DFT calculations and wrote the manuscript. Fabian Dankert synthesised [Ba(1,2-disila[15]crown-5)$(OSO_2CF_3)_2]_2$ and contributed to its characterisation, Carsten Donsbach performed the single crystal X-ray diffraction and refinement of [Ba(1,2-disila[15]crown-5)$(OSO_2CF_3)_2]_2$. Prof. Dr. Carsten von Hänisch contributed to interpretations and led the overarching research project.

Dalton Transactions **2017**, DOI: 10.1039/C6DT04018G

A structural study of alkaline earth metal complexes with hybrid disila-crown ethers

Fabian Dankert, Kirsten Reuter, Carsten Donsbach, Carsten von Hänisch

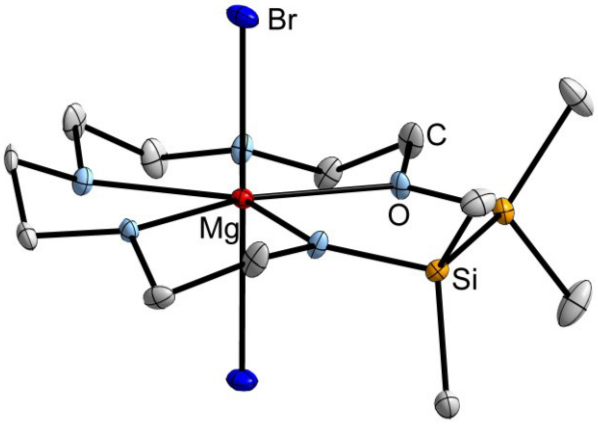

This report deals with the coordination ability of several disila-crown ethers towards salts of alkaline earth metals. The twofold charged cations are respectively located in one plane with the O_{crown} atoms, the coordination sphere being saturated by interaction with two anions. These are situated above and beneath the mean plane of the ligand. Furthermore, the first hybrid ligand with an aryl group as linker between the O atoms, 1,2-disila-benzo[18]crown-6 was synthesised. Additionally to the salts of weakly coordinating anions such as $(OSO_2CF_3)^-$ or PF_6^-, also the anions Br^- and I^- found application. Single crystal X-ray diffraction confirmed the successful incorporation of $MgBr_2$ and SrI_2 within the disila-crown ethers. These findings denote that the ligands are appropriate for the complexation of salts bearing a high lattice energy. DFT calculations reveal a significant release of energy for the transfer of Mg^{2+} from [15]crown-5 to 1,2-disila[15]crown-5 ($\Delta E = -217.4$ kJ·mol^{-1}). This result exceeds the hitherto quantified coordination ability of disila-crown ethers by far. It must be noted that beside the higher basicity of Si/C substituted O atoms, the increased ring diameter of the disila-crown ether in comparison to [15]crown-5 has to be taken into account.

Description of the Personal Contributions

Fabian Dankert conducted the syntheses, characterisation and interpretation of the presented compounds and wrote the manuscript. Kirsten Reuter initially supervised the project, performed the DFT calculations and contributed to interpretations. Carsten Donsbach performed the single crystal X-ray diffraction and refinement of the complexes. Prof. Dr. Carsten von Hänisch crucially contributed to interpretations and led the overarching research project.

Manuscript in Preparation

Crown ethers complexes of alkali metal chlorides from SO_2

Kirsten Reuter, Stefan S. Rudel, Magnus R. Buchner, Florian Kraus, Carsten von Hänisch

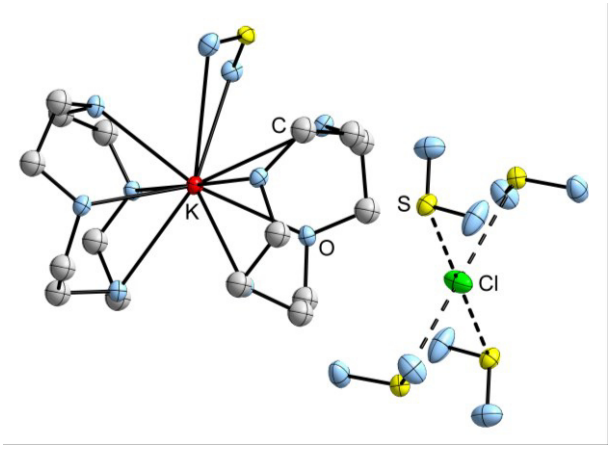

The number of complexes obtained by reaction of [12]crown-4 and 1,2-disila[12]crown-4 with the alkali metal chlorides (Li – Cs) in SO_2 displays the diversity of complexation modes of the ligands and the solvent. 1,2-Disila[12]crown-4 is reluctant to build sandwich complexes, so exclusively LiCl was successfully incorporated. This structure provides the first crystallographically described $[SO_2Cl]^-$ anion that was obtained from SO_2. Together with the alkali metal chlorides Na^+ - K^+, 1,2-disila[12]crown-4 does not form complexes. By contrast, [12]crown-4 willingly coordinates to Li^+, Na^+, K^+ and Rb^+ , except for CsCl. With LiCl, a 1:1 complex was observed, while in conjunction with the the heavier homologous salts NaCl, KCl and RbCl, sandwich complexes were determined by X-ray diffraction. Cl^- is respectively *S* coordinated by four SO_2 molecules, and in the case of $[M([12]crown\text{-}4)_2(SO_2)]Cl{\cdot}4SO_2$ (*M* = K, Rb), the first evidence for side on *O,O'* coordinated SO_2 was found. The reaction of [12]crown-4 and CsCl afforded crystals of $CsCl{\cdot}3SO_2$ as well as of [12]crown-4·$2SO_2$, indicating that the ionic radius of Cs^+ is too large for the coordination by this crown ether.

Compared to the lighter alkali metal chlorides, RbCl and CsCl show a slightly increased solubility in sulfur dioxide. Unexpectedly, the presence of 1,2-disila[12]crown-4 leads to a considerable increase of their solubility, although by NMR spectroscopy only minor interactions between the ligand and the respective salt were detected. Cooling of the saturated solutions afforded crystals, which were identified by single crystal X-ray diffraction as the homoleptic SO_2 solvates MCl·3SO_2 (M = Rb, Cs). These compounds reflect the versatile coordination modes of SO_2, since *O,O*-, bridging μ-*O* and *S*-interactions were found.

Description of the Personal Contributions

This project was collaboratively planned and conducted by Kirsten Reuter and Stefan S. Rudel: Kirsten Reuter performed the syntheses as well as the NMR and IR spectroscopic characterisation of the presented compounds contributed to interpretations. The manuscript was written by Kirsten Reuter and Stefan S. Rudel. Stefan S. Rudel conducted the crystal structure determination and refinement, solubility experiments by using flame sealed fused silica. Dr. Magnus R. Buchner provided support for the preparation of NMR samples containing SO_2 and was involved in NMR measurements. Prof. Dr. Florian Kraus provided the equipment and technical skills for X-ray measurements of single crystals grown in liquid SO_2 as well as valuable advice for the crystal structure determination of the solvates. Prof. Dr. Carsten von Hänisch provided the equipment and techniques for crystal growth from liquid SO_2, developed and led the research project on hybrid crown ethers.

Dalton Transactions **2017**, *accepted*.

Synthesis of Heteroatomic Bridged Paracyclophanes

Kirsten Reuter, R. G. Marlin Maas, Anna Reuter, Frank Kilgenstein, Yodita Asfaha, Carsten von Hänisch

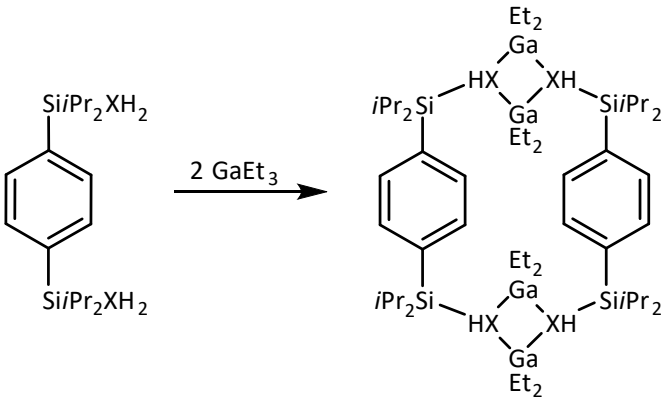

X = N, P

This report describes the access to heteroatomic bridged paracyclophanes starting from 1,4-(R_2SiCl)C_6H_4 (R = *i*Pr, Me). The reaction with NH_3 yields either the -SiNSi- bridged paracyclophane or the primary silylamine, depending on the steric hindrance of the rests R at the Si atoms. The analogous functionalisation with PH_2 groups was accomplished by the use of [$LiAl(PH_2)_4$] in the case of 1,4-$C_6H_4(Me_2SiCl)_2$ and [$LiPH_2$(dme)] in the case of 1,4-C_6H_4(*i*$Pr_2SiCl)_2$ and respectively yielded the primary silylphosphanes. Twofold lithiation of 1,4-C_6H_4(*i*$Pr_2SiPH_2)_2$ followed by salt metathesis with the corresponding chlorinated derivative gave access to the -SiPSi- bridged [3.3]paracyclophane. These compounds possess two coordination sites as they incorporate beside the π-aromatic systems the group 15 elements N and P. Their reactivity towards *Lewis* acids is an ongoing research issue. The second approach towards heteroatomic bridged paracyclophanes was found by the reaction of the primary silylamine and -phosphane with $GaEt_3$. After elimination of ethane, the two aryl bridges are

connected by two four membered $(GaN)_2$ or $(GaP)_2$ cycles. Both compounds show *cis* conformation in solid state and in solution owing to the rigid structure of the aryl bridged framework. Worth mentioning are the T-shape arranged aryl groups in the $(GaN)_2$ bridged paracyclophane, especially since coplanar conformations are the most common conformation mode of this compound class.

Description of the Personal Contributions

This publication represents in parts the Bachelor theses of R. G. Marlin Maas and Anna Reuter, which were accomplished under the supervision of Kirsten Reuter. Hereby, Anna Reuter conducted the synthesis and characterisation of 1,4-$C_6H_4(Me_2SiPH_2)_2$ and R. G. Marlin Maas that of the chlorosilane 1,4-$C_6H_4(i Pr_2SiCl)_2$ and the paracyclophane $[1,4\text{-}C_6H_4(i Pr_2SiPH)_2]_2$. As part of practical courses, Frank Kilgenstein synthesised the $(GaP)_2$ bridged paracyclophane and conducted the NMR spectroscopic analysis; Yodita Asfaha contributed to the synthesis and characterisation of the silanol 1,4-$C_6H_4(i Pr_2SiOH)_2$. Kirsten Reuter developed the initial concept to design aryl-bridged silylamines and -phosphanes, performed characterisation and syntheses and wrote the manuscript. Prof. Dr. Carsten von Hänisch contributed to interpretations, gave valuable support and led the research project.

6 Bibliography

[1] F. R. Boyd, *Science* **1964**, *145*, 13–20.

[2] S. L. Bass, J. F. Hyde, R. R. McGregor, *J. Am. Ceram. Soc.* **1946**, *29*, 66–70.

[3] I. Manners, *Angew. Chem. Int. Ed.* **1996**, *35*, 1602–1621.

[4] A. E. Martell, R. D. Hancock, R. J. Motekaitis, *Coord. Chem. Rev.* **1994**, *133*, 39-65.

[5] R. J. Gillespie, E. a Robinson, *Chem. Soc. Rev.* **2005**, *34*, 396-407.

[6] A. J. Blake, E. A. V. Ebsworth, S. G. D. Henderson, M. Dyrbusch, *Acta Crystallogr. Sect. C Cryst. Struct. Commun.* **1988**, *44*, 1–3.

[7] U. Blukis, P. H. Kasai, R. J. Myers, *J. Chem. Phys.* **1963**, *38*, 2753.

[8] A. Almenningen, O. Bastiansen, V. Ewing, K. Hedberg, M. Trætteberg, *Acta Chem. Scand.* **1963**, *17*, 2455–2460.

[9] B. Sternbach, A. G. MacDiarmid, *J. Am. Chem. Soc.* **1961**, *83*, 3384–3388.

[10] L. O. Brockway, F. T. Wall, *J. Am. Chem. Soc.* **1934**, *56*, 2373–2379.

[11] R. West, L. S. Whatley, K. J. Lake, *J. Am. Chem. Soc.* **1961**, *83*, 761–764.

[12] H. J. Emeléus, M. Onyszchuk, *J. Chem. Soc.* **1958**, 604–609.

[13] C. G. Pitt, *J. Organomet. Chem.* **1973**, *61*, 49–70.

[14] S. Shambayati, S. L. Schreiber, J. F. Blake, S. G. Wierschke, W. L. Jorgensen, *J. Am. Chem. Soc.* **1990**, *112*, 697–703.

[15] F. Weinhold, R. West, *Organometallics* **2011**, *30*, 5815–5824.

[16] F. Weinhold, R. West, *J. Am. Chem. Soc.* **2013**, *135*, 5762–5767.

[17] H. Bock, P. Mollère, G. Becker, G. Fritz, *J. Organomet. Chem.* **1973**, *61*, 113–125.

[18] H. Oberhammer, J. E. Boggs, *J. Am. Chem. Soc.* **1980**, *102*, 7241–7244.

[19] A. L. Allred, E. G. Rochow, *J. lnorg. Nucl. Chem* **1958**, *5*, 264–268.

[20] R. J. Gillespie, S. A. Johnson, *Inorg. Chem.* **1997**, *36*, 3031–3039.

[21] J. Passmore, J. M. Rautiainen, *Eur. J. Inorg. Chem.* **2012**, 6002–6010.

[22] S. Grabowsky, M. F. Hesse, C. Paulmann, P. Luger, J. Beckmann, *Inorg. Chem.* **2009**, *48*, 4384–4393.

[23] S. Grabowsky, J. Beckmann, P. Luger, *Aust. J. Chem.* **2012**, *65*, 785–795.

[24] C. Eaborn, P. B. Hitchcock, P. D. Lickiss, *J. Organomet. Chem.* **1984**, *264*, 119–126.

[25] a. Spielberger, P. Gspaltl, H. Siegl, E. Hengge, K. Gruber, *J. Organomet. Chem.* **1995**, *499*, 241–246.

[26] N. N. Yuzhelevskii, Y. A.; Pchelintsev, V. V.; Fedoseeva, *Vysokomol. Soedin. Seriya Bysokomolekulyarnye Soedin. Seriya B* **1976**, *18*, 873–874.

[27] M. A. Hossain, M. B. Hursthouse, M. A. Mazid, A. C. Sullivan, *J. Chem. Soc. Chem. Commun.* **1988**, *873*, 1305.

[28] V. A. Zeitler, C. A. Brown, *J. Am. Chem. Soc.* **1957**, *79*, 4618–4621.

[29] G. Gerritsen, R. Duchateau, G. P. A. Yap, *Organometallics* **2003**, *22*, 100–110.

[30] V. Lorenz, A. Fischer, S. Giessmann, J. W. Gilje, Y. Gun'ko, K. Jacob, F. T. Edelmann, *Coord. Chem. Rev.* **2000**, 321-368.

[31] F. J. Feher, T. A. Budzichowski, *Polyhedron* **1995**, *14*, 3239–3253.

[32] R. U. Lemieux, T. L. Nagabhushan, I. K. O'Neill, *Tetrahedron Lett.* **1964**, *5*, 1909–1916.

[33] M. A. Hossain, M. B. Hursthouse, A. Ibrahim, M. Mazid, A. C. Sullivan, *J. Chem. Soc., Dalton Trans.* **1989**, 2347–2352.

[34] A. Fridrichová, B. Mairychová, Z. Padělková, A. Lyčka, K. Jurkschat, R. Jambor, L. Dostál, *Dalton Trans.* **2013**, 16403–16411.

[35] S. Harder, B. Freitag, P. Stegner, J. Pahl, D. Naglav, *Z. Anorg. Allg. Chem.* **2015**, *641*, 2129–2134.

[36] A. Steiner, G. T. Lawson, B. Walfort, D. Leusser, D. Stalke, *J. Chem. Soc. Dalton Trans.* **2001**, *6*, 219–221.

[37] M. R. Churchill, C. H. Lake, S. L. Chao, T. Beachley, *J. Chem. Soc. Chem. Commun.* **1993**, 1577–1578.

[38] C. Eaborn, P. B. Hitchcock, K. Izod, J. D. Smith, *Angew. Chem., Int. Ed. Engl.* **1996**, *34*, 2679–2680.

[39] I. Haiduc, *Organometallics* **2004**, *23*, 3–8.

[40] E. Iravani, A. Dashti-Mommertz, B. Neumüller, *Z. Anorg. Allg. Chem.* **2003**, *629*, 1136–1146.

[41] I. Krossing, I. Raabe, *Angew. Chem.* **2004**, *116*, 2116–2142.

[42] I. Krossing, I. Raabe, *Angew. Chem., Int. Ed. Engl.* **2004**, *43*, 2066–2090.

[43] A. Decken, J. Passmore, X. Wang, *Angew. Chem., Int. Ed. Engl.* **2006**, *45*, 2773–2777.

[44] T. S. Cameron, A. Decken, I. Krossing, J. Passmore, J. M. Rautiainen, X. Wang, X. Zeng, *Inorg. Chem.* **2013**, *52*, 3113–3126.

[45] C. J. Pedersen, *J. Am. Chem. Soc.* **1970**, *92*, 386–391.

[46] P. P. Power, X. Xiaojie, *J. Chem. Soc. Chem. Commun.* **1984**, 358–359.

[47] D. Gingl, Hiller, Strähle, Borgholte, *Z. Anorg. Allg. Chem.* **1991**, *606*, 91–96.

[48] M. L. Cole, C. Jones, P. C. Junk, *J. Chem. Soc. Dalton Trans.* **2002**, 896–905.

[49] R. D. Ernst, A. Glöckner, A. M. Arif, *Z. Kristallogr. - New Cryst. Struct.* **2007**, *222*, 333–334.

[50] J. S. Ritch, T. Chivers, *Angew. Chem., Int. Ed.* **2007**, *46*, 4610–4613.

[51] C. von Hänisch, F. Weigend, O. Hampe, S. Stahl, *Chem. Eur. J.* **2009**, *15*, 9642–9646.

[52] C. Bimbös, M. Jost, C. Von Hänisch, K. Harms, *Eur. J. Inorg. Chem.* **2013**, *3*, 4645–4653.

[53] C. Von Hänisch, O. Hampe, F. Weigend, S. Stahl, *Angew. Chem. Int. Ed.* **2007**, *46*, 4775–4779.

[54] M. Ouchi, Y. Inoue, T. Kanzaki, T. Hakushi, *Bull. Chem. Soc. Jpn.* **1984**, *57*, 887–888.

[55] K. H. Pannell, C. K. La Neave, E. Rico, B. Arkles, *Pharmacol. Biochem. Behav.* **1984**, *21*, 77–80.

[56] T. Takano, N. Kasai, M. Kakudo, *Bull. Chem. Soc. Jpn.* **1963**, *36*, 585–590.

[57] J. Chojnowski, J. Kurjata, *Macromolecules* **1994**, *27*, 2302–2309.

[58] M. Cypryk, *Macromol. Theory Simul.* **2001**, *10*, 158–164.

[59] J. Kurjata, J. Chojnowski, *Makromol. Chem.* **1993**, *194*, 3271–3286.

[60] M. Cypryk, J. Kurjata, J. Chojnowski, *J. Organomet. Chem.* **2003**, *686*, 373–378.

[61] J. M. Markowitz, A. Arbor, *J. Chem. Edu.* **1960**, *37*, 75–81.

[62] H. Spandau, V. Gutmann, *Angew. Chem.* **1952**, *64*, 93–102.

[63] H. W. Foote, J. Fleischer, *J. Am. Chem. Soc.* **1931**, *53*, 1752–1763.

[64] W. Karcher, H. Hecht, *Chemie in Flüssigem Schwefeldioxid* in *Chemie in nichtwäßrigen ionisierenden Lösungsmitteln*, Bd. III, C. C: Addison, W. Karcher, H. Hecht (Hrsg.), Vieweg & Sohn,Braunschweig, **1967**.

[65] H. Kühnl, A. Strumpf, M. Gladziwa, *Z. Anorg. Allg. Chem.* **1979**, *449*, 145–156.

[66] A. Simon, K. Peters, E.-M. Peters, H. Kühnl, B. Koslowski, *Z. Anorg. Allg. Chem.* **1980**, *469*, 94–100.

[67] K. Peters, A. Simon, E.-M. Peters, H. Kühnl, B. Koslowski, *Z. Anorg. Allg. Chem.* **1982**, *492*, 7–14.

[68] R. Mews, E. Lork, P. G. Watson, Görtler, *Coord. Chem. Rev.* **2000**, *197*, 277–320.

[69] E. Lork, J. Petersen, R. Mews, *Angew. Chem., Int. Ed. Engl.* **1994**, *33*, 1663–1665.

[70] E. Lork, R. Mews, J. Petersen, M. Schröter, B. Žemva, *J. Fluor. Chem.* **2001**, *110*, 109–116.

[71] J. Derendorf, M. Keßler, C. Knapp, M. Rühle, C. Schulz, *Dalton Trans.* **2010**, *39*, 8671.

[72] A. Decken, C. Knapp, G. B. Nikiforov, J. Passmore, J. Mikko Rautiainen, X. Wang, X. Zeng, *Chem. Eur. J.* **2009**, *15*, 6504–6517.

[73] T. S. Cameron, G. B. Nikiforov, J. Passmore, J. M. Rautiainen, *Dalton Trans.* **2010**, *39*, 2587.

[74] C. Barbeau, R. J. Dubey, *Can. J. Chem.* **1973**, *51*, 3684–3689.

[75] G. J. Kubas, R. R. Ryan, V. McCarty, *Inorg. Chem.* **1980**, *19*, 3003–3007.

[76] S. Sun, Y. Niu, Q. Xu, Z. Sun, X. Wei, *RSC Adv.* **2015**, *5*, 46564–46567.

[77] S. Sun, Y. Niu, Z. Sun, Q. Xu, X. Wei, *RSC Adv.* **2015**, *5*, 8706–8712.

[78] J. D. Childs, D. Van der Helm, S. D. Christian, *Inorg. Chem.* **1975**, *14*, 1386–1390.

[79] R. A. Ando, L. J. A. Siqueira, F. C. Bazito, R. M. Torresi, P. S. Santos, *J. Phys. Chem. B* **2007**, *111*, 8717–8719.

[80] W. Eisfeld, M. Regitz, *J. Am. Chem. Soc.* **1996**, *118*, 11918–11926.

[81] K. Hoher, P. F. Cardoso, L. F. Lepre, R. A. Ando, L. J. A. Siqueira, *Phys. Chem. Chem. Phys.* **2016**, *18*, 28901–28910.

[82] W. Wu, B. Han, H. Gao, Z. Liu, T. Jiang, J. Huang, *Angew. Chem., Int. Ed.* **2004**, *43*, 2415–2417.

[83] J. Huang, A. Riisager, P. Wasserscheid, R. Fehrmann, *Chem. Commun.* **2006**, 4027.

[84] A. Kumar, G. S. McGrady, J. Passmore, F. Grein, A. Decken, *Z. Anorg. Allg. Chem.* **2012**, *638*, 744–753.

[85] N. Kuhn, A. Alsheikh, *Coord. Chem. Rev.* **2005**, *249*, 829–857.

[86] L. H. Finger, J. Guschlbauer, K. Harms, J. Sundermeyer, *Chem. Eur. J.* **2016**, *22*, 16292–16303.

[87] M. K. Denk, K. Hatano, A. J. Lough, *Eur. J. Inorg. Chem.* **2003**, *2003*, 224–231.

[88] A. Decken, F. A. LeBlanc, J. Passmore, X. Wang, *Eur. J. Inorg. Chem.* **2006**, *7*, 4033–4036.

[89] R. Minkwitz, W. Molsbeck, H. Preut, *Z. Naturforsch. B* **1989**, *44*, 1581–1583.

[90] R. Gleiter, W. Schafer, G. Krennrich, H. Sakurai, *J. Am. Chem. Soc.* **1987**, 4117–4120.

[91] B. Konig, M. Rodel, P. Bubenitschek, P. G. Jones, *Angew. Chem., Int. Ed.* **1995**, 661–662.

[92] C. J. Brown, A. C. Farthing, *Nature* **1949**, *164*, 915–916.

[93] H. Braunschweig, F. Breher, S. Capper, K. Dück, M. Fuß, J. O. C. Jimenez-Halla, I. Krummenacher, T. Kupfer, D. Nied, K. Radacki, *Chem. Eur. J.* **2013**, *19*, 270–81.

[94] J. Beckmann, S. L. Jänicke, *Eur. J. Inorg. Chem.* **2006**, *2006*, 3351–3358.

[95] A. Fürstner, M. Alcarazo, H. Krause, C. W. Lehmann, *J. Am. Chem. Soc.* **2007**, *129*, 12676–12677.

[96] M. Austeri, M. Enders, M. Nieger, S. Bräse, *Eur. J. Org. Chem.* **2013**, 1667–1670.

[97] S. Shirai, S. Iwata, Y. Maegawa, T. Tani, S. Inagaki, *J. Phys. Chem. A* **2012**, *116*, 10194–10202.

[98] C. Elschenbroich, B. Kanellakopulos, F. H. Köhler, B. Metz, R. Lescouëzec, N. W. Mitzel, W. Strauss, *Chemistry* **2007**, *13*, 1191–200.

[99] T. P. Tauer, M. E. Derrick, C. D. Sherrill, *J. Phys. Chem. A* **2005**, *109*, 191–196.

[100] D. J. Cram, D. I. Wilkinson, *J. Am. Chem. Soc.* **1960**, *82*, 5721–5723.

[101] F. Christiani, D. De Filippo, P. Deplano, F. Devillanova, A. Diaz, E. F. Trogu, G. Verani, *Inorg. Chim. Acta* **1975**, *12*, 119–122.

[102] P. K. Gantzel, K. N. Trueblood, *Acta Crystallogr.* **1965**, *18*, 958–968.

[103] C. Elschenbroich, R. Möckel, U. Zenneck, *Angew. Chem., Int. Ed. Engl.* **1978**, *17*, 531–532.

[104] C. Elschenbroich, J. Hurley, W. Massa, G. Baum, *Angew. Chem.* **1988**, *100*, 727–729.

[105] H. Schmidbaur, W. Bublak, B. Huber, G. Müller, *Helv. Chim. Acta* **1986**, *69*, 1742–1747.

[106] N. Mézailles, N. Maigrot, S. Hamon, L. Ricard, F. Mathey, Le Floch, *J. Org. Chem.* **2001**, *66*, 1054–1056.

[107] G. Meyer-Eppler, E. Vogelsang, C. Benkhäuser, A. Schneider, G. Schnakenburg, A. Lützen, *Eur. J. Org. Chem.* **2013**, *2013*, 4523–4532.

[108] C. Dutan, S. Choua, T. Berclaz, M. Geoffroy, N. Mézailles, A. Moores, L. Ricard, P. Le Floch, *J. Am. Chem. Soc.* **2003**, *125*, 4487–4494.

[109] A. Moores, C. Defieber, N. Mézailles, N. Maigrot, L. Ricard, P. Le Floch, *New J. Chem.* **2003**, *27*, 994–999.

[110] R. L. Merker, M. J. Scott, *J. Polym. Sci. Part A Gen. Pap.* **1964**, *2*, 15–29.

[111] A. Sekiguchi, T. Yatabe, C. Kabuto, H. Sakurai, *Angew. Chem.* **1989**, *101*, 778–780.

[112] N. Mireles, L. E. Sansores, a Martínez, R. Salcedo, *Int. J. Quantum Chem.* **2003**, *94*, 51–56.

[113] J. Beckmann, A. Duthie, G. Reeske, M. Schürmann, *Organometallics* **2005**, *24*, 3629–3633.

[114] H. Abdoul-Carime, *J. Chem. Soc. Faraday Trans.* **1998**, *94*, 2407–2410.

[115] R. Zadmard, A. Kraft, T. Schrader, U. Linne, *Chem. Eur. J.* **2004**, *10*, 4233–4239.

[116] M. K. Amini, M. Shamsipur, *J. Phys. Chem.* **1991**, *95*, 9601–9604.

7 Appendix

The presentation of the manuscripts follows the same order as shown in Section 5. The five already published reports are displayed in their original version. Two of them are open access sources; the others have the necessary permission of the publisher. The manuscript n° 5 with the title "Crown ethers complexes of alkali metal chlorides from SO_2" has not yet been published. If existing, adjusted Supplementary Information except for XYZ data is provided.

1) *Stable Alkali-Metal Complexes of Hybrid Disila-Crown Ethers*
   Reprinted with permission from „K. Reuter, M. Buchner, G. Thiele, C. von Hänisch, *Inorg. Chem.* **2016**, *55*, 4441-4447." Copyright © 2016, American Chemical Society.
2) *Synthesis and coordination ability of a partially Silicon based crown ether*
   „K. Reuter, G. Thiele, T. Hafner, F. Uhlig, C. von Hänisch, *Chem. Commun.* **2016**, *52*, 13265-13268." – Published by The Royal Society of Chemistry.
3) *Structural Study of Mismatched Disila-Crown Ether Complexes*
   „K. Reuter, F. M. Dankert, C. Donsbach, C. von Hänisch, *Inorganics* **2017**, *5(1)*, 11." – Published by MPDI.
4) *A structural study of alkaline earth metal complexes with hybrid disila-crown ethers*
   „F. Dankert, K. Reuter, C. Donsbach, C. von Hänisch, *Dalton Trans.* **2017**, DOI: 10.1039/C6DT04018G" – Published by The Royal Society of Chemistry.
5) *Crown ethers complexes of alkali metal chlorides from SO_2*
   K. Reuter, S. S. Rudel, M. R. Buchner, F. Kraus, C. v. Hänisch, *unpublished*.
6) *Synthesis of Heteroatomic Bridged Paracyclophanes*
   „K. Reuter, R. G. M. Maas, A. Reuter, F. Kilgenstein, Y. Asfaha, C. von Hänisch, Dalton Trans. 2017, DOI: 10.1039/c7dt00321h" – Published by The Royal Society of Chemistry

Inorganic Chemistry

Article

pubs.acs.org/IC

Stable Alkali-Metal Complexes of Hybrid Disila-Crown Ethers

Kirsten Reuter,[†] Magnus R. Buchner,[†] Günther Thiele,[‡] and Carsten von Hänisch*[,†]

[†]Fachbereich Chemie and Wissenschaftliches Zentrum für Materialwissenschaften (WZMW), Philipps-Universität Marburg, Hans-Meerwein-Straße 4, 35032 Marburg, Germany

[‡]Department of Chemistry, University of California, 210 Lewis Hall, Berkeley, California 94720, United States

Supporting Information

ABSTRACT: The complexation ability of hybrid disilane and ethylene containing crown ether ring systems was analyzed using 1,2-disila[12]crown-4 (**1**), 1,2-disila[15]crown-5 (**2**), 1,2-disila[18]crown-6 (**3**), and 1,2,7,8-tetrasila[12]crown-4 (**7**). Alkali-metal complexes (Li^+, Na^+, K^+) were obtained and analyzed via X-ray diffraction. The complex stability of $[Li(1,2\text{-disila}[12]\text{crown-4})]^+$ and $[Li(1,2,7,8\text{-tetrasila}[12]\text{crown-4})]^+$ was determined, in relation to the lithium complex of [12]crown-4, by density functional theory (DFT) calculations employing the BP86/def2-TZVP level of theory. In solution, the exchange of lithium cations between pure [12]crown-4 and hybrid [12]crown-4 is on even terms, as has been shown from the relative binding affinity of compounds **1** and **7** by means of dynamic proton nuclear magnetic resonance (NMR) spectroscopy.

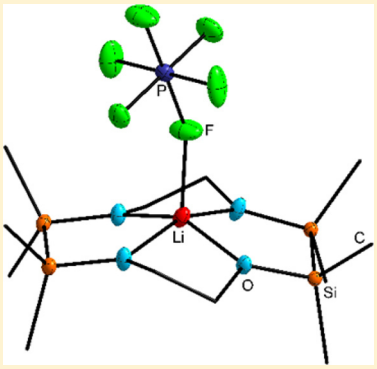

INTRODUCTION

Early studies on cyclosiloxanes have revealed a drastically reduced ability to interact with Lewis acids such as BCl_3 and BF_3, compared to crown ethers.[1−3] Until recently, the formation of complexes with cyclosiloxanes as ligands has only been successful upon the usage of salts of large, weakly coordinating anions (Scheme 1).[4−6] The lower basicity of the oxygen was suggested to be caused by the oxygen atom donating lone pair electron density into the σ^*-orbitals of the silicon−methyl bonds. Subsequent coordination of metal cations leads to a competing polarization of the $p^2(O) \rightarrow \sigma^*(Si\text{-}CH_3)$ interaction and is thus not favored.[7] Especially in alkylated siloxanes, the effects of hyperconjugative delocalization have been determined to be of greater relevance, compared to protonated siloxanes.[8]

According to a different approach based on calculations of the electron localization function, the oxygen atom in siloxanes exhibits higher anionicity as a result of the more electropositive Si atom, compared to carbon.[9,10] The polarized Si−O linkage then would suggest a higher coordination ability. However, recent quantum theory of atoms in molecules (QTAIM) analysis revealed that the lower complex stability of $[MD_6]^+$ (D = Me_2SiO), compared to $[M([18]\text{crown-6})]^+$ (M = Li, Ag) can be attributed to the less attractive electrostatic interaction of the metal ion with D_6, compared to [18]crown-6. The weaker electrostatic binding in D_6 metal complexes results from the repulsion between the positively charged Si atoms and the metal ions.[11]

Furthermore, a decrease in the complexation ability for contracted crown ether rings, such as [17]crown-6 and sila[17]crown-6, was already shown in the 1980s and accounted for distorted conformation rather than for electronic effects as observed for both CH_2 and $SiMe_2$ groups replacing one C_2H_4.[12]

Although cyclosiloxanes have been subject of intensive investigation, less attention has been paid to the corresponding cyclic silaethers, which are composed of Si_2 units. Merely the dioxane analogue, octamethyl-1,4-dioxatetrasilacyclohexane, is well-characterized[13] and gave rise to the finding that its basicity is increased, compared to that of cyclosiloxanes.[14] Consistent with this, quantum chemical studies indicate less significant hyperconjugation effects in compounds containing disilane units.[15,16] However, no metal complexes of these ligands are known to date.

Recent research indicate that the weak complexation ability of cyclosiloxanes, compared to ethers, is a result of electronic and structural factors. It is furthermore suggested that, in the sequence of intrinsic ring contraction in siloxanes, the O atoms cannot be aligned in-plane. The incorporation of Si_2 units reduces the distorted conformation observed in ring-contracted crown ethers and the positive charge at the Si atoms due to the nonpolar Si−Si bond. We herein report the synthesis and complexation properties of hybrid crown ethers, containing disilane as well as ethylene fragments between the O atoms.

EXPERIMENTAL SECTION

General Experimental Technique. All working procedures were conducted under rigorous exclusion of oxygen and moisture using Schlenk techniques under an argon atmosphere. Solvents were dried and freshly distilled before use. Nuclear magnetic resonance (NMR) spectra were recorded with Bruker Model Avance HD 300, Bruker Model DRX 400, or Bruker Model Avance 500 spectrometers, the

Received: February 1, 2016
Published: April 15, 2016

DOI: 10.1021/acs.inorgchem.6b00267
Inorg. Chem. 2016, 55, 4441−4447

Scheme 1. Binding Modes of Cyclosiloxanes in Li^+ and Ag^+ Complexes[a]

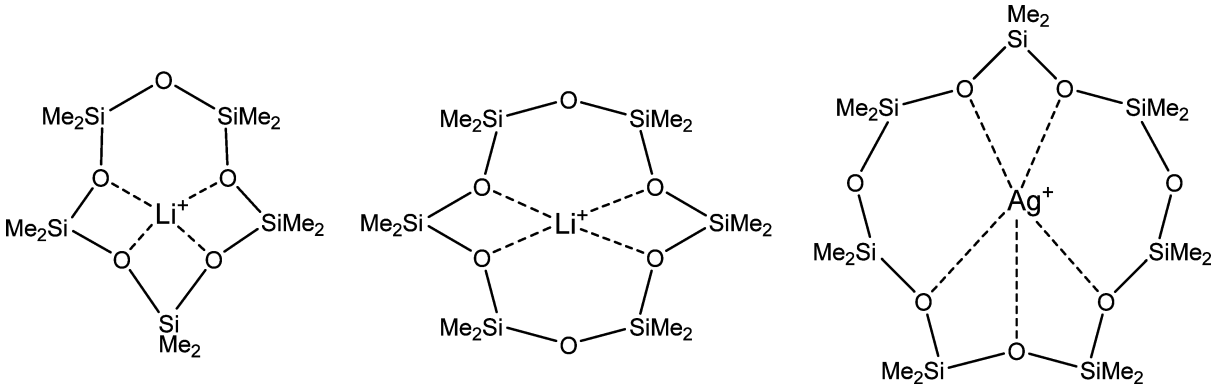

[a]Salts of these cationic complexes were obtained from the reaction of D_n (n = 5, 6) with $[LiAl\{OC(CF_3)_3\}_4]$ and D_5 with $AgSbF_6$, all in liquid SO_2.[4−6]

latter of which is equipped with a Prodigy CryoProbe. The structural analyses were carried out with appropriate single crystals on an automatic diffractometer (Bruker Model D8 Quest). Infrared (IR) spectra were recorded in attenuated total reflectance (ATR) mode on a Bruker Model Alpha FT-IR of the respective sample. MS spectrometry was measured on AccuTOF-GC (LIFDI) and LTQ-FT (ESI). The elemental analysis was performed on a Vario MicroCube.

Crystal Structures. Data collection was performed using a Bruker D8 Quest diffractometer at 100(2) K with Mo K_α radiation and graphite monochromatization (λ = 0.71073). Structure solution was realized by direct methods, refinement with full-matrix-least-squares against F^2 using SHELXS-2014, SHELXL-2014, and Olex2 software.[17,18] Crystal data for compounds **4**, **5**, **6**, and **8** are given as follows. (CCDC Nos. 1437285 (**4**), 1437286 (**5**), 1437287 (**6**), and 1437288 (**8**) contain the supplementary crystallographic data for this paper; these data can be obtained free of charge from The Cambridge Crystallographic Data Centre via www.ccdc.cam.ac.uk/data_request/cif.)

Compound **4** *($C_{11}H_{24}F_3Li_1O_7S_1Si_2$).* Molecular weight, M_W = 420.48 g/mol; monoclinic, $P2_1/c$, a = 13.7300(7) Å, b = 16.9864(7) Å, c = 16.9091(8) Å, β = 93.9527(17)°.

Compound **5** *($C_{18}H_{34}Cl_1Na_1O_9Si_2$).* M_W = 509.07 g/mol; triclinic, $P\bar{1}$, a = 9.8536(5) Å, b = 9.9654(5) Å, c = 13.0638(6) Å, α = 91.291(2)°, β = 92.820(2)°, γ = 97.259(2)°.

Compound **6** *($C_{14}H_{32}F_6K_1O_6P_1Si_2$).* M_W = 536.64 g/mol); monoclinic, $P2_1$, a = 10.4027(13) Å, b = 12.3519(11) Å, c = 10.4989(9) Å, β = 119.580(2)°.

Compound **8** *($C_{13}H_{34}Cl_2F_6Li_1O_4P_1Si_4$).* M_W = 589.57 g/mol; orthorhombic, $P2_12_12_1$, a = 10.1612(3) Å, b = 13.9035(5) Å, c = 19.6348(7) Å.

Computational Details. Calculations were performed with the program system TURBOMOLE V6.5.[19,20] The resolution of identity (RI) approximation,[21] dispersion corrections,[22] and the conductor-like screening model (COSMO)[23] were applied throughout, the latter with default settings. For all calculations, the BP86 functional[24,25] was chosen, utilizing a def2-TZVP basis set.[21,26]

Syntheses: Ligands 1−3. At ambient temperature, 1,1,2,2-tetramethyl-1,2-dichlorodisilane (2.0 mL, 0.01 mol) in THF (50 mL) and a solution of triethylene glycol (1.4 mL, 0.01 mol) (**1**), tetraethylene glycol (1.8 mL, 0.01 mol) (**2**) or pentaethylene glycol (2.2 mL, 0.01 mol) (**3**) in THF (50 mL) were added simultaneously to a well-stirred solution of triethylamine (2.9 mL, 0.02 mol) and tetrahydrofuran (THF) (150 mL). After 16 h, the solvent was evaporated *in vacuo*. The residue was extracted into *n*-pentane and filtered, and the solvent was removed from the filtrate. By heating the raw product to 200 °C at a pressure of 1×10^{-3} mbar, impurities were mostly withdrawn and the products **1**−**3** were obtained as colorless, viscous oils (**1**: 1.79 g, 64%; **2**: 2.4 g, 73%; **3**: 2.67 g, 70%).

Analytical Data for **1**. ^{1}H NMR (300 MHz, CD_2Cl_2): δ = 3.77 (m, 4H, CH_2), 3.62 (s, 4H, CH_2), 3.59 (m, 4H, CH_2), 0.23 ppm (s, 12H, CH_3); ^{13}C NMR (75 MHz, CD_2Cl_2): δ = 73.1 (s, CH_2), 71.7 (s, CH_2), 63.9 (s, CH_2), 0.3 ppm (s, CH_3); ^{29}Si NMR (60 MHz, CD_2Cl_2): δ = 10.7 ppm (s); IR (cm^{-1}): $\tilde{\nu}$ = 2949(w), 2865(w), 1457(w), 1351(w), 1295(w), 1245(m) (Si−CH_3), 1095(m) (Si−O), 990(m), 942(m), 824(m), 789(s), 761(vs), 718(m), 681(w), 627(m), 556(w), 508(w); MS (ESI^+): m/z (%) 265 $[MH]^+$ (100).

Analytical Data for **2**. ^{1}H NMR (300 MHz, CD_2Cl_2): δ = 3.76 (m, 4H, CH_2), 3.61 (s, 8H, CH_2), 3.57 (m, 4H, CH_2), 0.23 ppm (s, 12H, CH_3); ^{13}C NMR (75 MHz, CD_2Cl_2): δ = 73.0 (s, CH_2), 71.3 (s, CH_2), 71.3 (s, CH_2) 63.7 (s, CH_2), 0.0 ppm (s, CH_3); ^{29}Si NMR (60 MHz, CD_2Cl_2): δ = 11.0 ppm (s); IR (cm^{-1}): $\tilde{\nu}$ = 2974(m), 2865(m), 1452(w), 1350(w), 1294(w), 1245(m) (Si−CH_3), 1090(s) (Si−O), 990.7(m), 824(s), 790(s), 761(vs), 681(w), 656(w), 629(m), 506(w); MS (ESI^+): m/z (%) 309 $[MH]^+$ (5), 331 $[M-Na]^+$ (100).

Analytical Data for **3**. ^{1}H NMR (300 MHz, CD_2Cl_2): δ = 3.72 (t, $^3J_{HH}$ = 5.2 Hz, 4H, CH_2), 3.59 (s, 12H, CH_2), 3.51 (t, $^3J_{HH}$ = 5.2 Hz, 4H, CH_2), 0.24 ppm (s, 12H, CH_3); ^{13}C NMR (75 MHz, CD_2Cl_2): δ = 73.4 (s, CH_2), 71.2 (s, CH_2), 71.2 (s, CH_2), 63.6 (s, CH_2), 0.0 ppm (s, CH_3); ^{29}Si NMR (60 MHz, CD_2Cl_2): δ = 11.4 ppm (s); IR (cm^{-1}): $\tilde{\nu}$ = 2949(m), 2865(m), 1456(w), 1350(w), 1325(w), 1294(w), 1244(s) (Si−CH_3), 1088(vs) (Si−O), 944(m), 826(m), 789(s), 764(s), 681(w), 629(w), 534(m), 486(w), 422(w); MS (ESI^+): m/z (%) 353 $[MH]^+$

Synthesis of 4. Lithium triflate (183 mg, 1.2 mmol) was added to a solution of **1** (310 mg, 1.2 mmol) and DCM (20 mL). After stirring for 12 h, the solvent was evaporated *in vacuo*; the remaining solid was washed with *n*-pentane and dissolved in DCM and benzene (1:1). Slow reduction of the volume yielded colorless rods of **4** (310 mg, 65%). ^{1}H NMR (300 MHz, CD_2Cl_2): δ = 3.83 (m, 4H, CH_2), 3.76 (s, 4H, CH_2), 3.64 (m, 4H, CH_2), 0.36 ppm (s, 12H, CH_3); ^{13}C NMR (125 MHz, CD_2Cl_2): δ = 120.9 (q, $^1J_{CF}$ = 319 Hz, CF_3), 71.2 (s, CH_2), 68.8 (s, CH_2), 61.8 (s, CH_2), −0.8 ppm (s, CH_3); ^{29}Si NMR (60 MHz, CD_2Cl_2): δ = 15.4 ppm (s); ^{19}F NMR (283 MHz, CD_2Cl_2): δ = −79.1 ppm (s), ^{7}Li NMR (117 MHz, CD_2Cl_2): δ = −0.7 ppm (s). IR (cm^{-1}): $\tilde{\nu}$ = 2960(w), 2916(w), 2875(w), 1479(w), 1458(w), 1404(w), 1362(w), 1344(w), 1293(s), 1257(s) (Si−CH_3), 1246(s), 1225(m), 1128(s), 1108(m) (Si−O), 1066(m) (Si−O), 1038(vs), 943(s), 901(s), 864(m), 850(m), 818(m), 795(s), 769(s), 727(m), 636(vs), 584(m), 573(m), 517(m), 473(s), 452(w), 424(w); MS (ESI^+): m/z (%) 271 $[M]^+$ (100); elemental analysis calcd. (%) for $C_{11}H_{24}F_3Li_1O_7S_1Si_2$: C 31.42, H 5.75; found: C 31.17, H 5.835.

Synthesis of 5. Sodium perchlorate (160 mg, 1.3 mmol) was added to a stirred solution of **2** (400 mg, 1.3 mmol) and DCM (20 mL). After 12 h, the solvent was evaporated *in vacuo*, and the remaining solid was washed with *n*-pentane and dissolved in DCM and benzene (1:1). Slow reduction of the volume yielded colorless rods of **5** (180 mg, 64%).^{1}H NMR (300 MHz, CD_2Cl_2): δ = 3.76 (m, 4H, CH_2), 3.67 (s, 8H, CH_2), 3.61 (m, 4H, CH_2), 0.32 ppm (s, 12H, CH_3); ^{13}C NMR (75 MHz, CD_2Cl_2): δ = 71.7 (s, CH_2), 69.9 (s, CH_2), 69.7 (s, CH_2), 62.0 (s, CH_2), −1.0 ppm (s, CH_3); ^{29}Si NMR (60 MHz,

DOI: 10.1021/acs.inorgchem.6b00267
Inorg. Chem. 2016, 55, 4441−4447

Scheme 2. Synthesis Path of 1,2-Disila[12]crown-4 (1, *n* = 1), 1,2-Disila[15]crown-5 (2, *n* = 2), and 1,2-Disila[18]crown-6 (3, *n* = 3)

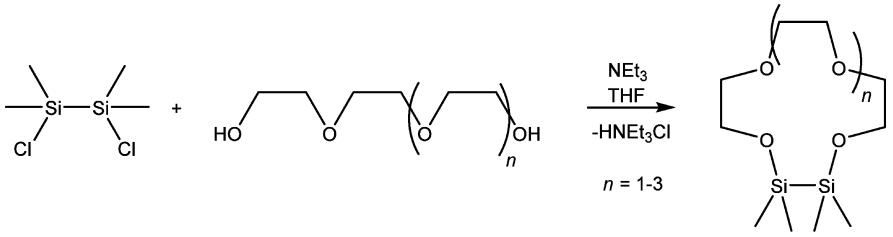

CD_2Cl_2): δ = 14.1 ppm (s); IR (cm^{-1}): $\tilde{\nu}$ = 2936(w), 2879(w), 1478(w), 1459(w), 1405(w), 1355(m), 1249(m) (Si−CH_3), 1144(w), 1092(s) (Si−O), 1064(vs) (Si−O), 1046(s), 956(s), 929(m), 865(m), 840(m), 815(m), 796(s), 767(s), 739(m), 687(w), 622(s), 546(w), 527(w), 452(w); MS (ESI$^+$): *m*/*z* (%) 331 $[M]^+$ (100); elemental analysis calcd (%) for $C_{12}H_{28}Cl_1Na_1O_9Si_2$: C 33.44, H 6.55; found: C 33.05, H 6.56.

Synthesis of 6. Potassium hexafluorophosphate (180 mg, 1.0 mmol) was added to a stirred solution of **3** (230 mg, 0.65 mmol) and DCM (20 mL). After 12 h, the solvent was evaporated *in vacuo*, the remaining solid was washed with *n*-pentane and dissolved in DCM. Slow reduction of the volume yielded colorless rods of **6** (150 mg, 51%). ^{1}H NMR (300 MHz, CD_2Cl_2): δ = 3.73 (m, 4H, CH_2), 3.62 (s, 12H, CH_2), 3.54 (m, 4H, CH_2), 0.28 ppm (s, 12H, CH_3); ^{13}C NMR (75 MHz, CD_2Cl_2): δ = 73.1 (s, CH_2), 70.7, (s, CH_2), 70.6, (s, CH_2), 70.5 (s, CH_2), 62.7 (s, CH_2), −1.0 ppm (s, CH_3); ^{29}Si NMR (60 MHz, CD_2Cl_2): δ = 13.0 ppm (s); ^{19}F NMR (283 MHz, CD_2Cl_2): δ = −72.9 ppm (d, $^1J_{PF}$ = 710 Hz, P−*F*), ^{31}P NMR (117 MHz, CD_2Cl_2): δ = −144.5 ppm (sept, $^1J_{PF}$ = 710 Hz, *P*−F); IR (cm^{-1}): $\tilde{\nu}$ = 2955(w), 2883(w), 2162(w), 2883(w), 1458(w), 1368(w), 1251(m) (Si−CH_3), 1088(m) (Si−O), 1057(m) (Si−O), 960(m), 940(m), 878(w), 832(vs), 792(s), 761(s), 734(s), 632(m), 555(s), 443(w), 422(w); MS (ESI$^+$): *m*/*z* (%) 391 $[M]^+$ (100); elemental analysis calcd. (%) for $C_{14}H_{32}F_6K_1O_6P_1Si_2$: C 31.33, H 6.01; found: C 30.74, H 5.91.

Synthesis of 7. A suspension of NaH (190 mg, 7.9 mmol) and THF (30 mL) was slowly added at −50 °C to a well-stirred solution of ethylene glycol (0.44 mL, 7.9 mmol) and THF (80 mL). The reaction was allowed to warm to room temperature and was stirred for additional 8 h. At −50 °C, 1,2-dichlorodisilane (1.5 mL, 7.9 mmol) and THF (30 mL) was slowly added to the suspension. After 12 h of stirring at room temperature, the solvent was removed under reduced pressure. The residue was extracted with *n*-pentane and filtered. After the removal of *n*-pentane and drying *in vacuo*, the product was obtained as a colorless oil (1.3 g, 65%). ^{1}H NMR (300 MHz, CD_2Cl_2): δ = 3.71 (s, 4H, CH_2), 0.22 ppm (s, 12H, CH_3); ^{13}C NMR (75 MHz, CD_2Cl_2): δ = 65.5 (s, CH_2), 0.1 ppm (s, CH_3); ^{29}Si NMR (60 MHz, CD_2Cl_2): δ = 10.8 ppm (s); IR (cm^{-1}): $\tilde{\nu}$ = 2951(w), 2863(w), 1455(w), 1393(w), 1291(w), 1245(m) (Si−CH_3), 1135(m), 1081(m) (Si−O), 1040(m) (Si−O), 949(m), 902(m), 824(m), 759(vs), 681(w), 658(w), 625(m), 531(w), 489(w); MS (LIFDI): *m*/*z* (%) 353 $[MH]^+$ (20).

Synthesis of 8. Lithium hexafluorophosphate (172 mg, 1.1 mmol) was added to a solution of **7** (400 mg, 1.1 mmol) and DCM (20 mL). After stirring for 12 h, the suspension was filtered and the solvent was evaporated *in vacuo*. The remaining solid was washed with *n*-pentane and dissolved in DCM and benzene (1:1). Slow reduction of the volume yielded colorless rods of **8** (280 mg, 49%). ^{1}H NMR (300 MHz, CD_2Cl_2): δ = 3.74 (s, 4H, CH_2), 0.35 ppm (s, 24H, CH_3); ^{13}C NMR (75 MHz, CD_2Cl_2): δ = 62.9 (s, CH_2), −1.2 ppm (s, CH_3); ^{29}Si NMR (60 MHz, CD_2Cl_2): δ = 15.8 ppm (s); ^{19}F NMR (283 MHz, CD_2Cl_2): δ = −74.0 ppm (d, $^1J_{FP}$ = 709 Hz, P−*F*), ^{7}Li NMR (117 MHz, CD_2Cl_2): δ = −0.7 ppm (s), ^{31}P NMR (117 MHz, CD_2Cl_2): δ = −144.1 ppm (sept, $^1J_{PF}$ = 709 Hz, *P*−F). IR (cm^{-1}): $\tilde{\nu}$ = 2952 (w), 2883(w), 1460(w), 1396(w), 1367(m), 1252(m) (Si−CH_3), 1116(w), 1088(m) (Si−O), 1054(s) (Si−O), 961(m), 939(m), 831(vs), 793(s), 760(vs), 731(s), 632(m), 555(s), 440(w), 416(w); MS (ESI$^+$): *m*/*z* (%) 359 $[M]^+$ (5); elemental analysis calcd. (%) for $C_{12}H_{32}F_6Li_1O_4P_1Si_2$: C 28.56, H 6.39; found: C 28.59, H 6.32.

RESULTS AND DISCUSSION

In the first step, one disilane unit is inserted in the ligand framework, which is achieved by Williamson ether synthesis of 1,1,2,2-tetramethyl-1,2-dichlorodisilane and the corresponding glycol (Scheme 2). Compounds **1**−**3** are colorless, viscous, and moisture-sensitive oils that instantly react in aqueous solution to form octamethyl-1,4-dioxatetrasilacyclohexane and the open-chained glycol.

Treatment of **1** with LiOTf (OTf = $F_3CSO_3^-$), **2** with $NaClO_4$, and **3** with KPF_6 in dichloromethane selectively yielded the corresponding complexes, which were highly sensitive toward traces of water. Analysis of the single crystals by X-ray diffraction (XRD) revealed a saturation of the cations' coordination sphere by interaction with all O atoms of the crown ether and, additionally, with the corresponding counterion. The respective salts crystallize in the space groups $P2_1/c$ (**4**), $P\bar{1}$ (**5**), and $P2_1$ (**6**).

In all of the complexes, the metal cations are shifted out of the crown ether ring center toward the counterions (Figures 1 and 2). For example, the transannular O−Li−O angles in [Li(1,2-disila[12]crown-4)]OTf (**4**) are notably smaller than 180° (124.0(2)° for O1−Li−O3 and 152.0(2)° for O2−Li−O4). In complexes **4** and **6**, the crown ether O atoms do not align in-plane, as usually observed in cyclosiloxane and crown ether complexes.[4,27] This is possibly the result of electrostatic interaction between the ring system and the counteranion, which is observed in both structures. For example, the F atoms of the triflate anion in **4** are pointing toward the methyl groups of the disilane units (F···H = 244.4(1) and 288.0(1) pm). In the sodium complex [Na(1,2-disila[15]crown-5)]ClO_4 (**5**), the

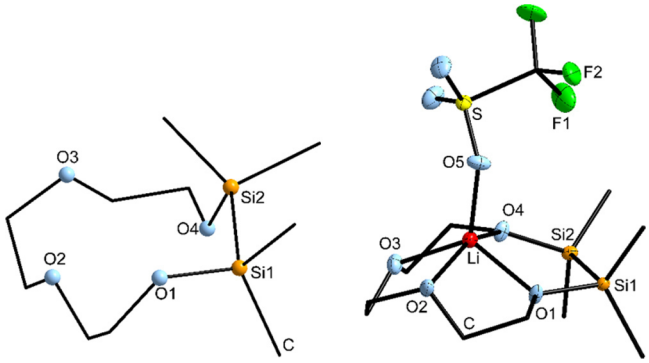

Figure 1. (Left) Optimized geometry of **1** and (right) molecular structure of **4**; thermal ellipsoids represent a 50% probability level, and H atoms are omitted for clarity and C atoms are represented by the stick/wires model.

DOI: 10.1021/acs.inorgchem.6b00267
Inorg. Chem. 2016, 55, 4441−4447

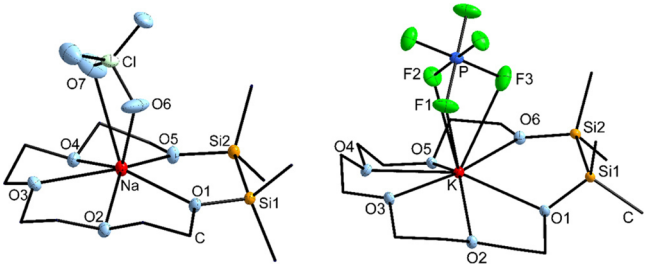

Figure 2. Molecular structure of (left) **5** and (right) **6**; thermal ellipsoids represent a 50% probability level, and H atoms are omitted for the sake of clarity. Selected bond lengths [pm] for **5**: Si1−O1, 167.0(2); Si2−O5, 167.1(2); Si1−Si2, 233.8(1); Si−C, 185.7(2)−186.7(2); O1−Na, 241.4(2); O2−Na, 250.2(2); O3−Na, 243.3(2); O4−Na, 250.8(2); O5−Na, 240.2(2); Na−O6, 240.0(2); Na−O7, 288.0(2). Selected bond lengths [pm] for **6**: Si1−O1, 166.6(3); Si2−O6, 166.0(3); Si1−Si2, 234.5(1); Si−C, 186.2(2)−186.7(5); O1−K, 278.0(3); O2−K, 287.5(3); O3−K, 287.8(3); O4−K, 280.1(2); O5−K, 293.2(3); O6−K, 284.4(3); F1−K, 282.4(4); F2−K, 291.4(4); and F3−K, 314.9(4). Selected bond angles [°] for **6**: O1−K−O4, 156.5(8); O2−K−O5, 139.9(8); and O6−K−O3, 172.5(8).

crown ether O atoms show only a slight deviation from a planar arrangement.

While the methyl groups in free 1,2-disila[12]crown-4 (**1**) adopt a staggered conformation, they are almost eclipsed in the corresponding lithium complex **4**, with torsion angles of only 20.1(1)° and 26.4(1)°, despite a considerable steric hindrance. An eclipsed arrangement of methyl groups is also known for cyclosiloxane complexes.[4−6] In contrast, the H atoms at the carbon moieties favor a perfectly staggered conformation in compounds **4**, **5**, and **6**, as well as in known crown ether complexes.

A comparison of the calculated models of compound **1** and [Li(1,2-disila[12]crown-4)]$^+$ indicates that complexation weakens the Si−O and Si−Si bonds and strengthens the Si−C bonds (see Table 1), which is consistent with the concept of negative hyperconjugation. Thus, the coordination of an O atom to a metal ion and the concomitant polarization toward the O atom diminishes this interaction.[7] Furthermore, oxygen atom O1, which is adjacent to the Si atom, shows the shortest O−Li bond length, whereas the largest O−Li bond length is observed for the fully carbon-substituted oxygen atom O2.

The ^{29}Si{^{1}H} NMR signal of **4** at δ = 15.4 ppm is considerably downfield shifted in comparison to the non-coordinating ligand **1** (δ = 10.7 ppm). However, the three ^{13}C{^{1}H} NMR signals of the glycole units undergo an upfield field shift from δ = 73.1, 71.7, and 63.9 ppm in **1** to 71.2, 68.8, and 61.8 ppm in **4**. Also, the resonance signals of the methyl groups at the Si atoms show high field shifts from δ = 0.3 ppm in **1** to −0.8 ppm in **4**, indicating an increase of electron density. Similar shifts have been observed for complexes **5** and **6**, in comparison to the corresponding free ligands in **2** and **3**.

These results encouraged us to increase the ratio of silicon in these hybrid crown ethers. Via asymmetric activation of ethylene glycol by irreversible deprotonation with sodium hydride and subsequent reaction with 1,2-dichlorodisilane, the desired product 1,2,7,8-tetrasila[12]crown-4 (**7**) was obtained in good yield as a colorless viscous oil (Scheme 3). Within this novel ligand, the disilane moieties are opposite to each other within the ring, and thus all four oxygen atoms are half disilane and half ethylene affected. Different than the one-fold silylated ligands **1**−**3**, compound **7** is stable toward water.

After the reaction with 1 equiv of $LiPF_6$, complex **8** crystallizes in the orthorhombic space group $P2_12_12_1$ as a monomeric contact ion pair, as observed in complexes **4**, **5**, and **6** (Figure 3).[17] Complex **8** shows an extremely high solubility in dichloromethane. Because of the symmetric arrangement of the silicon and carbon moieties, the O atoms are almost coplanar. In addition, regarding the values of the angles O1−Li−O3 (156.3(2)°) and O2−Li−O4 (149.4(2)°), the Li cation is only marginally shifted out of the crown ether ring center toward the anion. This results from an increased ratio of silicon and the enlarged cavity size of the ring system. This, in turn, leads to a contraction of the Li−O bonds (between 198.8(4) and 203.3(4) pm), which are slightly shorter than in **4**. The PF_6^- ion points toward the methyl groups of one disilane moiety, as a result of electrostatic interaction (F···H 268.8(2) and 258.8(2) pm).

The methyl groups at the Si atoms are in an almost perfectly eclipsed arrangement. The torsion angles of the methyl groups are comparably small (4.1(1)° and 8.0(1)°) and thus very similar to those in reported siloxane complexes.[4−6] Similar to [Li(1,2-disila[12]crown-4)]$^+$, the calculated Si−O bonds in [Li(1,2,7,8-tetrasila[12]crown-4)]$^+$ are longer, compared to the free molecule in **7**, while the Si−C bonds get shorter, as a result of the complexation (Table 1).

The relative binding affinities of the hybrid ligands **1** and **7** toward lithium were studied by quantum chemical methods and are presented in Scheme 4. The exchange of the Li ion from [12]crown-4 to 1,2-disila[12]crown-4 (**1**) was calculated by means of DFT employing the BP86 functional and def2-TZVP basis sets with inclusion of dispersion interactions and charge compensation, and is energetically favored by 10 kJ/mol. In contrast, the exchange of the Li ion toward the 2-fold silylated ligand **7** is energetically disfavored by 3 kJ/mol. Considering

Table 1. Experimental and Calculated Average Distances [pm] and Angles [°] for the Ligands 1,2-Disila[12]crown-4 (1) and 1,2,7,8-tetrasila[12]crown-4 (7) and the Lithium Complexes (4 and 8)

		Bond Length (Å)					Bond Angle (deg)	
compound	method	Li−O$_C$[a]	Li−O$_{Si}$[b]	Si−Si	Si−O	Si−C	C−O−Si	C−Si−Si−C
1	DFT[c]			235.5	168.6	188.4	122.7	78.5
[Li(1,2-disila[12]crown-4)]$^+$	DFT[c]	205.6	198.9	236.3	170.4	187.5	124.9	17.1
4	XRD[d]	208.1(3)	201.0(3)	235.3(1)	168.0(1)	186.2(2)	125.0(1)	23.3(1)
7	DFT[c]			236.0	169.9	188.5	122.8	97.6
[Li(1,2,7,8-tetra-sila[12]crown-4)]$^+$	DFT[c]		199.4	235.8	170.4	187.5	123.7	30.2
8	XRD[d]		201.3(4)	235.1(1)	167.0(2)	186.0(3)	125.2(2)	6.0(1)

[a]The subscript C denotes complete carbon-substituted crown ether O atoms. [b]O atoms bonded to silicon. [c]BP86 functional at the def2-TZVP level of theory. [d]Structures were determined by X-ray diffraction (XRD).

DOI: 10.1021/acs.inorgchem.6b00267
Inorg. Chem. 2016, 55, 4441−4447

Scheme 3. Synthesis Path of 1,2,7,8-Tetrasila[12]crown-4 (7)

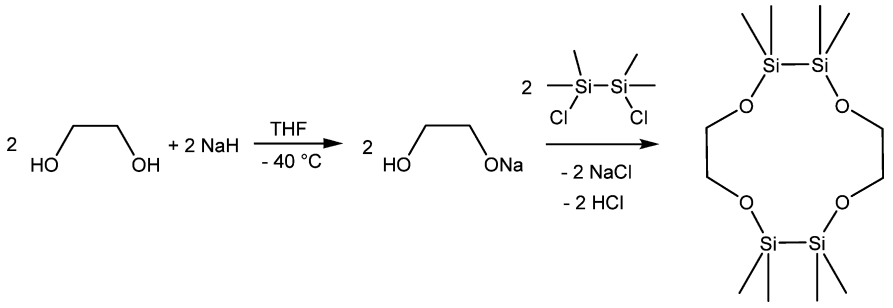

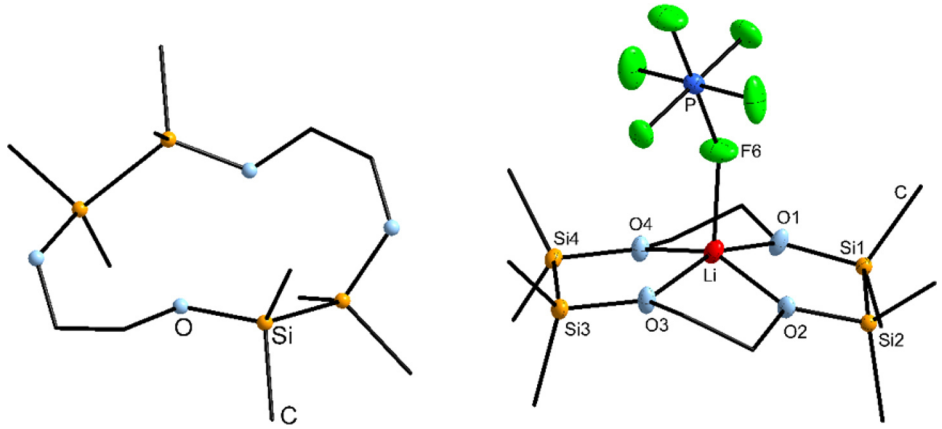

Figure 3. (Left) Optimized geometry of **7** calculated at the def2-TZVP level of theory; (right) molecular structure of **8**. Thermal ellipsoids represent a 50% probability level; hydrogen atoms are omitted for the sake of clarity.

Scheme 4. Relative Energies of the Lithium Exchange from [12]Crown-4 to 1,2-Disila[12]crown-4 (1) and 1,2,7,8-Tetrasila[12]crown-4 (7), as obtained from DFT Calculations

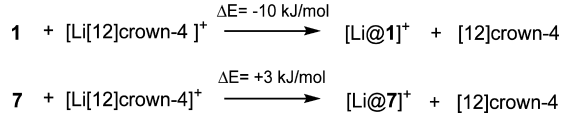

the typical error of DFT calculations, it can be assumed that ligands **1** and **7** have approximately the same ability to coordinate Li ions as the [12]crown-4. Nevertheless, the O−Li bond lengths in complex **8** are slightly shorter than those of **4**, indicating a stronger electrostatic interaction.

A more in-depth analysis of the bonding interactions within the $[Li[12]crown\text{-}4]^+$, and cations in **4** and **8**, reveal an increase of relaxation energy (determined as within EDA[28]) with

Scheme 5. 300 MHz, ^1H NMR Spectra in CD_2Cl_2 of (a) 1,2,7,8-Tetrasila[12]crown-4 (7), (b) [Li(1,2,7,8-Tetrasila[12]crown-4)]PF_6 (8), (c) [12]Crown-4/1,2,7,8-Tetrasila[12]crown-4 (7)/$LiPF_6$ Ratio 1:1:1, (d) [Li[12]crown-4]PF_6, and (e) [12]Crown-4

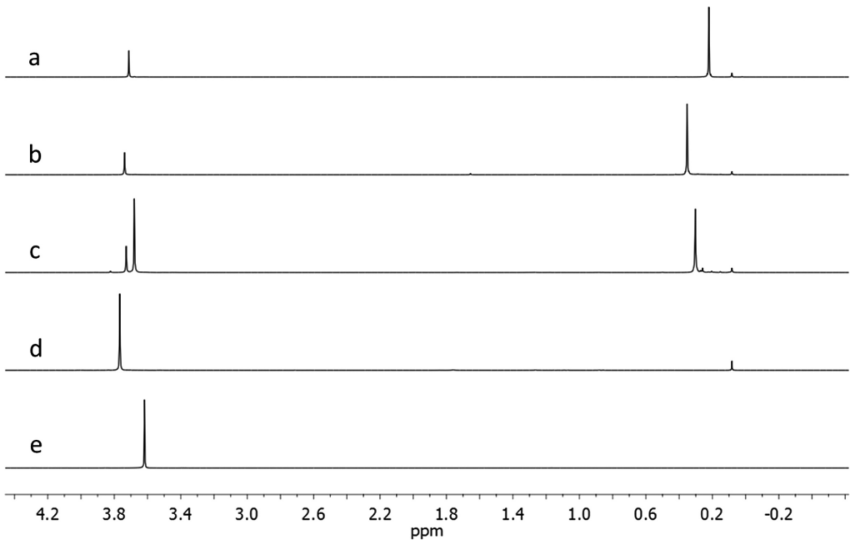

DOI: 10.1021/acs.inorgchem.6b00267
Inorg. Chem. 2016, 55, 4441−4447

increasing silicon content of the crown ethers. Thus, the rearrangement from free crown ether geometries toward the geometries found within the Li complexes requires more energy as the number of Si atoms increased ([12]crown-4, +17.96 kJ/mol; **1**, +33.77 kJ/mol; **7**, +60.41 kJ/mol), as would be expected. However, the overall reaction energies for all complexations (Scheme 4) are similar, independent of whether Si atoms are present or not, and independent of the amount of Si atoms present. Therefore, the electrostatic attraction between the O atoms of the ligands and the metal ions[11] must compensate for the relaxation energy and consequently increase significantly from [12]crown-4 to **1** and **7**.

Dynamic ^{1}H NMR spectroscopy was carried out to confirm the relative binding affinity of **1** and **7** toward Li cations. For this purpose, 1 equiv of [12]crown-4 was added to 1 equiv of complex **8** in deuterated dichloromethane. The purity of **8** was previously confirmed via CHN analysis. The resulting ^{1}H NMR spectrum shows that the signals of both ligands remain sharp, down to 230 K, indicating a fast exchange rate between the free ligands and the according alkali-metal complexes on the NMR time scale (Scheme 5, spectrum c). In the 1:1 mixture of [12]crown-4 and compound **8**, the signal of [12]crown-4 is present at δ = 3.68 ppm. Since the chemical shifts of [12]crown-4 (spectrum e; δ = 3.62 ppm) and [Li[12]crown-4]PF_6 (spectrum d; δ = 3.77 ppm) are known and the exchange is fast on the NMR time scale the percentage of coordinated and free ligand can be deducted from the average chemical shift in the mixture according to[29]

$$\delta_{\text{average}} = n_{\text{coordinated}}\delta_{\text{coordinated}} + n_{\text{noncoordinated}}\delta_{\text{noncoordinated}}$$

This reveals that, in spectrum c, which contains both ligands, 40% of [12]crown-4 are present as complex while 60% remain noncoordinated. Similarly, the proton resonances of 1,2,7,8-tetrasila[12]crown-4 are observed at δ = 0.30 ppm (methyl groups) and 3.73 ppm (ethylene bridge) in the 1:1 mixture. Comparison of the free ligand **7** (δ = 0.22 and 3.71 ppm) and the lithium complex **8** (δ = 0.34 and 3.74 ppm) results in a ratio of 60% coordinated and 40% noncoordinated 1,2,7,8-tetrasila[12]crown-4. Note that, in spectrum c, the ligand ratio of compound **7** to [12]crown-4, determined through comparison of the integrals in the ^{1}H NMR spectrum, is 6:4. Therefore, the observed coordination ratio may only depict the ligand ratio in solution. Nevertheless, the coordination ability of ligand **7** is comparable to [12]crown-4 in the case of lithium, which is consistent with the calculated binding affinities.

The analogous analysis of **1** with [12]crown-4 and 1 equiv of lithium triflate does not lead to similarly clear results, since both ligands have a tendency to build sandwich-like complexes with lithium. This was confirmed through NMR experiments with 1,2-disila[12]crown-4 (**1**) and a 1:2 metal-to-ligand stoichiometry. In the proton NMR, the observed average chemical shift of δ = 0.33 ppm for the SiMe_2 groups is downfield, compared to the calculated median shift of ligand **1** and complex **4**, which would be at δ = 0.30 ppm, proving that more than one ligand is coordinated to lithium. The analysis of the average chemical shifts in a mixture of ligand **1**, [12]crown-4, and LiOTf in a 1:1:1 ratio, indicates 82% of 1,2-disila[12]crown-4 (**1**) and 62% of [12]crown-4 are coordinated to lithium. The ratio of coordinated disila[12]crown-4 to [12]crown-4 is 1.3:1, while the exact ligand ratio, determined through comparison of the integrals in the ^{1}H NMR-spectrum, is 1.2:1. This supports the calculated superior binding properties of ligand **1**, in comparison to [12]-crown-4.

SUMMARY AND CONCLUSIONS

In conclusion, we have shown that, on a structural level, ethylene and disilane fragments in hybrid crown ether complexes differ, with respect to the eclipsed arrangement of the methyl groups at the disilane and the staggered arrangement of hydrogen at ethylene, respectively. According to the proton NMR studies, incorporation of disilane units in organic crown ether frameworks yields a comparable complexation ability of these ligands to that of organic crown ethers. Quantum chemical studies revealed a higher complex stability of [Li(1,2-disila[12]crown-4)]$^+$, in relation to [Li[12]crown-4]$^+$. The complex stability remains in a similar range through incorporation of an equal amount of disilane and ethylene between the O atoms, as present in complex **8**, despite the high energy value for the adoption of the molecular geometry in the complex. This indicates a highly attractive interaction between ligand **7** and the metal ion, which compensates the energy of the rearrangement in the complex. Calculated Si−O and Si−C bond lengths changes of the free ligands **1** and **7** and their lithium complexes are consistent with the concept of negative hyperconjugation. However, the O atoms adjacent to the disilane fragments adopt significantly shorter bond lengths to the metal cation than the all-ethylene substituted O atoms. We suggest that negative hyperconjugation has only a minor impact on the complexation ability of disilane containing crown ethers. Hence, in addition to the electrostatic repulsion of the metal ion and the positively charged Si atom, the decrease in complexation ability of cyclosiloxanes should be reflected, with respect to the inability of oxygen to arrange in-plane. Only all-disilane-substituted crown ether O atoms of the type SiSi−O−SiSi can finally give substantiated conclusions about the impact of negative hyperconjugation and the complexation ability, which is still a matter of ongoing research.

ASSOCIATED CONTENT

Supporting Information

The Supporting Information is available free of charge on the ACS Publications website at DOI: 10.1021/acs.inorgchem.6b00267.

CCDC Nos. 1437285 (**4**), 1437286 (**5**), 1437287 (**6**), and 1437288 (**8**) contain the supplementary crystallographic data for this paper. These data can be obtained free of charge from The Cambridge Crystallographic Data Centre via www.ccdc.cam.ac.uk/data_request/cif (PDF)

Crystal data overview of compound **4** (CIF)

Crystal data overview of compound **5** (CIF)

Crystal data overview of compound **6** (CIF)

Crystal data overview of compound **8** (CIF)

AUTHOR INFORMATION

Corresponding Author

*E-mail: haenisch@chemie.uni-marburg.de.

Notes

The authors declare no competing financial interest.

ACKNOWLEDGMENTS

This work was financially supported by the Deutsche Forschungsgemeinschaft (DFG). G.T. thanks the Leopoldina Nationale Akademie der Wissenschaften for a postdoctoral scholarship. K.R. thanks Dr. Ana Torvisco (Department of

DOI: 10.1021/acs.inorgchem.6b00267
Inorg. Chem. 2016, 55, 4441−4447

Inorganic Chemistry, TU Graz) for her valuable help with the crystal structure refinement.

REFERENCES

(1) West, R.; Whatley, L. S.; Lake, K. J. *J. Am. Chem. Soc.* **1961**, *83*, 761−764.
(2) Shepherd, B. D. *J. Am. Chem. Soc.* **1991**, *113*, 5581−5583.
(3) Emeléus, H. J.; Onyszchuk, M. *J. Chem. Soc.* **1958**, *0*, 604−609.
(4) Decken, A.; Passmore, J.; Wang, X. *Angew. Chem.* **2006**, *118*, 2839−2843.
(5) Ritch, J. S.; Chivers, T. *Angew. Chem., Int. Ed.* **2007**, *46*, 4610−4613.
(6) Decken, A.; LeBlanc, F. A.; Passmore, J.; Wang, X. *Eur. J. Inorg. Chem.* **2006**, *2006*, 4033−4036.
(7) Passmore, J.; Rautiainen, J. M. *Eur. J. Inorg. Chem.* **2012**, *2012*, 6002−6010.
(8) Weinhold, F.; West, R. *J. Am. Chem. Soc.* **2013**, *135*, 5762−5767.
(9) Grabowsky, S.; Hesse, M. F.; Paulmann, C.; Luger, P.; Beckmann, J. *Inorg. Chem.* **2009**, *48*, 4384−4393.
(10) Gillespie, R. J.; Johnson, S. A. *Inorg. Chem.* **1997**, *36*, 3031−3039.
(11) Cameron, T. S.; Decken, A.; Krossing, I.; Passmore, J.; Rautiainen, J. M.; Wang, X.; Zeng, X. *Inorg. Chem.* **2013**, *52*, 3113−3126.
(12) Ouchi, M.; Inoue, Y.; Kanzaki, T.; Hakushi, T. *Bull. Chem. Soc. Jpn.* **1984**, *57*, 887−888.
(13) Takano, T.; Kasai, N.; Kakudo, M. *Bull. Chem. Soc. Jpn.* **1963**, *36*, 585−590.
(14) Chojnowski, J.; Kurjata, J. *Macromolecules* **1994**, *27*, 2302−2309.
(15) Cypryk, M. *Macromol. Theory Simul.* **2001**, *10*, 158−164.
(16) Cypryk, M.; Kurjata, J.; Chojnowski, J. *J. Organomet. Chem.* **2003**, *686*, 373−378.
(17) Sheldrick, G. M. *SHELXL14, Program for the Refinement of Crystal Structures*; Universität Göttingen: Göttingen, Germany, 2014.
(18) Dolomanov, O. V.; Bourhis, L. J.; Gildea, R. J.; Howard, J. A. K.; Puschmann, H. *J. Appl. Crystallogr.* **2009**, *42*, 339−341.
(19) *TURBOMOLE Version 6*; TURBOMOLE GmbH, 2014. (TURBOMOLE is a development of University of Karlsruhe and Forschungszentrum Karlsruhe (1989−2007), which has been TURBOMOLE GmbH since 2007.)
(20) Furche, F.; Ahlrichs, R.; Hättig, C.; Klopper, W.; Sierka, M.; Weigend, F. *WIREs Comput. Mol. Sci.* **2014**, *4*, 91−100.
(21) Weigend, F. *Phys. Chem. Chem. Phys.* **2006**, *8*, 1057−1065.
(22) Grimme, S. *J. Comput. Chem.* **2004**, *25*, 1463−1473.
(23) Klamt, A.; Schüürmann, G. *J. Chem. Soc., Perkin Trans. 2* **1993**, *2*, 799−805.
(24) Becke, A. D. *Phys. Rev. A: At., Mol., Opt. Phys.* **1988**, *38*, 3098−3100.
(25) Perdew, J. P. *Phys. Rev. B: Condens. Matter Mater. Phys.* **1986**, *33*, 8822−8824.
(26) Weigend, F.; Ahlrichs, R. *Phys. Chem. Chem. Phys.* **2005**, *7*, 3297−3305.
(27) Gjikaj, M.; Adam, A. *Z. Anorg. Allg. Chem.* **2006**, *632*, 2475−2480.
(28) Hopffgarten, v. M.; Frenking, G. *Comput. Mol. Sci.* **2012**, *2*, 43−62.
(29) Crabtree, R. H. *The Organometallic Chemistry of the Transition Metals*, 4th Edition; John Wiley & Sons, Ltd.: Hoboken, NJ, 2005.

DOI: 10.1021/acs.inorgchem.6b00267
Inorg. Chem. 2016, 55, 4441−4447

Supplementary Information

"Stable Alkali Metal Complexes of Hybrid Disila-Crown Ethers"

Kirsten Reuter,[†] Magnus R. Buchner,[†] Günther Thiele[‡] and Carsten von Hänisch[†]*

[†]Fachbereich Chemie and Wissenschaftliches Zentrum für Materialwissenschaften (WZMW), Philipps-Universität Marburg, Hans-Meerwein-Straße 4, 35032 Marburg, Germany

‡Department of Chemistry, 210 Lewis Hall, University of California, Berkeley, California 94720, United States

Table 1. X-Ray measurement, structure solution and refinement of **4**.

Compound	**4**
Empirical formula	$C_{11}H_{24}F_3Li_1O_7S_1Si_2$
Formula weight /g·mol^{-1}	420.48
Crystal color, shape	colorless needle
Crystal size /mm^3	0.365 x 0.154 x 0.126
Crystal system	monoclinic
Space group	$P2_1/c$
a / Å	13.7300(7)
b / Å	16.9864(7)
c / Å	16.9091(8)
β / °	93.9527(17)°
V /Å^3	3934.2(3)
Z	8
ρ_{calc} / g·cm^{-3}	1.420
μ ($Mo_{K\alpha}$) /mm^{-1}	0.341
2 θ range /°	2.75 – 26.97
Reflections measured	47121
Independent reflections	8569, R_{int} = 0.0671
R_1 ($I > 2\sigma(I)$)	0.0381
wR_2 (all data)	0.0910
GooF (all data)	1.134
Largest diff. peak and hole /e.Å^{-3}	0.700 and -0.462

Table 2. X-Ray measurement, structure solution and refinement of **5**.

Compound	**5** · C_6H_6
Empirical formula	$C_{18}H_{34}Cl_1Na_1O_9Si_2$
Formula weight /g·mol^{-1}	509.07
Crystal color, shape	Colorless needle
Crystal size /mm^3	0.537 x 0.167 x 0.124
Crystal system	triclinic
Space group	$P\bar{1}$
a / Å	9.8536(5)
b / Å	9.9654(5)
c / Å	13.0638(6)
α /°	91.291(2)
β / °	92.820(2)
γ /°	97.259(2)
V /Å^3	1270.4(1)
Z	2
ρ_{calc} / g·cm^{-3}	1.331
μ ($Mo_{K\alpha}$) /mm^{-1}	0.305
2 θ range /°	2.540 – 27.183
Reflections measured	33119
Independent reflections	5632 , R_{int} = 0.0338
R_1 ($I > 2\sigma(I)$)	0.043
wR_2 (all data)	0.1141
GooF (all data)	1.068
Largest diff. peak and hole /e.Å^{-3}	1.006 and -0.305

Table 3. X-Ray measurement, structure solution and refinement of **6**.

Compound	**6**
Empirical formula	$C_{14}H_{32}F_6K_1O_6P_1Si_2$
Formula weight /g·mol^{-1}	536.64
Crystal color, shape	Colorless block
Crystal size /mm^3	0.394 x 0.155 x 0.125
Crystal system	monoclinic
Space group	$P2_1$
a / Å	10.4027(13)
b / Å	12.3519(11)
c / Å	10.4989(9)
β / °	119.580(2)
V /Å^3	1173.2(2)
Z	2
ρ_{calc} / g·cm^{-3}	1.519
μ ($Mo_{K\alpha}$) /mm^{-1}	0.471
2 *θ* range /°	2.25 – 25.29
Reflections measured	15778
Independent reflections	4295 , R_{int} = 0.0631
R_1 ($I > 2\sigma(I)$)	0.0330
wR_2 (all data)	0.0603
GooF (all data)	1.020
Largest diff. peak and hole /e.Å^{-3}	0.292 and -0.208

Table 4. X-Ray measurement, structure solution and refinement of **8**.

Compound	**8** · CH_2Cl_2
Empirical formula	$C_{13}H_{34}Cl_2F_6Li_1O_4P_1Si_4$
Formula weight /g·mol^{-1}	589.57
Crystal color, shape	colorless rhomb
Crystal size /mm^3	0.534 x 0.500 x 0.488
Crystal system	orthorhombic
Space group	$P2_12_12_1$
a / Å	10.1612(3)
b / Å	13.9035(5)
c / Å	19.6348(7)
V /Å^3	2773.93(16)
Z	4
ρ_{calc} / g·cm^{-3}	1.412
μ ($Mo_{K\alpha}$) /mm^{-1}	0.522
2 θ range /°	2.539 – 31.755
Reflections measured	31968
Independent reflections	9322, R_{int} = 0.0454
R_1 ($I > 2\sigma(I)$)	0.0355
wR_2 (all data)	0.0732
GooF (all data)	1.035
Largest diff. peak and hole /e.Å^{-3}	0.363 and -0.396

ChemComm

COMMUNICATION

View Article Online
View Journal | View Issue

Cite this: *Chem. Commun.*, 2016, 52, 13265

Received 14th September 2016,
Accepted 14th October 2016

DOI: 10.1039/c6cc07520g

www.rsc.org/chemcomm

Synthesis and coordination ability of a partially silicon based crown ether†

Kirsten Reuter,[a] Günther Thiele,[b] Thomas Hafner,[c] Frank Uhlig[c] and Carsten von Hänisch*[a]

The first hybrid crown ether with two adjacent disilane fragments was synthesized through reaction of $O(Si_2Me_4Cl)_2$ (3) with $O(C_2H_4OH)_2$. By means of DFT calculations, the complexation ability of 1,2,4,5-tetrasila[12]crown-4 (7) towards Li^+ was determined to be considerably higher compared to [12]crown-4.

Compared to ethers, siloxanes show low coordination ability towards Lewis acids.[1] This has been attributed to both electronic and structural effects: the electron density of the O atom is less available as a result of the interaction between the lone pairs of the O atom and the σ*-orbitals of the Si–C bonds.[2] This negative hyperconjugation is then not only competing with the coordination of a cation, it also leads to a widening of the Si–O bond angle.[3] On the other hand, the ionic character of the Si–O bond increases with larger Si–O angles.[4] The high anionicity of the O atom would rather suggest an increased coordination ability. This is especially not the case for linear Si–O linkages, which can be related to the delocalized and hardly polarizable electron density at the O atom.[5] Additionally, recent studies revealed that the positively polarized Si atoms in siloxanes show a considerable repulsion towards cations.[6]

Lately, we reported on hybrid crown ethers which partially incorporate a disilane and an ethylene framework (Scheme 1).[7] The presence of Si_2-units leads to a structural equivalence of organic and inorganic fragments with respect to the number of atoms between the donor atom. By DFT calculations and dynamic proton NMR studies, the stability of these hybrid disila-crown ethers complexes was determined to be in the range of organic crown ether complexes. Unexpectedly, the insertion of disilane units does not reduce the coordination ability of the ligand as has been observed for ring contracted crown ethers like [17]crown-6 and sila[17]crown-6.[8] However, all hitherto described disila-crown ethers incorporate fully C or half C and half Si affected donor atoms.[7] In this work, we report on the synthesis and the complex stability of a novel crown ether bearing organic, hybrid and fully inorganic substituted O atoms.

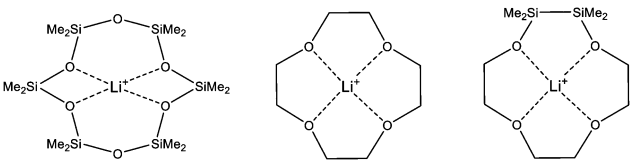

Scheme 1 Binding modes of Li^+ in D_6 (D = Me_2SiO) (left), [12]crown-4 (centre) and 1,2-disila[12]crown-4 (right) with increasing complex stability from left to right.

A suitable synthesis path for the required inorganic fragment, $O(Si_2Me_4Cl)_2$ (**3**), starts with the asymmetric chlorination of 1,1,2,2-tetramethyldisilane by the use of trichloroisocyanuric acid (TCCA) (Scheme 2).[9] The chlorination of the two Si atoms appears not to happen statistically. The distribution of the three resulting disilane species can be estimated from comparison of the intensities of the respective similar substituted Si atoms in the ^{29}Si NMR spectrum (Fig. 1). 10% of $H_2Si_2Me_4$ (**I**), 70% of HSi_2Me_4Cl (**1**) and 20% of $Cl_2Si_2Me_4$ (**II**) can thusly be detected in the reaction solution. Since a small excess of TCCA has been used, the proportion of **I** and **II** is not precisely equal. After distillative purification, 64% of the asymmetrically chlorinated species **1** was obtained.

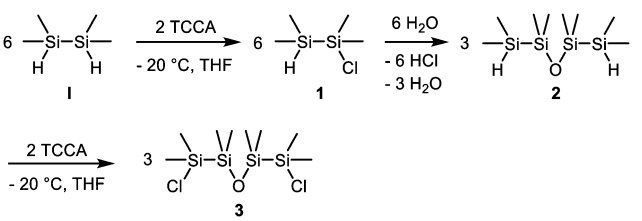

Scheme 2 Synthesis path for the inorganic building block of a partially Si based crown ether.

[a] *Fachbereich Chemie and Wissenschaftliches Zentrum für Materialwissenschaften (WZMW), Philipps-Universität Marburg, Hans-Meerwein-Straße 4, 35043 Marburg, Germany. E-mail: haenisch@chemie.uni-marburg.de; Fax: +49-6421-2825653*
[b] *Department of Chemistry, University of California, 210 Lewis Hall, Berkeley, California 94720, USA*
[c] *Institut für Anorganische Chemie, TU Graz, 6330 Graz, Austria*

† Electronic supplementary information (ESI) available: Experimental details, computational and crystallographic data. CCDC 1499542 (7) and 1499541 (8). For ESI and crystallographic data in CIF or other electronic format see DOI: 10.1039/c6cc07520g

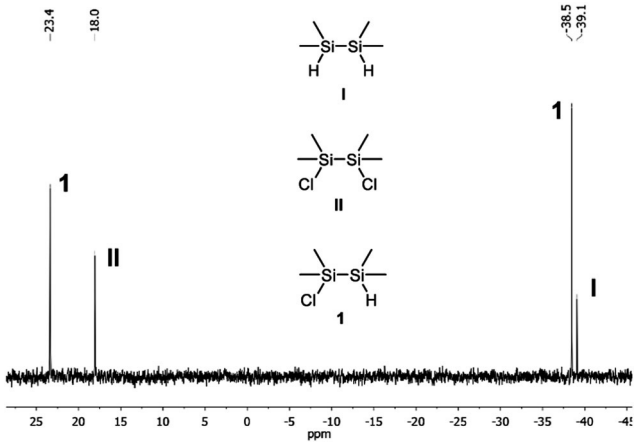

Fig. 1 ^{29}Si{H} NMR spectrum (D_2O-capillary, 59.60 MHz, DEPT) of the formation of HSi_2Me_4Cl after removal of the cyanuric acid.

Through treatment with water, compound **1** hydrolysed and condensed immediately in a clean reaction to $O(Si_2Me_4H)_2$ (**2**). In case of impurities, **2** was purified *via* distillation (b.p. 86 °C, 10 mmHg). In the next step, the remaining H atoms at the terminal Si atoms were again substituted by the use of TCCA. In this reaction, the purity of the educt **2** is crucial, since **3** cannot be purified by distillation as a result of its low decomposition temperature. Simultaneously, another synthesis path for **3** was investigated. However, the abstraction of the phenyl groups of $O(Si_2Me_4Ph)_2$ (**5**) by trifluoromethanesulfonic acid was not successful so that this route was finally abandoned.[10]

In high dilution, the inorganic building block **3** reacts selectively with diethylene glycol and triethylamine (NEt_3) to the hybrid crown ether 1,2,4,5-tetrasila[12]crown-4 (**6**) (Scheme 3). Compound **6** is a highly viscous oil which is well miscible in DCM, THF and *n*-pentane, but only poorly miscible in water. Differently to the before described hybrid crown ethers like 1,2-disila[12]crown-4, no decomposition of **6** was observed in water. Ligand **6** incorporates three different types of O atoms, C, C/Si and Si substituted ones, which generates ideal conditions for comparing the respective coordination ability.

Lithium triflate, which is only poorly soluble in DCM, was the salt of choice. The complexation by compound **6** in DCM was successfully completed after 4 h, resulting in a clear solution. Removal of the solvent led to a colourless solid, which gave colourless rods after recrystallization from DCM/cyclopentane. [Li(1,2,4,5-tetrasila[12]-crown-4)OTf] (**7**) crystallizes in the orthorhombic space group *Pbca* with sixteen molecules per unit cell. Different to the free ligand **6**, complex **7** is highly sensitive towards traces of water as has also been observed for other disila-crown ether complexes.[7]

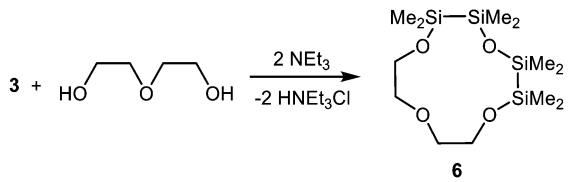

Scheme 3 Reaction path for ligand **6**.

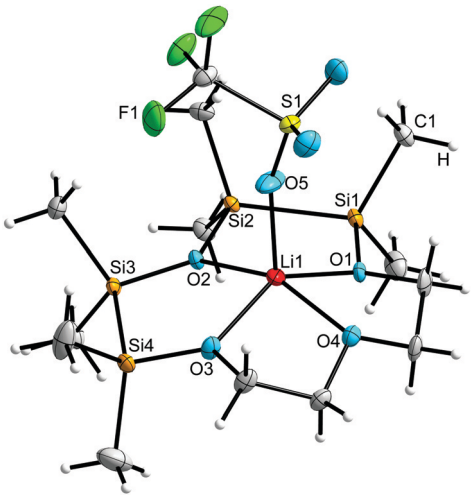

Fig. 2 Molecular structure of **7** in the crystal. Thermal ellipsoids represent the 50% probability level.

In complex **7**, the lithium cation is coordinated by the four crown ether O atoms and one O atom of the trifluoromethanesulfonate anion (OTf^-), giving a coordination number of five (Fig. 2). The three different types of O atoms in the ligand show strong deviations in their bond lengths to Li^+. While the completely C and the hybrid substituted O atoms O4, O1 and O3 establish similar bond lengths of 209.4(6) pm and 201.4(6) pm respectively, the fully Si substituted O atom O2 exhibits a considerably long bonding (231.0(6) pm, Table 1). These results, based on X-ray diffraction, differ from the calculated structure of [Li(1,2,4,5-tetrasila[12]crown-4)]$^+$, wherein the anion has not been considered. As can be deducted from the bond lengths between Li^+ and the three types of O atoms, the cation is more centrally located, with the hybrid substituted O atoms showing the shortest and the C substituted O atom the longest bonding (Table 1). These deviations may be a result of the hydrogen bonding between the anion $F_3CSO_3^-$ and the H atoms of the methyl groups. The distance between one of the H and one F atom (260.0(2) pm) is beneath the sum of the van-der-Waals-radii. The orientation of $F_3CSO_3^-$ towards the methyl groups may push the cation in the direction of the carbon bonded O atom (O4).

As expected, the presence of two disilane units leads to an increased diameter of the crown ether. The ring diameter affects – beside the donor ability of the used anion – the position of the cation in the crown ether. For example in [Li([12]crown-4)OTf] (**8**),‡ Li^+ is located 83.6(9) pm above the plane generated by the ring systems' O atoms. In the hybrid crown ether complex **7**, the Li^+ cation is located only 56.8(4) pm above the plane of the ligands' O atoms, indicating a better matching with respect to the ring diameter. Moreover, the adjacent disilane units lead to an asymmetric structure of the ligand as a result of the mean Si–Si bond length of 233.8(1) pm and the comparatively smaller mean C–C bonding of 150.1(1) pm (Fig. 3). As reported before, C–O–C bond angles are generally smaller compared to Si–O–Si angles.[11] In complex **7**, the bond angles widen in the series C–O–C < C–O–Si < Si–O–Si (Table 1).

As observed in the reported disila-crown ether complexes, the interaction p(O) → σ*(Si–C) can be observed with respect to

Table 1 Selected bond lengths and angles of compound **7**, the calculated cationic complex [Li@**6**]$^+$ and ligand **6**

		Selected bond lengths [pm]						Selected angles [°]		
Compound	Method	Li–O_C[a]	Li–$O_{C/Si}$[b]	Li–O_{Si}[c]	Si–O_C[a]	Si–O_{Si}[c]	Si–C	C–O–C	C–O–Si	Si–O–Si
7	XRD[d]	209.4(6)	201.4(6)	231.0(6)	167.2(2)	166.7(1)	185.8(5)	113.6(2)	123.4(2)	134.3(1)
[Li(1,2,4,5-tetrasila[12]crown-4)]$^+$	DFT[e]	207.1	197.1	201.6	171.3	170.8	187.3	114.8	123.6	129.1
6	DFT[e]	—	—	—	168.2	165.2	188.4	114.7	124.2	149.2

[a] The subscript C denotes complete carbon-substituted O atoms. [b] O atoms bonded to both carbon and silicon. [c] Completely Si bonded O atoms. [d] Structures determined by X-ray diffraction. [e] BP86 functional at the def2-TZVP level of theory.

the bond lengths changes between the calculated free ligand structure and the calculated complex.[8] Compound **6** incorporates two types of Si bonded O atoms: completely Si (Si–O_{Si}) or Si and C bonded (Si–O_C) oxygen atoms. As expected, the impact of the negative hyperconjugation is stronger in the Si–O_{Si} bond, which shows a considerable increase of the calculated bond length by complexation from 165.2 pm in the free ligand to 170.8 pm in the lithium complex. The impact is smaller for the Si–O_C bonds, which increase from 168.2 pm to 171.3 pm (Table 1). Simultaneously, the eight Si–C bonds length show a minor decrease as a result of the complexation.

In the ^{29}Si{H} NMR spectrum, the two signals show a considerable downfield shift from δ = 0.9/10.9 ppm in the free ligand to 9.4/15.9 ppm in the complex, indicating a strong electron withdrawing effect through the complexation of Li^+. The signal at 0.9 ppm in the free ligand corresponds to the equivalent Si atoms Si2 and Si3 (Fig. 3), which undergo a downfield shift of $\Delta(\delta)$ = 8.5 ppm, while Si1 and Si4 show a smaller shift of $\Delta(\delta)$ = 5.0 ppm. This can be attributed to the stronger polarisation of the completely Si bonded O atom O2 in the solution, in comparison to the Si/C bonded O atoms O1 and O3.

The relative binding affinity of **6** was studied by means of DFT, implemented in Turbomole V7.0.1,[12] using the BP86 functional[13] and the def2-TZVP basis set with inclusion of dispersion interactions.[14] As presented in Scheme 4, the exchange of Li^+ from [12]crown-4 to the hybrid crown ether **6** releases 29.51 kJ mol^{-1}. Particularly with respect to the before described constitution isomer 1,2,7,8-tetrasila[12]crown-4,[7] the complexation ability of **6** is considerably high. Hybrid disila-crown ethers generally require an increased amount of energy for changing from the free ligand structure to the structure found within the complex compared to organic crown ethers. This can be related to the adoption of the ecliptic arrangement of the methyl groups in the complex, which has also been observed in cyclosiloxane complexes.[6] The methyl groups in complex **7** also adopt an approximately eclipsed conformation with dihedral angles between 4.2(1)°–13.5(1)°. This is not only the case between directly bonded Si atoms, but also consistently between the O bridged Si atoms Si2 and Si3.

Calculation of the energy differences ΔE_{geom} between the free and the complex geometries of 1,2,4,5-tetrasila[12]crown-4 (**6**) reveals a value of 69.89 kJ mol^{-1} (Scheme 5), which is 9.48 kJ mol^{-1} higher compared to the constitution isomer 1,2,7,8-tetrasila[12]crown-4.[7] The increased amount of energy refers to the steric hindrance of the ecliptic Me groups between the O bridged disilane fragments. Although ΔE_{geom} is high, ligand **6** shows a considerably coordination ability (Scheme 4), which implies a significant electrostatic attraction between the completely Si substituted O atom and Li^+. With respect to the before described complex stabilities of disila-crown ethers,[7] the basicity of the C_2H_4 and/or Si_2Me_4 substituted O atoms increases in the series $O_C < O_{Si/C} < O_{Si}$.

In conclusion, the synthesis of O bridged disilane fragments like $O(Si_2Me_4Cl)_2$ (**3**) provides access to Si based crown ethers. For this purpose, TCCA serves as versatile agent for the asymmetric chlorination of tetramethyldisilane. The hybrid crown ether **6** was obtained through reaction of **3** with diethylene glycol and incorporates three types of O atoms: completely C, half C and Si and completely Si substituted ones. Complexation of lithium triflate yielded single crystals of [Li(1,2,4,5-tetrasila[12]crown-4)OTf] (**7**), which were characterized by X-ray diffraction. DFT calculations (BP86 functional and def2-TZVP basis set) revealed that the presence of the completely Si substituted O atom leads to a considerable increase of the coordination ability compared to [12]crown-4 as well as the hitherto known disila-crown ethers.[7] The strong interaction between the lithium cation and the completely Si bonded O2 atom has also been confirmed by ^{29}Si NMR spectroscopy by reference to the significantly high downfield shift of the equivalent Si atoms Si2 and Si3.

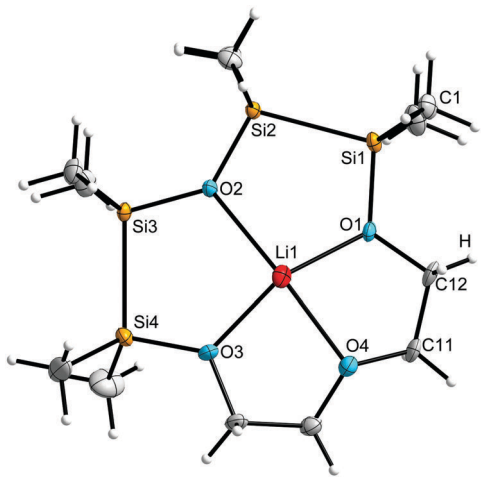

Fig. 3 A top-view of the molecular structure in the crystal of [Li(1,2,4,5-tetrasila[12]crown-4)]$^+$. The anion is not displayed.

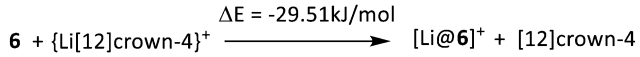

Scheme 4 Relative energy for the lithium exchange from [12]crown-4 to 1,2,4,5-tetrasila[12]crown-4 (**6**) as obtained from DFT calculations.

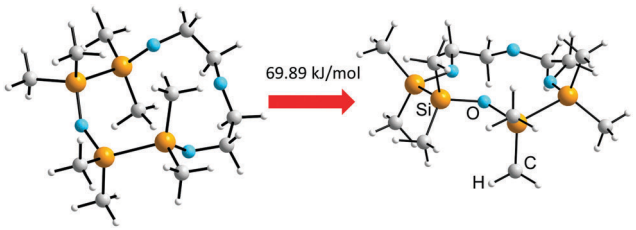

Scheme 5 Illustration of the transformation from the free ligand structure to the molecular structure found within the complex and the resulting energetic effort.

These results challenge the so far accepted theories concerning the low coordination ability of siloxanes. Negative hyperconjugation – although present – doesn't significantly reduce the basicity of disila-crown ethers. Through insertion of disilane instead of monosilane fragments, the distance between the Si atoms and the metal cation is high enough to prevent electrostatic repulsion – a major factor for the low coordination ability of cyclosiloxanes.[6] The synthesis and complexation of completely disilane based crown ethers will give further insights into the coordination ability of Si bonded O atoms, which is still a matter of ongoing research.

This work was financially supported by the Deutsche Forschungsgemeinschaft (DFG). G. T. thanks the Leopoldina Nationale Akademie der Wissenschaften for a postdoctoral scholarship.

Notes and references

‡ For details concerning compound **8** see ESI.†

1 (*a*) H. J. Emeléus and M. Onyszchuk, *J. Chem. Soc.*, 1958, 604; (*b*) R. West, L. S. Whatley and K. J. Lake, *J. Am. Chem. Soc.*, 1961, **83**, 761; (*c*) B. D. Shepherd, *J. Am. Chem. Soc.*, 1991, **113**, 5581; (*d*) C. von Hänisch, O. Hampe, F. Weigend and S. Stahl, *Angew. Chem., Int. Ed.*, 2007, **46**, 4775; (*e*) U. Dittmar, H. C. Marsmann and E. Rikowski, in *Organosilicon Chemistry Set: From Molecules to Materials*, ed. N. Auner and J. Weis, Wiley-VCH Verlag GmbH, Weinheim, Germany, 2005, ch. 64b.
2 (*a*) A. Decken, J. Passmore and X. Wang, *Angew. Chem., Int. Ed.*, 2006, **118**, 2839; (*b*) J. S. Ritch and T. Chivers, *Angew. Chem., Int. Ed.*, 2007, **46**, 4610.
3 F. Weinhold and R. West, *J. Am. Chem. Soc.*, 2013, **135**, 5762.
4 (*a*) R. J. Gillespie and S. A. Johnson, *Inorg. Chem.*, 1997, **36**, 3031; (*b*) J. Passmore and J. M. Rautiainen, *Eur. J. Inorg. Chem.*, 2012, 6002.
5 S. Grabowsky, M. F. Hesse, C. Paulmann, P. Luger and J. Beckmann, *Inorg. Chem.*, 2009, **48**, 4384.
6 (*a*) A. Decken, F. A. LeBlanc, J. Passmore and X. Wang, *Eur. J. Inorg. Chem.*, 2006, 4033; (*b*) T. S. Cameron, A. Decken, I. Krossing, J. Passmore, J. M. Rautiainen, X. Wang and X. Zeng, *Inorg. Chem.*, 2013, **52**, 3113.
7 K. Reuter, M. R. Buchner, G. Thiele and C. von Hänisch, *Inorg. Chem.*, 2016, **55**, 4441.
8 M. Ouchi, Y. Inoue, T. Kanzaki and T. Hakushi, *Bull. Chem. Soc. Jpn.*, 1984, **57**, 887.
9 (*a*) S. Varaprath and D. H. Stutts, *J. Organomet. Chem.*, 2007, **692**, 1892; (*b*) T. Hafner, Master thesis, TU Graz, 2013.
10 Experimental details on the synthesis of $PhSi_2Me_4Cl$ (**4**) and $O(Si_2Me_4Ph)_2$ (**5**) can be found in the ESI†.
11 S. Shambayati, J. F. Blake, S. G. Wierschke, W. L. Jorgensen and S. L. Schreiber, *J. Am. Chem. Soc.*, 1990, **112**, 697.
12 Turbomole Version 7.0.1, Turbomole GmbH 2016. Turbomole is a development of University of Karlsruhe and Forschungszentrum Karlsruhe 1989–2007, Turbomole GmbH since 2007.
13 (*a*) F. Weigend and R. Ahlrichs, *Phys. Chem. Chem. Phys.*, 2005, **7**, 3297; (*b*) F. Weigend, *Phys. Chem. Chem. Phys.*, 2006, **8**, 1057; (*c*) M. Dolg, H. Stoll, A. Savin and H. Preuss, *Theor. Chim. Acta*, 1989, **75**, 173; (*d*) H. Stoll, B. Metz and M. Dolg, *J. Comput. Chem.*, 2002, **23**, 767.
14 (*a*) S. Grimme, J. Antony, S. Ehrlich and H. Krieg, *J. Chem. Phys.*, 2010, **132**, 154104; (*b*) S. Grimme, S. Ehrlich and L. Goerigk, *J. Comput. Chem.*, 2011, **32**, 1456.

Supplementary Information

"Synthesis and Coordination Ability of a Partially Silicon Based Crown Ethers"

Kirsten Reuter,[a] Günther Thiele,[b] Thomas Hafner,[c] Frank Uhlig[c] and Carsten von Hänisch[a]*

[a] Fachbereich Chemie and Wissenschaftliches Zentrum für Materialwissenschaften (WZMW), Philipps-Universität Marburg, Hans-Meerwein-Straße, 35043 Marburg, Germany, Fax: +49-6421-2825653. E-Mail: haenisch@chemie.uni-marburg.de

[b] Department of Chemistry, 210 Lewis Hall, University of California, Berkeley, California 94720, United States

[c] Institut für Anorganische Chemie, TU Graz, 6330 Graz, Austria

Content

Alternative Synthesis Path for $O(Si_2Me_4Cl)$

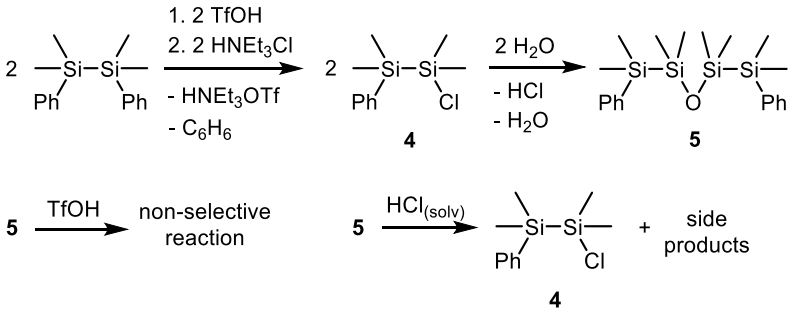

Scheme 1: Synthesis path for the Si based fragment of a hybrid crown ether based on the substitution of phenyl groups at the silicon atoms with trifluoromethanesulfonic acid (TfOH). Abstraction of the phenyl groups as the final step is not possible with strong acids.

Another suitable reaction path for compound **3** seemed to be the asymmetric chlorination of 1,1,2,2-tetramethyl-1,2-diphenyldisilane by the use of trifluoromethanesulfonic acid (TfOH)[1] and subsequent chlorination with $HNEt_3Cl$ leading to compound **4**. The asymmetric chlorodisilane **4** reacts in aqueous solution to the condensed species **5**, which can be purified *via* column chromatography. However, the O atom in **5** inhibits the following abstraction of the terminal phenyl groups by strong acids as can be seen from the reaction with $HCl_{(solv)}$, which leads to the chlorinated compound **4** (Scheme 3). Since the O atom is preferably being attacked by acids rather than the Ph-groups, this synthesis path turned out to be an impasse.

Experimental Section

General: Except the synthesis of compound **5**, all working procedures were conducted under rigorous exclusion of oxygen and moisture using a Schlenk line and nitrogen atmosphere. Solvents were dried and freshly distilled before use. NMR spectra were recorded with BRUKERACANCEHD 300, BRUKERDRX400 or with BRUKERAVANCE 500 and visualized with MESTRENOVA.[2] IR vibrational spectra were gathered with the BRUKER ALPHA ATR-FT-IR. The starting materials 1,2-dihydrido-1,1,2,2-tetramethyldisilane[3] and 1,2-diphenyl-1,1,2,2-tetramethyldisilane[4] were prepared by reported methods.

Computational Details. Calculations were performed with the program system TURBOMOLE V7.0.1.[8,9] The RI approximation[10], and dispersion corrections[11,12] were applied throughout. For all calculations the BP86 functional[13,14] was chosen, utilizing a def2-TZVP basis set.[15-17]

Me_4Si_2HCl (**1**): To 26.0 g (0.22 mol, 3eq.) of 1,1,2,2-tetramethyldisilane diluted in 600 mL of THF, 17.0 g (0.73 mol, 1eq.) of TCCA at -20 °C was slowly added. The reaction was allowed to warm to room temperature and stirred for 4 h. The solvent and the raw product were separated *in vacuo* from the cyanuric acid, followed by distillative removal of THF and purification of compound **1** (bp. 125-128 °C) at ambient pressure. 21,5 g (64%) of **1** was obtained as a colourless oil.
^{1}H NMR (C_6D_6, 300 MHz): δ = 0.09 (d, $^3J_{HH}$ = 4.5 Hz, C*H*$_3$, 6H), 0.34 (s, C*H*$_3$, 6H), 3.89 (h, $^3J_{HH}$ = 4.5 Hz, Si*H*, 1H) ppm; ^{13}C NMR (C_6D_6, 75 MHz): δ = -7.3 (s, *C*H$_3$), 2.4 (s, *C*H$_3$) ppm; ^{29}Si{H} NMR (C_6D_6, 60 MHz): δ = -39.1 (s, *Si*H), 22.8 (s, *Si*Cl) ppm; ^{29}Si NMR (C_6D_6, 60 MHz): δ = -39.1 (d *br*, $^1J_{SiH}$ = 181.3 Hz, *Si*H), 22.8 (br, *Si*Cl) ppm. IR: $\tilde{\nu}$ = 2963(m), 1261(s), 1091(s), 1019(s), 799(vs), 701(w).

$O(Si_2Me_4H)_2$ (**2**): At ambient temperature, 5.0 mL of H_2O was added to 10.0 mL (9.30 g, 0.61 mol) of **1** diluted in 50 mL of *n*-pentane and stirred for 1 h. The aqueous phase was removed and washed two times with 30 mL of *n*-pentane. The combined organic phases were dried over $MgSO_4$ for 4 h and subsequently filtered. The solvent was removed *in vacuo* and 7,55 g (99%) of product **2** was obtained as a colourless oil.
^{1}H NMR (C_6D_6, 300 MHz): δ = 0.16 (d, $^3J_{HH}$ = 4.6 Hz, C*H*$_3$, 12H), 0.27 (s, C*H*$_3$, 12H), 3.92 (h, $^3J_{HH}$ = 4.6 Hz, Si*H*, 2H) ppm; ^{13}C NMR (C_6D_6, 75 MHz): δ = -6.7 (s, *C*H$_3$), 2.7 (s, *C*H$_3$) ppm; ^{29}Si{H} NMR (C_6D_6, 60 MHz): δ = -43.1 (s, *Si*H), 6.0 (s, *Si*O) ppm; ^{29}Si NMR (C_6D_6, 60 MHz): δ = -43.1 (d *br*, $^1J_{SiH}$ = 172.8 Hz, *Si*H), 6.0 (br, *Si*O) ppm. IR: $\tilde{\nu}$ = 2957(m), 2093(m), 1411(w), 1257(s), 1024(vs), 910(m), 882(s), 767(vs), 699(m), 655(s), 417(w).

$O(Si_2Me_4Cl)_2$ (**3**): At -20 °C, 1.27 g (5.5 mmol, 2eq.) of TCCA was slowly added to 2.05 g (8.2 mmol, 3eq.) of **2** diluted in 50 mL of THF. The reaction was allowed to warm to room temperature and stirred for 4 h. The solvent was removed under at reduced pressure and the product dissolved in *n*-pentane. Insoluble cyanuric acid was removed *via* filtration and the product washed two times with *n*-pentane. The solvent was removed *in vacuo* and 2.31 g (88%) of compound **3** was obtained as a colourless oil.
^{1}H NMR (C_6D_6, 300 MHz): δ = 0.25 (s, C*H*$_3$, 12H), 0.38 (s, C*H*$_3$, 12H) ppm; ^{13}C NMR (C_6D_6, 75 MHz): δ = 1.4 (s, *C*H$_3$), 1.9 (s, *C*H$_3$) ppm; ^{29}Si{H} NMR (C_6D_6, 60 MHz): δ = 2.4 (s, *Si*O), 16.7 (s, *Si*Cl) ppm. IR $\tilde{\nu}$ = 2955(w), 1400(w), 1249(s), 1038(s), 823(s), 765(vs), 721(m), 686(m), 666(s), 651(s), 554(w), 482(s), 407(s).

$PhMe_4Si_2Cl$ (4): At 0 °C, 1.28 g (8.6 mmol, 1eq.) of freshly distilled trifluoromethanesulfonic acid was slowly added to 2.32 g (8.6 mmol, 1eq.) of 1,2-diphenyl-1,1,2,2-tetramethyldisilane diluted in 60 mL of toluene. The solution was allowed to warm to ambient temperature and stirred for additional 3 h. Subsequently, 2.37 g (17.2 mmol, 2eq.) of triethylammoniumchloride was added and the suspension was stirred for 9 d. Insoluble salts were filtered and the solvent was removed at reduced pressure. After distillative purification (32 °C, $1\cdot10^{-3}$mbar) 0.94 g (48%) of **4** was obtained as a colourless oil.
^{1}H NMR (C_6D_6, 300 MHz): δ = 0.17 (s, C*H*$_3$, 6H), 0.20 (s, C*H*$_3$, 6H), 7.02-7.04 (m, $H_{arom.}$, 3H), 7.26-7.29 (m, $H_{arom.}$, 2H) ppm; ^{13}C NMR (C_6D_6, 75 MHz): δ = -4.6 (s, *C*H$_3$), 2.1 (s, *C*H$_3$), 128.4 (s, $C_{arom.}$), 129.4 (s, $C_{arom.}$), 134.2 (s, $C_{arom.}$), 136.9 (s, $C_{arom.}$) ppm; ^{29}Si{H} NMR (C_6D_6, 60 MHz): δ = -22.0 (s, *Si*Ph), 22.8 (s, *Si*Cl) ppm. IR $\tilde{\nu}$ = 3068(w), 2955(w), 2895(w), 1486(m), 1427(w), 1248(s), 1106(s), 1053(w), 999(w), 831(s), 814(s), 786(vs), 768(s), 729(s), 696(vs), 670(m), 644(m), 618(m), 495(s), 465(s), 419(m).

$O(Si_2Me_4Ph)_2$ (5): To 0.94 g (4.1 mmol) of **4** in 20 mL of *n*-pentane, 5 mL of 1M HCl_{aq} was added at ambient temperature. The solution was stirred for 2 h. The aqueous phase was was extracted with 20 mL *n*-pentane twice. The combined organic phases were dried over $MgSO_4$ for 4 h and subsequently filtered. The solvent was evaporated *in vacuo* and the resulting colourless oil was purified using column chromatography (silicagel; heptane : di*iso*propyl ether = 3:1) yielding 0.66 g (81%) of **5** as colourless oil.
^{1}H NMR (C_6D_6, 300 MHz): δ = 0.19 (s, C*H*$_3$, 12H), 0.34 (s, C*H*$_3$, 12H), 7.18-7.26 (m, $H_{arom.}$, 6H), 7.48-7.51 (m, $H_{arom.}$, 4H) ppm; ;
^{13}C NMR (C_6D_6, 75 MHz): δ = -3.8 (s, *C*H$_3$), 2.4 (s, *C*H$_3$), 128.2 (s, $C_{arom.}$), 128.9 (s, $C_{arom.}$), 134.3 (s, $C_{arom.}$), 139.2 (s, $C_{arom.}$) ppm;

^{29}Si{H} NMR (C_6D_6, 60 MHz): δ = -25.8 (s, *Si*Ph), 4.9 (s, *Si*O) ppm. IR $\tilde{\nu}$ = 3068(w), 2951(m), 2894(w), 1427(m), 1403(w), 1246(s), 1105(m), 1036(s), 825(s), 793(s), 768(vs), 729(s), 695(vs), 658(m), 638(s), 470(m), 441(w).

1,2,4,5-Tetrasila[12]crown-4 (**6**): At room temperature, 1.0 mL (1.09 g, 3.4 mmol, 1eq.) of **5** diluted in 50 mL of Et_2O and 0.23 mL (0.36 g, 3.4 mmol, 1eq.) of dihydroxydiethylether, 0.95 mL (0.69 g, 6.8 mmol, 2eq.) of NEt_3 in 50 mL of Et_2O were simultaneously dropped into 50 mL of Et_2O. The solution was stirred for 12 h. Subsequently, the solvent was removed at reduced pressure and 50 mL of *n*-pentane was added to the residue, followed by filtration. The solvent from the resulting clear solution was evaporated under reduced pressure and 1.13 g (94%) of compound **6** was obtained as a viscous colourless oil.
^{1}H NMR (CD_2Cl_2, 300 MHz): δ = 0.19 (s, C*H*$_3$, 12H), 0.22 (s, C*H*$_3$, 12H), 3.55-3.58 (m, C*H*$_2$, 4H), 3.76-3.79 (m, C*H*$_2$, 4H) ppm; ^{13}C NMR (CD_2Cl_2, 75 MHz): δ = -0.17 (s, *C*H$_3$), 3.1 (s, *C*H$_3$), 64.4 (s, *C*H$_2$), 73.4 (s, *C*H$_2$) ppm; ^{29}Si{H} NMR (CD_2Cl_2, 60 MHz): δ = 0.9 (s, *Si*O$_{Si}$), 10.9 (s, *Si*O$_C$) ppm. IR $\tilde{\nu}$ = 2950(w), 2866(w), 1245(s), 1143(m), 1094(m), 1032(s), 940(m), 854(m), 825(m), 798(s), 759(vs), 716(m), 680(m), 658(m), 634(m). MS (ESI$^+$): *m/z* (%) 353.1451 [*M*H]$^+$ (45).

[Li(1,2,4,5-tetrasila[12]crown-4)OTf] (**7**): To 1.13 g (3.2 mmol, 1eq.) of **6** diluted in 50 mL of dichloromethane, 0.65 g (4.2 mmol, 1eq.) of lithium triflate was added at ambient temperature and stirred for 18 h. In the case of an excess of the lithium salt, the resulting suspension was filtered and the solvent of the resulting clear solution was evaporated *in vacuo*. The remaining white powder was washed twice with 20 mL of *n*-pentane and subsequently dried under reduced pressure. 0.95 g (57%) of **7** was obtained as an amorphous colourless powder. Single crystals in form of colourless rods were grown after 4 d in a mixture of dichloromethane and cyclopentane (2:1) at -35 °C.
^{1}H NMR (CD_2Cl_2, 300 MHz): δ = 0.37 (s, C*H*$_3$, 12H), 0.40 (s, C*H*$_3$, 12H), 3.69-3.72 (m, C*H*$_2$, 4H), 3.84-3.87 (m, C*H*$_2$, 4H) ppm; ^{13}C NMR (CD_2Cl_2, 75 MHz): δ = -1.3 (s, *C*H$_3$), 2.9 (s, *C*H$_3$), 61.4 (s, *C*H$_2$), 71.4 (s, *C*H$_2$) ppm; ^{29}Si{H} NMR (CD_2Cl_2, 60 MHz): δ = 9.4 (s, *Si*O$_{Si}$), 15.9 (s, *Si*O$_C$) ppm; ^{7}Li NMR (CD_2Cl_2, 194 MHz): δ = -0.9 (s) ppm; ^{19}F NMR (CD_2Cl_2, 283 MHz): δ = -78.8 (s) ppm. IR $\tilde{\nu}$ = 2955(w), 2874(w), 2834(w), 2791(w), 1572(w), 1548(w), 1523(w), 1478(w), 1349(m), 1254(s), 1157(s), 1131(m), 1042(s), 950(m), 928(s), 855(s), 829(s), 800(m), 766(m), 729(s), 696(vs), 637(s), 598(m), 571(vs), 524(w), 514(w), 493(w), 476(w), 449(w), 410(w). MS (ESI$^+$): *m/z* 359.1533 (%) [*M*]$^+$-OTf (100).

[Li([12]crown-4)OTf] (**8**): To 0.52 g (2.9 mmol, 1eq.) of [12]crown-4 and 0.46 g (2.9 mmol, 1eq.) of lithium triflate, 15 mL of dichloromethane was added. The suspension was stirred for 18 h resulting in a clear solution. The quantity of the solvent was reduced until saturation. After 7 d at room temperature, crystals of **8** (0.72 g, 75%) were obtained as colourless needles.
^{1}H NMR (CD_2Cl_2, 300 MHz): δ = 3.77 (s, C*H*$_2$, 16H) ppm; ^{13}C NMR (CD_2Cl_2, 75 MHz): δ = 67.8 (s, *C*H$_2$) ppm; ^{7}Li NMR (CD_2Cl_2, 194 MHz): δ = -0.7 (s) ppm; ^{19}F NMR (CD_2Cl_2, 283 MHz): δ = -79.2 (s) ppm. IR $\tilde{\nu}$ = 2940.3(w), 1492.8(w), 1449(w), 1363(w), 1290(s), 1255(s), 1226(s), 1158(s), 1132(s), 1082(vs), 1037(s), 1018(s), 928(s), 862(m), 757(w), 638(vs), 589(w), 572(w), 530(w), 516(m), 448(m). MS (ESI$^+$): *m/z* 183.1203 (%) [*M*]$^+$-OTf (60).

Crystal Structure Data collection was performed using a BRUKER D8 QUEST diffractometer at 100(2) K with MoK_α radiation and graphite monochromatization (λ = 0.71073). Structure solution was realized by direct methods, refinement with full-matrix-least-squares against F^2 using SHELXL-14 and Olex2 software.[5,6] The presentation of crystal structures was done with DIAMOND4.2.2[7]

Table S1. X-Ray measurement, structure solution and refinement details of **7**.

Empirical formula	$C_{13}H_{32}F_3Li_1O_7S_1Si_4 \cdot CH_2Cl_2$
Formula weight /g·mol^{-1}	593.67
Crystal color, shape	colourless plate
Crystal size /mm^3	0.525 x 0.225 x 0.214
Crystal system	orthorhombic
Space group	*Pbca*
a / Å	14.6745(7)
b / Å	24.0048(11)
c / Å	32.5952 (14)
V /Å^3	11481.9(9)
Z	16
ρ_{calc} / g·cm^{-3}	1.374
μ (Mo$_{K\alpha}$) /mm^{-1}	0.515
2 ϑ range /°	2.52 – 25.19
Reflections measured	146908
Independent reflections	10456, R_{int} = 0.0774
R_1 ($I > 2\sigma(I)$)	0.0534
wR_2 (all data)	0.1273
GooF (all data)	1.040
Largest diff. peak and hole /e.Å^{-3}	2.079 and -0.982

Table S2. X-Ray measurement, structure solution and refinement details of **8**.

Empirical formula	$C_9H_{16}F_3Li_1O_7S_1$
Formula weight /g·mol^{-1}	332.22
Crystal color, shape	colourless needle
Crystal size /mm^3	0.543 x 0.216 x 0.201
Crystal system	monoclinic
Space group	$P2_1/n$
a / Å	7.0179(3)
b / Å	13.5605(6)
c / Å	14.8661(7)
β /°	96.427(2)°
V /Å^3	1405.86(11)
Z	4
ρ_{calc} / g·cm^{-3}	1.570
μ (Mo$_{K\alpha}$) /mm^{-1}	0.293
2 ϑ range /°	2.76 – 28.48
Reflections measured	45249
Independent reflections	3538, R_{int} = 0.0258
R_1 ($I > 2\sigma(I)$)	0.0259
wR_2 (all data)	0.0663
GooF (all data)	1.087
Largest diff. peak and hole /e.Å^{-3}	0.376 and -0.495

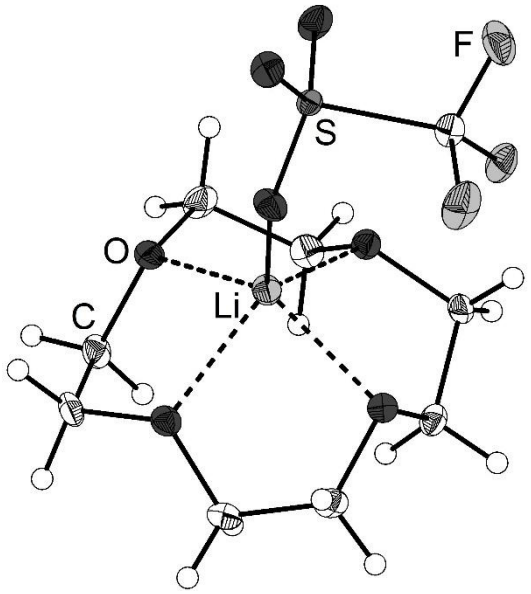

Figure S1: Molecular structure of **8** in the crystal. Thermal ellipsoids represent the 50% probability level.

[1] W. Uhlig, *Prog. Polym. Sci.* **2002**, *27*, 255.
[2] M. R. Willcott, *J. Am. Chem. Soc.* **2009**, *131*, 13180.
[3] C. Ackerhans, P. Böttcher, P. Müller, H. W. Roesky, I. Usón, H.-G. Schmidt, M. Noltemeyer, *Inorg. Chem.* **2001**, *40*, 3766.
[4] H. Gilman, K. Shiina, D. Aoki, B. J. Gaj, D. Wittenberg, T. Brennan, *J. Organomet. Chem.* **1968**, *13*, 323.
[5] G. M. Sheldrick, SHELXL14, Program for the Refinement of Crystal Structures, Universität Göttingen, **2014**.
[6] O. V. Dolomanov, L. J. Bourhis, R. J. Hildea, J. A. K. Howard, H. Puschmann, *J. Appl. Crystallogr.* **2009**, 42, 339-341.
[7] H. Putz, K. Brandenburg, Diamond – Crystal and Molecular Structure Visualization, Crystal Impact, Kreuzherrenstr. 102, 53227 Bonn, Germany.
[8] TURBOMOLE Version 7.0.1, TURBOMOLE GmbH 2016.TURBOMOLE is a development of University of Karlsruhe and Forschungszentrum Karlsruhe 1989–2007, TURBOMOLE GmbH since 2007.
[9] F. Furche, R. Ahlrichs, C. Hättig, W. Klopper, M. Sierka, F. Weigend, *WIREs Comput. Mol. Sci.* **2014**, *4*, 91-100.
[10] F. Weigend, *Phys. Chem. Chem. Phys.* **2006**, *8*, 1057-1065.
[11] S. Grimme, J. Antony, S. Ehrlich, H. Krieg, *J. Chem. Phys.* **2010**, *132*, 154104.
[12] S. Grimme, S. Ehrlich, L. Goerigk, *J. Comput. Chem.* **2011**, *32*, 1456.
[13] A. D. Becke, *Phys. Rev. A* **1988**, *38*, 3098-3100.
[14] J. P. Perdew, *Phys. Rev. B* **1996**, *33*, 8822-8824.
[15] F. Weigend, R. Ahlrichs, *Phys. Chem. Chem. Phys.* **2005**, *7*, 3297.
[16] F. Weigend, *Phys. Chem. Chem. Phys.* **2006**, *8*, 1057.
[17] M. Dolg, H. Stoll, A. Savin, H. Preuss, *Theor. Chim. Acta* **1989**, *75*, 173.
[18] H. Stoll, B. Metz, M. Dolg, *J. Comput. Chem.*, **2002**, *23*, 767.

inorganics

MDPI

Article

Structural Study of Mismatched Disila-Crown Ether Complexes

Kirsten Reuter, Fabian Dankert, Carsten Donsbach and Carsten von Hänisch *

Fachbereich Chemie and Wissenschaftliches Zentrum für Materialwissenschaften (WZMW), Philipps-Universität Marburg, Hans-Meerwein Straße 4, D-35032 Marburg, Germany; kirsten.reuter@staff.uni-marburg.de (K.R.); Dankert@students.uni-marburg.de (F.D.); donsbach@students.uni-marburg.de (C.D.)

* Correspondence: haenisch@chemie.uni-marburg.de; Tel.: +49-0-6421-282-5612

Academic Editor: Matthias Westerhausen

Received: 21 December 2016; Accepted: 2 February 2017; Published: 9 February 2017

Abstract: Mismatched complexes of the alkali metals cations Li^+ and Na^+ were synthesized from 1,2-disila[18]crown-6 (**1** and **2**) and of K^+ from 1,2,4,5-tetrasila[18]crown-6 (**4**). In these alkali metal complexes, not all crown ether O atoms participate in the coordination, which depicts the coordination ability of the C-, Si/C-, and Si-bonded O atoms. Furthermore, the inverse case—the coordination of the large Ba^{2+} ion by the relatively small ligand 1,2-disila[15]crown-5—was investigated, yielding the dinuclear complex **5**. This structure represents a first outlook on sandwich complexes based on hybrid crown ethers.

Keywords: hybrid crown ether; siloxane; disilane; mismatch complex; host–guest chemistry

1. Introduction

The nature of the Si–O bond has been intensively studied over the past six decades. In the 1960s especially, the large valence angle in disiloxanes and the unusual short Si–O bond length, e.g., in $O(SiH_2Me_2)_2$, were issued in numerous publications [1,2]. The low basicity of siloxanes was originally attributed to an electron-withdrawing tendency of the silyl groups of the type p(O)→d(Si) [3–5]. This approach was later discarded in favor of hyperconjugation interactions between p(O)→σ*(Si–C) [6–8]. Alternatively, in an opposed model based on calculations of the electron density function, the Si–O bond was described as essentially ionic due to the high difference in electronegativity between Si and O [9,10]. Careful theoretical studies on the basicity of $O(SiH_2Me_2)_2$ and OEt_2 revealed that the lower electrostatic attraction in siloxanes results from the repulsion between the positively charged Si atoms and Lewis acids [11]. This proceeding has recently been extended on cyclosiloxanes [12], which were previously described as pseudo crown ethers or inorganic crown ethers [13–15]. However, the structural analogy to organic crown ethers is poor, since siloxanes feature O atoms linked by $–SiMe_2–$ rather than $–CH_2CH_2–$. Additionally, organic ring-contracted crown ethers exhibit an eminently reduced coordination ability, as has been shown in the referencing of [17]crown-6, in which only one $–CH_2CH_2–$ unit was replaced by $–CH_2–$ [16,17]. Consequently, higher comparability between organic crown ethers and cyclosiloxanes can be provided by extension of the $–SiMe_2–$ unit to $–SiMe_2SiMe_2–$. Recent studies of hybrid [12]crown-4 featuring one or two disilane fragments in a residuary organic crown ether framework revealed an increasing coordination ability towards Li^+ in the series C–O–C < C–O–Si < Si–O–Si (Scheme 1) [18,19].

Another deviation between the hitherto discussed cyclosiloxanes and organic crown ethers concerns the substituents at Si and C. Up to date, neither cyclosiloxanes with H-substituents at the Si atoms nor permethylated crown ethers have been synthesized, which complicates a meaningful comparison of the two types of ligands. Calculation of the energy changes for crown

ethers, cyclosiloxanes and hybrid crown ethers going from the free ligand geometries to complex geometries—determined as relaxation energy—revealed that $SiMe_2$ or Si_2Me_4 containing ligands require steadily more energy for adopting the complex geometry [12,18,19]. The complex stability is directly affected by the relaxation energy, which is in the case of the hybrid crown ethers compensated by the particularly high donor ability of the O atoms [18].

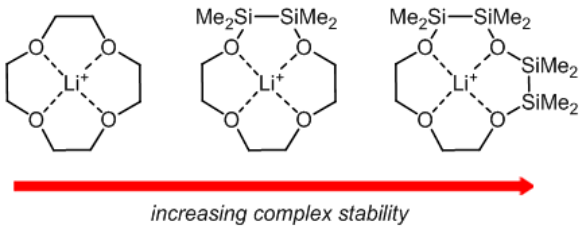

Scheme 1. Binding modes and relative binding affinities of Li^+ in [12]crown-4, 1,2-disila[12]crown-4, and 1,2,4,5-tetrasila[12]crown-4.

The hitherto described hybrid crown ethers exhibit up to three different types of O atoms—all C-, C/Si-, and all Si-bonded ones (Scheme 1). To experimentally explore the competition between the basicity of the inequivalent O atoms and the energy effort for reaching the ligand geometry in the complex, we performed complexation reactions using small alkali and alkaline earth metal ions and comparatively large ligands. As a result, the ligand exceeds with its ring diameter the ionic radius of the Lewis acid. Since particularly Si-based crown ethers show limited flexibility [11–15,18,19], we expected not all O_{crown} atoms to participate in the coordination of the metal center [20–22]. The first mismatch structure of a hybrid crown ether was very recently published and is constituted of 1,2-disila[18]crown-6 and $Ca(OTf)_2$ ($OTf = {}^-OSO_2CF_3$) [23]. Therein, one of the C-bonded O atoms does not participate in the coordination of Ca^{2+}, showing the preference of the metal ion to be coordinated by the Si/C-linked O atoms. This preference depicts the coordination ability of the O atoms in partially Si-based crown ethers and is a matter of investigation in this work.

2. Results and Discussion

2.1. Mismatch Complexes Involving 1,2-Disila[18]crown-6 with Li^+ and Na^+

The hybrid ligand 1,2-disila[18]crown-6 was synthesized in a single step reaction from 1,2-dichlorodisilane and pentaethylene glycol (Scheme 2). Prior studies have shown that Li^+ matches well with 1,2-disila[12]crown-4 and Na^+ with 1,2-disila[15]crown-5 [18], so that the two cations together with 1,2-disila[18]crown-6 are supposed to fulfil the criteria of a mismatch. Reaction of 1,2-disila[18]crown-6 with lithium hexafluorophosphat in a 1:1 stoichiometry yielded a highly viscous oil. After freezing at −196 °C and subsequent storage at −35 °C for 3 days, Compound **1** crystallized in the space group $P2_1/c$ in the form of colorless planks. In the solid-state structure of Compound **1**, Li^+ is coordinated by five of the six crown ether O atoms (Figure 1). The non-coordinating completely carbon-bonded O atom O5 shows an atomic distance of 295.7(5) pm to the Li^+ cation. The PF_6 anion does not interact with the cation. The coordination polyhedron can be described as a distorted trigonal bipyramid (Figure 2). The three equatorial O atoms (O2, O4, O6) establish shorter bond lengths to the cation than the two axial O atoms. The shortest Li–O bond length has a value of 194.9(5) pm (Li1–O6), while the longest bond length measures 224.8(5) pm (Li1–O1). Compared to the hitherto known lithium complexes of hybrid sila-crown ethers, the Li1–O1 bond length is elongated, which may be the result of the strongly twisted ligand. Typically, the O atoms in sila-crown ethers complexes adopt an approximately planar conformation [13–15,18,19]. The disilane fragment in **1** is roughly coplanar to the thereon bonded O atoms O1 and O2, but the organic part of the ligand is strongly twisted and is wrapped around the metal center.

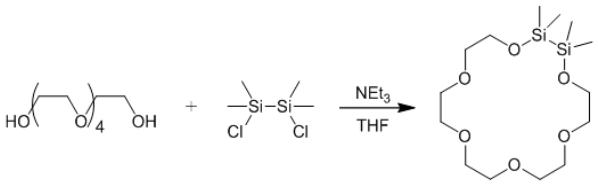

Scheme 2. Synthesis path for 1,2-disila[18]crown-6 [18].

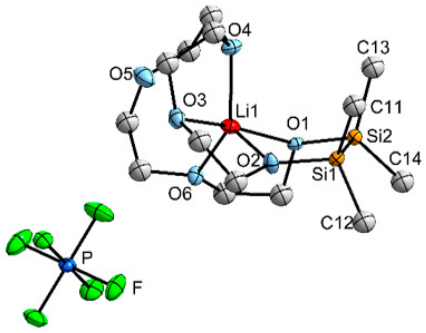

Figure 1. Molecular structure of [Li(1,2-disila[18]crown-6)]PF_6 (**1**) in the crystal. Thermal ellipsoids represent the 50% probability level. Hydrogen atoms are omitted for clarity. Selected bond lengths (pm) and angles (°): Si1–Si2: 235.1(1), Si1–O1: 168.9(2), Si2–O2: 167.9(2), Li1–O1: 224.8(5), Li1–O2: 200.4(5), Li1–O3: 212.1(5), Li1···O5: 295.7(5), Li1–O6: 194.9(5), O3–Li1–O1: 169.4(2), O2–Li1–O4: 115.9(2), O2–Li1–O6: 111.6(2), O4–Li1–O6: 132.5(2), O1–Li1–O4: 102.3(2), O1–Li1–O2: 88.9(2), O1–Li1–O6: 79.5(2), C11–Si2–Si1–C13: 9.6(1), C12–Si2–Si1–C14: 8.9(1).

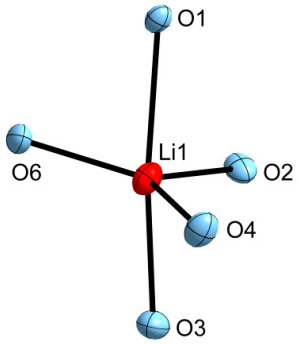

Figure 2. Trigonal bipyramidal coordination polyhedron of the lithium cation in [Li(1,2-disila[18]crown-6)]PF_6 (**1**).

Trigonal bipyramidal coordination is common for mismatched crown ether complexes of lithium [24,25], while in [12]crown-4 complexes the square-pyramid [26,27] or in sandwich complexes the square antiprism is the usual coordination polyhedron [28]. In prior studies on sila-crown ether complexes, it was already shown that the Me groups at the Si atoms take in a roughly eclipsed conformation [18,19,23]. In **1**, the Me groups adopt with dihedral angles of 9.6(1)° for C11–Si2–Si1–C13, and 8.9(1)° for C12–Si2–Si1–C14 the expected conformation of the complex. As a result, the attractive electrostatic interaction between the Si/C-bonded O atoms and the Li^+ cation must compensate for the required energy effort of the ecliptic arrangement. The $^{29}Si\{^1H\}$-NMR signal shifts from δ = 11.4 ppm in the free ligand to δ = 15.6 ppm in **1**, indicating a strong electrostatic interaction between Li^+ and O1 and O2. The strong shift also reflects the hard Lewis acidity in comparison to K^+, since in [K(1,2-disila[18]crown-6)PF_6] the respective $^{29}Si\{^1H\}$-NMR signal is at δ = 13.0 ppm [18].

By an analogous reaction of $NaPF_6$ with 1,2-disila[18]crown-6, single crystals in form of colorless blocks were obtained from dichloromethane/benzene (2:1). [Na(1,2-disila[18]crown-6)PF_6] (**2**) crystallizes in the triclinic space group $P\bar{1}$ as a monomeric contact ion pair (Figure 3). Na^+ is

coordinated by five of the six crown ether O atoms and additionally by two F atoms of the PF_6 anion. The coordination sphere of Na^+ cannot be assigned to a hitherto described polyhedron as a result of its strong distortion. Compared to K^+, the ionic radius of Na^+ is still too small for the cavity diameter of 1,2-disila[18]crown-6. As a result, O1 is with a distance of 453.2(3) pm not participating in the coordination of the metal ion. This leads to a strong distortion of the ring system, as O1 is located significantly beneath the mean plane of the other crown ether O atoms. Additionally, the Me groups at the Si atoms show a staggered arrangement, which is the common structure in free hybrid crown ethers [18]. In the case of Compound **2**, the electrostatic attraction between O1 and Na^+ apparently does not compensate for the adoption of an ecliptic arrangement, so the cation is preferably coordinated by the C-bonded O atoms. The coordinating Si- and C-linked O atom O2 establishes a bond length of 238.5(3) pm to the metal, while the completely C-linked O atoms show values between 237.0(3) and 247.3(2) pm. The $^{29}Si\{^1H\}$-NMR signal of Compound **2** appears at δ = 14.3 ppm and, according to the respective Lewis acidity of Li^+ and Na^+, is less low-field shifted compared to **1**.

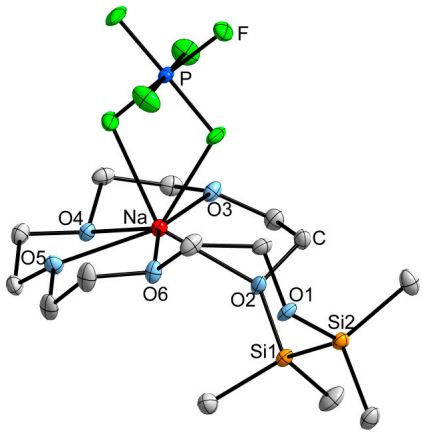

Figure 3. Molecular structure of [Na(1,2-disila[18]crown-6)PF_6] (**2**) in the crystal. Thermal ellipsoids represent the 50% probability level. Hydrogen atoms are not displayed. Selected bond lengths (pm) and angles (°): Na···O1: 453.2(3), Na–O2: 238.5(3), Na–O3: 247.3(2), Na–O4: 244.9(3), Na–O5: 237.0(3), Si1–Si2: 235.8(1), Si2–O1: 166.2(3), Si1–O2: 167.5(2), Si2–O1–C10: 122.7(2), Si1–O2–C1: 121.7(2), C4–O4–C5: 113.5(2), C13–Si1–Si2–C11: 66.0(2), C14–Si1–Si2–C12: 65.6(2).

2.2. Determination of ΔE_{geom} in 1,2-Disila[18]crown-6 Complexes

As was shown in prior studies, hybrid crown ethers require steadily more energy than organic crown ethers for adopting the ligand structure within the complex [18,19,23]. The increase in relaxation energy was partially attributed to the sterically disfavored ecliptic arrangement of the Me groups bonded at the Si atoms. That was found to be the predominant conformation in the hybrid crown ether complex structures. The mismatched complexes **1** and **2** offer two different coordination modes of the Si/C-bonded O atoms: In the case of the Li-complex **1**, both Si-bonded O atoms participate in the coordination, while in the Na-complex **2**, only one of the Si/C-bonded O atoms binds to the metal center, which results in a staggered arrangement of the Me groups. It follows that 1,2-disila[18]crown-6 is expected to exhibit considerable different energy levels in the complex structures **1** and **2**. The energy difference ΔE_{geom} was determined by DFT calculations, implemented in Turbomole V7.0 [28], using the BP86 functional [29–32] and the def2-TZVP basis set with inclusion of dispersion interactions [33,34]. Accordingly, the energy of the ligand increases by 77.58 $kJ \cdot mol^{-1}$ for adopting the structure found within $[Li(1,2\text{-disila}[18]\text{crown-}6)]^+$ and by 29.24 $kJ \cdot mol^{-1}$ for $[Na(1,2\text{-disila}[18]\text{crown-}6)]^+$. The electrostatic attraction between the Si/C-bonded O atoms and Na^+ does not compensate for the ecliptic conformation of the Me groups. By contrast, Li^+ must exhibit a significantly increased electrostatic attraction to the hybrid-bonded O atoms. The mismatched

hybrid crown ether complexes **1** and **2** therefore suggest that the cation exerts a major impact on the coordination modes of the ligand.

The optimized structure of the free ligand 1,2-disila[18]crown-6 shows, as expected, a staggered conformation of the methyl groups at the silicon atoms. The DFT calculated structures of the cations in Compounds **1** and **2** exhibit only very small differences in the structural parameter in comparison to the structures obtained by X-ray diffraction (see XYZ data in the ESI).

2.3. Mismatch Involving 1,2,4,5-Tetrasila[18]crown-6 and K^+

The synthesis of hybrid crown ethers with a higher amount of disilane units was very recently described for 1,2,4,5-tetrasila[12]crown-4 [19]. In an analogous reaction of $O(Si_2Me_4Cl)_2$ with tetraethylene glycol, the ligand 1,2,4,5-tetrasila[18]crown-6 (**3**) was synthesized using high dilution of the agents to prevent polymerization (Scheme 3). Compound **3** is a highly viscous, colorless oil. Through the presence of two disilane units, the ring size is further increased in comparison to 1,2-disila[18]crown-6. In the $^{29}Si\{^1H\}$-NMR spectrum, Compound **3** shows two signals which can be assigned to the two types of Si atoms: The Si–O–Si entity appears at δ = 2.1 ppm, the C–O–Si entity is low-field shifted and appears at δ = 11.0 ppm.

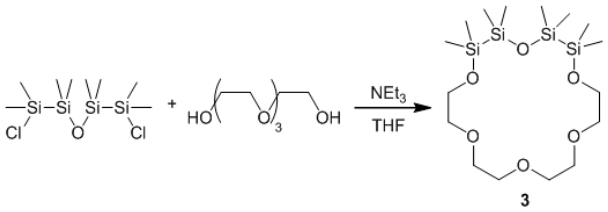

Scheme 3. Synthesis path of 1,2,4,5-tetrasila[18]crown-6 (**3**).

Treatment of **3** with KPF_6 yielded the corresponding, highly water sensitive complex [K(1,2,4,5-tetrasila[18]crown-6)PF_6] (**4**). Different to the hitherto known hybrid disila-crown ether complexes, **4** is directly after removal of the volatiles an oily compound, which crystallizes within 18 h at ambient temperature in form of colorless planks in the space group $P2_1/n$.

As observed in the Na^+ complex **2**, Compound **4** is a monomeric contact ion pair (Figure 4). The cation is coordinated by five of the six crown ether O atoms and three F atoms of the anion, giving a coordination number of eight. The incorporation of two disilane units into the ring system leads to an increased ring diameter so that K^+, which commonly matches perfectly with [18]crown-6, has a too small ionic radius for the ligand **3**. The inorganic part sticks out, showing an interatomic distance of 505.5(2) pm between the completely Si substituted O atom O2 and the metal ion. The Me groups at the Si atoms adopt an approximately staggered conformation with average dihedral angles of 84.2(2)° at Si1/Si2 and 59.8(2)° at Si3/Si4. Worth mentioning is the unusual orientation of Si4: In all hitherto known sila-crown ether complexes, the Si atoms bonded to coordinating O atoms are approximately arranged in plane with the crown ether O atoms [12–15,18,19,23]. In contrast to this, Si4 is considerably located beneath the mean plane of the coordinating O atoms. The Si/C-bonded O atoms O1 and O3 show O–K bond lengths of 283.8(2) and 279.4(2) pm, whereas the fully C-substituted O atoms O4–O6 establish average bond lengths of 273.7(2) pm. It can therefore be assumed that K^+ is stronger coordinated by the carbon-based part of the hybrid crown ether **3**. Compared to [K(1,2-disila[18]crown-6)PF_6], which incorporates only one disilane unit and in which all crown ether atoms are participating in the coordination, the mean O–K bond lengths are in **4** considerably shorter [18]. This can be related to the coordination number of 8 in **4** compared to 9 in [K(1,2-disila[18]crown-6)PF_6]. The Si2–O2–Si3 bond angle is 143.8(1)°, this is a typical value for siloxanes [1,2]. Also the Si4–O3–C9 bond angle of 123.3(2)° is in the expected range [18,19]. Only the Si1–O1–C16 angle is with 117.8(1)° smaller than usually observed and is similar to that found in C–O–C bindings, e.g., C14–O6–C15 with 112.3(2)°.

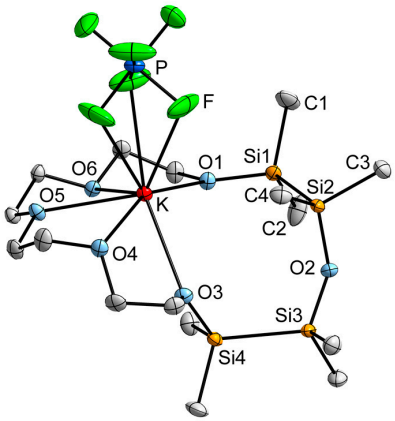

Figure 4. Molecular structure of [K(1,2,4,5-tetrasila[18]crown-6)PF_6] (**4**) in the crystal. Thermal ellipsoids represent the 50% probability level. Hydrogen atoms are not displayed. Selected bond lengths (pm) and angles (°): K–O1: 283.8(2), K···O2: 505.5(2), K–O3: 279.4(2), K–O4: 274.4(2), K–O5: 272.3(2), K–O6: 274.3(2), Si1–Si2: 234.9(1), Si1–O1: 166.5(2), Si2–O2: 164.5(2), Si3–O2: 165.2(2), Si4–O3: 166.7(2); Si4–O3–C9: 123.3(2), Si2–O2–Si3: 143.8(1), Si1–O1–C16: 117.8(1), C14–O6–C15: 112.3(2), C1–Si1–Si2–C4: 84.1(2), C2–Si1–Si2–C3: 84.2(1), C6–Si3–Si4–C8: 59.5(1), C5–Si3–Si4–C7: 60.1(1).

The reluctance of K^+ to interact with the Si-substituted O atoms was also observed in solution and can be deducted from the shifts in the $^{29}Si\{^1H\}$-NMR spectrum: The resonance signal of Si2/Si3 shows only a slight low-field shift to δ = 2.7 ppm (Δ(δ) = 0.6 ppm) and the signal of Si1/Si4 appears at δ = 11.9 ppm (Δ(δ) = 0.9 ppm). In comparison, the $^{29}Si\{^1H\}$-NMR signals of 1,2-disila[18]crown-6 shift from δ = 11.4 ppm in the free ligand to δ = 13.0 ppm in the potassium complex [18]. The small shift of the $^{29}Si\{^1H\}$ signal indicates that also in solution O2 shows only minor interaction with the K^+ ion, owing to the high energy effort of Si_2Me_4 fragments to adopt the ecliptic geometry.

2.4. The Inverse Case: 1,2-Disila[15]crown-5 and Ba^{2+}

Beside experiments involving large ligands with comparatively small cations, we also investigated the inverse mismatch case, i.e., 1,2-disila[15]crown-5 with $BaOTf_2$ (OTf = $^-OSO_2CF_3$). Prior studies revealed that Ba^{2+} perfectly matches with 1,2-disila[18]crown-6 and 1,2-disila-benzo[18]crown-6. In the corresponding complex, Ba^{2+} is located in one plane with the coordinating O atoms and is saturated by two triflate groups, which are arranged upon and beneath the crown ether mean plane [23]. Reaction of 1,2-disila[15]crown-5 with $BaOTf_2$ in 1:1 stoichiometry yielded colorless blocks of [Ba(1,2-disila[15]crown-5)OTf_2]$_2$ (**5**) in the triclinic space group $P\bar{1}$. Different to the hitherto known sila-crown ether complexes, **5** forms a dinuclear complex (Figure 5). The four triflate anions act as bridges between the two metal centers and participate in the saturation of the coordination sphere with four O atoms, respectively. Furthermore, Ba^{2+} is coordinated by the five crown ether O atoms, giving a coordination number of 9. The ion Ba(1) is located 156.8(2) pm above the calculated mean plane of the O_{crown} atoms, which reflects the small ring diameter of 1,2-disila[15]crown-5 compared to the ionic radius of Ba^{2+}. The disilane units of the crown ethers show in opposite directions to each other as a result of the sterically demanding methyl groups. The typical approximately ecliptic arrangement of the methyl groups in sila-crown ethers complexes can also be found in Compound **5**. However, the dihedral angles have values of 26.1(3)° and 22.8(3)° and accordingly show stronger deviations from the ideal ecliptic arrangement compared to those found in other hybrid-crown ether complexes. The Si/C-bonded O atoms O1 and O5 establish bond lengths of 283.4(1) and 286.5(1) pm to the cation and are in a similar range with C-bonded O atoms, which show O–Ba bonds between 280.4(1) and 287.7(1) pm. Ba^{2+} is furthermore strongly coordinated by the triflate O atoms since the bonding to Ba(1) has an average value of 275.7(4) pm. Another indication for the weak coordination of Ba^{2+} by

1,2-disila[15]crown-5 was revealed by mass spectrometric analysis: Only [Na(1,2-disila[15]crown-5)]$^+$ was detected. Na^+ is a common impurity in mass spectrometers, so Ba^{2+} was immediately replaced.

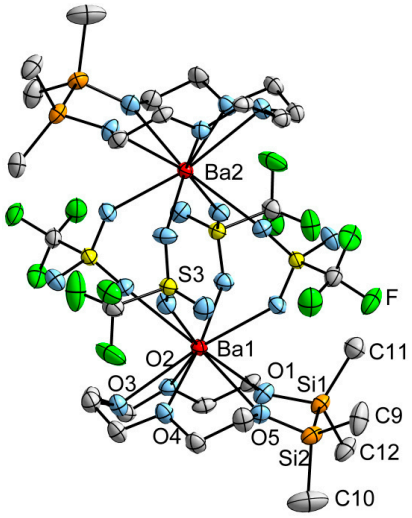

Figure 5. Molecular structure of [Ba(1,2disila[15]crown-5)$OTf_2]_2$ (**5**) in the crystal. Thermal ellipsoids represent the 50% probability level. Hydrogen atoms are not displayed. Selected bond lengths (pm) and angles (°): Ba1–O1: 283.4(1), Ba1–O2: 287.7(1), Ba1–O3: 280.4(1), Ba1–O4: 287.7(4), Ba1–O5: 286.5(1), Ba1–O_{OTf}: 269.4(1)–278.7(1), Si1–Si2: 234.6(2), Si1–O1: 167.2(4), 165.9(3), Ba1···Ba2: 527.1(2), Si1–O1–C1: 121.5(3), Si2–O5–C8: 121.6(3), C4–O3–C5: 114.9(4), C11–Si1–Si2–C9: 26.1(3), C12–Si1–Si2–C10: 22.8(3).

3. Materials and Methods

3.1. General Experimental Technique

All working procedures were conducted under exclusion of oxygen and moisture using Schlenk techniques under a nitrogen atmosphere. Solvents were dried and freshly distilled before use. Nuclear magnetic resonance (NMR) spectra were recorded with BRUKER Model AVANCE HD300, BRUKER Model DRX400, or BRUKER Model AVANCE500 spectrometers (Bruker Corporation, Rheinstetten, Germany) and were visualized with MestReNova [35]. Infrared (IR) spectra were recorded in attenuated total reflectance (ATR) mode on a BRUKER model ALPHA FT-IR. MS spectrometry was measured on a LTQ-FT (ESI, Thermo Fischer Scientific, Darmstadt, Germany) or on a JEOL AccuTOF-GC (LIFDI, JEOL, Freising, Germany). Elemental analysis data cannot be provided due to the presence of fluorine in the samples, which harm the elemental analysis devices. The ligands 1,2-disila[18]crown-6 and 1,2-disila[15]crown-5 [18] and $O(Si_2Me_4Cl)_2$ [19] were prepared by reported methods.

3.2. Computational Details

Calculations were performed with Turbomole V7.0 [28]. The resolution of identity (RI) approximation, dispersion corrections [29–32], and the conductor-like screening (COSMO) model [36] were applied, the latter with default settings. For all calculations the BP86 functional and def2-TZVP basis set [33,34] were chosen.

3.3. Crystal Structures

Data collection was performed on a Bruker D8 Quest or a Stoe IPDS II diffractometer at 100(2) K with Mo Kα radiation and graphite monochromatization. Structure solution was done by direct methods, refinement with full-matrix-least-squares against F^2 using shelxs-2014, shelxl-2014, shelxt-2014, and olex2 software (Table 1) [37,38]. The presentation of crystal structures was done

with Diamond4.2.2 [39]. CCDC 1517535 (**1**), 1517536 (**2**), 1517537 (**4**), and 1517538 (**5**) contain the supplementary crystallographic data for this paper. These data can be obtained free of charge from The Cambridge Crystallographic Data Centre via www.ccdc.cam.ac.uk/data_request/cif.

Table 1. Crystal Structure Data.

Empirical Formula	$C_{14}H_{30}Li_1O_6Si_2F_6P_1$	$C_{14}H_{32}F_6Na_1O_6P_1Si_2$	$C_{16}H_{40}F_6K_1O_6Si_4P_1$	$C_{28}H_{55}Ba_2F_{12}O_{22}S_4Si_4$
Formula weight ($g \cdot mol^{-1}$)	502.47	520.53	624.91	1487.00
Crystal color, shape	colorless plank	colorless block	colorless plank	colorless block
Crystal size (mm)	0.134 × 0.189 × 0.382	0.060 × 0.271 × 0.284	0.138 × 0.140 × 0.539	0.232 × 0.245 × 0.509
Crystal system	monoclinic	triclinic	monoclinic	triclinic
Space group	$P2_1/c$	$P\bar{1}$	$P2_1/n$	$P\bar{1}$
Formula units	4	2	4	2
Temperature (K)	100(2)	100(2)	100(2)	100(2)
Unit cell dimensions	a = 9.189(1) b = 23.663(1) c = 10.608(1) β = 94.332(1)	a = 8.512(1) b = 11.468(1) c = 13.996(1) α = 105.64(1) β = 103.51(1) γ = 103.20(1)	a = 9.379(1) b = 22.608(2) c = 14.906(1) β = 104.62(1)	a = 11.269(2) b = 12.458(3) c = 20.817(4) α = 78.69(3) β = 83.62(3) γ = 78.63(3)
Cell volume ($Å^3$)	2300.0(2)	1215.83(17)	3058.4(4)	2801.6(11)
Pcalc (g/cm^3)	1.451	1.422	1.357	1.763
μ (Mo Kα) (mm^{-1})	0.298	0.301	0.446	1.739
2θ range	2.384–25.299	2.578–25.237	2.289–25.319	1.695–26.373
Reflections measured	47204	13274	86701	24025
Independent Reflections	4181 [Rint = 0.0402]	4422 [Rint = 0.0882]	5566 [Rint = 0.0290]	11417 [Rint = 0.0848]
$R1$ ($I > 2\sigma(I)$)	0.0455	0.0535	0.0191	0.0435
$wR2$ (all data)	0.1103	0.1504	0.0360	0.1091
GooF	1.023	1.021	0.800	0.926
Largest diff. peak and hole ($e \cdot Å^{-3}$)	1.02/−0.65	0.60/−0.56	0.60/−0.61	1.61/−2.25

3.4. Experimental Section

Li(1,2-disila[18]crown-6)]PF_6 (**1**): At ambient temperature, 159 mg (1.05 mmol, 1 equiv) of $LiPF_6$ was added to 370 mg (1.1 mmol, 1 equiv) of 1,2-disila[18]crown-6 in 15 mL of dichloromethane. The suspension was stirred for 18 h and was subsequently filtered. The solvent was removed under reduced pressure, and the residue was washed with *n*-pentane. The resulting colorless greasy solid was recrystallized with traces of dichloromethane after freezing at −196 °C and subsequently storage at −35 °C for 3 days. 45% (275 mg, 0.5 mmol) of **1** was obtained in form of colorless planks. ^{1}H NMR (300 MHz, CD_2Cl_2): δ = 0.34 (s, 12H, CH_3), 3.71–3.73 (m, 4H, CH_2), 3.76 (s, 12H, CH_2), 3.81–3.82 ppm (m, 4H, CH_2); ^{13}C{^{1}H} NMR (75 MHz, CD_2Cl_2): δ = −0.5 (s, CH_3), 61.7 (s, CH_2), 68.1 (s, CH_2), 68.2 (s, CH_2), 68.4 (s, CH_2), 71.4 ppm (s, CH_2); ^{29}Si{^{1}H} NMR (CD_2Cl_2): δ = 15.6 ppm (s); ^{7}Li NMR (194 MHz, CD_2Cl_2): δ = −0.9 ppm (s); ^{31}P{^{1}H} NMR (117 MHz, CD_2Cl_2): δ = −144.0 ppm (h, $^1J_{PF}$ = 710 Hz); ^{19}F NMR (283 MHz, CD_2Cl_2): δ = −73.7 ppm (d, $^1J_{PF}$ = 710 Hz). IR $\tilde{\upsilon}$ = 2962(w), 2885(vw), 1456(vw), 1410(vw), 1351(vw), 1258(m), 1057(s), 1011(s), 923(w), 789(vs), 701(w), 661(w), 635(w), 556(m), 466(m). MS (ESI$^+$): *m/z* 359.1893% $[M]^+ - PF_6$ (95).

[Na(1,2-disila[18]crown-6)PF_6] (**2**): At ambient temperature, 48 mg (0.3 mmol, 1 equiv) of $NaPF_6$ was added to 100 mg (0.28 mmol, 1 equiv) of 1,2-disila[18]crown-6 in 10 mL of dichloromethane. The suspension was stirred for 1 h, followed by filtration and removal of the solvent. The residue was washed twice with 10 mL of *n*-pentane and was dried in vacuo. Recrystallization from dichloromethane: benzene (2:1) at −35 °C yielded 44% (64 mg, 0.12 mmol) of **2** in form of colorless blocks after 1 day. ^{1}H NMR (300 MHz, CD_2Cl_2): δ = 0.29 (s, 12H, CH_3), 3.61–3.63 (m, 4H, CH_2), 3.67 (s, 12H, CH_2), 3.80–3.83 ppm (m, 4H, CH_2); ^{13}C{^{1}H} NMR (75 MHz, CD_2Cl_2): δ = −0.4 (s, CH_3), 62.8 (s, CH_2), 69.9 (s, CH_2), 72.0 (s, CH_2), 72.9 ppm (s, CH_2); ^{29}Si{^{1}H} NMR (CD_2Cl_2): δ = 14.3 ppm (s); ^{31}P{^{1}H} NMR (117 MHz, CD_2Cl_2): δ = −143.9 ppm (h, $^1J_{PF}$ = 710 Hz); ^{19}F NMR (283 MHz, CD_2Cl_2): δ = −74.8 ppm

(d, $^1J_{PF}$ = 710 Hz). IR $\tilde{\upsilon}$ = 2912(w), 2880(w), 1457(w), 1399(w), 1350(w), 1291(w), 1250(m), 1131(s), 1082(s), 1056(s), 955(s), 931(m), 834(vs), 816(vs), 794(s), 771(s), 740(m), 720(m), 635(m), 556(s), 504(w), 471(w). MS (ESI$^+$): *m/z* 375.1634% $[M]^+ - PF_6$ (100).

1,2,4,5-Tetrasila[18]crown-6 (**3**): 0.7 mL (4.1 mmol, 1 equiv) of tetraethylene glycol and 1.1 mL (8.2 mmol, 2 equiv) of NEt_3 in 50 mL of THF was simultaneously, with 1.30 g (4.1 mmol, 1 equiv) of $O(Si_2Me_4Cl)_2$ in 50 mL of THF, dropped into a three-neck flask with 50 mL of stirred THF. The resulting white suspension was stirred for 12 h. Subsequently, the solvent was removed under reduced pressure, the product was extracted with 50 mL of *n*-pentane followed by filtration. The solvent was removed in vacuo, and 85% (1.5 g, 3.5 mmol) of **3** was obtained in form of a colorless oil. ^{1}H NMR (300 MHz, CD_2Cl_2): δ = 0.20 (s, 12H, CH_3), 0.22 (s, 12H, CH_3), 3.54–3.56 (m, 4H, CH_2), 3.60 (s, 8H, CH_2), 3.72–3.76 ppm (m, 4H, CH_2); ^{13}C{^{1}H} NMR (75 MHz, CD_2Cl_2): δ = −0.5 (s, *C*H$_3$), 2.9 (s, *C*H$_3$), 63.9 (s, *C*H$_2$), 71.2 (s, *C*H$_2$), 71.6 (s, *C*H$_2$), 73.1 (s, *C*H$_2$); ^{29}Si{^{1}H} NMR (CD_2Cl_2): δ = 2.1 (s, *Si*OSi), 11.0 ppm (s, CO*Si*). IR $\tilde{\upsilon}$ = 2949(w), 2867(w), 1456(w), 1400(w), 1350(w), 1294(w), 1246(m), 1091(s), 1031(s), 947(m), 826(m), 797(s), 761(s), 682(m), 660(m), 635(m), 553(w), 546(w). MS (ESI$^+$): *m/z* 441.1977% $[MH]^+$ (15).

[K(1,2,4,5-tetrasila[18]crown-6)PF_6] (**4**): 58 mg (0.32 mmol, 1 equiv) of KPF_6 was added to a stirred solution of 140 mg (0.32 mmol, 1 equiv) of 1,2,4,5-tetrasila[18]crown-6 in 15 mL of dichloromethane. The resulting suspension was stirred for 12 h at ambient temperature, followed by filtration. The solvent was removed in vacuo, and the product was obtained in form of a colorless, highly viscous oil. After 18 h at ambient temperature, colorless blocks were obtained, yielding 61% (120 mg, 0.2 mmol) of **4**. ^{1}H NMR (300 MHz, CD_2Cl_2): δ = 0.08 (s, 12H, CH_3), 0.23 (s, 12H, CH_3), 3.54–3.57 (m, 4H, CH_2), 3.62 (s, 8H, CH_2), 3.73–3.77 ppm (m, 4H, CH_2); ^{13}C{^{1}H} NMR (75 MHz, CD_2Cl_2): δ = −0.6 (s, *C*H$_3$), 2.8 (s, *C*H$_3$), 63.6 (s, *C*H$_2$), 71.0 (s, *C*H$_2$), 71.1 (s, *C*H$_2$), 73.1 ppm (s, *C*H$_2$); ^{29}Si{^{1}H} NMR (CD_2Cl_2): δ = 2.7 (s, *Si*OSi), 11.9 ppm (s, CO*Si*); ^{31}P{^{1}H} NMR (117 MHz, CD_2Cl_2): δ = −143.9 ppm (h, $^1J_{PF}$ = 710 Hz); ^{19}F NMR (283 MHz, CD_2Cl_2): δ = −73.8 ppm (d, $^1J_{PF}$ = 710 Hz). IR $\tilde{\upsilon}$ = 2948(w), 2886(w), 1470(w), 1458(w), 1401(w), 1360(w), 1349(w), 1301(w), 1247(m), 1126(m), 1110(m), 1095(m), 1085(m), 1065(m), 1051(m), 1017(m), 945(m), 931(m), 916(m), 825(vs), 797(vs), 762(vs), 738(m), 719(w), 684(m), 659(m), 555(s), 441(w), 427(w), 414(w). MS (ESI$^+$): *m/z* 479.1531% $[M]^+ - PF_6$ (100).

[Ba(1,2-disila[15]crown-5)OTf_2]$_2$ (**5**): 119 mg (0.27 mmol, 1 equiv) of $BaOTf_2$ was added to 84 mg (0.27 mmol, 1 equiv) of 1,2-disila[15]crown-5 in 15 mL of dichloromethane. The suspension was stirred for 18 h followed by filtration. The solvent was removed under reduced pressure, and the residue was washed twice with 15 mL of *n*-pentane. The product was recrystallized from dichloromethane and pentane (2:5). After 1 day at ambient temperature, colorless plates of **5** were obtained with 22% (87 mg, 0.06 mmol) yield. ^{1}H NMR (300 MHz, CD_2Cl_2): δ = 0.37 (s, 24H, CH_3), 3.71–4.04 ppm (m, 32H, CH_2); ^{13}C{^{1}H} NMR (75 MHz, CD_2Cl_2): δ = −0.8 (s, *C*H$_3$), 62.0 (s, *C*H$_2$), 69.0 (s, *C*H$_2$), 70.3 (s, *C*H$_2$), 72.6 (s, *C*H$_2$), 120.9 ppm (q, $^1J_{CF}$ = 322 Hz, *C*F$_3$); ^{19}F NMR (283 MHz, CD_2Cl_2): δ = −79.4 ppm (s, CF_3); ^{29}Si{^{1}H} NMR (CD_2Cl_2): δ = 17.8 ppm (s); IR $\tilde{\upsilon}$ = 2952(w), 2869(w), 1468(w), 1358(w), 1263(s), 1228(s), 1171(s), 1156(s), 1121(m), 1084(s), 1061(s), 1030(s), 948(s), 917(m), 867(m), 838(s), 793(s), 770(s), 728(s), 631(s), 575(s), 515(s), 454(w), 416(w); MS (LIFDI$^+$): *m/z* 331.136% [1,2-disila[15]crown-5+Na]$^+$ (100).

4. Conclusions

In this work, the competing coordination ability of C-, Si/C-, and fully Si-bonded O atoms was studied. 1,2-disila[18]crown-6 as well as 1,2,4,5-tetrasila[18]crown-6 turned out to be suitable ligands, since the presence of Si_2 units further increases the ring diameter in comparison to the organic crown ether [18]crown-6. Single crystals of [Li(1,2-disila[18]crown-6)]PF_6 (**1**) and of [Na(1,2-disila[18]crown-6)PF_6] (**2**) were obtained and revealed a divergent coordination of the cation. In **1**, the highly flexible ligand completely saturates the coordination sphere of Li^+, while the PF_6 anion does not show any interaction with the cation. The Li^+ ion is preferably coordinated by the Si- and C-bonded O atoms. Contrary to that, Na^+ shows stronger interaction with the C-bonded O atoms of 1,2-disila[18]crown-6. Only one of the Si/C-bonded O atoms participates in the coordination. As a result, the Me groups of the Si-based part of the ligand remain in the staggered conformation, which is

also the preferred geometry of the free ligand [18]. Contrary to Compound **1**, the interaction of the Si/C-bonded O atoms with the cation does not compensate for the required change of conformation. The energy effort of 1,2-disila[18]crown-6 for adopting the geometry of the Li^+ and Na^+ complex was determined by DFT calculations. ΔE_{geom}, in the case of **1**, has a value of 77.58 kJ·mol^{-1}, which is considerably increased. In contrast, the ligand shows with 29.24 kJ·mol^{-1} smaller energy changes by coordination of Na^+, which can be partially attributed to the staggered arrangement of the Si-bonded methyl groups. It follows that the electrostatic attraction between the hybrid-bonded O atoms and Na^+ do not compensate for the required energy effort of the ecliptic arranged methyl groups. The Lewis acids therefore show a major impact on the coordinative properties of the different types of O atoms within hybrid crown ethers.

Similar coordination modes were also found in 1,2,4,5-tetrasila[18]crown-6 (**3**), which incorporates three types of O atoms: C-, Si/C-, and Si-bonded ones. Ordinary, K^+ perfectly fits in [18]crown-6 and 1,2-disila[18]crown-6 [18]. The presence of two disilane units leads to a further increase of the ligand such that **3** does not match with K^+. The completely Si-bonded O atom, which requires the highest amount of energy to adopt the complex geometry [19], does not participate in the coordination. The complexation of the heavier homologue Rb^+ by **3** is an issue of current investigation. In this study, no superiority in coordination ability of each of the different types of O atoms was found.

The experiment on the inverse case, e.g., small ligands with large cations in 1:1 stoichiometry, leads to the dinuclear complex (**5**), which is bridged by four triflate anions. This crystal structure represents an initial outlook on the ability of disila-crown ethers to build sandwich complexes. Therefore, reactions in 2:1 stoichiometry of ligand to salt are crucial.

Supplementary Materials: The following are available online at www.mdpi.com/2304-6740/5/1/11/s1, Figures S1–S3: Calculated structure of 1,2-disila[18]crown-6, [Li(1,2-disila[18]crown-6)]+, [Na(1,2-disila[18]crown-6)]$^+$; Tables S1–S3: XYZ data of 1,2-disila[18]crown-6, [Li(1,2-disila[18]crown-6)]+, [Na(1,2-disila[18]crown-6)]$^+$.

Acknowledgments: This work was financially supported by the Deutsche Forschungsgemeinschaft (DFG).

Author Contributions: Kirsten Reuter performed the syntheses and analytics of Compounds **1**–**4**, DFT calculations, and interpretations and wrote the paper; Fabian Dankert conducted the synthesis and characterization of Compound **5**; Carsten Donsbach accomplished the measurement, crystal structure solution, and refinement of **5**; Carsten von Hänisch contributed to interpretation and led the over-arching research project.

Conflicts of Interest: The authors declare no conflict of interest.

References

1. Liebau, F. Untersuchungen über die Grösse des Si–O–Si–Valenzwinkels. *Acta Cryst.* **1961**, *14*, 1103–1109. [CrossRef]
2. Almenningen, A.; Bastiansen, O.; Ewing, V.; Hedberg, K.; Trætteberg, M. The Molecular Structure of Disiloxane, $(SiH_3)_2O$. *Acta Chem. Scand.* **1963**, *17*, 2455–2460. [CrossRef]
3. Stone, F.G.A.; Seyferth, D. The Chemistry of Silicon Involving Probable Use of *d*-Type Orbitals. *J. Inorg. Nucl. Chem.* **1955**, *1*, 112–118. [CrossRef]
4. Craig, D.P.; Maccoll, A.; Nyholm, R.S.; Orgel, L.E. Chemical bonds involving *d*-orbitals. Part I. *J. Chem. Soc.* **1954**, 332–353. [CrossRef]
5. Emeléus, H.J.; Onyszchuk, M. The Reaction of Methyldisoxanes and 1:1 Dimethyldisilthiane with Boron and Hydrogen Halides. *J. Chem. Soc.* **1958**, 604–609. [CrossRef]
6. Pitt, C.G. Hyperconjugation and its Role in Group IV Chemistry. *J. Organomet. Chem.* **1973**, *61*, 49–70. [CrossRef]
7. Shambayati, S.; Schreiber, S.L.; Blake, J.F.; Wierschke, S.G.; Jorgenson, W.L. Structure and basicity of silyl ethers: A crystallographic and ab initio inquiry into the nature of silicon-oxygen interactions. *J. Am. Chem. Soc.* **1990**, *112*, 697–703. [CrossRef]
8. Cypryk, M.; Apeloig, Y. Ab Initio Study of Silyloxonium Ions. *Organometallics* **1997**, *16*, 5938–5949. [CrossRef]
9. Gillespie, R.J.; Johnson, S.A. Study of Bond Angles and Bond Lenghts in Disiloxane and Related Molecules in Terms of the Topology of the Electron Density and Its Laplacian. *Inorg. Chem.* **1997**, *36*, 3031–3039. [CrossRef] [PubMed]

10. Grabowski, S.J.; Hesse, M.F.; Paulmann, C.; Luger, P.; Beckmann, J. How to Make the Ionic Si–O Bond More Covalent and the Si–O–Si Linkage a Better Acceptor for Hydrogen Bonding. *Inorg. Chem.* **2009**, *48*, 4384–4393. [CrossRef] [PubMed]
11. Passmore, J.; Rautiainen, J.M. On The Lower Basicity of Siloxanes Compared to Ethers. *Eur. J. Inorg. Chem.* **2012**, 6002–6010. [CrossRef]
12. Cameron, T.S.; Decken, A.; Krossing, I.; Passmore, J.; Rautiainen, J.M.; Wang, X.; Zeng, X. Reactions of a Cyclodimethyldisiloxane $(Me_2SiO)_6$ with Silver Salts of Weakly Coordinating Anions; Crystal Structures of $[Ag(Me_2SiO)_6][Al]$ ([Al] = $FAl\{OC(CF_3)_3\}_3]$, $[Al\{OC(CF_3)_3\}_4]$) and Their Comparison with $[Ag(18\text{-Crown-6})]_2[SbF_6]_2$. *Inorg. Chem.* **2013**, *52*, 3113–3126. [CrossRef] [PubMed]
13. Decken, A.; Passmore, J.; Wang, W. Cyclic Dimethylsiloxanes as Pseudo Crown Ethers: Syntheses and Characterization of $Li(Me_2SiO)_5[Al\{OC(CF_3)_3\}_4]$, $Li(Me_2SiO)_6[Al\{OC(CF_3)_3\}_4]$ and $Li(Me_2SiO)_6[Al\{OC(CF_3)_2Ph\}_4]$. *Angew. Chem. Int. Ed.* **2006**, *45*, 2773–2777. [CrossRef] [PubMed]
14. Ritch, J.S.; Chivers, T. Silicon Analogues of Crown Ethers and Cryptands: A New Chapter in Host–Guest Chemistry? *Angew. Chem. Int. Ed.* **2007**, *46*, 4610–4613. [CrossRef] [PubMed]
15. Von Hänisch, C.; Hampe, O.; Weigend, F.; Stahl, S. Stepwise Synthesis and Coordination Compound of an Inorganic Cryptand. *Angew. Chem. Int. Ed.* **2007**, *46*, 4775–4779. [CrossRef] [PubMed]
16. Inoue, Y.; Ouchi, M.; Hakushi, T. Molecular Design of Crown Ethers. 3. Extraction of Alkaline Earth and Heavy Metal Picrates with 14- to 17-Crown-5 and 17- to 22-Crown-6. *Bull. Chem. Soc. Jpn.* **1985**, *58*, 525–530. [CrossRef]
17. Ouchi, M.; Inoue, Y.; Kanzaki, T.; Hakushi, T. Ring-contracted Crown Ethers: 14-Crown-5, 17-Crown-6, and Their Sila-analogues. Drastic Decrease in Cation-binding Ability. *Bull. Chem. Soc. Jpn.* **1984**, *57*, 887–888. [CrossRef]
18. Reuter, K.; Buchner, M.R.; Thiele, G.; von Hänisch, C. Stable Alkali-Metal Complexes of Hybrid Disila-Crown Ethers. *Inorg. Chem.* **2016**, *55*, 4441–4447. [CrossRef] [PubMed]
19. Reuter, K.; Thiele, G.; Hafner, T.; Uhlig, F.; von Hänisch, C. Synthesis and coordination ability of a partially silicon based crown ether. *Chem. Commun.* **2016**, *52*, 13265–13268. [CrossRef] [PubMed]
20. Dalley, N.K.; Lamb, J.D.; Nazarenko, A.Y. Crystal Structure of the Complex of 1,4,7,10,13,16-Hexacyclooctadecane with Lithium Picrate Dihydrate. *Supramol. Chem.* **1997**, *8*, 345–350.
21. Chadwick, S.; Ruhlandt-Senge, K. The Remarkable Structural Diversity of Alkali Metal Pyridine-2-thiolates with Mismatched Crown Ethers. *Chem. Eur. J.* **1998**, *4*, 1768–1780. [CrossRef]
22. Akutagawa, T.; Hasegawa, T.; Nakamura, T.; Takeda, S.; Inabe, T.; Sugiura, K.; Sakata, Y.; Underhill, A.E. Ionic Channel Structures in $[(M^+)_x([18]\text{crown-6})][Ni(dmit)_2]_2$ Molecular Conductors. *Chem. Eur. J.* **2001**, *7*, 4902–4912. [CrossRef]
23. Dankert, F.; Reuter, K.; Donsbach, C.; von Hänisch, C. A Structural Study of Alkaline Earth Metal Complexes with Hybrid Disila-Crown Ethers. *Dalton Trans.* **2017**. [CrossRef] [PubMed]
24. Olsher, U.; Izatt, R.M.; Bradshaw, J.S.; Dalley, N.K. Coordination chemistry of lithium ion: A crystal and molecular structure review. *Chem. Rev.* **1991**, *91*, 137–164. [CrossRef]
25. Gingl, F.; Hiller, W.; Strähle, J. [Li(12-Krone-4)]Cl: Kristallstruktur und IR-Spektrum. *Z. Anorg. Allg. Chem.* **1991**, *606*, 91–96. [CrossRef]
26. Liddle, S.T.; Clegg, W. A homologous series of crown-ether-complexed alkali metal amides as discrete ion-pair species: Synthesis and structures of $[M(12\text{-crown-4})_2][PyNPh{\cdot}PyN(H)Ph]$ (M = Li, Na and K). *Polyhedron* **2003**, *22*, 3507–3513. [CrossRef]
27. Feldmann, C.; Okrut, A. Two Tricyclic Polychalcogenides in $[Li(12\text{-crown-4})_2]_2[Sb_2Se_{12}]$ and $[Li(12\text{-crown-4})_2]_4[Te_{12}]{\cdot}(12\text{-crown-4})_2$. *Z. Anorg. Allg. Chem.* **2009**, *635*, 1807–1811. [CrossRef]
28. *Turbomole*, version 7.0; Turbomole Is a Development of University of Karlsruhe and Forschungszentrum Karlsruhe 1989–2007, Turbomole GmbH 2016. Turbomole GmbH: Karlsruhe, Germany, 2007.
29. Weigend, F.; Ahlrichs, R. Balanced bass sets of split valence, triple zeta valence and quadruple zeta valence quality for H to Rn: Design and assessment of accuracy. *Phys. Chem. Chem. Phys.* **2005**, *7*, 3297–3305. [CrossRef] [PubMed]
30. Weigend, F. Accurate Coulomb-fitting basis sers for H to Rn. *Phys. Chem. Chem. Phys.* **2006**, *8*, 1057–1065. [CrossRef] [PubMed]
31. Dolg, M.; Stoll, H.; Savin, A.; Preuss, H. Energy-adjusted pseudopotentials for the rare earth elements. *Theoret. Chim. Acta* **1989**, *75*, 173–194. [CrossRef]

32. Stoll, H.; Metz, B.; Dolg, M. Relativistic energy-consistent pseudopotentials—Recent developments. *J. Comput. Chem.* **2002**, *23*, 767–778. [CrossRef] [PubMed]
33. Grimme, S.; Antony, J.; Ehrlich, S.; Krieg, H. A consistent and accurate ab initio parametrization of density functional dispersion correction (DFT-D) for the 94 elements H–Pu. *J. Chem. Phys.* **2010**, *132*, 154104–154119. [CrossRef] [PubMed]
34. Grimme, S.; Ehrlich, S.; Goerigk, L. Effect of the damping function in dispersion corrected density functional theory. *J. Comput. Chem.* **2011**, *32*, 1456–1465. [CrossRef] [PubMed]
35. Willcott, M.R. MestRe Nova. *J. Am. Chem. Soc.* **2009**, *131*, 13180. [CrossRef]
36. Klamt, A.; Schüürmann, G. COSMO: A new approach to dielectric screening in solvents with explicit expressions for the screening energy and its gradient. *J. Chem. Soc. Perkin. Trans.* **1993**, *2*, 799–805. [CrossRef]
37. Sheldrick, G.M. *SHELXL14*; Program for the Refinement of Crystal Structures; Universität Göttingen: Göttingen, Germany, 2014.
38. Dolomanov, O.V.; Bourhis, L.J.; Hildea, R.J.; Howard, J.A.K.; Puschmann, H. *Olex2*: A complete structure solution, refinement and analysis program. *J. Appl. Crystallogr.* **2009**, *42*, 339–341. [CrossRef]
39. Putz, H.; Brandenburg, K. *Diamond—Crystal and Molecular Structure Visualization*; Crystal Impact: Bonn, Germany, 2012.

Dalton Transactions

PAPER

View Article Online
View Journal

Cite this: DOI: 10.1039/c6dt04018g

A structural study of alkaline earth metal complexes with hybrid disila-crown ethers†

Fabian Dankert, Kirsten Reuter, Carsten Donsbach and Carsten von Hänisch*

Received 19th October 2016,
Accepted 24th November 2016

DOI: 10.1039/c6dt04018g

www.rsc.org/dalton

Compounds consisting of $[M(1,2\text{-disila-}[3n]\text{crown-}n)]^{2+}$ (M = Mg, Ca, Sr, Ba; n = 5, 6) and $[Ba(1,2\text{-disila-benzo}[18]\text{crown-}6)]^{2+}$ cations and different anions were obtained by equimolar reaction of the hybrid disila-crown ethers 1,2-disila[15]crown-5 (**1**), 1,2-disila[18]crown-6 (**2**) and 1,2-disila-benzo[18]crown-6 (**7**) with alkaline earth metal salts. Even with strongly coordinating anions such as Br^- or I^- stable complexes could be obtained, showing the good coordination ability of these ligands. The structures of all coordination compounds were determined *via* single crystal X-ray diffraction (XRD). By means of DFT calculations, the complexation ability of 1,2-disila[15]crown-5 (**1**) towards magnesium bromide was determined to be considerably higher compared to [15]crown-5. The opposite case was observed in solution as the exchange of calcium cations between [18]crown-6 and 1,2-disila[18]crown-6 (**2**) was studied *via* dynamic proton nuclear magnetic resonance (NMR) spectroscopy.

Introduction

Within the scope of developing macrocycles, there has also been an increased interest in ring compounds which are made of an inorganic skeleton.[1–3] Unlike crown ether complexes, coordination compounds with cyclosiloxanes are very rare. They are mostly constituted of a weakly coordinating anion such as Al_F (Al_F = $[Al\{OC(CF_3)_3\}_4]^-$), $[SbF_6]^-$ or $[InH\{CH_2C(CH_3)\}_3]^-$ as counterion where the charge is widely spread over a non-nucleophilic, chemically robust moiety.[2,4–6] The Zr(IV) compound $[Zr(D_6)Br_2][Zr_2Br_9]_2$ (D = Me_2SiO) is a unique example of a cyclosiloxane complex with a more strongly coordinating halide anion.[7]

One model to describe the reduced basicity of siloxanes is the negative hyperconjugation. An occupied p-orbital of the oxygen atom donates electron density into the σ*-orbital of the silicon–methyl bond, which strengthens the Si–O bond. The complexation of metal ions leads to a competing polarization.[2,8] According to Weinhold and West, negative hyperconjugation plays a major role in permethylated siloxanes, which was recently shown *via* natural-bond-orbital-analysis.[9,10] Another approach to explain the low basicity of siloxanes consists of an ionic consideration of the Si–O bond.[11–13] Despite the high anionicity of the O atoms, siloxanes do not exhibit an increased coordination ability owing to the energetically unfavoured further polarisation of the already polar Si–O bond. In this respect changes in the $n_O \rightarrow \sigma^*_{Si-C}$ interaction play a significant role.[8] Recent work suggests that repulsion between the positively polarized Si atom and the metal ion is eminently important beside the negative hyperconjugation to explain the low coordination ability of cyclosiloxanes.[14] Furthermore, extraction experiments have shown that the complexation abilities of ring contracted crown ethers like [17]crown-6 and sila[17]crown-6 are notably smaller than those of common crown ethers revealing that not only electronic effects but also the conformation of the macrocycle determines the complexation ability of such compounds.[15,16]

These facts motivated us to incorporate a Si_2Me_4 unit rather than one $SiMe_2$ in between the oxygen atoms of crown ethers (Scheme 1). Less attention has been paid to this function and its coordination chemistry even though it is known for quite some time.[17,18] However, in our recent work on hybrid disila-crown ethers we were able to synthesize crown ethers of the type 1,2-disila[3n]crown-n and their alkali metal complexes. The reaction of 1,2-dichloro-1,1,2,2-tetramethyldisilane and the appropriate glycole yielded the hybrid crown ether.

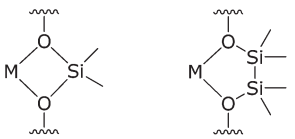

Scheme 1 Binding modes of siloxanes (left) and disila-crowns (right) in metal complexes.

Fachbereich Chemie and Wissenschaftliches Zentrum für Materialwissenschaften (WZMW), Philipps-Universität Marburg, Hans-Meerwein-Straße 4, D-35032, Marburg, Germany. E-mail: haenisch@chemie.uni-marburg.de

†Electronic supplementary information (ESI) available. CCDC 1497467–1497471. For ESI and crystallographic data in CIF or other electronic format see DOI: 10.1039/c6dt04018g

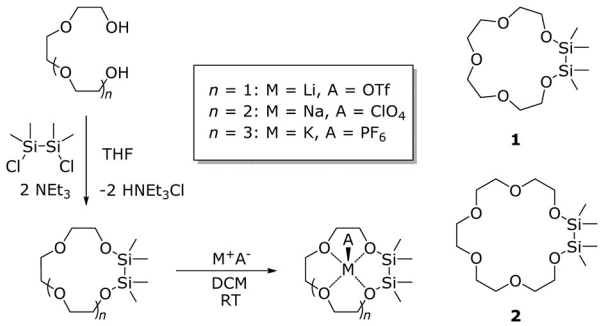

Scheme 2 Synthesis of hybrid disila-crown-ethers and their alkali metal complexes.

Complexation with selected alkali metal salts in dichloromethane (DCM) then yielded their alkali metal complexes (Scheme 2). By means of DFT calculations as well as dynamic proton NMR experiments, we revealed a comparable complexation ability of these crown ethers and their organic analogues.[19] We therefore assume that the reduced complexation ability of siloxanes is rather the result of structural and electrostatic factors. As the next step in understanding the coordination chemistry of disila-crown ethers we herein report the incorporation of alkaline earth metal cations.

Results and discussion

Treatment of **1** with $MgBr_2$ in trifluorotoluene led to the coordination compound [Mg(1,2-disila[15]crown-5)Br_2] (**3**). Neat **3** is a white powder which can be recrystallized after dissolution in DCM and layering with *n*-pentane. The resulting colourless plates were analysed *via* XRD. **3** crystallizes in the orthorhombic space group *Pbca*. The magnesium cation is coordinated by all oxygen atoms of the cyclic ligand as well as by two bromide ions giving a coordination number of seven (Fig. 1). The oxygen atoms are in almost coplanar arrangement with the magnesium cation, which is apparent from the Br1–Mg1–O–angles of approximately 90°. The $MgBr_2$ fragment is in well-nigh linear shape showing a Br1–Mg1–Br2 angle of 178.5(1)°. This is consistent with the [$Mg(THF)_4Br_2$] (THF = tetrahydrofuran) complex, whose Br–Mg–Br-angle is 178.0(1)°.[20]

The O–Mg–O-angles differ from 67.5(1) to 81.5(1)°. The O1–Mg1–O5-angle is enlarged as a result of the Si–Si bond of 232.2(1) pm. The methyl groups are taking an almost ecliptic arrangement, which can be seen in the C–Si–Si–C-torsion angles of 9.3(1)° and 6.2(1)°. This eclipsed arrangement was also reported for different cyclosiloxane and disila-crown ether complexes.[2,4,14,19,21] The O–Mg-bond lengths vary from 223.3(2) to 235.1(2) pm. Hence they are slightly longer than the O–Mg-bond lengths in related compounds with [15]crown-5 as ligand (see Table 1) and quite as long as those of [Mg([18]crown-6)(Cl–H–Cl)$_2$].[22] However, the O–Mg-bond lengths of fully carbon substituted oxygen atoms in **3** are comparable to those which are half carbon and half silicon substituted, so there is no hint for lower complexation ability of the silicon bonded oxygen atoms.

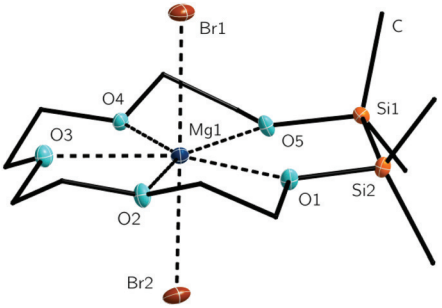

Fig. 1 Molecular structure of **3** in the crystal. Thermal ellipsoids represent a probability level of 50%. Hydrogen atoms are omitted for clarity. Selected bond lengths [pm]: O1–Mg1 227.5(2), O2–Mg1 225.3(2), O3–Mg1 235.1(2), O4–Mg1 223.8(2), O5–Mg1 222.3(2), Br1–Mg1 260.9(1), Br(2)–Mg1 258.9(1), Si1–O5 168.9(2), Si2–O1 168.5(2), Si1–Si2 232.3(1). Selected bond angles [°]: O1–Mg1–O5 81.5, O1–Mg1–Br1 88.8(1), O2–Mg1–Br1 89.2(1), O3–Mg1–Br1 88.9(1), O4–Mg1–Br1 91.4(1), O5–Mg1–Br1 89.5(1), Br1–Mg1–Br2 178.5(1).

Table 1 Selected bond lengths [pm] for compounds **3–5** and their related crown ether complexes

Compound	O_{crown}–M [pm]	CN[a]	Ref.
3	223.3(2)–235.1(2)	7	*b*
[Mg([15]crown-5)($SCPh_3$)$_2$]	214.3(3)–219.2(4)	7	26
[Mg([15]crown-5)(H_2O)$_2$](NO_3)$_2$	201.2(7)–235.7(8)	7	27
[Mg([15]crown-5)(NCS)$_2$]	214.2(2)–223.9(7)	7	28
[Mg([15]crown-5)([$CuCl_4$])CH_3CN]	211.7(4)–219.1(3)	7	29
4	243.6(1)–247.9(1)	7	*b*
[Ca([18]crown-6)(OTf)$_2$(H_2O)]	255.5(1)–265.7(1)	9	30
[Ca([18]crown-6)I_2]	264.9(5)[c]	8	31
[Ca([15]crown-5)(NCS)$_2$$H_2O$]	251.2(2)–258.5(2)	8	28
[Ca([15]crown-5)(NO_3)$_2$]	247.4(3)–258.1(4)	9	27
5	270.0(2)–277.7(2)	8	*b*
[Sr([18]crown-6)(NO_3)$_2$]	266.7(5)–275.5(3)	10	27
[Sr([18]crown-6)(HSO_4)$_2$]	268.2(8)–268.0(8)	10	32
[Sr([18]crown-6)(H_2O)$_3$][$CuCl_4$]	267.2(3)–270.0(3)	9	33
[Sr([18]crown-6)($MeCN$)$_3$][BPh_4]$_2$	262.4(2)–271.4(2)	9	34
[Sr([18]crown-6)(hmpa)$_2$][$Sn(SnPh_3)_3$]$_2$	258.9(4)–273.6(4)	8	35

[a] Coordination number. [b] This work. [c] All symmetry generated.

The shortest O–Mg bond is attributed to the silicon bonded oxygen atom O5 whereas the longest O–Mg bond is observed for the fully carbon substituted oxygen atom O3. The relative binding affinity of the hybrid ligand **1** towards magnesium bromide was further studied by quantum chemical calculations and is presented in Scheme 3. The exchange of magnesium bromide from [15]crown-5 to 1,2-disila[15]crown-5 (**1**) was calculated by means of DFT using the BP86 functional and def2-TZVP basis sets with inclusion of dispersion interactions together with charge compensation and is energetically favoured by 217.63 kJ mol^{-1}. This result implies a significantly better coordination ability of **1** compared to [15]crown-5 and is in well accordance to previous calculations for 1,2-disila[12]crown-4 towards Li^+.[19] Unfortunately, the results of quantum chemical calculations could not be underlined with

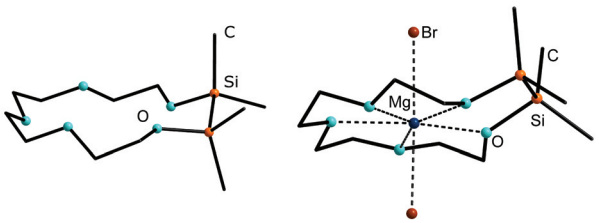

ΔE = -217,36 kJ/mol

1 + [Mg([15]crown-5)Br_2] ⟶ [$MgBr_2$@**1**] (**3**) + [15]crown-5

Scheme 3 Optimized structures of **1** (left) and **3** (right) and relative energies of the cation exchange from [15]crown-5 to 1,2-disila[15]crown-5 (**1**). Calculations performed at the def2-TZVP level of theory. For XYZ-Data and related structures see ESI.†

experimental data such as dynamic ^{1}H NMR spectroscopy. **3** does only barely dissolve in DCM and thus no proton NMR study was possible for this compound.

The heavier calcium cation was incorporated by treating **2** with $Ca(OTf)_2$ (OTf = $F_3CSO_3^-$) in DCM. The resulting coordination compound [Ca(1,2-disila[18]crown-6)OTf_2] (**4**) was obtained as colourless powder. After recrystallization from dichloromethane, single crystals suitable for XRD were obtained in shape of colourless rods. **4** crystallizes in the monoclinic space group $P2_1/n$. This coordination compound shows a mismatch: one of the crown ether oxygen atoms does not participate in the coordination of the central atom. The crown acts as "pseudo-1,2-disila[15]crown-5", so overall five crown ether oxygen atoms together with the two triflate groups coordinate to the calcium cation giving a total coordination number of seven (Fig. 2). The O4–Ca1 atomic distance is 321.4(1) pm. The distorted O7–Ca1–O10 bond angle of 163.0(1)° is a result of the repulsion between O4 and one of the triflate groups.

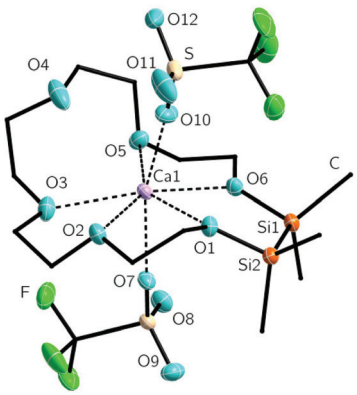

Fig. 2 Molecular structure of **4** in the crystal. Thermal ellipsoids represent a probability level of 50%. Hydrogen atoms are omitted for clarity. Selected bond lengths [pm]: O1–Ca1 244.9(1), O(2)–Ca(1) 245.8(1), O(3)–Ca(1) 247.9(1), O4···Ca1 321.4(1), O5–Ca1 243.6(1), O(6)–Ca1 247.5(1), O(7)–Ca(1) 234.8(1), O(10)–Ca(1) 230.2(2), Si(1)–O(6) 169.6(1), Si(2)–O(1) 169.1(1). Selected bond angles [°]: O1–Ca1–O6 76.1(1), O7–Ca1–O1 85.5(1), O7–Ca1–O2 84.6(1), O7–Ca1–O3 78.3(1), O7–Ca1–O5 99.4(1), O7–Ca1–O6 81.6(1), O7–Ca1–O10 63.0(1).

Hence this angle is slightly smaller than the expected 180° angle which is found in $[Ca(CH_3CH_2OH)_4OTf_2]$.[23]

The O7–Ca1–O(1,2,3,5,6) bond angles differ from 78.3(1) to 99.41(1)° leading to a distorted arrangement of the crown ether oxygen atoms around the calcium cation. The mismatch is obviously caused by the small ion diameter of Ca^{2+}, which is 200 pm, and the enlarged cavity of the ligand **2** compared to [18]crown-6.[24] The coordination pattern of **4** is known for different crown ether complexes.[22,25] However, no mismatched calcium complexes of [18]crown-6 are known to date. Due to the mismatch, the O_{crown}–Ca bond lengths in **4** are slightly shorter than those of complexes of [18]crown-6 and close to [15]crown-5 complexes of calcium (see Table 1). In case of this mismatched crown ether complex, we observed a significantly lower complexation ability of **2** in comparison to [18]crown-6 which was confirmed by means of dynamic ^{1}H NMR spectroscopy (see Scheme 4). An equimolar reaction of **2**, [18]crown-6 and $Ca(OTf)_2$ was carried out. The percentage of coordinated and free ligand was calculated from the average chemical shifts in the mixture according to[36]

$$\delta_{average} = (n_{coordinated}\delta_{coordinated} + n_{noncoordinated}\delta_{noncoordinated})/n_{total}$$

Chemical shifts of compound **4** are significantly high-field shifted in the 1 : 1 mixture of **4** and [18]crown-6, whereas the singlet of [18]crown-6 is significantly down-field shifted (see Scheme 4, spectrum c). As calculated with the above given equation, the ratio of **4** to [Ca([18]crown-6)OTf_2] is 14 : 86. This result is contradicted to experimental data[19] which was observed

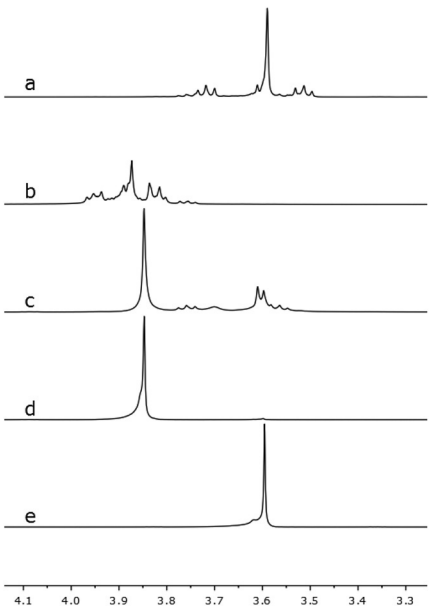

Scheme 4 Segments of 300 MHz ^{1}H NMR Spectra in CD_2Cl_2 of (a) 1,2-disila[18]crown-6, (b) [Ca(1,2-disila[18]crown-6)$(OTf)_2$] (c) [18]crown-6/1,2-disila[18]crown-6/$Ca(OTf)_2$ ratio 1 : 1 : 1 (d) [Ca([18]crown-6)OTf_2] and (e) [18]crown-6.

for the system 1,2,7,8-tetrasila[12]crown-4/$LiPF_6$/[12]crown-4 but attention should be paid to the enlarged cavity size of **2**.

As reported for different supramolecules, the coordination ability of such compounds highly depends on the characteristics of the host-molecule. Especially the size complementarity between cation and host cavity influences the magnitude of the binding constant.[37] The molecular structure of $[Ca([18]crown-6)(OTf)_2(H_2O)]$ reveals that [18]crown-6 enables all six oxygen atoms for the coordination to the metal ion rather than only five as in **4**.[30] This is presumably the key advantage of [18]crown-6 over the corresponding disila crown ether **2**.

The halide complex $[Sr(1,2\text{-disila}[18]crown\text{-}6)I_2]$ (**5**) was synthesized by reaction of **2** with SrI_2 in trifluorotoluene. After recrystallization, **5** was obtained as colourless blocks which were suitable for XRD. **5** crystallizes in the monoclinic space group *C*2/*c* with one solvent molecule DCM. In contrast to **4**, all crown ether oxygen atoms are coordinating to the larger strontium cation (Fig. 3). With two additional iodine atoms, the strontium cation has a coordination number of eight. No crown ether complex of the halide salt SrI_2 is known to date. Actually, different approaches to obtain crown ether complexes of strontium halides yielded $[Sr([12]crown\text{-}4)(H_2O)_3Br]Br$ or $[Sr([18]crown\text{-}6)(H_2O)_3]X_2$ ($X = Cl^-$, Br^-). Therein no or no more than one halide anion is placed in the coordination sphere of the metal ion.[38,39] Having an ion diameter of 236 pm, the strontium cation is still too small for the hole diameter of **2**.[24] The twisted arrangement of the ligand enables all oxygen atoms to participate in the coordination. The O–Sr1–I1 bond angles differ from 86.1(1) to 96.9(1)° stronger than for example the O–Mg1–Br1 bond angles in **3**. In addition, the $Sr(OSiMe_2)_2$ fragment shows an envelope conformation where the disilane-unit is buckling with Sr–O–O–Si torsion angles of 151.0(1) and 146.8(1)°. The methyl groups are again in an almost eclipsed arrangement with C–Si–Si–C torsion angles of 5.1(1) and 6.2(1)°. The I1–Sr1–I2 bond angle of 177.4(1)° is very close to 180° showing a well-nigh linear coordination of the SrI_2-fragment, which is also observed for $[Sr(DME)_2(THF)I_2]$ (DME = 1,2-dimethoxyethane), whose I–Sr–I bond angle is 178.6(1)°.[40]

With bond lengths of 320.1(1) and 320.5(1) pm, the Sr–I bonds are similar to those of different ether adducts such as for example $[Sr(DME)_3I_2]$, $[Sr(diglyme)_2I_2]$ (diglyme = bis(2-methoxyethyl)ether) or $[Sr(DME)_2(THF)I_2]$.[40] Again all carbon substituted oxygen atoms show almost the same bond lengths to the metal ion as the half carbon and half silicon affected oxygen atoms (270.0(2) to 277.7(2) pm). However, the O6–Sr1 bond is the longest one, but should be considered with respect to the twisting of the crown ether. The $Sr–O_{crown}$ bonds of $[Sr([18]crown\text{-}6)(NO_3)_3]$ and $[Sr([18]crown\text{-}6)(HSO_4)_2]$ are marginally shorter.[27,32] The cationic crown compounds $[Sr([18]crown\text{-}6)(hmpa)_2]^{2+}$ (hmpa = hexamethylphosphoramide) and $[Sr([18]crown\text{-}6)L_3]^{2+}$ (L = H_2O, CH_3CN) show notably smaller $Sr–O_{crown}$ bond lengths (see also Table 1).[33,34,39]

Finally, the heaviest non-radioactive alkaline earth metal was incorporated into the macrocycle by treating **2** with Ba$(OTf)_2$ in DCM. After recrystallization, $[Ba(1,2\text{-disila}[18]crown\text{-}6)OTf_2]$ (**6**) crystallizes in the triclinic space group $P\bar{1}$ with two independent molecules within the asymmetric unit. The metal ion is coordinated by all of the crown ether oxygen atoms as well as by the two triflate groups. One triflate group is coordinating as bidentate ligand giving the barium cation a total coordination number of nine (Fig. 4). With its ion diameter of 270 pm the barium cation is larger than the strontium cation, but the crown is still twisting as shown by the O5–Ba1–O10 and O6–Ba1–O10 bond angles, which are 78.1(1) and 77.4(1)°

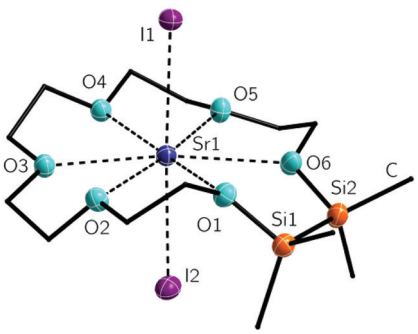

Fig. 3 Molecular structure of **5** in the crystal. Thermal ellipsoids represent a probability level of 50%. Hydrogen atoms and one solvent molecule DCM are omitted for clarity. Selected bond lengths [pm]: O1–Sr1 273.8(1), O2–Sr1 273.8(1), O3–Sr1 270.0(2), O4–Sr1 273.5(1), O5–Sr1 271.0(1), O6–Sr1 277.7(2), I1–Sr1 320.1(1), I2–Sr1 320.5(1), Si1–O1 167.6(2), Si2–O6 167.7(2), Si1–Si2 233.4(1). Selected bond angles [°]: O1–Sr1–I1 88.0(1), O2–Sr1–I1 93.2(1), O3–Sr1–I1 96.9(1), O4–Sr1–I1 87.0(1), O5–Sr1–I1 86.1(1), O6–Sr1–I1 93.2(1), I1–Sr1–I2 177.4(1), Sr1–O1–O6–Si2 151.0(1), Sr1–O6–O1–Si1 146.8(1).

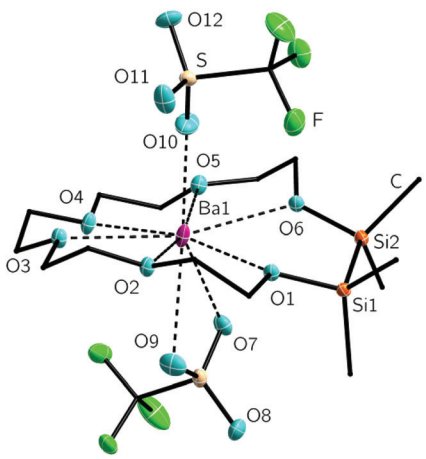

Fig. 4 Molecular structure of **6** in the crystal. Thermal ellipsoids represent a probability level of 50%. Hydrogen and disordered atoms with lower occupancy are omitted for clarity. Only one of two independent molecules per asymmetric unit is shown. Selected bond lengths [pm]: O1–Ba1 283.8(1), O2–Ba1 277.5(1), O3–Ba1 285.3(1), O4–Ba(1) 285.9, O5–Ba1 284.0(1), O6–Ba1 279.8(1), O7–Ba1 292.1(1), O9–Ba1 288.7, O10–Ba1 253.9(3), Si1–O1 168.5(1), Si2–O6 168.1(1), Si1–Si2 234.6(1). Selected bond angles [°]: O1–Ba1–O6 69.3(1), O1–Ba1–O4 168.6(1), O2–Ba1–O5 167.3(1), O3–Ba1–O6 166.0(1), Ba1–O1–O6–Si2 157.6(1), Ba1–O6–O1–Si1 156.5(1).

Table 2 Selected bond lengths [pm] for compounds **6**, **8** and their related crown ether complexes

Compound	O_{crown}–Ba [pm]	CN[a]	Ref.
$[Ba([18]crown-6)(hmpa)_2][BPh_4]_2$	277.2(2)–281.3(2)	8	34
$[Ba([18]crown-6)(hmpa)_2][SnPh_3]$	277(1)–280(1)	8	35
$[Ba([18]crown-6)(HCPh_2)_2]$	275.0(2)–280.2(3)	8	41
$[Ba([18]crown-6)(PPh)_2]$	271.7(2)–280.7(2)	8	42
$[Ba([18]crown-6)(hmpa)_2](SeMes^*)_2$[b]	276.7(3)–280.3(2)	8	43
6	277.5(1)–285.9(1)	9	[c]
8	277.5(2)–289.9(2)	9	[c]
$[Ba([18]crown-6)(NCS)_2(H_2O)]$	280.8(6)–287.5(5)	9	44
$[Ba([18]crown-6)\{O_2P(OnBu)_2\}(H_2O)]$	281(2)–290(2)	9	45
$[Ba([18]crown-6)(O_2CCF_3)_2(py)]$	282.0(5)–284.5(7)	10	46
$[Ba([18]crown-6)(pta)_2]$[d]	278.6(3)–283.1(3)	10	47
$[Ba(DB[18]crown-6)(pta)_2]$[e]	292.9(4)–317.1(4)	10	47
$[Ba([18]crown-6)(H_2O)_3Cl]Cl$	277.0(2)–285.4(1)	10	48
$[Ba([18]crown-6)(O_2CCH_3)_2]$	275.3(2)–283.5(2)	10	49
$[Ba([18]crown-6)(NO_3)_2H_2O]$	283(1)–290.8(8)	11	27

[a] Coordination number. [b] Mes* = 2,4,6-$tBu_3C_6H_2$. [c] This work. [d] pta = 1,1,1-trifluoro-5,5-dimethylhexane-2,4-dione. [e] DB = dibenzo.

respectively.[24] The O1–4–Ba1–O10 angles are much closer to 90°. The O_{crown}–Ba bond lengths of 277.5(1) to 285.9(1) pm are in accordance with those of different [18]crown-6 complexes with barium. Nevertheless these distances are dependent on several factors such as coordination number, donor strength and the sterically demand of coligands (see Table 2).

Similar to the compounds **3–5**, the silicon bonded oxygen atoms do not differ significantly concerning the oxygen metal distance in comparison to the fully carbon substituted oxygen atoms. Again an eclipsed arrangement of the methyl groups at the silicon atoms is found. With 2.3(1) and 2.7(1)° the C–Si–Si–C torsion angles are even smaller. The monodentate coordinating triflate group binding to the metal ion has a O(10)–Ba1 bond length of 253.9(3) pm. The chelating triflate group has significantly longer bond lengths of 288.7(1) and 292.1(1) pm. This is very similar to the trifluoroacetate groups in the complex $[Ba(O_2CCF_3)_2([18]crown-6)(py)]$ (py = pyridine). The trifluoroacetate group, which acts as monodentate ligand, has O–Ba bond length of 263.1(9) pm. The chelating one has a bond length of 287.6(1) pm.[46] To what extend these complexes are affected by negative hyperconjugation is still a matter of interest. We therefore claimed to crystallize a free ligand which can be compared to coordination compounds and started to prepare the heavier benzylic crown ether 1,2-disila-benzo[18]crown-6 (**7**). The organic fragment of 1,2-disila-benzo[18]crown-6 was synthesized by reaction of catechol and 2-(2-chlorethoxy)ethanol.[50] Subsequent addition of 1,2-dichloro-1,1,2,2-tetramethyldisilane yielded compound **7** (Scheme 5). However, **7** was obtained as a viscous oil, so no crystal structure could be obtained. An investigation regarding the coordination ability of **7** was still interesting because the benzylic unit as well as the Si_2Me_4 fragment are considerably unpliable. Coordination chemistry was performed by reaction of **7** with $Ba(OTf)_2$, yielding $[Ba(1,2\text{-disila-Benzo}[18]crown\text{-}6)OTf_2]$ (**8**), which crystallizes in the orthorhombic space group $P2_12_12_1$ (Fig. 5).

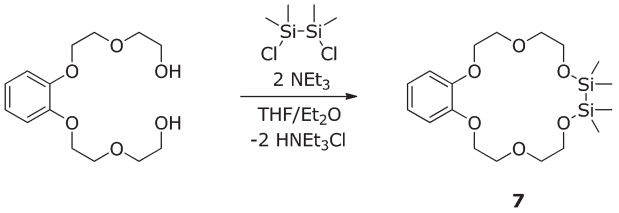

7

Scheme 5 Synthesis of 1,2-disila-benzo[18]crown-6.

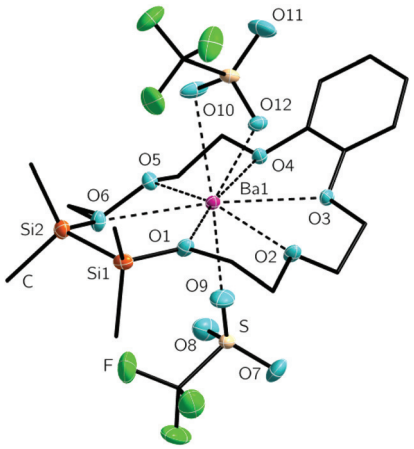

Fig. 5 Molecular structure of **8** in the crystal. Thermal ellipsoids represent a probability level of 50%. Hydrogen and disordered atoms with lower occupancy are omitted for clarity. Selected bond lengths [pm]: O1–Ba1 279.6(2), O2–Ba1 278.2(2), O3–Ba1 289.9(2), O4–Ba(1) 284.9(1), O5–Ba1 277.5(2), O6–Ba1 286.6(2), O9–Ba1 263.0(7), O10–Ba1 282.8(4), O12–Ba1 279.9(1), Si1–O1 167.8(2), Si2–O6 167.5(2), Si1–Si2 233.9(1). Selected bond angles [°]: O1–Ba1–O6 70.8(1), O1–Ba1–O4 170.0(1), O2–Ba1–O5 157.0(1), O3–Ba1–O6 166.3(1).

As previously shown for **6**, the metal ion in **8** is coordinated by all of the crown ether oxygen atoms as well as the two triflate groups. The barium ion is only slightly shifted out of the center of the crown ether. The transannular angles of 157.0(1) to 170.0(1)° are close to 180°, so the barium cation fits well into the cavity of **7**.

In contrast to **6**, the twisting of the crown is absent. The crown ether is rather bent with the benzylic as well as the disilane unit buckling to one side. With 277.5(2)–289.9(2) pm, the O_{crown}–Ba distances have almost the same lengths as in **6**. So have those of related compounds (see Table 2). Similar to **6**, one triflate group is chelating, the other one bonds to the metal ion only by a single oxygen atom. In comparison to O9, whose atomic distance to the metal ion is 263.0(7) pm, the chelating oxygen atoms of the triflate group have O10–Ba1 and O12–Ba1 atomic distances of 282.8(4) and 279.1(6) pm, respectively. The methyl groups of the $SiMe_2$ units are only slightly contorted to each other and show torsion angles of 16.8(1) and 18.3(1)°.

According to recently published work another key role in understanding the complexation ability of silicon based crown ethers analogues is the repulsion between the positively

charged metal ion and the positively polarized silicon atoms.[14] The use of Si_2Me_4 rather than one $SiMe_2$ allows lower repulsion, which can be seen in the average Si–M distances. This might also be an explanation for the higher complexation ability of these hybrid disila-crown ethers in comparison to cyclosiloxanes which we reported before. Further calculations would be helpful to quantify though. Experimental data of metal complexes with disila units, however, features longer average Si–M distances than the sila units in siloxanes. While [Li(1,2-disila[12]crown-4)OTf] has average M–Si distances of 321.6 pm they are shortened to 272–275 pm in the cyclosiloxane complexes $[Li(D_6)Al_F]$ and $[Li(D_6)Al_{PhF}]$ (Al_{PhF} = $[Al\{OC(CF_3)_2Ph\}_4]^-$).[2,19] [K(1,2-disila[18]crown-6)PF_6] has Si–M average distances of 392.4(1) pm.[19] $[K(D_7)]^+$ has average distances of 358–365 pm, so these are shortened as well.[4,21] Analogous observations were made in the comparison of alkaline earth metal complexes reported in this work like **5** and **6** with siloxane complexes such as $[Sr(NBN\text{-}SiMe_2OSiMe_2O)THF]_2$ or $[Ba(THF)_6(dmpz)_8\{(OSiMe_2)O\}_2]$ (dmpz = 3,5-dimethylpyrazolate).[51,52] Still no complexes of common cyclosiloxanes and alkaline earth metal salts are known today, so the reported complexes in this work are the first crown-type structures containing an alkaline earth metal as well as ligands bearing Si–O donors.

Conclusions

In a recent work, we described the synthesis of hybrid disila-crown ethers of the type 1,2-disila[3*n*]crown-*n* (**1**: *n* = 5, **2**: *n* = 6) and the formation of alkaline metal complexes.[19] Within this study, we reported the synthesis of 1,2-disila-benzo[18]crown-6 (**7**) using similar conditions.

By equimolar reaction of alkaline earth metal salts with the disila-crown ethers **1**, **2** and **7**, we obtained the alkaline earth metal complexes **3–6** and **8**. The structures of all coordination compounds were determined *via* X-ray crystallographic studies. The O_{crown}–M bond lengths indicate that all carbon substituted oxygen atoms show almost the same bond lengths to the metal ion as the half carbon and half silicon affected oxygen atoms, so that on a structural level no reduced complexation ability of these O–Si_2Me_4–O fragments can be observed. The variation of ion diameter and cavity diameter of the crown then gives interesting coordination patterns: in compound **4**, the cavity diameter of **2** is too large for the calcium ion resulting in a mismatch structure. This structure reveals that it's not inevitably the silicon affected oxygen atom which does not participate in the coordination but according to proton NMR-studies, the complexation ability of 1,2-disila[18]crown-6 (**2**) was determined to be significantly lower than those of [18]crown-6. The size complementarity between cation and host cavity significantly influences the complex stabilities.

Beside the triflate complexes **4**, **6** and **8**, we also obtained complexes with strongly coordinating anions such as Br^- or I^- (compound **3** and **5**). These results show a better coordination ability of disila-bridged donor atoms in comparison to R_2Si bridges, which results from longer Si–M distance within the metal complexes and a reduced cyclic stress. Furthermore DFT calculations (BP86 functional and def2-TZVP basis set) revealed that the coordination ability of 1,2-disila[15]crown-5 (**1**) towards magnesium bromide is considerably higher compared to [15]crown-5. Nonetheless, all disila-substituted crown ether oxygen atoms of the type SiSi–O–SiSi would still be useful to give more meaningful results in how far disila-affected crown ethers can challenge organic crown compounds. Most recent work hints a considerably higher complexation ability of the partially silicon substituted crown ether 1,2,4,5-tetrasila[12]crown-4 towards Li^+ than [12]crown-4.[53] Thus, further investigations for this kind of crown ethers and a stepwise synthesis of a fully silicon substituted crown ether are intended for the future.

Experimental section

General

All working procedures were carried out with rigorous exclusion of oxygen and moisture using Schlenk techniques under inert gas atmosphere. Solvents were dried and freshly distilled before use. Compounds **1**, **2** and the organic fragment of **7** were synthesized using methods described in literature.[19,50] Alkaline earth metal salts were stored and handled under argon atmosphere using a glovebox. NMR spectra were recorded on a Bruker AV III HD 300 MHz or AV III 500 MHz. Infrared (IR) spectra of the respective samples were measured using attenuated total reflectance (ATR) mode on a Bruker Model Alpha FT-IR. MS-spectrometry was measured on JEOL AccuTOF-GC (LIFDI) or LTQ-FT (ESI). Elemental analysis was performed on a Vario MicroCube. Fluorine-containing compounds led to ongoing damage of the elemental analyser and were not measured.

Synthesis of [Mg(1,2-disila[15]crown-5)Br_2] (3). 0.244 g 1,2-disila[15]crown-5 (0.79 mmol) are dissolved in 15 mL trifluorotoluene, and 0.146 g (0.79 mmol) $MgBr_2$ are added. The suspension is stirred for four days and then filtered. The residue is washed with 4 mL DCM, and the filtrate is freed of the solvent. The resulting solid is washed with three portions of 5 mL *n*-pentane, dissolved in 2 mL DCM and layered with 10 mL *n*-pentane. After two days, **3** is obtained as colourless blocks (0.12 g, 30%). Elemental Analysis [%] found (calc.): C 28.83 (29.26) H 6.18 (5.73).

^{1}H NMR: (300 MHz, CD_2Cl_2) δ = 0.44 (s, 12H, Si(CH_3)$_2$), 3.77–3.80 (m, 4H, CH_2), 3.86 (s, 8H, CH_2), 3.95–3.98 (m, 4H, CH_2) ppm; $^{13}C\{^1H\}$ NMR: (75 MHz, CD_2Cl_2) δ = −0.8 (s, Si(CH_3)$_2$), 61.8 (s, CH_2), 68.1 (s, CH_2), 68.5 (s, CH_2), 69.9 (s, CH_2) ppm; $^{29}Si\{^1H\}$ NMR: (99 MHz, CD_2Cl_2) δ = 18.0 (s, *Si*(CH_3)$_2$) ppm; MS: LIFDI(+) *m*/*z* (%): 411.051 $[M - Br]^+$ (83); IR (cm^{-1}): 2948 (m), 2884 (w), 1634 (w), 1467 (m), 1345 (w), 1297 (w), 1243 (m), 1084 (s), 1058 (s), 1046 (s), 959 (s), 922 (m), 896 (m), 824 (m), 803 (m), 774 (w), 730 (s), 696 (w), 639 (w), 568 (w).

Synthesis of [Ca(1,2-disila[18]crown-6)OTf_2] (4). 0.192 g 1,2-disila[18]crown-6 (0.79 mmol) are dissolved in 15 mL DCM,

and 0.146 g (0.79 mmol) $CaOTf_2$ are added. The suspension is stirred vigorously overnight and then filtered. The residue is washed with 2 mL DCM and the filtrate is freed of the solvent. The resulting solid is washed with three portions of 5 mL *n*-pentane, dissolved in 5 mL DCM and layered with 10 mL *n*-pentane. After two days, **4** is obtained as colourless rods (0.187 g, 39%).

^{1}H NMR: (300 MHz, CD_2Cl_2) δ = 0.41 (s, 12H, Si(CH_3)$_2$), 3.80–3.84 (m, 4H, CH_2), 3.87–3.89 (m, 12H, CH_2), 3.94–3.97 (m, 4H, CH_2) ppm; ^{13}C{^{1}H} NMR: (75 MHz, CD_2Cl_2) δ = −0.9 (s, Si(*C*H$_3$)$_2$), 62.9 (s, *C*H$_2$), 69.7 (s, *C*H$_2$), 70.3 (s, *C*H$_2$), 70.7 (s, *C*H$_2$), 72.7 (s, *C*H$_2$), 120.7 (q, $^1J_{CF}$ = 318 Hz, *C*F$_3$) ppm; ^{29}Si{^{1}H} NMR: (99 MHz, CD_2Cl_2) δ = 19.7 (s, *Si*(CH$_3$)$_2$) ppm; ^{19}F NMR: (282 MHz, CD_2Cl_2) δ = −79.3 (s, C*F*$_3$) ppm; MS LIFDI(+) *m*/*z* (%): 375.165 [1,2-disila[18]crown-6 + Na]$^+$ (100), 541.088 [M − OTf]$^+$ (40); IR (cm^{-1}): 2954 (w), 2887 (w), 1471 (w), 1357 (w), 1305 (s), 1240 (s), 1219 (s), 1164 (s), 1059 (s), 1028 (s), 935 (s), 868 (m), 838 (s), 817 (s), 795 (s), 775 (s), 760 (s), 726 (s), 634 (s), 579 (m), 514 (s), 460 (w).

Synthesis of [Sr(1,2-disila[18]crown-6)I$_2$] (5). 0.355 g 1,2-disila[18]crown-6 (1.00 mmol) are dissolved in 20 mL trifluorotoluene, and 0.343 g (0.79 mmol) SrI_2 are added. The suspension is stirred under exclusion of light for 12 h and then filtered. The residue is washed with 2 mL DCM, and the filtrate is freed of the solvent. The resulting solid is washed with three portions of 5 mL *n*-pentane, dissolved in 3 mL DCM and layered with 15 mL *n*-pentane. After two days, **5** is obtained as colourless plates (0.227 g, 33%). Elemental Analysis [%] found (calc.): C 24.23 (23.96) H 5.05 (4.65).

^{1}H NMR: (300 MHz, CD_2Cl_2) δ = 0.46 (s, 12H, Si(CH_3)$_2$), 3.81–3.84 (m, 4H, CH_2), 3.90 (s, 4H, CH_2), 3.91–3.96 (m, 8H, CH_2), 4.05–4.08 (m, 4H, CH_2) ppm; ^{13}C{^{1}H} NMR: (75 MHz, CD_2Cl_2) δ = 0.0 (s, Si(*C*H$_3$)$_2$), 63.1 (s, *C*H$_2$), 70.4 (s, *C*H$_2$), 70.5 (s, *C*H$_2$), 70.5 (s, *C*H$_2$), 73.0 (s, *C*H$_2$) ppm; ^{29}Si{^{1}H} NMR: (99 MHz, CD_2Cl_2) δ = 18.2 (s, *Si*(Me)$_2$) ppm. MS: LIFDI(+) *m*/*z* (%): 566.984 [M − I]$^+$ (100); IR (cm^{-1}): 2943 (w), 2881 (w), 1457 (w), 1353 (w), 1320 (w), 1245 (m), 1082 (s), 1039 (s), 972 (s), 957 (s), 930 (s), 919 (s), 862 (s), 841 (s), 823 (s), 797 (s). 769 (s), 729 (s), 696 (m), 657 (w), 628 (m), 532 (w), 461 (w).

Synthesis of [Ba(1,2-disila[18]crown-6)OTf$_2$] (6). 0.100 g 1,2-disila[18]crown-6 (0.28 mmol) are dissolved in 15 mL DCM, and 0.124 g (0.28 mmol) $BaOTf_2$ are added. The suspension is stirred overnight and then filtered. The residue is washed with 2 mL DCM and the filtrate is freed of the solvent. The resulting solid is washed with three portions of 5 mL *n*-pentane, dissolved in 4 mL DCM and layered with 10 mL *n*-pentane. After two days, **6** is obtained as colourless blocks (0.103 g, 38%).

^{1}H NMR: (300 MHz, CD_2Cl_2) δ = 0.36 (s, 12H, Si(CH_3)$_2$), 3.68–3.70 (m, 4H, CH_2), 3.78 (s, 12H, CH_2), 3.86–3.88 (m, 4H, CH_2) ppm; ^{13}C{^{1}H} NMR: (75 MHz, CD_2Cl_2) δ = −0.9 (s, Si(*C*H$_3$)$_2$), 63.6 (s, *C*H$_2$), 70.7 (s, *C*H$_2$), 70.9 (s, *C*H$_2$), 71.3 (s, *C*H$_2$), 73.2 (s, *C*H$_2$), 120.9 (q, $^1J_{CF}$ = 321 Hz, *C*F$_3$) ppm; ^{19}F NMR: (282 MHz, CD_2Cl_2) δ = −79.1 (s, C*F*$_3$) ppm; ^{29}Si{^{1}H} NMR: (99 MHz, CD_2Cl_2) δ = 17.6 (s, *Si*(CH$_3$)$_2$) ppm; MS ESI(+) *m*/*z* (%): 639.031 [M − OTf]$^+$ (100); IR (cm^{-1}): 2951 (w), 2925 (w), 2888 (w), 1475 (w), 1456 (w), 1353 (w), 1296 (s), 1242 (s), 1223 (s), 1164 (s), 1123 (s), 1105 (s), 1083 (s), 1074 (s), 1024 (s), 964 (s), 952 (s), 917 (w), 896 (w), 873 (m), 864 (s), 842 (s), 821 (s), 799 (m), 774 (s), 759 (m), 736 (s), 719 (m), 698 (w), 631 (s), 580 (s), 574 (s), 540 (s), 514 (s), 456 (w).

Synthesis of 1,2-disila-benzo[18]crown-6 (7). 0.73 g of 1,2-bis (5-hydroxy-3-oxa-1-pentyloxy)benzene (2.55 mmol) and 0.49 mL 1,2-dichloro-1,1,2,2-tetramethyldisilane (2.55 mmol) are dissolved in 50 mL of THF each and added dropwise into a stirred solution of 100 mL THF, 20 mL Et_2O and 0.7 mL triethylamine (5.1 mmol) simultaneously over a period of 90 min. After stirring the solution overnight, the solvent is removed under reduced pressure. The residue is resolved in 20 mL toluene and filtered. The solvent is removed again and 4 mL acetonitrile is added. The crude product is gently washed and the solution is decanted. The solvent is yet again removed under reduced pressure and the resulting oil is dried *in vacuo* at 1×10^{-3} mbar for several hours. The crown ether is obtained as colourless, slightly yellow oil (0.77 g, 75%).

^{1}H NMR: (300 MHz, CD_3CN) δ = 0.21 (s, 12H, Si(CH_3)$_2$), 3.60–3.63 (m, 4H, CH_2), 3.75–3.80 (m, 8H, CH_2), 4.08–4.11 (m, 4H, CH_2), 6.87–6.98 (m, 4H, CH_{AR}) ppm; ^{13}C{^{1}H} NMR: (75 MHz, CD_3CN) δ = −0.29 (s, Si(*C*H$_3$)$_2$), 63.9 (s, *C*H$_2$), 69.8 (s, *C*H$_2$), 70.4 (s, *C*H$_2$), 73.6 (s, *C*H$_2$), 114.7 (s, *C*H$_2$), 122.2 (s, *C*H$_{Ar}$), 149.8 (s, C_{qAr}) ppm. ^{29}Si{^{1}H} NMR: (99 MHz, CD_3CN): δ = 11.0 (s, *Si*(CH$_3$)$_2$) ppm; MS (LIFDI+) *m*/*z* (%): 400.17443 [M]$^+$ (20); IR (cm^{-1}): 2947 (m), 2868 (m), 1593 (m), 1501 (s), 1453 (m), 1396 (w), 1356 (w), 1328 (w), 1248 (s), 1219 (s), 1125 (s), 1088 (s), 1051 (s), 943 (s), 826 (s), 789 (s), 763 (s), 740 (s), 682 (w), 658 (m), 630 (w), 481 (w).

Synthesis of [Ba(1,2-disila-benzo[18]crown-6)OTf$_2$] (8). 0.164 g 1,2-disila-benzo[18]crown-6 (0.41 mmol) are dissolved in 15 mL DCM, and 0.178 g (0.28 mmol) $BaOTf_2$ are added. The suspension is stirred for 6 h and then filtered. The residue is washed with 2 mL DCM and the filtrate is freed of the solvent. The resulting solid is washed with four portions of 10 mL *n*-pentane, dissolved in 4 mL DCM and layered with 15 mL *n*-pentane. After two days, **8** is obtained as colourless blocks (0.120 g, 35%).

^{1}H NMR: (300 MHz, CD_2Cl_2) δ = 0.36 (s, 12H, Si(CH_3)$_2$), 3.81–3.88 (m, 8H, CH_2), 4.03–4.06 (m, 4H, CH_2), 4.24–4.27 (m, 4H, CH_2), 6.93–7.03 (m, 4H, CH_{AR}) ppm; ^{13}C{^{1}H} NMR: (75 MHz, CD_2Cl_2) δ = −0.9 (s, Si(*C*H$_3$)$_2$), 63.4 (s, *C*H$_2$), 68.4 (s, *C*H$_2$), 69.6 (s, *C*H$_2$), 73.4 (s, *C*H$_2$), 112.3 (s, *C*H$_{AR}$), 120.8 (q, $^1J_{CF}$ = 319 Hz, *C*F$_3$), 122.8 (s, *C*H$_{Ar}$), 146.9 (s, $C_{q,Ar}$) ppm; ^{19}F NMR: (282 MHz, CD_2Cl_2) δ = −78.7 (s, C*F*$_3$) ppm; ^{29}Si{^{1}H} NMR: (99 MHz, CD_2Cl_2) δ = 17.7 (s, *Si*(CH$_3$)$_2$) ppm; MS LIFDI (+) *m*/*z* (%): 687.031 [M − OTf]$^+$ (100), 1523.014 [2M − OTf]$^+$ (100); IR (cm^{-1}): 2945 (w), 2885 (w), 1596 (w), 1506 (s), 1477 (m), 1456 (w), 1357 (s), 1300 (s), 1240 (s), 1220 (s), 1171 (s), 1115 (s), 1063 (s), 1034 (s), 1023 (s), 961 (s), 941 (s), 914 (s), 865 (m), 852 (s), 837 (s), 819 (s), 795 (s), 772 (s), 756 (s), 737 (s), 634 (s), 604 (m), 583 (m), 573 (m), 528 (m), 513 (s), 454 (w).

Computational details

Calculations were performed with the program system TURBOMOLE V7.0.1.[54] The resolution of identity (RI) approxi-

mation, dispersion corrections, and the conductor-like screening model (COSMO) were applied throughout, the latter with default settings. For all calculations, the BP86 functional was chosen, utilizing a def2-TZVP basis set.[55]

Crystal structures

Single crystal X-ray diffraction was carried out using Bruker D8 Quest (**3**, **6**, **8**) or IPDS 2 diffractometer (**4**, **5**) at 100–110 K with MoK_α radiation and X-ray optics or graphite monochromatization, respectively (λ = 0.71073). The structures were solved by direct methods and refinement with full-matrix-least-squares against F^2 using SHELXT- and SHELXL-2015 on OLEX2 platform.[56–58] Triflate groups were refined with help of DSR.[59] Crystallographic data for compounds **3–6** and **8** are denoted as follows: CCDC No. 1497469 (**3**), 1497467 (**4**), 1497468 (**5·DCM**), 1497471 (**6**) and 1497470 (**8**).

Crystal data of 3. $C_{12}H_{28}Br_2MgO_5Si_2$, orthorhombic, *Pbca*, Z = 8, 100 K, a = 10.8339(6) Å, b = 14.1089(7) Å, c = 27.7505(14) Å, V = 4241.8(4) Å^3, ρ = 1.543 g cm^{-3}, multiscan absorption correction using SADABS-2014,[60] μ = 3.980 mm^{-1}, T_{min}, T_{max} = 0.622, 0.745, 2Θ range 4.77–50.54°, reflections measured 22 357, independent reflections 3841 [R(int) = 0.0724], 203 parameters, R-index [$I \geq 2\sigma(I)$] 0.0322, wR_2 (all data) 0.0553, GOOF 1.023, $\Delta\rho_{max}$, $\Delta\rho_{min}$ 0.40/−0.41 e Å^3.

Crystal data of 4. $C_{16}H_{32}CaF_6O_{12}S_2Si_2$, monoclinic, $P2_1/n$, Z = 4, 100 K, a = 8.9460(18) Å, b = 34.272(7) Å, c = 9.6976(19) Å, β = 103.04°, V = 2896.6(11) Å^3, ρ = 1.584 g cm^{-3}, numerical absorption correction using X-AREA and X-RED32,[61] μ = 0.535 mm^{-1}, T_{min}, T_{max} = 0.874, 0.951, 2Θ range 4.48–49.62°, reflections measured 13 664, independent reflections 4991 [R(int) = 0.0780], 358 parameters, R-index [$I \geq 2\sigma(I)$] 0.0408, wR_2 (all data) 0.1089, GOOF 1.008, $\Delta\rho_{max}$, $\Delta\rho_{min}$ 0.73/–0.67 e Å^3.

Crystal data of 5·DCM. $C_{15}H_{34}Cl_2I_2O_6Si_2Sr$, monoclinic, $C2/c$, Z = 8, 100 K, a = 14.037(3) Å, b = 10.896(2) Å, c = 37.359(8) Å, β = 99.19(3)°, V = 5641(2) Å^3, ρ = 1.834 g cm^{-3}, numerical absorption correction using X-AREA and X-RED32,[61] μ = 4.400 mm^{-1}, T_{min}, T_{max} = 0.482, 0.709, 2Θ range 4.756–52.016°, reflections measured 15 303, independent reflections 5516 [R(int) = 0.0290], 257 parameters, R-index [$I \geq 2\sigma(I)$] 0.0191, wR_2 (all data) 0.0360, GOOF 0.800, $\Delta\rho_{max}$, $\Delta\rho_{min}$ 0.60/−0.61 e Å^3.

Crystal data of 6. $C_{16}H_{32}BaF_6O_{12}S_2Si_2$, triclinic, $P\bar{1}$, Z = 4, Z' = 2, 100 K, a = 9.7531(4) Å, b = 17.5485(8) Å, c = 18.5666(8) Å, α = 72.5040(10)°, β = 86.902(2)° γ = 89.5490(10)°, V = 3026.2(2) Å^3, ρ = 1.617 g cm^{-3}, multiscan absorption correction using SADABS-2014,[60] μ = 1.617 mm^{-1}, T_{min}, T_{max} = 0.544, 1.000, 2Θ range 4.518–61.68°, reflections measured 103 763, independent reflections 18 918 [R(int) = 0.0254], 982 parameters, R-index [$I \geq 2\sigma(I)$] 0.0237, wR_2 (all data) 0.0509, GOOF 1.093, $\Delta\rho_{max}$, $\Delta\rho_{min}$ 1.03/−2.70 e Å^3.

Crystal data of 8. $C_{20}H_{32}BaF_6O_{12}S_2Si_2$, orthorhombic, $P2_12_12_1$, Z = 4, 110 K, a = 9.0173(4) Å, b = 10.3761(5) Å, c = 35.6495(16) Å, V = 3335.5(3) Å^3, ρ = 1.665 g cm^{-3}, numerical absorption correction using SADABS-2014,[60] μ = 1.473 mm^{-1}, T_{min}, T_{max} = 0.668, 0.904, 2Θ range 4.542–57.452°, reflections measured 32 181, independent reflections 8616 [R(int) = 0.0346], 525 parameters, R-index [$I \geq 2\sigma(I)$] 0.0274, wR_2 (all data) 0.0481, GOOF 1.037, $\Delta\rho_{max}$, $\Delta\rho_{min}$ 0.59/−0.60 e Å^3, Flack parameter 0.002(6).

Acknowledgements

This work was financially supported by the Deutsche Forschungsgemeinschaft (DFG).

References

1 J. S. Ritch and T. Chivers, *Angew. Chem.*, 2007, **119**, 4694–4697, (*Angew. Chem., Int. Ed.*, 2007, **46**, 4610–4613).
2 A. Decken, J. Passmore and X. Wang, *Angew. Chem.*, 2006, **118**, 2839–2843, (*Angew. Chem., Int. Ed.*, 2006, **45**, 2773–2777).
3 C. von Hänisch, O. Hampe, F. Weigend and S. Stahl, *Angew. Chem.*, 2007, **119**, 4859–4863, (*Angew. Chem., Int. Ed.*, 2007, **46**, 4775–4779).
4 M. R. Churchill, C. H. Lake, S.-H. L. Chao and O. T. Beachley, *J. Chem. Soc., Chem. Commun.*, 1993, **1**, 1577–1578.
5 A. Decken, F. A. LeBlanc, J. Passmore and X. Wang, *Eur. J. Inorg. Chem.*, 2006, 4033–4036.
6 I. Krossing and I. Raabe, *Angew. Chem.*, 2004, **116**, 2116–2142, (*Angew. Chem., Int. Ed.*, 2004, **43**, 2066–2090).
7 R. D. Ernst, A. Glöckner and A. M. Arif, *Z. Kristallogr.*, 2007, **222**, 333–334.
8 J. Passmore and J. M. Rautiainen, *Eur. J. Inorg. Chem.*, 2012, 6002–6010.
9 F. Weinhold and R. West, *Organometallics*, 2011, **30**, 5815–5824.
10 F. Weinhold and R. West, *J. Am. Chem. Soc.*, 2013, **135**, 5762–5767.
11 H. Oberhammer and J. E. Boggs, *J. Am. Chem. Soc.*, 1980, **102**, 7241–7244.
12 R. J. Gillespie and S. A. Johnson, *Inorg. Chem.*, 1997, **36**, 3031–3039.
13 S. Grabowsky, M. F. Hesse, C. Paulmann, P. Luger and J. Beckmann, *Inorg. Chem.*, 2009, **48**, 4384–4393.
14 T. S. Cameron, A. Decken, I. Krossing, J. Passmore, J. M. Rautiainen, X. Wang and X. Zeng, *Inorg. Chem.*, 2013, **52**, 3113–3126.
15 M. Ouchi, Y. Inoue, T. Kanzaki and T. Hakushi, *Bull. Chem. Soc. Jpn.*, 1984, **57**, 887–888.
16 Y. Inoue, M. Ouchi and T. Hakushi, *Bull. Chem. Soc. Jpn.*, 1985, **58**, 525–530.
17 D. J. Harrison, D. R. Edwards, R. McDonald and L. Rosenberg, *Dalton Trans.*, 2008, 3401–3411.
18 M. K. Skjel, A. Y. Houghton, A. E. Kirby, D. J. Harrison, R. McDonald and L. Rosenberg, *Org. Lett.*, 2010, **12**, 376–379.
19 K. Reuter, M. R. Buchner, G. Thiele and C. von Hänisch, *Inorg. Chem.*, 2016, **55**, 4441–4447.

20 M. Stürmann, W. Saak, M. Weidenbruch and K. W. Klinkhammer, *Eur. J. Inorg. Chem.*, 1999, 579–582.
21 C. Eaborn, P. B. Hitchcock, K. Izod and J. D. Smith, *Angew. Chem.*, 1995, **107**, 2936–2937, (*Angew. Chem., Int. Ed. Engl.*, 1996, **34**, 2679–2680).
22 J. L. Atwood, S. G. Bott, C. M. Means, A. W. Coleman, H. Zhang and M. T. May, *Inorg. Chem.*, 1990, **29**, 467–470.
23 M. Barboiu and A. van der Lee, *Acta Crystallogr., Sect. C: Cryst. Struct. Commun.*, 2003, **59**, m366–m368.
24 M. Trömel, *Z. Naturforsch.*, 2000, **55b**, 243–247.
25 S. Chadwick and K. Ruhlandt-Senge, *Chem. – Eur. J.*, 1998, **4**, 1768–1780.
26 S. Chadwick, U. Englich and K. Ruhlandt-Senge, *Inorg. Chem.*, 1999, **38**, 6289–6293.
27 P. C. Junk and J. W. Steed, *J. Chem. Soc., Dalton Trans.*, 1999, 407–414.
28 Y. Y. Wei, B. Tinant, J. P. Declercq, M. Van Meerssche and J. Dale, *Acta Crystallogr., Sect. C: Cryst. Struct. Commun.*, 1988, **44**, 73–77.
29 T. B. Rubtsova, O. K. Kireeva, B. M. Bulychev, N. P. Streltsova, V. K. Belsky and B. P. Tarasov, *Polyhedron*, 1992, **11**, 1929–1938.
30 P. Farina, W. Levason and G. Reid, *Dalton Trans.*, 2013, **42**, 89–99.
31 J. Langer, S. Krieck, R. Fischer, H. Görls and M. Westerhausen, *Z. Anorg. Allg. Chem.*, 2010, **636**, 1190–1198.
32 D. Braga, M. Gandolfi, M. Lusi, D. Paolucci, M. Polito, K. Rubini and F. Grepioni, *Chem. – Eur. J.*, 2007, **13**, 5249–5255.
33 A. N. Chekhlov, *Russ. J. Coord. Chem.*, 2009, **35**, 492–495.
34 A. Verma, M. Guino-O, M. Gillett-Kunnath, W. Teng and K. Ruhlandt-Senge, *Z. Anorg. Allg. Chem.*, 2009, **635**, 903–913.
35 U. Englich, K. Ruhlandt-Senge and F. Uhlig, *J. Organomet. Chem.*, 2000, **613**, 139–147.
36 R. H. Crabtree, *The Organometallic Chemistry of the Transition Metals*, John Wiley & Sons, Ltd., Hoboken, NJ, 4th edn, 2005.
37 A. N. Swinburne and J. W. Steed, *Podands. Supramolecular Chemistry: From Molecules to Nanomaterials*, John Wiley & Sons, Ltd., see DOI: 10.1002/9780470661345.smc058.
38 P. C. Junk, L. M. Louis and M. K. Smith, *Z. Anorg. Allg. Chem.*, 2002, **628**, 1196–1209.
39 P. C. Junk and J. W. Steed, *J. Coord. Chem.*, 2007, **60**, 1017–1028.
40 W. Maudez and K. M. Fromm, *Z. Anorg. Allg. Chem.*, 2012, **638**, 1810–1819.
41 J. S. Alexander and K. Ruhlandt-Senge, *Chem. – Eur. J.*, 2004, **10**, 1274–1280.
42 M. R. Crimmin, A. G. M. Barrett, M. S. Hill, P. B. Hitchcock and P. A. Procopiou, *Inorg. Chem.*, 2007, **46**, 10410–10415.
43 K. Ruhlandt-Senge and U. Englich, *Chem. – Eur. J.*, 2000, **6**, 4063–4070.
44 B. Wei, Y. Tinant, M. Declercq, J. Van Meerssche and J. Dale, *Acta Crystallogr., Sect. C: Cryst. Struct. Commun.*, 1988, **44**, 77–80.
45 J. H. Burns, *Inorg. Chim. Acta*, 1985, **102**, 15–21.
46 W. A. Wojtczak, M. J. Hampden-Smith and E. N. Duesler, *Inorg. Chem.*, 1998, **37**, 1781–1790.
47 T. S. Pochekutova, V. K. Khamylov, Y. A. Kurskii, G. K. Fukin and B. I. Petrov, *Polyhedron*, 2010, **29**, 1381–1386.
48 M.-M. Zhao, *Acta Crystallogr., Sect. E: Struct. Rep. Online*, 2012, **68**, m286–m286.
49 L. Archer, M. J. Hampden-Smith and E. Duesler, *Polyhedron*, 1998, **17**, 713–723.
50 H.-F. Ji, R. Dabestani, G. M. Brown and R. L. Hettich, *J. Chem. Soc., Perkin Trans. 2*, 2001, 585–591.
51 S. Harder, B. Freitag, P. Stegner, J. Pahl and D. Naglav, *Z. Anorg. Allg. Chem.*, 2015, **641**, 2129–2134.
52 A. Steiner, G. T. Lawson, B. Walfort, D. Leusser and D. Stalke, *J. Chem. Soc., Dalton Trans.*, 2001, 219–221.
53 K. Reuter, G. Thiele, T. Hafner, F. Uhlig and C. von Hänisch, *Chem. Commun.*, 2016, **52**, 13265–13268.
54 (*a*) Turbomole Version 7.0.1, Turbomole GmbH 2016. Turbomole is a development of University of Karlsruhe and Forschungszentrum Karlsruhe 1989–2007, Turbomole GmbH since 2007; (*b*) F. Furche, R. Ahlrichs, C. Hättig, W. Klopper, M. Sierka and F. Weigend, *Wiley Interdiscip. Rev.: Comput. Mol. Sci.*, 2014, **4**, 91–100.
55 (*a*) F. Weigend and R. Ahlrichs, *Phys. Chem. Chem. Phys.*, 2005, **7**, 3297; (*b*) F. Weigend, *Phys. Chem. Chem. Phys.*, 2006, **8**, 1057; (*c*) M. Dolg, H. Stoll, A. Savin and H. Preuss, *Theor. Chim. Acta*, 1989, **75**, 173; (*d*) H. Stoll, B. Metz and M. Dolg, *J. Comput. Chem.*, 2002, **23**, 767; (*e*) S. Grimme, J. Antony, S. Ehrlich and H. Krieg, *J. Chem. Phys.*, 2010, **132**, 154104; (*f*) S. Grimme, S. Ehrlich and I. Goerigk, *J. Comput. Chem.*, 2011, **32**, 1456.
56 G. M. Sheldrick, *Acta Crystallogr., Sect. A: Fundam. Crystallogr.*, 2015, **71**, 3–8.
57 G. M. Sheldrick, *Acta Crystallogr., Sect. C: Cryst. Struct. Commun.*, 2015, **71**, 3–8.
58 O. V. Dolomanov, L. J. Bourhis, R. J. Gildea, J. A. K. Howard and H. Puschmann, *J. Appl. Crystallogr.*, 2009, **42**, 339–341.
59 D. Kratzert, J. J. Holstein and I. Krossing, *J. Appl. Crystallogr.*, 2015, **48**, 933–938.
60 Bruker, *SADABS*, Bruker AXS Inc., Madison, Wisconsin, USA, 2014.
61 Stoe & Cie, *X-AREA and X-RED32*, Stoe & Cie, Darmstadt, Germany, 2009.

Crown ether complexes of alkali metal chlorides from SO_2

Kirsten Reuter,[a] Stefan S. Rudel,[b] Magnus R. Buchner,[b] Florian Kraus*[b] and Carsten von Hänisch*[a]

Abstract: The structures of the alkali metal chloride SO_2 solvates (Li – Cs) in conjunction with 12-crown-4 or 1,2-disila-12-crown-4 show strong discrepancies, despite the structural similarity of the ligands. With LiCl both types of crown ethers form 1:1 complexes and give [Li(1,2-disila-12-crown-4)(SO_2Cl)] (**1**) and [Li(12-crown-4)Cl]·4SO_2 (**2**). 1,2-disila-12-crown-4 turned out to be unable to coordinate cations too large for the cavity diameter, for example under formation of sandwich-type complexes. As a result, exclusively 12-crown-4 reacts with the heavier alkali metal chlorides NaCl, KCl and RbCl. [Na(12-crown-4)$_2$]Cl·4SO_2 (**3**) and [*M*(12-crown-4)$_2$(SO_2)]Cl·4SO_2 (**4**: *M* = K; **5**: *M* = Rb) all show *S* coordination to the chloride ions by four SO_2 molecules, respectively. Compounds **4** and **5** additionally exhibit the first crystallographically evidenced non-bridging *O,O'* coordination mode of SO_2. Unexpectedly, the disila-crown ether supports the dissolution of RbCl and CsCl in the solvent and yields the homoleptic SO_2 solvated alkali metal chlorides *M*Cl·3SO_2 (**6**: *M* = Rb; **7**: *M* = Cs), which incorporate bridging *μ-O,O'* coordinating moieties as well as the unprecedented side on *O,O*' coordination mode. All compounds were characterised by single crystal X-ray diffraction. The crown ether complexes were additionally studied by means of NMR spectroscopy, the presence of SO_2 at ambient temperature was proven by IR spectroscopy on the neat compounds.

Introduction

Liquid sulfur dioxide has been established as one of the most important non-aqueous, aprotic and polar solvents[1] for synthetic organic and inorganic chemistry.[2] Especially compounds having covalent bonding character such as $AlCl_3$ and BCl_3 are significantly more soluble in SO_2 than salts with a typical ionic lattice as for example LiCl and NaCl.[3][4] Numerous reported coordination compounds with SO_2 as a ligand display the variety of bonding modes.[5] *S* (e.g. [Mn(C_5H_5)(CO_2)(SO_2)])[6] and *S,O* coordination (e.g. [Mo(CO)$_3$(phen)(SO_2)])[7] were observed towards electron-rich complexes.[8] *O* (e.g. [Ni(SO_2)$_6$][AsF_6]$_2$)[9] and bridging *μ-O,O*' coordination (e.g. [Li(OSO)$_{6/2}$][$AlCl_4$][10] was reported for hard d- and f-block as well as main group metal atoms. The latter require the presence of almost non-coordinating anions[11] such as [$B_{12}Cl_{12}$]$^{2-}$ [12], [AsF_6]$^-$ [13] or [Al{OC(CF_3)$_3$}$_4$]$^-$ [14] to provide sufficient

[a] K. Reuter, Prof. Dr. C. v. Hänisch
Anorganische Chemie and Wissenschaftliches Zentrum für Materialwissenschaften (WZMW)
Philipps-Universität Marburg
Hans-Meerwein Straße 4, 35032 Marburg, Germany
E-mail: haenisch@chemie.uni-marburg.de
[b] S. S. Rudel, Dr. M. R. Buchner, Prof. Dr. F. Kraus
Anorganische Chemie, Fluorchemie and Wissenschaftliches Zentrum für Materialwissenschaften (WZMW)
Philipps-Universität Marburg
Hans-Meerwein Straße 4, 35032 Marburg, Germany
E-mail: florian.kraus@chemie.uni-marburg.de

solubility of the corresponding salts.[15] Thus, the resulting 'naked' cations are enabled to rather interact with the weakly coordinating SO_2 ligands than with the anion or in some cases with both.[16] By contrast, reactions of SO_2 with salts containing strongly coordinating anions such as the alkali metal chlorides have only scarcely been investigated, owing to their low solubility in SO_2.[4] Organic compounds, for example amines[17] and glycols,[18] are well-miscible with SO_2 and find application as absorber materials for the flue gas desulfurization.[19] Especially room temperature ionic liquids based on alkylammonium salts turned out to be valuable for the reversible removal of sulfur from flue gas.[20][21] In these systems, SO_2 in conjunction with the anion is acting as an electron acceptor[22][23] and shows non covalent electrostatic interactions. [24][25] In the case of F^- as an anion, also the formation of the fluorosulfite anion has been observed.[26][24]

We recently reported on hybrid crown ethers that incorporate Si_2Me_4 bridges instead of C_2H_4 bridges between the O_{crown} atoms.[27][28] By theoretical and experimental methods, the complexation ability of these ligands was determined to be superior to that of organic crown ethers. However, all reported alkali metal complexes include weakly coordinating anions such as PF_6^- or $(SO_3CF_3)^-$.[29][30] Attempts to coordinate alkali metal cations from their chlorides did not succeed in organic solvents such as dichloromethane; water turned out to be an inappropriate solvent due to its reactivity with the disila-crown ether complexes. In this work, we report on the adequacy of liquid sulfur dioxide as a solvent for the complexation of the alkali metal chlorides by 1,2-disila-12-crown-4. To obtain substantial information about the specific coordination ability of hybrid crown ethers, we furthermore performed complexation reactions involving the organic crown ether 12-crown-4.

Results and Discussion

One equivalent of LiCl and two equivalents of 1,2-disila-12-crown-4 were suspended in liquid SO_2. The colourless solids of lithium chloride disappeared within one day at ambient temperature and cooling of the saturated solution to –35 °C yielded colourless crystals suitable for single crystal X-ray diffraction. Due to the high solubility of the complex in SO_2, only tiny amounts of the solvent were required. [Li(1,2-disila-12-crown-4)(SO_2Cl)] (**1**) crystallises in the orthorhombic crystal system, space group *Pna*2_1 with four molecules per unit cell. The structure was refined as an inversion twin. The molecular structure reveals an *O*-coordinated chlorosulfite ligand which itself is pyramidal (Figure 1). Attractive interaction between chloride and SO_2 has been widely reported,[24] but the generally observed interatomic S–Cl distance is larger than 280 pm.[31][32]

By contrast, the S1–Cl1 atom distance in compound **1** is with 241.6(1) pm slightly shorter compared to the literature (249.2(5) pm).[33] It should be noted that only one crystallographic characterization of the chlorosulfite anion has been published to date and the latter was synthesised by reduction of SO_2Cl_2. So, compound **1** represents the first example of a $[SO_2Cl]^-$ anion obtained from SO_2. Notwithstanding the previously reported structure of the chlorosulfite anion, both S–O bonds in compound **1** show only small disparity with 145.7(1) pm (S1-O5) and

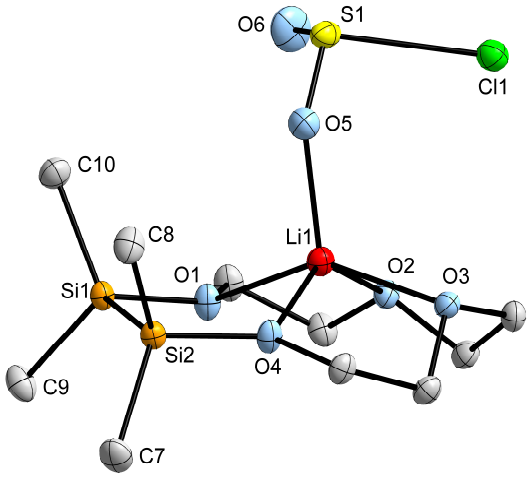

Figure 1. Molecular structure of [Li(1,2-disila-12-crown-4)SO_2Cl] (**1**) in the solid state. The non-hydrogen atoms are represented by displacement ellipsoids at the 50% probability level at 100(2) K. Hydrogen atoms are omitted. Selected bond lengths (pm) and angles (°): O1-Li1: 201.9(3), O2-Li1: 202.7(3), O3–Li1: 206.6(3), O4–Li1: 199.5(3), O5–Li1: 196.7(3), Si1–Si2: 235.6(1), Si2–C7: 186.3(2), S1–O5: 145.7(1), S1–O6: 144.5(2), S1–Cl1: 241.6(1); O5–S1–O6: 114.0(9), O6–S1–Cl1: 101.6(7), O5–S1–Cl1: 99.8(6), C9–Si1–Si2–C7: 6.3(1), C10–Si1–Si2–C8: 6.6(1).

144.5(2) pm (S1–O6). The IR spectrum of compound **1** dried *in vacuo* confirms the presence of the $[SO_2Cl]^-$ anion, showing the stretching vibrations $\tilde{\nu}_{as}$ (SO) at 1246 cm^{-1}, $\tilde{\nu}_{s}$ (SO) at 1107 cm^{-1} and the bending vibration δ (SO_2) at 528 cm^{-1} (Table 1).[33][34] The square-pyramid-like coordination sphere of the Li cation is built up by a terminally O-coordinated $[SO_2Cl]^-$ anion with a Li1–O5 distance of 196.7(3) pm and by the four O_{crown} atoms with O(1-4)–Li1 distances between 199.5(3) pm and 206.6(3) pm. These are similar to those in the related compound [Li(1,2-disila-12-crown-4)(OSO_2CF_3)].[27] The Me groups at the Si atoms show an almost eclipsed arrangement with dihedral angles of 6.3(1)° and 6.6(1)°, which is common for coordinating cyclosiloxanes[35][36] and disila-crown ethers[27][28]. The NMR measurements were performed with a 1:1 ratio of LiCl to 1,2-disila-12-crown-4 in SO_2. In the $^{29}Si\{^1H\}$ NMR spectrum, compound **1** shows a signal at δ = 17.1 ppm and is considerably shifted downfield compared to the free ligand (Table 2), due to the coordination of the *Lewis* acid Li^+. Furthermore, by NMR spectroscopy, small amounts of the decomposition products of 1,2-disila-12-crown-4 were identified. These are octamethyltetrasila-1,4-dioxane ($^2D_2$)[37] and the open chained glycol. In the $^{29}Si\{^1H\}$ NMR spectrum, a signal assigned to $^2D_2$ was detected at 5.4 ppm and the IR spectrum reveals the presence of the OH stretching vibration at $\tilde{\nu}$ = 3328 and 3256 cm^{-1}. Decomposition may be caused by traces of moisture, since in prior studies the sensitivity of disila-crown ether complexes towards moisture has already been observed.[27]

Table 1. IR data (/cm^{-1}) for SO_2,[38] $[SO_2Cl]^-$,[33] $[SO_2Cl]^-$ in compound **1** and SO_2 in compounds **2** – **5**.

Species	$\tilde{\nu}_{as}$ S-O[a]	$\tilde{\nu}_{s}$ S-O[b]	δ S-O[c]
SO_2	1340	1150	524
$[SO_2Cl]^-$	1248	1105	530
1	1246	1107	528
2	1311	1131	527
3	1304	1133	527
4	1304	1133	527
5	1307	1131	527

[a] Antisymmetric stretching mode. [b] Symmetric stretching mode. [c] Bending mode.

In an analogous synthetic approach, 12-crown-4 and LiCl were suspended in SO_2, giving a clear solution within one day at ambient temperature. Cooling of the saturated reaction to –35 °C within two days afforded colourless blocks of [Li(12-crown-4)Cl]·4SO_2 (**2**), suitable for single crystal X-ray diffraction. Compound **2** crystallises in the tetragonal crystal system, space

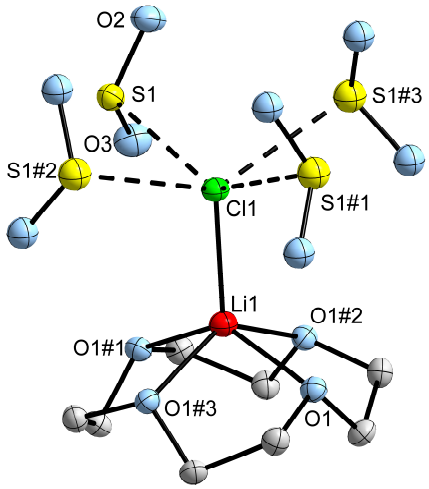

Figure 2. Molecular structure of [Li(12-crown-4)Cl]·4SO_2 (2) in the solid state. The non-hydrogen atoms are represented by displacement ellipsoids at the 50% probability level at 100(2) K. Hydrogen atoms are omitted. Symmetry transformations for the generation of equivalent atoms: #1: −x+3/2, −y+3/2, z; #2: −y+3/2, x, z; #3: y, −x+3/2, z. Selected atom distances (pm) and angles (°): O1–Li1: 206.6(2), Li1–Cl1: 230.9(4), S1–O2: 143.0(1), S1–O3: 142.4(1), S1–Cl1: 293.03(4); O2–S1–O3: 116.8(1), O1–Li1–Cl1: 112.4(1).

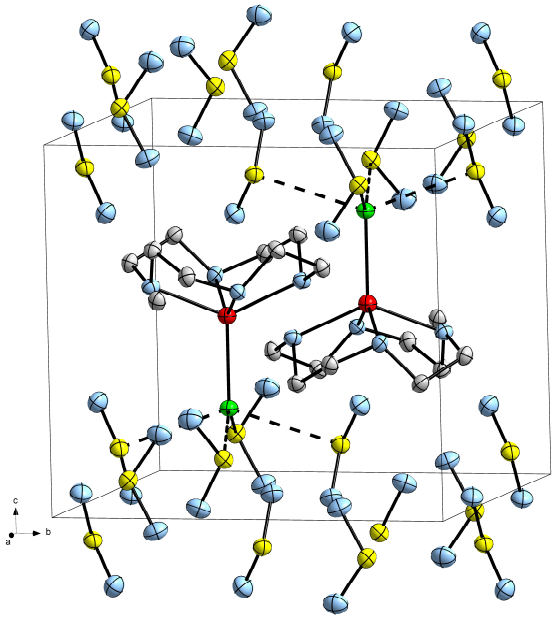

Figure 3. A section of the crystal structure of compound **2**. The non-hydrogen atoms are represented by displacement ellipsoids at the 50% probability level at 100(2) K. Hydrogen atoms are omitted.

group *P*4/*n*, with two molecules per unit cell. As in compound **1**, the lithium atom is coordinated in the shape of a square pyramid. Atom O1, situated in the crown ether, is quadrupled by a fourfold symmetry axis through Cl1 and Li1, thus forming the base of the pyramid. In contrast to compound **1** not $[SO_2Cl]^-$ but the chloride ion Cl1 makes up the top of the pyramid with a Li1–Cl1 distance of 230.8(4) pm similar to that found in [Li(12-crown-4)Cl][39]. The Cl1 atom itself is coordinated by SO_2 *via* the S1 atom. To our knowledge, fourfold solvation of halides has not yet been reported for solid state structures. Said symmetry axis leads to four molecules of SO_2 forming a square pyramid with the Cl1 atom (Figure 2). The S1–Cl1 distance is 293.03(4) pm. The consistent antiparallel orientation of the crown ether complexes together with the solvation of the chloride ion leads to a layered crystal structure as can be seen in Figure 3.

The IR spectrum does not hint to the presence of $[SO_2Cl]^-$ anions, but SO_2 can easily be detected by reference to the characteristic stretching vibrations at $\tilde{\nu}$ = 1311 and 1131 cm^{-1} and the bending vibration at δ = 527 cm^{-1}. It is however remarkable that, in the case of the hybrid disila-crown ether, the chloride ion reacted with SO_2 to form the chlorosulfite anion. This might be the result of a stronger coordination of Li^+ in compound **1** compared to compound **2**.[27][28] The weaker interaction of Cl^- and Li^+ in compound **1** may lead to an increased *Lewis* basicity of Cl^-, that raises its reactivity towards SO_2 to form the chlorosulfite anion. For example a similar reaction was observed for F^-.[24] The bond lengths and angles in the SO_2 molecule are with 143.0(1) pm and 116.8(1)° within the expected range.[32] The complexation of lithium by

12-crown-4 in solution can be deduced from the downfield shift of the single signal in the ^{1}H NMR spectrum from δ = 4.24 ppm in 12-crown-4 to δ = 4.42 ppm in compound **2** (Table 2). As opposed to the observations made in the syntheses of compounds **1** and **2**, no clear solutions were obtained after suspending respectively two equivalents of 1,2-disila-12-crown-4 with one equivalent NaCl or KCl in liquid SO_2. Subsequent removal of the solvent yielded a colourless oil and a white appearing precipitate respectively. NaCl was exemplarily identified by single crystal X-ray diffraction. The NMR spectroscopic analysis was performed using the analogous 2:1 mixture. The ^{29}Si{^{1}H} NMR spectrum revealed that in the presence of NaCl the signal splits from one signal at 14.1 ppm of the original disila-crown ether into one at 13.5 ppm and one at 14.4 ppm, indicating a weak interaction with Na^{+}. The coordination attempt of 1,2-disila-12-crown-4 and KCl afforded one signal in the ^{29}Si{^{1}H} NMR with a chemical shift of δ = 14.3 ppm. The weak interaction of 1,2-disila-12-crown-4 with NaCl and KCl is presumably inefficient for the dissolution of the salt, especially as 1,2-disila-12-crown-4 was hitherto found unable to form sandwich-type complexes. After removal of the solvent the storage of 1,2-disila-12-crown-4 and KCl at –35 °C for three months yielded colourless crystals, which were identified by X-ray diffraction as the known decomposition product $^{2}D_2$. To obtain insights into the decomposition process, long term NMR experiments of two equivalents of 1,2-disila-12-crown-4 and one equivalent of KCl in SO_2 were performed. Only after ten weeks of storage at room temperature small amounts of the decomposition product $^{2}D_2$ were detected *via* the signal at 5.6 ppm in the ^{29}Si{^{1}H} NMR spectrum. These observations made us assume that the use of a PTFE valve enabled the diffusion of significant amounts of moisture into the NMR tube. This would affect batches on a preparative scale even stronger due to the larger sealing surface and the cooling of the reaction vessels, so flame sealed ampoules would be recommended.

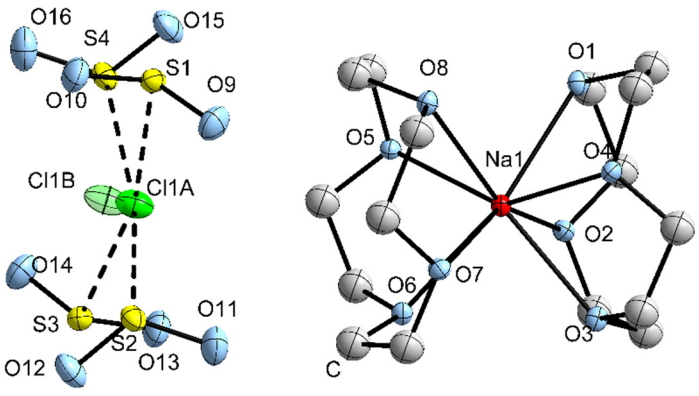

Figure 4. Molecular structure of [Na(12-crown-4)$_2$]Cl·4SO_2 (3) in the solid state. The non-hydrogen atoms are represented by displacement ellipsoids at the 50% probability level at 100(2) K. Hydrogen atoms are omitted. Selected atom distances (pm) and angles (°): Na1–O1: 251.3(1), Na1–O5: 242.0(1), S1–O9: 142.7(1), S1–O10: 142.9(1), S1–Cl1A: 283.6(2), S1–Cl1B: 285.0(3), O9–Si1–O10: 115.9(1).

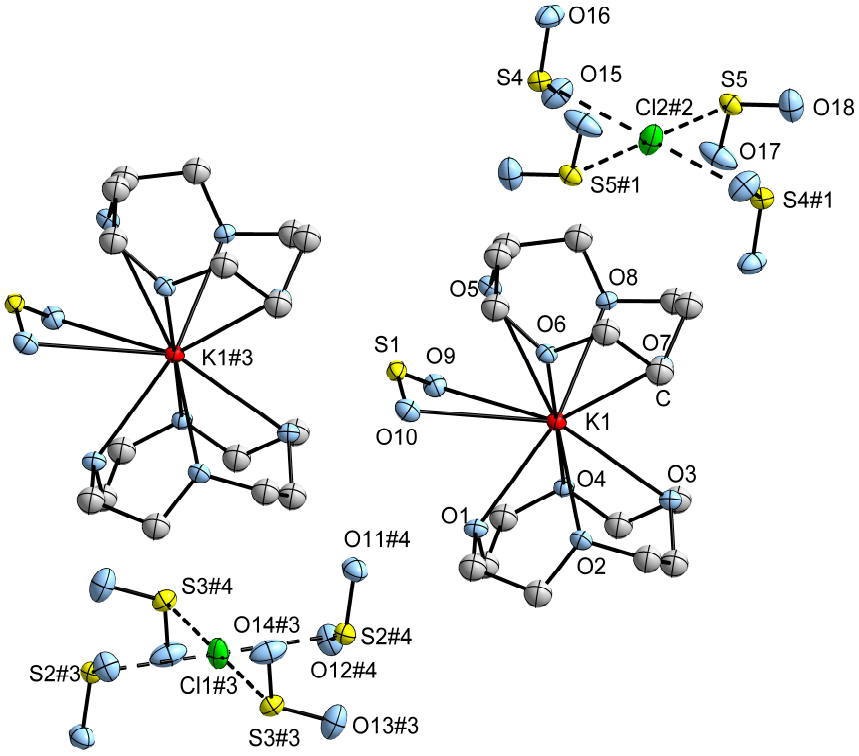

Figure 5. Molecular structure of $[K(12\text{-crown-}4)_2(SO_2)]Cl{\cdot}4SO_2$ (**4**) in the solid state. The complex $[Rb(12\text{-crown-}4)_2(SO_2)]Cl{\cdot}4SO_2$ (**5**) crystallises isotypically and will not be separately displayed. Atom assignment was maintained accordingly. The non-hydrogen atoms are represented by displacement ellipsoids at the 50% probability level at 100(2) K. Hydrogen atoms are omitted. Symmetry transformations for the generation of equivalent atoms: #1: −x+2, −y, −z+1; #2: x, y, z/2; #3: −x+1, y, z; #4: −x+2, −y, −z+2. Selected atom distances (pm) and angles (°) of **4**: K1–O1: 281.0(2), K1–O2: 282.0(3), K1–O3: 295.0(2), K1–O4: 284.2(2), K1–O5: 311.7(3), K1–O6: 295.6(3), K1–O7: 272.5(3), K–O8: 289.5(2), K1–O9: 299.2(3), K1–O10: 320.6(3), S1–O9: 143.4(3), S1–O10: 143.3(3), S2–O11: 143.0(3), S2–O12: 142.9(3), S2–Cl1: 282.5(1); O9–S1–O10: 116.7(1), O11–S2–O12: 116.4(2). Selected atom distances (pm) and angles (°) of **5**: Rb1–O1: 293.1(1), Rb1–O2: 292.9(1), Rb1–O3: 302.6(1), Rb1–O4: 293.0(1), Rb1–O5: 315.7(1), Rb1–O6: 300.5(1), Rb1–O7: 284.2(2), Rb1–O8: 300.7(1), Rb1–O9: 306.7(1), Rb1–O10: 324.0(2), S1–O9: 142.9(2), S1–O10: 143.2(2), S5–O17: 141.9(2), S5–O18: 141.8(3), S2–Cl1: 282.4(1), O9–S1–O10: 116.4(1), O11–S2–O12: 116.3(1).

Sandwich complexes are particularly described for organic crown ethers[40] and indeed the reaction of two equivalents of 12-crown-4 with one equivalent of NaCl, KCl or RbCl respectively in SO_2, led to clear solutions within one day. Single crystals suitable for X-ray diffraction were afforded by cooling of the saturated SO_2 solutions and storage at –35 °C. $[Na(12\text{-crown-}4)_2]Cl{\cdot}4SO_2$ (**3**), $[K(12\text{-crown-}4)_2(SO_2)]Cl{\cdot}4SO_2$ (**4**) and $[Rb(12\text{-crown-}4)_2(SO_2)]Cl{\cdot}4SO_2$ (**5**) each crystallise in the space group $P\bar{1}$ as discrete ions.

The coordination sphere of Na^+ in compound **3** is saturated by the eight O_{crown} atoms arranged in a shape similar to a square antiprism (Figure 4). The Na1–O(1-8) distances with values between 242.0(1) and 251.3(1) pm are slightly shorter than in other $[Na(12\text{-crown-}4)_2]^+$ complexes (e.g. 246.4(7) – 251.9(6) pm).[41][42] The chloride anion is slightly disordered

(0.49(3) : 0.51(3)) on the central position between the crown ether ligands of two [Na(12-crown-4)$_2$]$^+$ cations, thus forming infinite [Na(12-crown-4)$_2$]Cl columns.

As in compound **2** it is solvated by four SO_2 molecules, with S–Cl distances between 282.8(2) and 299.7(3) pm. The columns are stacked so that again a layered structure is formed. The ^{1}H and ^{13}C{^{1}H} NMR spectra of compound **3** reveal splitting as well as broadening of the signals of the free ligand, which is indicative for exchange processes between crown ether and the salt in solution. In difference to compounds **1** and **2**, the signals in the ^{1}H and ^{13}C{^{1}H} NMR spectra of compound **3** undergo a significant upfield shift (see Table 2), which was attributed to conformational effects.[43]

Additional to the eight O_{crown} atoms, the potassium ion in compound **4** is side on *O,O'* coordinated by one SO_2 molecule (Figure 4). Despite the numerous reported coordination compounds involving SO_2,[11] this bidentate binding mode is hitherto unprecedented. To the best of our knowledge, SO_2 coordination of a metal atom to date occurred either of the type *O* [10][34], *S,O*[7][8] or *μ-O,O'* in polynuclear complexes with bridging SO_2 moieties[12][44] and exclusively in conjunction with weakly coordinating anions. The distances between the O atoms of SO_2 and K1 have values of 299.2(3) and 320.6(3) pm, indicating that the atoms O9 and O10 are not bonded equally strong to the metal centre. The K1–O_{crown} distances range from 272.5(3) to 311.7(3) pm and beside the larger ionic radius of K^+ compared to Li^+ and Na^+ reflect also its coordination number of ten. In comparison, [K(12-crown-4)$_2$]$^+$ with coordination number eight commonly shows K–O_{crown} distances of 277 – 284 pm.[40] The non-equivalent chloride ions Cl1 and Cl2 are similarly to those in compounds **2** and **3** coordinated by four SO_2 molecules. The O9–S1–O10 angle of the *side on O,O'* coordinating SO_2 molecule is 116.7(1)° and does not differ significantly from that of *S* coordinating SO_2 (O11–S2–O12 angle of 116.4(2)°). Due to the additional SO_2 ligand at the metal atom, the two crown ether ligands are not oriented coplanar but angled slightly towards each other. With the chlorine atom still centred in relation to the crown ether, this results in an overall structure made up of zig zag chains. Due to the crooked growth of the crystals, the structure was solved from a non-merohedral two component twin. The NMR spectroscopic analysis revealed that the ^{1}H and ^{13}C{^{1}H} signals of compound **4** become broader upon coordination as was also observed in compound **3**. They furthermore undergo an upfield shift in the ^{1}H NMR spectrum from δ = 4.24 ppm in 12-crown-4 to 4.19 ppm in the complex of compound **4** and from δ = 70.7 to 68.2 ppm in the ^{13}C{^{1}H} NMR spectrum.

The structure of [Rb(12-crown-4)$_2$(SO_2)]Cl·4SO_2 (**5**) is isotypic to [K(12-crown-4)$_2$(SO_2)]Cl·4SO_2 (**4**). The O_{crown}–Rb distances measure between 284.2(2) pm and 315.7(1) pm and also the *O,O'* coordinated SO_2 molecule shows with 306.7(1) and 324.0(2) pm longer atomic distances compared to those in compound **4**, which nicely depicts the larger ionic radius of Rb^+. The ^{1}H and ^{13}C{^{1}H} NMR spectra reveal the same tendency as

observed for the sandwich type complexes of compounds **3** and **4**. In the ^{1}H NMR spectrum the signal of compound **5** undergoes a significant upfield shift from δ = 4.24 ppm in the free ligand to δ = 3.92 ppm. Accordingly, in the $^{13}C\{^{1}H\}$ NMR spectrum the signal of compound **5** shows an upfield shift to 68.4 ppm (Δ(*δ*) = 2.3 ppm) (Table 2). To gather IR spectra of the compounds **3** - **5**, the supernatant solvent was completely evaporated at ambient temperature and atmospheric pressure. The neat crystals of the sodium compound **3** showed opacification under those conditions, but remained solid. However, the potassium and the rubidium compounds **4** and **5** melted to liquids with considerably high surface tension. The recorded asymmetric and symmetric stretching vibrations as well as the bending vibration of SO_2 all occurred at very similar frequencies (Table 1). The fact that SO_2 remains bound to the complexes at ambient temperature and normal pressure proves the comparably strong attractive interactions of the complex and sulfur dioxide.

Table 2. Chemical shifts of 1,2-disila-12-crown-4, 12-crown-4, compounds **1** – **5** as well as *M*Cl (*M* = Na[a], Rb[b], Cs[b]) and1,2-disila-12-crown-4 in SO_2 and CsCl and 12-crown-4[c] in SO_2 using a TMS capillary.

	$\delta^{1}H$ /ppm		$\delta^{13}C\{^{1}H\}$ /ppm		$\delta^{29}Si\{^{1}H\}$ /ppm
Compound	$O(CH_2)_2$	$Si(CH_3)_2$	$O(CH_2)_2$	$Si(CH_3)_2$	
1,2-disila-12-crown-4	4.12-4.14 (m), 4.15 (s) 4.29-4.31 (m)	0.80 (s)	63.6 (s), 71.1 (s) 72.5 (s)	0.7 (s)	14.1 (s)
12-crown-4	4.24 (s)		70.7		
1	3.94-3.96 (m), 4.05 (s) 4.13-4.15 (m)	0.63 (s)	62.0 (s), 68.5 (s) 71.1 (s)	–0.8 (s)	17.1 (s)
NaCl + 1,2-disila-12-crown-4[a]	3.86-3.88 (m), 3.92 (s), 3.97 (s), 4.06-4.07 (m), 4.10-4.12 (m)	0.55 (s) 0.58 (s)	62.7 (s), 62.9 (s), 69.7 (s), 69.8 (s), 72.0 (s), 72.3 (s)	0.2 (s), 0.30 (s)	13.5 (s), 14.4 (s)
2	4.42 (s)		68.0		
3	3.91 (br) 3.92 (br)		67.9 (br) 68.1 (br)		
4	4.19 (br)		68.2 (s)		
7	3.92 (s)		68.4 (s)		
RbCl + 1,2-disila-12-crown-4[b]	4.21-4.23 (m), 4.25 (s), 4.28-4.29 (m), 4.31 (s), 4.39-4.40 (m), 4.44-4.45 (m)	0.84 (s) 0.94 (s)	63.1 (s), 63.6 (s), 70.3 (s), 70.8 (s), 72.5 (s), 72.9 (s)	–0.2 (s), –0.2 (s), 0.2 (s), 0.7 (s)	14.1 (s), 14.3(s)
CsCl + 12-crown-4[c]	4.25 (s)		69.7 (s)		

[a] Chemical shifts of the suspension consisting of 2 equiv. of 1,2-disila-12-crown-4 and 1 equiv. of NaCl in SO_2. [b] Solution of 2 equiv. of 1,2-disila-12-crown-4 and 1 equiv. of *M*Cl (*M* = Rb, Cs) in SO_2. [c] Solution of 2 equiv. of 12-crown-4 and 1eq. of CsCl in SO_2.

Unexpectedly, two equivalents of the sila-crown ether and one equivalent of RbCl and CsCl, respectively, gave clear solutions in SO_2 within one day of stirring at ambient temperature. The amount of SO_2 was subsequently reduced to saturation and storage at –35 °C afforded xenomorph crystals intergrown in the shape of columns, which still proofed to be suitable for X-ray diffraction. However, in neither crystal structure the inclusion of crown ethers was observed. Instead, mere SO_2 solvates of RbCl and CsCl respectively had formed. $RbCl{\cdot}3SO_2$ (**6**) and $CsCl{\cdot}3SO_2$ (**7**) crystallise isotypical in the cubic crystal system, space group $Im\bar{3}$, with eight formula units per unit cell.

The structures were solved in the space group $Im\bar{3}m$ and corrected for twinning by choosing the lower symmetry space group plus a mirror plane as a twin law. In the following, only the structure of compound **6** is described exemplary. The structure contains two crystallographically distinguishable Rb atoms. Rb1 is positioned in the origin of the unit cell with $m\bar{3}$ symmetry. It is solely surrounded by the O1 atoms, of twelve *μ-O* coordinating SO_2 molecules in a shape resembling an icosahedron. The O1 atoms on the other hand are connected to six Rb2 atoms. These surround the atom Rb1 in a shape resembling an octahedron (Figure 6, left). The coordination number of Rb2 is also twelve. Here four *O,O'* bound SO_2 molecules form a stretched octagon out of O1 and O2 atoms which is capped on each side by two O2 atoms originating from *μ-O* bridging SO_2. Every O2 atom connects this polyhedron to the neighbouring Rb2 atom. Thus, every Rb2 atom is itself surrounded square planar by four other Rb2 atoms. Perpendicular to this plane O1 bridges to Rb1 (Figure 6, right).

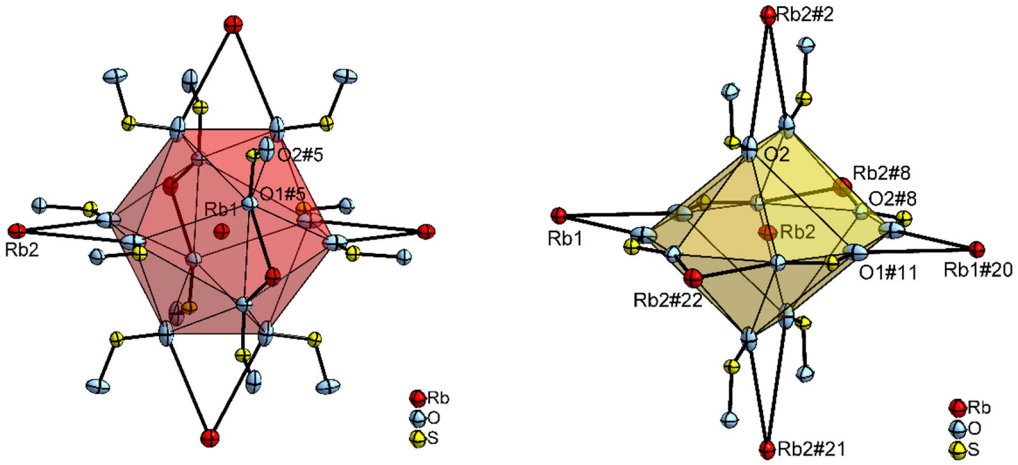

Figure 6. Coordination of Rb1 (left) and Rb2 (right) in crystalline $RbCl{\cdot}3SO_2$ (**6**). $CsCl{\cdot}3SO_2$ (**7**) crystallises isotypically and will not be separately displayed. Atom assignment was maintained accordingly. Atoms are represented by displacement ellipsoids at the 50% probability level at 100(2) K. Symmetry transformations for the generation of equivalent atoms: #1: x+1/2, y+1/2, z+1/2; #2: y+1/2, z+1/2, x−1/2; #5: −x+1/2, −y+1/2, z−1/2; #8: z+1/2, x−1/2, y−1/2;.#20: x+1, y, z; #21: y+1, z−1/2, x−1/2; #22: z+1/2,x–1/2, y+1/2. Selected atom distances (pm) and angles (°) of **6**: Rb1–O1: 326.2(2), Rb2–O1: 333.7(3), Rb2–O2: 298.8(3), S1–O1: 143.4(3), S1–O2: 143.4(2), O1–S1–O2: 116.0(1). Selected bond lengths (pm) and angles (°) of **7**: Cs1–O1: 322.5(9), Cs2–O1: 349.2(10), Cs2–O2: 355.1(11), S1–O1: 145.8(11), S1–O2: 144.3(8) O1–S1–O2: 112.2(5).

Seen from the oxygen positions: O1 solely bridges between Rb1 and Rb2, whereas O2 is exclusively connecting Rb2 atoms. The SO_2 molecule thus combines all three *O* coordination modes at once – *O,O' side-on*, *μ-O* bridging and *μ-O,O'* bridging (Figure 7).

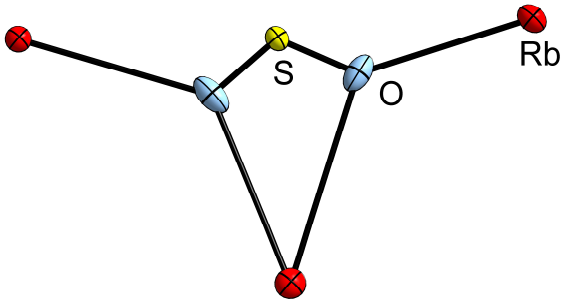

Figure 7. Coordination mode of SO_2 in crystals of $RbCl{\cdot}3SO_2$ (**6**). $CsCl{\cdot}3SO_2$ (**7**).crystallises isotypically and will not be separately displayed. Atom assignment was maintained accordingly. Atoms are represented by displacement ellipsoids at the 50% probability level at 100(2) K. Symmetry transformations for the generation of equivalent atoms: #1: x+1/2, y+1/2, z+1/2; #2: y+1/2, z+1/2, x–1/2.

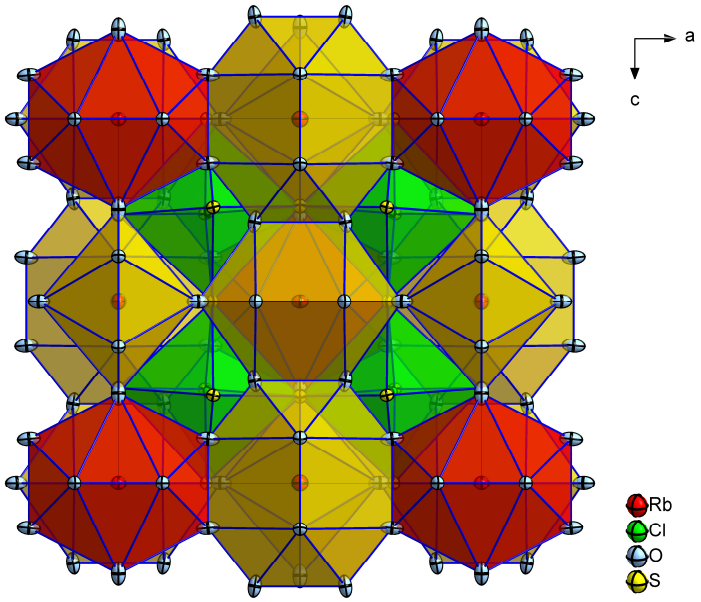

Figure 8. View along the *b*-axis of the crystal structure of compound **6.** The red polyhedra represent the coordination sphere of Rb1, in gold, the coordination sphere of Rb2 is displayed, and the green octahedra show S1 surrounded Cl1. Atoms are represented by displacement ellipsoids at the 50% probability level at 100(2) K.

The sulfur atoms of the SO_2 molecules form corner sharing octahedra, which are centred by the chlorine atoms. Figure 8 shows the arrangement of the described polyhedra in the unit cell of compound **6**. Neglecting the SO_2 molecules as well as the symmetry inequivalence of the rubidium atoms, the structure still resembles the CsCl structure type.

With 116,0(1)° the O1–S1–O2 angle is practically identical to that in compounds **3**-**5.** As to be expected, the Rb-O distances are observed from 298.8(3) to 333.7(3) pm, which is comparable

to those in compound **5**. It must be noted that RbCl and CsCl show a slightly increased solubility in SO_2 compared to the almost insoluble chlorides of Li, Na and K.[2] Thus we were able to produce the microcrystalline compounds **6** and **7** at room temperature from RbCl and CsCl respectively with liquid SO_2 inside flame-sealed fused silica capillaries, whereas the other alkali metal halides did not show any sign of reaction over several weeks of storage, as was shown by *in situ* powder X-ray diffraction.

Although the solubility of RbCl and CsCl is increased tremendously, the NMR spectra of two equivalents of 1,2-disila-12-crown-4 and one equivalent of RbCl in SO_2 reveal that the ligand shows only minor interactions with the cations (see Table 2). This becomes most visible in the $^{29}Si\{^1H\}$ NMR spectrum. Besides the main signal at δ = 14.1 ppm, which is assigned to the free ligand, the small signal at δ = 14.3 ppm is indicative for a weak interaction with the cations. Similar shifts were also observed for 1,2-disila-12-crown-4 and CsCl in SO_2. The sole crystallisation of the solvates **6** and **7** indicates that the hybrid crown ether acts preferably as an auxiliary for the dissolution of RbCl and CsCl in sulfur dioxide. Attempts to afford solvates of RbCl and CsCl in SO_2 under exclusion of 1,2-disila[12]crown-4, likewise gave crystalline material of compounds **6** and **7**. It must still be noted that the obtained crystals exhibited lower quality in comparison to those synthesised in the presence of 1,2-disila-12-crown-4 due to their growth in a suspension of the salts in contrast to crystallisation out of a clear solution.

Finally, also the suspension of two equivalents of 12-crown-4 and one equivalent of CsCl in SO_2 gave a clear solution within one day at ambient temperature. Cooling of the saturated solution yielded two types of crystals. Colourless isotropic crystals constitute the large proportion and were identified by single crystal X-ray diffraction as the SO_2 solvate of CsCl (**7**), which was also observed in conjunction with 1,2-disila-12-crown-4. Apart from that, colourless plates were identified as the SO_2 solvate of the free ligand 12-crown-4 (Figure 9).

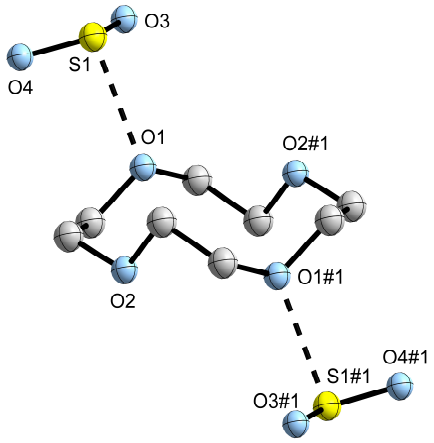

Figure 9. Molecular structure of 12-crown-4·2SO_2 (**8**) in the solid state. The non-hydrogen atoms are represented by displacement ellipsoids at the 50% probability level at 100(2) K. Hydrogen atoms are omitted. Symmetry transformations for the generation of equivalent atoms: #1: –x+1, –y+1, –z+1. Selected atom distances (pm) and angles (°): S1–O4: 142.5(2), S1–O3: 142.7(1), S1–O1: 260.1(2), O3–S1–O4: 116.9(1).

It crystallises in the space group $P2_1/c$, with four molecules per unit cell. The asymmetric unit consists of half a molecule 12-crown-4 and one molecule SO_2. A center of inversion leads to the complete 12-crown-4·2SO_2 moiety (**8**). Two SO_2 molecules thereby respectively show *S* interaction with the O_{crown} atoms O1 and O1#1. The coordination mode is similar to that observed between chloride ions and sulphur atoms in compounds **2** – **4**. The interatomic S1–O1 distance measures 260.1(2) pm. To our knowledge compound **8** represents the first crystallographically described SO_2 solvate of an ether group, although ethers and glycols find broad application in the removal of SO_2 from flue gas.[18][19] The ^{1}H and ^{13}C{^{1}H} NMR spectra reveal that 12-crown-4 shows almost no interaction with CsCl, since the chemical shifts do not deviate significantly from those of the free ligand (see Table 2). Apparently, the ionic radius of Cs^+ is too large for the complexation by 12-crown-4 so that CsCl and 12-crown-4 each rather crystallise as SO_2 solvates (Scheme 1).

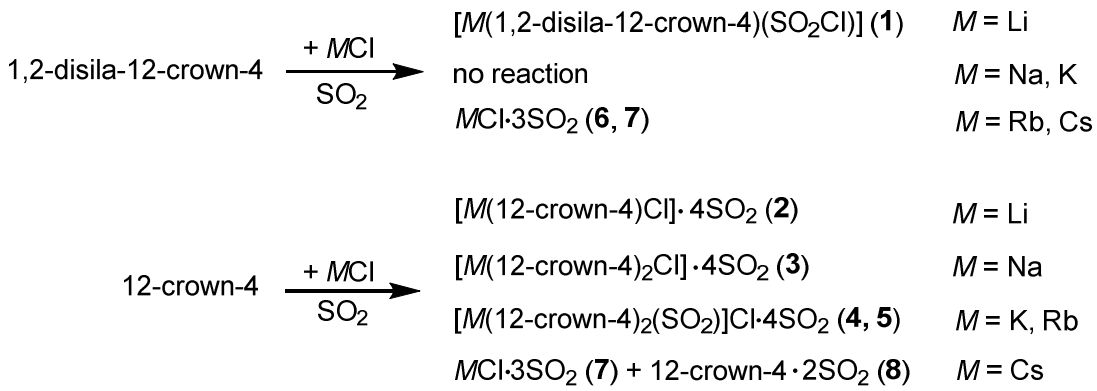

Scheme 1. Comprising reaction paths of the ligands 1,2-disila-12-crown-4 and 12-crown-4 with *M*Cl (*M* = Li, Na, K, Rb, Cs).

Conclusions

1,2-disila-12-crown-4 selectively coordinates in SO_2 to LiCl and yields [Li(1,2-disila-12-crown-4)(SO_2Cl)] (**1**). Additionally to the four O_{crown} atoms the Li^+ cation is coordinated by an O atom of $[SO_2Cl]^-$. This anion was formed by the reaction of SO_2 and Cl^- and was furthermore characterized by IR spectroscopy. In contrast, the larger cations Na^+ and K^+ remain non-complexed by 1,2-disila-12-crown-4. This is presumably a result of the sterically demanding methyl groups at the Si atoms. In conjunction with RbCl and CsCl, we observed that 1,2-disila-12-crown-4 acts as an auxiliary for the dissolution of the salts, although by NMR spectroscopic measurements only minor interactions between the salts and the hybrid ligand were detected. The SO_2 solvates *M*Cl·3SO_2 (**6**: *M* = Rb; **7**: *M* = Cs) combine three types of binding modes of the solvent: *O,O' side-on*, *μ-O* bridging and *μ-O,O'* bridging. To compare the coordination ability of 1,2-disila-12-crown-4 with that of 12-crown-4, the analogous experiments were

performed using the latter compound as a ligand. 12-crown-4 forms a 1:1 complex with LiCl. The cation hereby shows interactions with the O_{crown} atoms and the Cl^- anion. Together with NaCl, KCl and RbCl, 12-crown-4 forms the sandwich complex compounds [Na(12-crown-4)$_2$]Cl·4SO_2 (**3**), [K(12-crown-4)$_2$(SO_2)]Cl·4SO_2 (**4**) and [Rb(12-crown-4)$_2$(SO_2)]Cl·4SO_2 (**5**). In the case of the potassium complex in compound **4** and the rubidium complex in compound **5**, the cations are additionally saturated by *O,O' side-on* coordination of SO_2. This unprecedented coordination mode of SO_2 enhances, together with the combined *O,O'* and *μ-O* coordination observed in the compounds **6** and **7**, the number of known SO_2 binding types. All complexes containing 12-crown-4 retain SO_2 at ambient temperature, as was proven by IR spectroscopic measurements. Compounds **4** and **5** melt at ambient temperature to liquids with considerable high surface tension, whereas compound **3** remains solid. This can possibly be related to the different binding modes of SO_2. In this series, the cavity of 12-crown-4 appears to be too small for the coordination of Cs^+, so CsCl·3SO_2 as well as the solvated ligand 12-crown-4·2SO_2 were obtained and identified by single crystal X-ray diffraction (Scheme 1).

Experimental Section

General remarks: All reactions were performed in glass vessels equipped with fine thread glass spindles. All work was conducted under dry N_2 atmosphere. Solid reagents were stored in a LabStar Glovebox by MBraun Inc. under Ar-atmosphere (99.999, Praxair). The salts LiCl (99.9%), NaCl (99.9%), KCl (99.99%), RbCl (99.8%) and CsCl (99.5%) were commercially purchased from Sigma Aldrich and were dried in vacuum at 150 °C for at least 3 h. 12-crown-4 (97%) was purchased from Acros Organics. 1,2-Disila-12-crown-4 was prepared by reported methods.[27] The solvent SO_2 (Air Liquide, 99.999%) was dried over CaH_2 and was distilled directly into the reaction vessel *via* a vacuum line. NMR spectra were gathered in 5 mm thin wall precision low pressure NMR sample tubes fitted with a PTFE piston (Wilmad-LabGlass) on a Bruker Model Avance 500 spectrometer and were visualized with MestReNova.[45] Infrared spectra were recorded in attenuated total reflectance (ATR) mode in a Bruker Model Alpha FT-IR, the data were processed using the OPUS 7.2 spectroscopy software.[46]

Single crystal X-ray diffraction:

Single crystals were selected under exclusion of air in cooled perfluorinated polyether (Galden, *Solvay* Solexis) and mounted using the *MiTeGen* MicroLoop system. X-ray diffraction data were collected using the graphite monochromated Mo-K_α radiation of a *Stoe* IPDS2 or IPDS2T diffractometer equipped with an Image Plate detector. The diffraction data were reduced with the X-Area software package and, where applicable, corrected for absorption numerically using X-Red.[47-49] Due to the lack of coloured crystals and the preparation method, in some

cases size and shape could hardly be estimated. Regarding the negligible effect owing to low absorption coefficients, the absorption correction was omitted for those crystals (compounds **4**, **8**). The structures were solved using Direct Methods (SHELXT-2014/4 for compounds **1**, **3**, **8** or SHELXS-97) and refined against F^2 (SHELXL-2016/4) using the ShelXle software package.[50-52] Non hydrogen atoms were located by Difference Fourier synthesis and refined anisotropically. Hydrogen atoms were located by using a riding model and refined isotropically. Crystallographic data and structure refinement results are summarized in Table 3.

Reactions to afford single crystals:

[Li(1,2-disila-12-crown-4)(SO_2Cl)] (**1**): At –30 °C 180 mg (0.68 mmol, 2 equiv.) of 1,2-disila-12-crown-4 and 14.4 mg (0.34 mmol, 1 equiv.) of LiCl were dissolved in ca. 5 mL of SO_2. The suspension was allowed to warm to ambient temperature and was stirred for 12 h. The quantity of the resulting clear solution was reduced until saturation. Storage at –35 °C afforded colourless crystals of 1 within 3 d. IR [cm^{-1}]: 3328(m), 3256(m), 294(w), 2926(m), 2877(m), 1478(w), 1453(w), 1401(w), 1362(w), 1346(w), 1287(m), 1246(m, $\tilde{\nu}_{as}$: *S-O*), 1128(s), 1107(s, $\tilde{\nu}_{s}$: *S-O*), 1066(vs), 1031(s), 951(vs), 923(s), 895(m), 867(w), 837(m), 817(s), 794(s), 771(vs), 733(m), 720(m), 694(m), 669(m), 634(m), 554(m), 528(m, *δ: SO_2*); MS (ESI^+): *m/z* [%] calcd.: 271.1368, found: 271.1363 $[Li(1,2\text{-disila-12-crown-4})]^+$ (100).

The preparation of compounds **2** – **8** is analogous to that of **1**:

[Li(12-crown-4)Cl]·SO_2 (**2**): LiCl: 16.6 mg, 0.39 mmol, 1 equiv.; 12-crown-4: 138 mg, 0.78 mmol, 2 equiv.; Storage at –35 °C yielded colourless blocks within 2 d. IR [cm^{-1}]: 3278(br), 2857(w), 2927(w), 2880(w), 1718(w), 1476(w), 1445(w), 1438(w), 1355(w), 1311(w, $\tilde{\nu}_{as}$: *S-O*), 1291(w), 1280(m), 1252(w), 1131(s, $\tilde{\nu}_{s}$: *S-O*), 1079(s), 1016(s), 1016(s), 928(s), 860(m), 606(w), 561(m), *δ*: 527(m, *SO_2*), 490(w), 430(s); MS (ESI^+): *m/z* [%] calcd.: 183.1203 found: 183.1200 $[Li(12\text{-crown-4})]^+$ (100).

[$Na(12\text{-crown-4})_2Cl$]·$4SO_2$ (**3**): NaCl: 30.0 mg, 0.51 mmol, 1 equiv.; 12-crown-4: 180 mg, 1.02 mmol, 2 equiv.; Storage at –35 °C yielded colourless blocks within 1 h. IR [cm^{-1}]: 3400(br), 2962(w), 2962(w), 2920(m), 2872(m), 1721(w), 1489(w), 1473(w), 1446(m), 1365(m), 1350(w), 1304(s, $\tilde{\nu}_{as}$: *S-O*), 1289(s), 1250(s), 1133(vs, $\tilde{\nu}_{s}$: *S-O*), 1089(vs), 1020(vs), 915(vs), 849(s), 553(s), *δ*: 527(vs, *SO_2*).

[$K(12\text{-crown-4})_2(SO_2)$]Cl·$4SO_2$ (**4**): KCl: 36.0 mg, 0.48 mmol, 1 equiv.; 12-crown-4: 170 mg, 0.96 mmol, 2 equiv.; Storage at –35 °C yielded colourless plates within 3 d. IR [cm^{-1}]: 3398(br), 2920(m), 2872(m), 1721(w), 1473(w), 1446(m), 165(m), 1304(s, $\tilde{\nu}_{as}$: *S-O*), 1289(s), 1250(s), 1133(vs, $\tilde{\nu}_{s}$: *S-O*), 1089(vs), 1020(vs), 915(vs), 849(s), 553(s), *δ*: 527(s, *SO_2*).

[$Rb(12\text{-crown-4})_2(SO_2)$]Cl·$4SO_2$ (**5**): RbCl: 60.0 mg, 0.50 mmol, 1 equiv.; 12-crown-4: 175 mg, 0.99 mmol, 2 equiv.; Storage at –35 °C yielded aggregates of colourless columns within 1 d.

IR [cm^{-1}]: 2909(m), 2865(m), 1722(w), 1450(w), 1364(m), 1306(s, $\tilde{\nu}_{as}$: *S-O*), 1291(s), 1249(m), 1131(vs, $\tilde{\nu}_{s}$: *S-O*), 1093(vs), 1070(s), 1024(vs), 970(w), 912(s), 844(s), 814(w), δ: 526(s, SO_2). $RbCl{\cdot}12SO_2$ (**6**): RbCl: 23.0 mg, 0.19 mmol, 1 equiv.; 1,2-disila-12-crown-4: 100 mg, 0.37 mmol, 2 equiv.; Storage at –35 °C afforded **6** in form of colourless columns within 12 h. $CsCl{\cdot}12SO_2$ (**7**): CsCl: 32.0 mg, 0.19 mmol, 1 equiv.; 1,2-disila-12-crown-4: 103 mg, 0.39 mmol, 2 equiv.; Storage at –35 °C afforded **8** in form of colourless 'spheres' within 1 d. 12-crown-4$\cdot SO_2$ (**8**): CsCl: 84.0 mg, 0.50 mmol, 1 equiv.; 12-crown-4: 175 mg, 0.99 mmol, 2 equiv.; Storage at –35 °C yielded colourless plates of **8** and colourless 'spheres' of **7** within 4 d.

Synthetic approach for NMR measurements:

1,2-disila-12-crown-4: 0.7 mL of SO_2 was condensed at –30 °C onto 20.0 mg ($7.5{\cdot}10^{-5}$ mol) of 1,2-disila-12-crown-4. Prior to the measurement, the sample was allowed to warm to ambient temperature. ^{1}H NMR (TMS, 500 MHz): δ = 0.80 (s, C*H*$_3$, 12H), 4.12-4.14 (m, C*H*$_2$, 4H), 4.15 (s, C*H*$_2$, 4H), 4.29-4.31 ppm (m, C*H*$_2$, 4H); ^{13}C{^{1}H} NMR (TMS, 126 MHz): δ = 0.7 (s, *C*H$_3$), 63.6 (s, *C*H$_2$), 71.1 (s, *C*H$_2$), 72.5 ppm (s, *C*H$_2$); ^{29}Si{^{1}H} NMR (TMS, 99 MHz): δ = 14.1 ppm (s).

12-crown-4: The sample preparation is similar to that of 1,2-disila-12-crown-4. ^{1}H NMR (TMS, 500 MHz): δ = 4.24 ppm (s, C*H*$_2$); ^{13}C{^{1}H} NMR (TMS, 126 MHz): δ = 70.7 ppm (s, *C*H$_2$).

1: 0.7 mL of SO_2 was condensed at –30 °C onto 3.4 mg ($7.9{\cdot}10^{-5}$ mol, 1 equiv.) of LiCl and 21 mg ($7.9{\cdot}10^{-5}$ mol, 1 equiv.) of 1,2-disila-12-crown-4. Prior to the measurement, the NMR tube was kept at ambient temperature for at least 2 d until complete dissolution of the precipitate. ^{1}H NMR (TMS, 500 MHz): δ = 0.63 (s, C*H*$_3$, 12H), 3.94-3.96 (m, C*H*$_2$, 4H), 4.05 (s, C*H*$_2$, 4H), 4.13-4.15 ppm (m, C*H*$_2$, 4H); ^{13}C{^{1}H} NMR (TMS, 126 MHz): δ = –0.8 (s, *C*H$_3$), 62.0 (s, *C*H$_2$), 68.5 (s, *C*H$_2$), 71.1 ppm (s, *C*H$_2$); ^{29}Si{^{1}H} NMR (TMS, 99 MHz): δ = 17.1 ppm (s); ^{7}Li NMR (TMS, 194 MHz): δ = 1.1 ppm (s).

The sample preparation of compounds **2**-**8** is similar to that of **1**.

2: LiCl: 4.3 mg, 0.1 mmol, 1 equiv.; 12-crown-4: 18 mg, 0.1 mmol, 1 equiv.
^{1}H NMR (TMS, 500 MHz): δ = 4.42 ppm (s, C*H*$_2$); ^{13}C{^{1}H} NMR (TMS, 126 MHz): δ = 68.0 ppm (s, *C*H$_2$); ^{7}Li NMR (TMS, 194 MHz): δ = 1.0 ppm (s).
3: NaCl: 4.6 mg, $7.9{\cdot}10^{-5}$ mol, 1 equiv.; 12-crown-4: 28 mg, $1.6{\cdot}10^{-4}$ mol, 2 equiv.; ^{1}H NMR (TMS, 500 MHz): δ = 3.91 (br, C*H*$_2$), 3.92 ppm (br, C*H*$_2$); ^{13}C{^{1}H} NMR (TMS, 126 MHz): δ = 67.9 ppm (br, *C*H$_2$), 68.1 (br, *C*H$_2$).

4: KCl: 4.2 mg, $6.0 \cdot 10^{-5}$ mol, 1 equiv.; 12-crown-4: 20 mg, $1.1 \cdot 10^{-4}$ mol, 2 equiv.; ^{1}H NMR (TMS, 500 MHz): δ = 4.19 ppm (br, C*H*$_2$); ^{13}C{^{1}H} NMR (TMS, 126 MHz): δ = 68.2 ppm (s, *C*H$_2$).

7: RbCl: 4.8 mg, $4.0 \cdot 10^{-5}$ mol, 1 equiv.; 12-crown-4: 14 mg, $8.0 \cdot 10^{-5}$ mol, 2 equiv.; ^{1}H NMR (TMS, 500 MHz): δ = 3.92 ppm (s, C*H*$_2$); ^{13}C{^{1}H} NMR (TMS, 126 MHz): δ = 68.4 ppm (s, *C*H$_2$).

8: CsCl: 8.1 mg, $4.8 \cdot 10^{-5}$ mol, 1 equiv.; 12-crown-4: 17 mg, $9.6 \cdot 10^{-5}$ mol, 2 equiv.; ^{1}H NMR (TMS, 500 MHz): δ = 4.25 (s, C*H*$_2$); ^{13}C{^{1}H} NMR (TMS, 126 MHz): δ = 69.7 (s, *C*H$_2$), 69.7 (s, *C*H$_2$), 69.9 ppm (s, *C*H$_2$).

Acknowledgements

This work was financially supported by the Deutsche Forschungsgemeinschaft (DFG). F.K. thanks the DFG for a Heisenberg-Professorship. We thank the X-ray, MS and NMR facilities for their kind support.

Keywords: SO_2 solvate • crown ether • hybrid crown ether • *host-guest* chemistry

[1] H. Spandau, V. Gutmann, *Angew. Chem.* **1952**, *64*, 93–102.

[2] W. Karcher, H. Hecht, *Chemie in Flüssigem Schwefeldioxid* in *Chemie in nichtwäßrigen ionisierenden Lösungsmitteln*, Bd. III, C. C: Addison, W. Karcher, H. Hecht (Hrsg.), Vieweg & Sohn,Braunschweig, **1967**.

[3] G. W. Watt, W. A. Jenkins, C. V. Robertson, *Anal. Chem.* **1950**, *22*, 330–331.

[4] P. Elving, J. M. Markowitz, *J. Chem. Educ.* **1960**, *37*, 75–81.

[5] W. A. Schenk, *Angew. Chem., Int. Ed. Engl.* **1987**, *26*, 98–109.

[6] C. Barbeau, R. J. Dubey, *Can. J. Chem.* **1973**, *51*, 3684–3689.

[7] G. J. Kubas, R. R. Ryan, V. McCarty, *Inorg. Chem.* **1980**, *19*, 3003–3007.

[8] D. M. P. Mingos, *Transit. Met. Chem.* **1978**, *3*, 1–15.

[9] E. Lork, J. Petersen, R. Mews, *Angew. Chem., Int. Ed. Engl.* **1994**, *33*, 1663–1665.

[10] A. Simon, K. Peters, E.-M. Peters, H. Kühnl, B. Koslowski, *Z. Anorg. Allg. Chem.* **1980**, *469*, 94–100.

[11] R. Mews, E. Lork, P. G. Watson, Görtler, *Coord. Chem. Rev.* **2000**, *197*, 277–320.

[12] J. Derendorf, M. Keßler, C. Knapp, M. Rühle, C. Schulz, *Dalton. Trans.* **2010**, *39*, 8671.

[13] R. Hoppenheit, W. Isenberg, R. Mews, *Zeitschrift für Naturforsch. B* **1982**, *37*, 1116–1121.

[14] T. S. Cameron, G. B. Nikiforov, J. Passmore, J. M. Rautiainen, *Dalton Trans.* **2010**, *39*, 2587.

[15] H. Kühnl, A. Strumpf, M. Gladziwa, *Z. Anorg. Allg. Chem.* **1979**, *449*, 145–156.

[16] E. Lork, R. Mews, J. Petersen, M. Schröter, B. Žemva, *J. Fluor. Chem.* **2001**, *110*, 109–116.

[17] J. D. Childs, D. Van der Helm, S. D. Christian, *Inorg. Chem.* **1975**, *14*, 1386–1390.

[18] K. Hoher, P. F. Cardoso, L. F. Lepre, R. A. Ando, L. J. A. Siqueira, *Phys. Chem. Chem. Phys.* **2016**, *18*, 28901–28910.

[19] W. Wu, B. Han, H. Gao, Z. Liu, T. Jiang, J. Huang, *Angew. Chem. Int. Ed.* **2004**, *43*, 2415–2417.

[20] J. Huang, A. Riisager, P. Wasserscheid, R. Fehrmann, *Chem. Commun.* **2006**, 4027.

[21] L. E. Barrosse-Antle, C. Hardacre, R. G. Compton, *J. Phys. Chem. B* **2009**, *113*, 1007–1011.

[22] R. A. Ando, L. J. A. Siqueira, F. C. Bazito, R. M. Torresi, P. S. Santos, *J. Phys. Chem. B* **2007**, *111*, 8717–8719.

[23] A. Kumar, G. S. McGrady, J. Passmore, F. Grein, A. Decken, *Z. Anorg. und Allg. Chem.* **2012**, *638*, 744–753.

[24] W. Eisfeld, M. Regitz, *J. Am. Chem. Soc.* **1996**, *118*, 11918–11926.

[25] A. Kornath, O. Blecher, *Z. Anorg. und Allg. Chem.* **2002**, *628*, 570–574.

[26] U. Keßler, M. Jansen, *Z. Anorg. und Allg. Chem.* **1999**, *625*, 385–388.

[27] K. Reuter, M. R. Buchner, G. Thiele, C. von Hänisch, *Inorg. Chem.* **2016**, *55*, 4441–4447.

[28] K. Reuter, G. Thiele, T. Hafner, F. Uhlig, C. von Hänisch, *Chem. Commun.* **2016**, *52*, 13265–13268.

[29] K. Reuter, F. Dankert, C. Donsbach, C. von Hänisch, *Inorganics* **2017**, *5*, 11.

[30] F. Dankert, K. Reuter, C. Donsbach, C. von Hänisch, *Dalton Trans.* **2017**, DOI 10.1039/C6DT04018G.

[31] E. G. Awere, N. Burford, R. C. Haddon, S. Parsons, J. Passmore, J. V Waszczak, P. S. White, *Inorg. Chem.* **1990**, *29*, 4821–4830.

[32] P. D. Boyle, S. M. Godfrey, R. G. Pritchard, *J. Chem. Soc., Dalton Trans.* **1999**, 4245–4250.

[33] N. Kuhn, H. Bohnen, D. Bläser, R. Boese, A. H. Maulitz, *J. Chem. Soc., Chem. Commun.* **1994**, *53*, 2283–2284.

[34] A. Decken, C. Knapp, G. B. Nikiforov, J. Passmore, J. Mikko Rautiainen, X. Wang, X. Zeng, *Chem. - Eur. J.* **2009**, *15*, 6504–6517.

[35] T. S. Cameron, A. Decken, I. Krossing, J. Passmore, J. M. Rautiainen, X. Wang, X. Zeng, *Inorg. Chem.* **2013**, *52*, 3113–3126.

[36] A. Decken, J. Passmore, X. Wang, *Angew. Chem., Int. Ed. Engl.* **2006**, *45*, 2773–2777.

[37] T. Takano, N. Kasai, M. Kakudo, *Bull. Chem. Soc. Jpn.* **1963**, *36*, 585–590.

[38] E. R. Lippincott, F. E. Welsh, *Spectrochim. Acta* **1961**, *17*, 123–124.

[39] F. Gingl, W. Hiller, J. Strähle, H. Borgholte, K. Dehnicke, *Z. Anorg. Allg. Chem.* **1991**, *606*, 91–96.

[40] S. T. Liddle, W. Clegg, *Polyhedron* **2003**, *22*, 3507–3513.

[41] M. Gjikaj, A. Adam, *Z. Anorg. Allg. Chem.* **2006**, *632*, 2475–2480.

[42] E. Mason, H. A. Eick, *Acta Crystallogr., Sect. B: Struct. Crystallogr. Cryst. Chem.* **1982**, *38*, 1821–1823.

[43] K. Torizuka, T. Sato, *Org. Magn. Reson.* **1979**, *12*, 190–195.

[44] K. Peters, A. Simon, E.-M. Peters, H. Kühnl, B. Koslowski, *Z. Anorg. Allg. Chem.* **1982**, *492*, 7–14.

[45] M. R. Willcott, *J. Am. Chem. Soc.* **2009**, *131*, 13180.

[46] OPUS, *Bruker Opt. GmbH* **2012**.

[47] *X-Area.* Stoe & Cie GmbH, Darmstadt, Germany, **2011**.

[48] *X-Shape.* Stoe & Cie GmbH, Darmstadt, Germany, **2009**.

[49] *X-Red32.* Stoe & Cie GmbH, Darmstadt, Germany, **2009**.

[50] G. M. Sheldrick, *SHELXS-2013/1*, Göttingen, **2013**.

[51] G. M. Sheldrick, *SHELXL-2016/4*, Göttingen (Germany), **2016**.

[52] C. B. Hübschle, G. M. Sheldrick, B. Dittrich, *J. Appl. Crystallogr.* **2011**, *44*, 1281–1284.

Dalton Transactions

PAPER

View Article Online
View Journal

Cite this: DOI: 10.1039/c7dt00321h

Synthesis of heteroatomic bridged paracyclophanes†‡

K. Reuter, R. G. M. Maas, A. Reuter, F. Kilgenstein, Y. Asfaha and C. von Hänisch*

Received 30th January 2017,
Accepted 23rd February 2017

DOI: 10.1039/c7dt00321h

rsc.li/dalton

Heteroatomic bridged paracyclophanes were obtained by two independent synthetic approaches. The required precursors consist of *para* R_2SiCl (R = Me, *i*Pr) substituted aromatic rings (**2** and **4**). They were subsequently functionalised by using NH_3, $[LiPH_2(dme)]$ or $LiAl(PH_2)_4$. In the case of the Me-substituted species **2**, the reaction with NH_3 directly yielded the Si_2N bridged paracyclophane **5**. The Si_2P incorporated derivative **10** was obtained by lithiation of *p*-$C_6H_4(SiiPr_2PH_2)_2$ (**9**) and subsequent salt metathesis with the chlorosilane **4**. The second approach involves the use of $GaEt_3$ in the formation of four membered $(GaPn)_2$ cycles (Pn = N, P). *p*-$[C_6H_4\{SiiPr_2N(H)GaEt_2\}_2]_2$ (**11**) and *p*-$[C_6H_4\{SiiPr_2P(H)GaEt_2\}_2]_2$ (**12**) represent the first examples of stable $(GaPn)_2$ *cis* isomers as the *trans* species did not appear in solution. Although **11** and **12** show a similar coordination pattern, they differ in the orientation of the aromatic systems: in the solid structure, **11** adopts a – for paracyclophanes so far unique – T-shape conformation of the phenyl rings, while **12** shows the predominant coplanar orientation. All cyclophanes were characterized by X-ray diffraction, elemental analysis, NMR and IR spectroscopy.

Introduction

In the last few years reactions of primary silylamines and -phosphanes with group 13 organyls have intensively been studied and have yielded a broad spectrum of group 13/15 compounds.[1] The structure of the products strongly depends on the silyl group bonded to the pnictogen atoms (Scheme 1). For example, four-membered $(GaPn)_2$ cycles (Pn = N, P) were obtained by the reaction of $GaEt_3$ and $R_2R'SiPnH_2$ (**I**).[2] When two PH_2 groups are linked by one Si atom, as present in $iPr_2Si(PH_2)_2$, the reaction with $GaEt_3$ leads to the compound $[iPr_2Si\{P(H)GaEt_2\}_2]_2$ (**II**), which incorporates an eight membered Ga_4P_4 ring system.[3] However, experiments with the corresponding N-analogues have not been reported to date. The enlargement of the spacer between the two PH_2 groups by a disiloxane fragment as in $O(SiiPr_2PH_2)_2$ results in an analogous reaction giving a sixteen-membered Ga_8P_8 ring system, which is incorporated in four disiloxane frameworks (**III**).[4] Hitherto, aryl groups as spacers between two silylamines or -phosphanes are barely known,[5] and also the reactivity of aryl bridged bis(silylpnictogens) towards group 13 organyls has not been the issue of investigation to date. Since benzene as a spacer provides an increased distance in comparison to $iPr_2Si(PH_2)_2$ and $O(SiiPr_2PH_2)_2$ between the two PnH_2 groups located at the *para* position, different Ga_xPn_x-patterns as shown in Scheme 1 can be expected. Compounds of the type *p*-$C_6H_4(SiR_2PnH_2)$ can also be considered as precursors for heteroatomic bridged paracyclophanes. Most notably C_2 and Si_2 bridged [2.2]paracyclophanes have intensively been investigated,[6] owing to their application as auxiliaries in the enantioselective synthesis[7] and their coordination chemistry.[8] In the

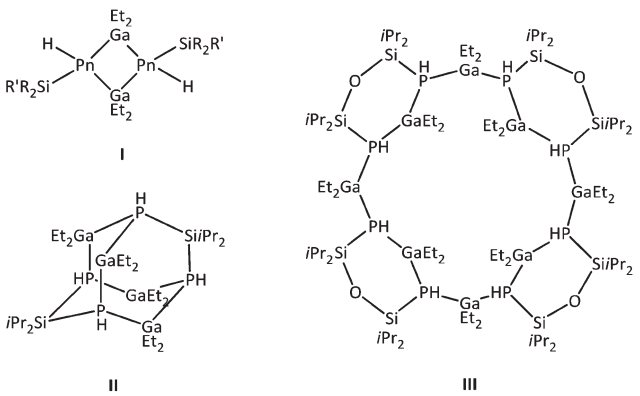

Scheme 1 Structures of $[Et_2GaPn(H)SiR_2R']_2$ (Pn = N; R,R′ = Et and Pn = P; R = Me, R′ = CMe_2iPr) (**I**), $[iPr_2Si\{P(H)MEt_2\}_2]_2$ (**II**) and $[O(SiiPr_2)_2\{P(H)MEt_2\}_2]_4$ (**III**).

Fachbereich Chemie and Wissenschaftliches Zentrum für Materialwissenschaften (WZMW), Philipps-Universität Marburg, Hans-Meerwein-Straße 4, 35043 Marburg, Germany. E-mail: haenisch@chemie.uni-marburg.de; Fax: +49-6421-2825653

†Dedicated to Professor Evamarie Hey-Hawkins on the occasion of her 60th birthday.

‡CCDC 1527336 (**2**), 1527337 (**4**), 1527338 (**5**), 1527339 (**6**), 1527340 (**7**), 1527341 (**8**), 1527342 (**9**), 1527343 (**10**), 1527344 (**11**) and 1527345 (**12**). For crystallographic data in CIF or other electronic format see DOI: 10.1039/c7dt00321h

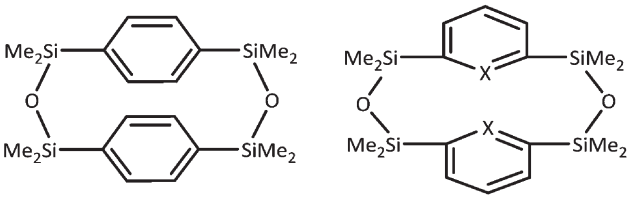

Scheme 2 Examples of siloxane-bridged silacyclophanes (X = CH, N, P).

field of heteroatomic bridged paracyclophanes, especially the disiloxane bridged cyclophanes were matter of particular interest.[9] However, still no coordination compounds involving Si–O bridged paracyclophanes have been published (Scheme 2). The weak coordination ability of oxygen in siloxanes is well-known for quite some time[10] and was attributed to the interaction of the p(O) electron density with the σ*(Si–C) orbitals[11] and moreover to the electrostatic repulsion between the positively polarized Si atoms and the Lewis acid.[12] By replacing the weakly coordinating O atom of the siloxane group by a group 15 compound, *e.g.* NH or PH, the bridging moiety could, especially after deprotonation, participate in the coordination of Lewis acids.

In this work, we present the synthesis of heteroatomic bridged paracyclophanes by two independent approaches, involving condensation reactions as well as σ-donor–σ-acceptor interactions.

Results

Precursors for [3.3]paracyclophanes

The required building blocks for the aryl bridged bis(silanes) were synthesised by a twofold Grignard reaction of 1,4-dibromobenzene and subsequent addition of two equivalents of R_2SiHCl (R = Me (**1**),[13] *i*Pr (**3**)). Trichloroisocyanuric acid (TCCA) serves as a highly selective reagent for the chlorination of silicon hydrides,[14] so that the resulting products were obtained without the formation of impurities (Scheme 3).

p-$C_6H_4(SiMe_2Cl)$ (**2**) and *p*-$C_6H_4(Si{i}Pr_2Cl)$ (**4**) are colourless oils, and both crystallise within 2 h at room temperature in the space groups $P2_1/n$ and $P2_1/c$, respectively. The molecular structures show that the chlorine atoms are oriented in opposite directions (Fig. 1). The bond lengths between Si1 and Cl1

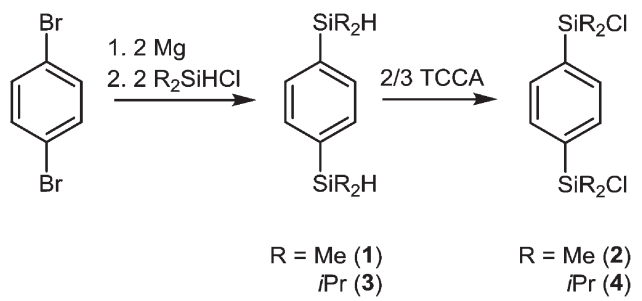

Scheme 3 Synthesis pathway for the aryl bridged bis(silanes) *p*-$C_6H_4(SiR_2H)_2$ (R = Me (**1**), *i*Pr (**3**)) and chlorination by TCCA.

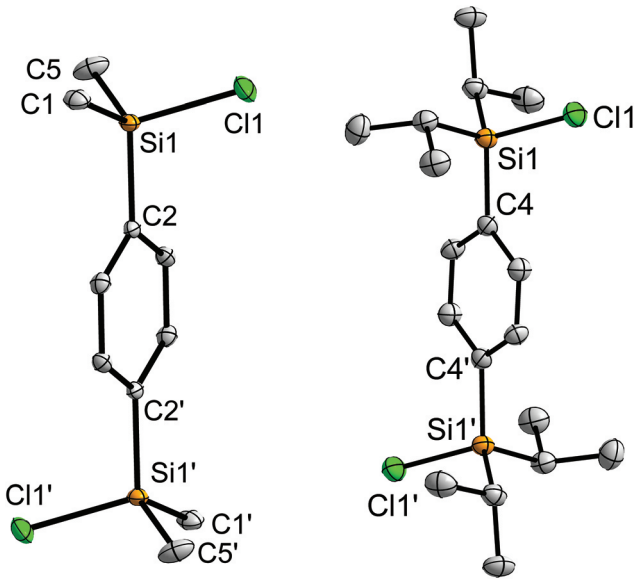

Fig. 1 Molecular structures of *p*-$C_6H_4(SiMe_2Cl)$ (**2**, left) and *p*-$C_6H_4(Si{i}Pr_2Cl)$ (**4**, right) in the crystal. Thermal ellipsoids represent the 50% probability level. Hydrogen atoms are not displayed for clarity. Selected bond lengths [pm] and angles [°]. **2**: Si1–Cl1: 208.4(1), Si1–C2: 187.2(1), Si1–C2···C2′ 179.0(1), Cl1–Si1–C2: 105.8(1). **4**: Si1–Cl1: 208.1(1), Si1–C4: 187.2(1), Si1–C4···C4′: 176.4(1), Cl1–Si1–C4: 107.6(1).

are 208.4(1) pm in **2** and 208.1(1) pm in **4**. The Si atoms of compound **2** are, with a deviation of 1.0°, almost coplanar with the aromatic system, while the bulkier *i*Pr groups in **4** lead to a stronger displacement of the Si atoms from the planar aromatic ring with a value of 3.6°. In the $^{29}Si\{^1H\}$ NMR spectra, the signals of Si1/Si1′ appear at 19.9 ppm for **2** and 27.1 ppm for **4**. Compound **2** is sensitive towards traces of water and hydrolysis of the Si–O–Si bridged paracyclophane, as shown in Scheme 2.[9] However, the *i*Pr groups in **4** provide sufficient steric hindrance, and so the Si–Cl moiety remains stable in aqueous solution, independent of the presence of $NaOH_{(aq.)}$.

Functionalisation with group 15 elements

Chlorine is a versatile leaving group and offers various possibilities for further functionalisation of the Si atoms with group 15 elements. Nitrogen can be introduced – driven by the formation of solid NH_4Cl – by the reaction of the chlorosilanes **2** and **4** with NH_3 in toluene at room temperature. The reaction completes after *ca.* 2 h, when no further NH_4Cl emerges as a white precipitate. By $^{29}Si\{^1H\}$ NMR measurement of the reaction with a D_2O capillary as the standard, the completeness of the reaction can finally be ensured.

The reaction of **2** with NH_3 yielded a colourless solid, which was recrystallized from dichloromethane and toluene at −35 °C. After 4 d, colourless plates suitable for X-ray diffraction were obtained. Compound **5** crystallises in the space group $P2_1/n$ with four molecules per unit cell. As a result of the low steric hindrance, the reaction with NH_3 leads directly to the condensed product $[1,4\text{-}C_6H_4(SiMe_2NH)_2]_2$ (**5**) under elim-

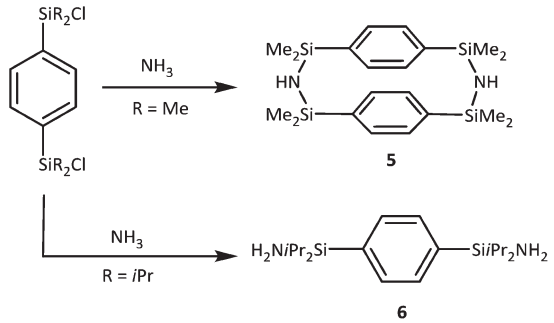

Scheme 4 Overview of the reaction of *p*-$C_6H_4(SiMe_2Cl)_2$ (**2**) and *p*-$C_6H_4(SiiPr_2Cl)_2$ (**4**) with ammonia yielding the SiNSi-bridged paracyclophane **5** and the primary silylamine **6**.

ination of NH_3 (Scheme 4). The primary amine cannot be detected by $^{29}Si\{^1H\}$ NMR measurement from the reaction. The molecular structure of **5** can best be described as a silylamine bridged paracyclophane (Fig. 2). More than the open chained species **2**, the Si–C_{ar} bonds deviate from the planes defined by the two benzene rings between 6.2° and 4.1°. Similar values were found in disiloxane bridged paracyclophanes.[9] The coplanar arranged aromatic ring systems do not lie exactly above one another as a result of the flexible Si–N–Si bridge. The inter-ring distance is 331.8 pm, which is significantly smaller than that in the siloxane bridged [3.3]paracyclophane, owing to smaller Si–N–Si angles (Si–N–Si: ∅134.0(1)° *vs.* Si–O–Si: 150.2(1)°). Besides single crystal X-ray crystallography, compound **5** was fully characterized by NMR and IR spectroscopy, mass spectrometry, and elemental analysis. The $^{29}Si\{^1H\}$ chemical shift undergoes the expected highfield-shift from δ = 19.9 ppm in **2** to δ = −3.9 ppm in the paracyclophane **5**.

The analogous reaction of the isopropyl substituted chlorosilane **4** with NH_3, yielded a colourless solid. After 2 d at −25 °C colourless plates of *p*-$C_6H_4(iPr_2SiNH_2)_2$ (**6**) were obtained from toluene. **6** crystallizes in the space group $P\bar{1}$ with two molecules per unit cell. The *i*Pr groups prevent the diamine from condensation, and so the primary amine was obtained (Fig. 3). The molecular structure shows similarities to the educt **4**, since the NH_2 groups are again oriented in opposite directions as noted above. Worth mentioning is the enlarged Si–N bond length of 178.5(1) pm. In comparison, the secondary silylamine **5** shows a Si–N bond length of 172.8(1) pm, and similar values were also found in other primary and secondary silylamines.[15]

Due to the higher basic NH_2 substituents, compound **6** is – different from the chlorinated species **4** – sensitive towards water and hydrolysis to the corresponding silanol $C_6H_4(SiiPr_2OH)_2$ (**7**) (Fig. 3, right). Therein, the OH groups are not oriented in exactly opposite directions as can be deduced from the dihedral angle (O1–Si1···Si2–O2) of 54.7(1)°. This might be the result of H-bonding, which is visualised in Fig. 4. Three OH-groups respectively show interactions on both sides of each molecule, giving a strand-like coordination pattern. The O···O distances range between 268.8(2) pm and 272.9(3) pm, indicative of medium strength H-bonding.[16] The presence of one single intense absorption at 3299 cm^{-1} in the IR spectrum confirms that all OH groups are involved in hydrogen bonding. Compound **7** represents, with its silanol entities, a suitable precursor for the corresponding disiloxane bridged

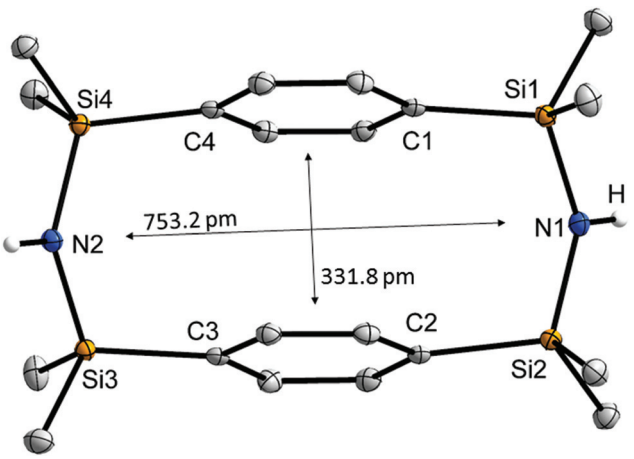

Fig. 2 Molecular structure of [1,4-$C_6H_4(SiMe_2NH)_2]_2$ (**5**) in the crystal. Thermal ellipsoids represent the 50% probability level. Carbon bonded hydrogen atoms are not displayed. Selected bond lengths [pm], interatomic distances [pm] and angles [°]. Si1–N1: 172.8(1), Si2–N1: 173.1(1), Si3–N2: 172.4(1), Si4–N2: 173.8(1), Si1–C1: 187.3(1), Si2–C2: 187.7(1), Si3–C3: 187.4(1), Si4–C4: 188.0(1), N1···N2: 753.2(2), Si1–N1–Si2: 133.9(1), Si3–N2–Si4: 134.1(1), C4···C1–Si1 175.9(1), C3···C2–Si2: 173.9(1).

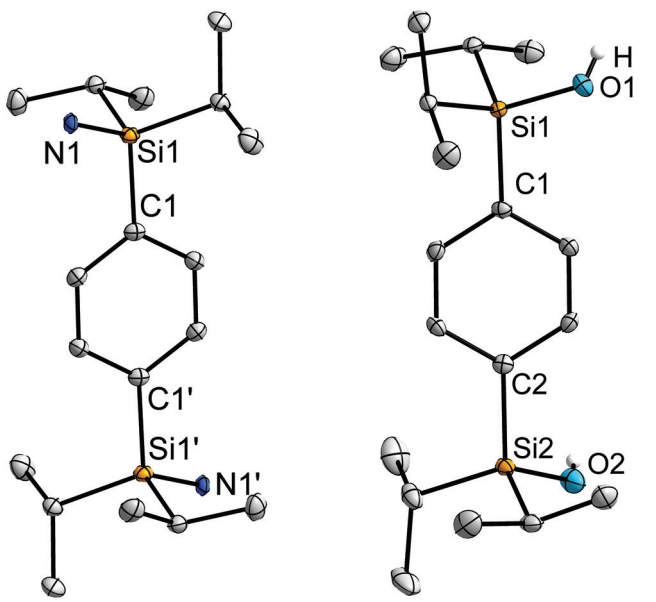

Fig. 3 Molecular structures of *p*-$C_6H_4(iPr_2SiNH_2)_2$ (**6**, left) and the hydrolysis product *p*-$C_6H_4(SiiPr_2OH)_2$ (**7**, right) in the crystal. Thermal ellipsoids represent the 50% probability level. C bonded H atoms are not displayed, N bonded H atoms were not found. Selected bond lengths [pm], interatomic distances [pm] and angles [°]. **6**: Si1–N1: 178.5(1), Si1–C1: 188.3(2). **7**: Si1–O1: 165.6(1), Si2–O2: 165.7(2), Si1–C1: 187.2(3), Si2–C2: 188.0(3); O1–Si1···Si2–O2: 54.7(1).

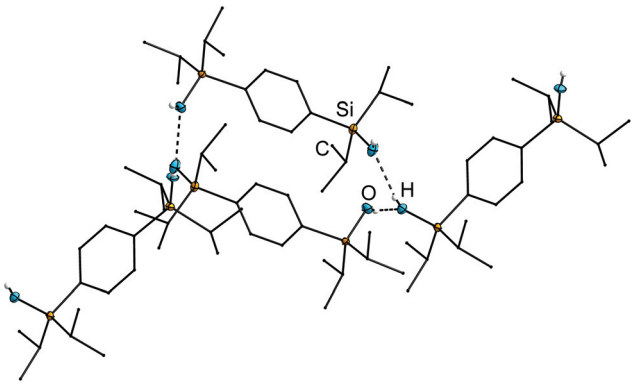

Fig. 4 A perspective view of the H-bonding in p-$C_6H_4(SiiPr_2OH)_2$ (**7**). Thermal ellipsoids represent the 50% probability level. C bonded H atoms are not displayed for clarity, C atoms are represented in the wires and sticks model.

paracyclophane. The Si–OH functional group additionally offers various possibilities for further functionalisation.

Besides nitrogen we were also interested in the functionalisation with phosphorus, *e.g.* PH_2. Several methods are known to date to transfer PH_2 groups. In particular, the use of $[LiAl(PH_2)_4]$, developed by Baudler *et al.*,[17] and $[LiPH_2(dme)]$[18] proved to be valuable.

The methyl substituted derivative p-$C_6H_4(SiMe_2PH_2)_2$ (**8**) was obtained in quantitative yield by the reaction of **2** with an excess of $[LiAl(PH_2)_4]$. Contrary to this, $[LiPH_2(dme)]$ didn't turn out to be an acceptable agent for the synthesis of **8**, owing to its high tendency to undergo acid–base reactions with primary silyl phosphanes followed by condensation as well as decomposition (Scheme 5). **8** crystallises from benzene at 6 °C within 2 d in the space group $P2_1/n$ with two molecules per unit cell. On a structural level, compound **8** doesn't differ significantly from the above described educt **2**. In the ^{31}P NMR spectrum, the P atoms appear as a triplet at δ = −237.5 ppm with a coupling constant of $^1J_{P,H}$ = 184 Hz. An additional coupling to the H atoms at the adjacent methyl groups leads to a broadening of the signal pattern as was also observed in similar compounds.[17] The doublet of the P–*H* hydrogen atoms was also detected in the ^1H NMR spectrum at δ = 1.42 ppm. In the $^{29}Si\{^1H\}$ NMR spectrum, one doublet can be observed at δ = −1.4 ppm with a coupling constant of $^1J_{Si,P}$ = 18 Hz. The P–H stretching vibration appears at $\tilde{\nu}$ = 2287 cm^{-1} in the IR spectrum. Furthermore, compound **8** was fully characterized by elemental analysis and mass spectrometry.

The *i*Pr substituted species **4** turned out to be suitable for the reaction with $[LiPH_2(dme)]$, as p-$C_6H_4(SiiPr_2PH_2)_2$ (**9**) was obtained selectively.[19] For this purpose, a solution of chlorosilane **4**, diethylether and 1,2-dimethoxyethane was purged with PH_3 under simultaneous addition of *n*-BuLi in hexane. At −20 °C, the acid–base reaction of *n*-BuLi and PH_3 to form $[LiPH_2(dme)]$ is faster than the competing salt metathesis reaction of *n*-BuLi and **4**. By distillation (1×10^{-3} mbar, 85 °C), compound **9** was purified, giving 64% yield. **9** crystallises from benzene within 2 d at 6 °C in the space group $P2_1/n$ with two molecules per unit cell. The molecular structure is visualised in Fig. 5 (right) and exhibits strong analogies to the methyl substituted primary silylphosphane **8**. The ^{31}P NMR spectrum shows one triplet at δ = −275.7 ppm with a coupling constant of $^1J_{SiH}$ = 186 Hz. In the ^1H NMR spectrum the expected doublet of the P–*H* hydrogen atoms can be detected at δ = 1.29 ppm, and in the $^{29}Si\{^1H\}$ NMR spectrum the two identical Si atoms split into a doublet at δ = 14.3 ppm with a coupling constant of $^1J_{Si,P}$ = 14 Hz. The P–H stretching vibration was found at $\tilde{\nu}$ = 2289 cm^{-1}. Compound **9** was additionally characterized by mass spectrometry, and the purity was confirmed by elemental analysis.

Selective synthesis of a Si_2P bridged [3.3]paracyclophane

Compound **9** represents a suitable building block for –SiPSi– bridged [3.3]paracyclophanes. Deprotonation of the primary silylphosphane by using 2eq. of $Li\{N(SiMe_3)_2\}$ selectively

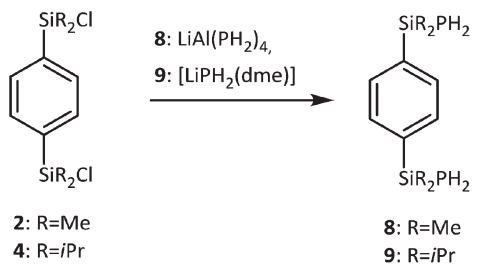

Scheme 5 Synthesis pathway for p-$C_6H_4(SiMe_2PH_2)_2$ (**8**) by using $[LiAl(PH_2)_4]$ and p-$C_6H_4(SiiPr_2PH_2)_2$ (**9**) by using $[LiPH_2(dme)]$.

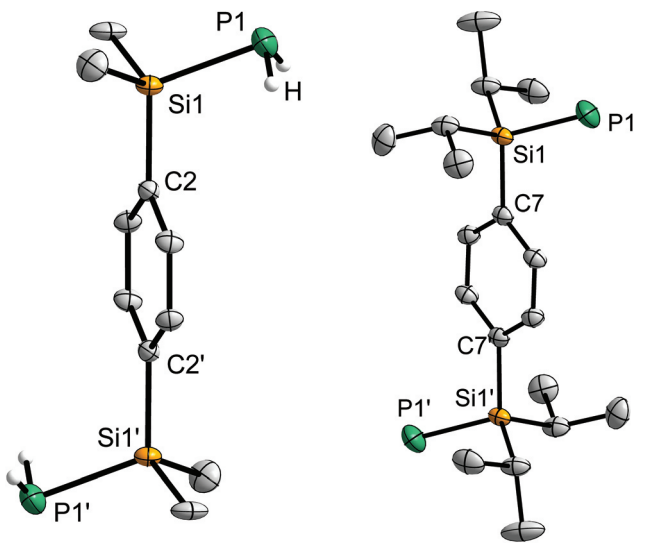

Fig. 5 Molecular structures of p-$C_6H_4(Me_2SiPH_2)_2$ (**8**, left) and p-$C_6H_4(SiiPr_2PH_2)_2$ (**9**, right) in the crystal. Thermal ellipsoids represent the 50% probability level. C bonded H atoms are not displayed, in compound **9**, the P bonded H atoms were not found. Selected bond lengths [pm], interatomic distances [pm] and angles [°]. **8**: Si1–P1: 227.1(3), Si1–C2: 187.6(2), Si1–C2···C2′: 178.9(1). **9**: Si1–P1: 216.2(1), Si1–C7: 187.6(2), Si1–C7···C7′: 177.2(1).

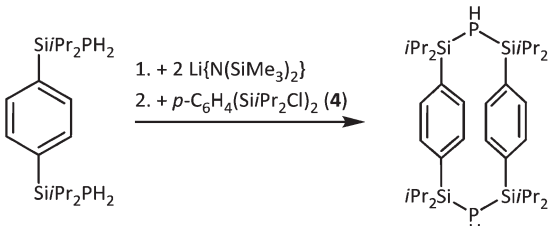

9 **10**

Scheme 6 Twofold lithiation of **9** followed by salt metathesis with **4** gives the SiPSi bridged [3.3]paracyclophane **10**.

yielded the twofold lithiated species. In the next step, *p*-C$_6$H$_4$(Si*i*Pr$_2$Cl)$_2$ (**4**) was added stoichiometrically with high dilution, in order to prevent polymerisation (Scheme 6). The raw product is a colourless solid, which crystallises in toluene within 2 d at −25 °C in the space group $P\bar{1}$ with two molecules per unit cell. On a structural level, [*p*-C$_6$H$_4$(Si*i*Pr$_2$PH)$_2$]$_2$ (**10**) shows similarities to the SiNSi-bridged paracyclophane **5**. The two benzene cycles are parallelly displaced owing to the flexible SiPSi linker. In **10**, the distance between the two stacked π-systems is 402.8(4) pm which is more than that in **5**, due to the larger Si–P distances of 225.9(1) and 226.4(1) pm. For secondary silylphosphanes they fall in the typical range.[20] As expected, the Si1–P1–Si2 bond angle (117.6(1)°) is smaller than that of Si–N–Si found in the [3.3]paracyclophane **5**. The P atoms adopt, together with the aryl fragments, an extended chair conformation as one P atom is located beneath and one above the mean plane generated by the four Si atoms (Fig. 6).

In the ^{31}P NMR spectrum, one doublet at δ = −275.5 ppm with a coupling constant of $^{1}J_{P,H}$ = 197 Hz was observed. The P–*H* hydrogen atoms were also detected in the ^{1}H NMR spectrum at δ = 0.99 ppm. The Si satellites were detected in the ^{31}P{^{1}H} NMR spectrum with a coupling constant of $^{1}J_{Si,P}$ = 39 Hz. In the ^{29}Si{^{1}H} NMR spectrum, the Si atoms of compound **10** appear at δ = 8.4 ppm as a doublet. The P–H stretching vibration was detected by IR spectroscopy at $\tilde{\nu}$ = 2283 cm^{-1}.

Reactivity towards GaEt$_3$

Lithiation of the silylphosphane **9** followed by salt metathesis with the corresponding chlorosilane **4** represents one possibility to obtain heteroatomic bridged paracyclophanes as presented in Scheme 6. Another approach consists of the use of group 13 organyls. For this purpose, the primary amine *p*-C$_6$H$_4$(*i*Pr$_2$SiNH$_2$)$_2$ (**6**) and the primary silylphosphane *p*-C$_6$H$_4$(*i*Pr$_2$SiPH$_2$)$_2$ (**9**) were respectively reacted with GaEt$_3$ (Scheme 7). As reported, group 13 organyls are likely to react with primary silylamines and -phosphanes, and undergo alkane elimination followed by Ga–N or Ga–P bond formation.[1–4]

After the reaction of **6** with GaEt$_3$ at ambient temperature, colourless crystals of the space group $P2_12_12_1$ were grown within 4 d at −35 °C (Table 1). By single crystal X-ray diffraction, a dimeric species was found, possessing a Ga–N donor–

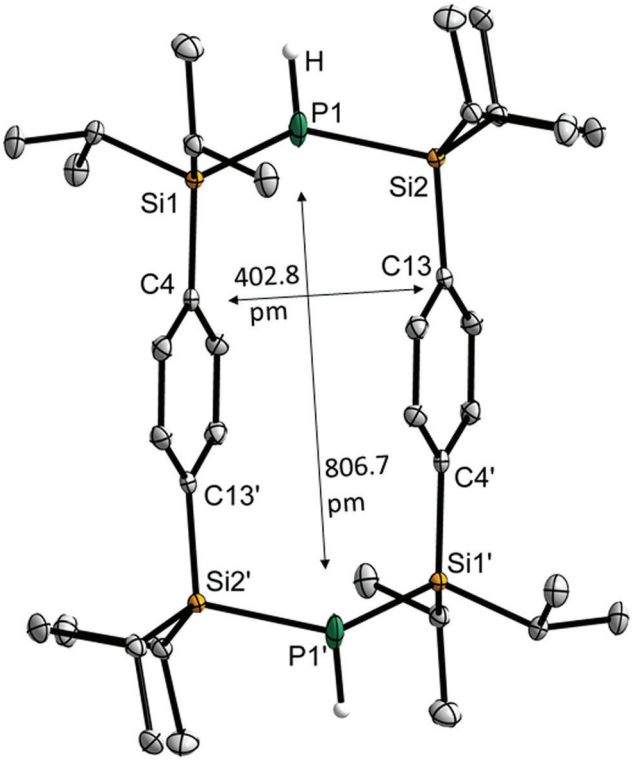

Fig. 6 Molecular structures of *p*-[C$_6$H$_4$(Si*i*Pr$_2$PH)$_2$]$_2$ (**10**) in the crystal. Thermal ellipsoids represent the 50% probability level. C bonded H atoms are not displayed. Selected bond lengths [pm], interatomic distances [pm] and angles [°]: Si1–P1: 225.9(1), Si2–P1: 226.4(1), Si1–C4: 187.9(2), Si2–C13′: 188.2(3), P1···P1′: 806.7(1), C4···C13: 402.8(4), Si1–P1–Si2: 117.6(1), Si1–C4···C13′: 178.6(1).

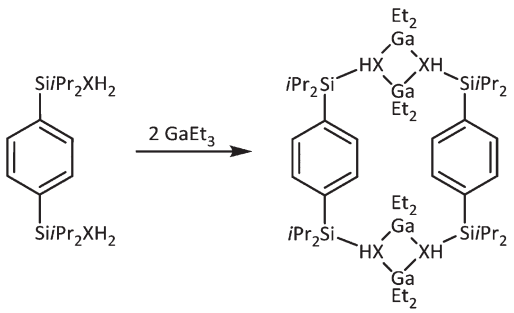

6: X = N
9: X = P

11: X = N
12: X = P

Scheme 7 Reaction of **6** and **9** with GaEt$_3$ gives the paracyclophanes [*p*-C$_6$H$_4${Si*i*Pr$_2$N(H)GaEt$_2$}$_2$]$_2$ (**11**) and [*p*-C$_6$H$_4${Si*i*Pr$_2$P(H)GaEt$_2$}$_2$]$_2$ (**12**).

acceptor bonding interaction (Fig. 7). The two resulting (GaN)$_2$ cycles act as bridges between two aryl entities so that **11** can be described as a Si(GaN)$_2$Si bridged paracyclophane. The most eye-catching feature of compound **11** represents the T-shaped arrangement of the π-systems. This type of non-covalent interaction is common for the stabilisation of DNA[21]

Table 1 Crystal structure data for the compounds **2** and **4–12**

	2	**4**	**5**	**6**
Empirical formula	$C_{10}H_{16}Cl_2Si_2$	$C_{18}H_{32}Cl_2Si_2$	$C_{20}H_{34}N_2Si_4$	$C_{18}H_{32}N_2Si_4$
Formula weight [g mol^{-1}]	263.31	375.51	414.85	332.63
Crystal colour, shape	Colourless block	Colourless plank	Colourless plate	Colourless block
Crystal size [mm]	0.059 × 0.170 × 0.172	0.06 × 0.120 × 0.320	0.120 × 0.148 × 0.228	0.114 × 0.265 × 0.530
Crystal system	Monoclinic	Monoclinic	Monoclinic	Triclinic
Space group	$P2_1/n$	$P2_1/c$	$P2_1/n$	$P\bar{1}$
Formula units	2	2	4	1
Temperature [K]	100(2)	153(2)	100(2)	100(2)
Unit cell dimensions [Å] and [°]	a = 6.4554(4) b = 10.2475(6) c = 10.4165(7) β = 96.700(3)	a = 8.7688 (4) b = 10.4447(5) c = 11.9094(6) β = 103.242(4)	a = 8.7323(3) b = 12.0878(4) c = 22.5265(9) β = 94.950(1)	a = 7.1205(4) b = 8.6746(5) c = 9.1371(5) α = 82.356(2) β = 76.703(2) γ = 9.1371(5)
Cell volume [Å^3]	648.36(7)	1061.75(9)	2368.90(15)	511.29 (5)
ρ_{calc} [g cm^{-3}]	1.278	1.175	1.163	1.080
μ (Mo K$_\alpha$) [mm^{-1}]	0.614	0.415	0.258	0.173
$\Theta_{min}/\Theta_{max}$ [°]	2.798–27.101	1.757–26.732	2.437–25.328	2.294–28.334
Reflections measured	2977	2251	4314	9365
Independent reflections	1506[R_{int} = 0.0207]	1814[R_{int} = 0.0525]	3839[R_{int} = 0.0313]	2461[R_{int} = 0.0202]
R_1 ($I > 2\sigma(I)$)	0.0242	0.0319	0.0269	0.0384
wR_2 (all data)	0.0609	0.0846	0.0784	0.1215
GooF	1.111	0.961	1.080	1.131
Largest diff. peak and hole [e Å^{-3}]	0.365/−0.349	0.216/−0.313	0.393/−0.263	0.807/−0.258

7	**8**	**9**	**10**	**11**	**12**
2·($C_{18}H_{34}O_2Si_2$)·$CHCl_3$	$C_{10}H_{16}P_2Si_2$	$C_{18}H_{32}P_2Si_2$	$C_{18}H_{32}P_1Si_2$	$C_{52}H_{108}Ga_4N_4Si_4$	$C_{33}H_{62}Ga_2P_2Si_2$
796.63	254.35	366.55	336.59	1180.66	716.38
Colourless plates	Colourless needle	Colourless plank	Colourless needle	Colourless block	Colourless plate
0.052 × 0.251 × 0.332	0.030 × 0.040 × 0.280	0.072 × 0.332 × 0.379	0.045 × 0.063 × 0.202	0.307 × 0.391 × 0.411	0.072 × 0.332 × 0.379
Triclinic	Monoclinic	Triclinic	Triclinic	Orthorhombic	Triclinic
$P\bar{1}$	$P2_1/n$	$P\bar{1}$	$P\bar{1}$	$P2_12_12_1$	$P\bar{1}$
2	2	1	2	4	2
100(2)	105(2)	115(2)	100(2)	100(2)	100(2)
a = 12.4377(9)	a = 6.5882(7)	a = 7.1303(4)	a = 9.2321(10)	a = 16.6181(6)	a = 11.4453(7)
b = 12.9833(8)	b = 10.5545(11)	b = 8.7216(5)	b = 9.5654(10)	b = 18.9494(8)	b = 13.4431(9)
c = 15.6637(10)	c = 10.6184(12)	c = 9.2829(6)	c = 12.1031(12)	c = 19.7553(8)	c = 14.5944(8)
α = 104.231(2)	β = 95.877(4)	α = 82.676(2)	α = 103.979(2)		α = 67.504(2)
β = 105.552(2)		β = 83.138(2)	β = 94.721(4)		β = 68.993(2)
γ = 101.563(2)		γ = 72.688(2)	γ = 109.762(3)		γ = 88.105(2)
2263.9(3)	734.47(2)	544.60(6)	960.21(17)	6221.0(4)	1922.6(2)
1.169	1.150	1.118	1.164	1.261	1.237
0.342	0.426	0.306	0.262	1.825	1.566
2.480–25.301	2.728–28.330	2.220–25.242	2.362–25.318	2.325–25.000	2.314
7614	1332	6246	3496	23 303	25.323
8233[R_{int} = 0.0773]	1108[R_{int} = 0.0751]	2399[R_{int} = 0.0261]	2905[R_{int} = 0.0403]	9696[R_{int} = 0.0396]	7610[R_{int} = 0.0475]
0.0424	0.0369	0.0354	0.0437	0.0325	0.0317
0.0955	0.1016	0.1092	0.1087	0.0810	0.0707
1.028	1.059	1.096	1.068	1.097	1.024
0.416/−0.372	0.396/−0.197	0.614/−0.289	0.913/−0.804	2.251/−1.458	0.498/−0.310

and has intensively been studied on a practical and theoretical level. Careful DFT calculations on benzene dimers revealed that the T-shaped and the parallel-displaced conformations are almost isoenergetic.[22] However, compound **11** represents the first example of a T-shaped aromatic system in paracyclophanes. As illustrated in Fig. 7, the H atoms bonded to C8 and C9, are oriented in the direction of the orthogonally placed aromatic system C1–C4. T-shaped aromatic interactions are commonly described for only one H atom with another π-system,[23] which is however not possible for compound **11**.

The aromatic rings adopt an orthogonal arrangement with respect to each other (Fig. 8, left), which is a typical geometry for T-shaped π–π interactions.[21] The C atoms C8 and C9 show a distance of 481.5(3) pm and 479.1(3) pm to the calculated median plane of the orthogonally arranged aromatic cycle (C1–C4). Besides the above described intramolecular interaction, no intermolecular π-interactions were observed in the crystal structure. As was determined by ^{1}H NMR spectroscopy, the aryl H atoms give one sharp signal at δ = 7.50 ppm, proving that in solution the aromatic rings have a low rotational barrier. As expected, also in the $^{13}C\{^1H\}$ NMR spectrum, two signals for the aromatic C atoms can be detected at 134.0 and 136.4 ppm. Owing to the electron withdrawing effect of Ga, the $^{29}Si\{^1H\}$ NMR signal shows a downfield shift to 4.1 ppm.

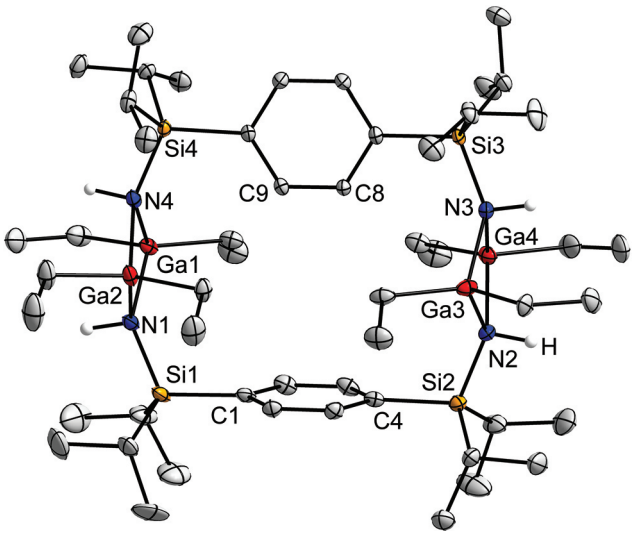

Fig. 7 Molecular structures of *p*-[C_6H_4{Si*i*Pr$_2$N(H)GaEt$_2$}$_2$]$_2$ (**11**) in the crystal. Thermal ellipsoids represent the 50% probability level. C bonded H atoms are not displayed. Selected bond lengths [pm], interatomic distances [pm] and angles [°]: Ga1–N1: 204.4(2), N4–Ga1: 203.9(2), Si1–N1: 176.0(3), Si2–N2: 176.4(2), Si1–C1: 188.5(3), Ga1···Ga2: 296.3(1), Ga3···Ga4: 295.8(1), Ga1···Ga4: 758.5(1), Ga2···Ga3: 753.6(1), C8···∅C$_{ar}$1–6: 481.5(3), C9···∅C$_{ar}$1–6: 479.1(3), N1–Ga1–N4: 86.6(1), N1–Ga2–N4: 86.3(1), Ga1–N4–Ga2: 92.9(1), Ga1–N1–Ga2: 92.8(1), Si1–N1–Ga2: 127.3(1), Si4–N4–Ga2: 128.1(1), Si1–C1···C4: 178.6(1).

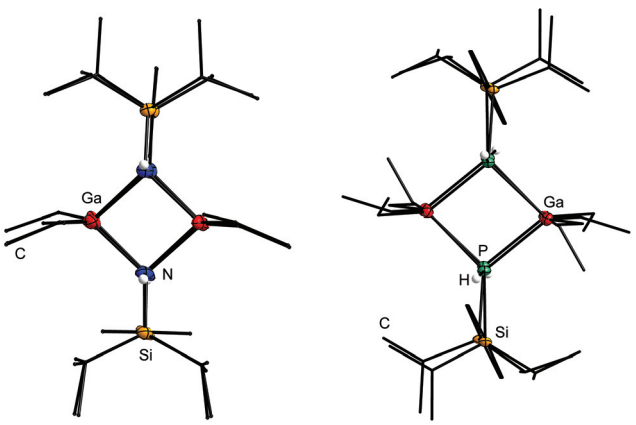

Fig. 8 A perspective view of **11** along the (GaN)$_2$ cycles (left) and of **12** along the (GaP)$_2$ cycles (right). Thermal ellipsoids represent the 50% probability level. C atoms are displayed in the wire and stick model, C bonded H atoms are omitted.

Different from the hitherto described paracyclophanes, **11** shows no significant strain. On the contrary, the π-systems tend to decrease the large inter-ring distance as can be deduced from the deviations in the angles of the Si–C$_{ar}$ bonds to the planes defined by phenyl groups. Si1 and Si2 with 1.4° and 1.5° deviation are almost coplanar with the aromatic system. Even Si3 and Si4 exhibit only small distortions from planar arrangement relative to the aryl ring, with values ranging from 2.8° to 4.0°.

Owing to the rigidity of the Si–C$_{aryl}$ group, the N bonded H atoms and the Si*i*Pr$_2$ groups adopt a *cis* orientation. By contrast, most of the hitherto described (GaN)$_2$ cycles show a *trans*-conformation in the solid state and generally isomerise in solution.[1,24] The first example of a crystallographically described dimeric *cis*-silylamidogallane was very recently published,[25] but also in that case, isomerisation was observed in solution. By contrast, in **11** the *cis* isomer remains predominant as by NMR spectroscopy only one set of signals was detected.

The GaN-rings deviate from the planar arrangement and adopts a butterfly structure as a result of the inflexible Si–C$_{aryl}$ moiety. The Ga atoms of the opposite (GaN)$_2$ cycles exhibit an intramolecular distance of 758.5(1) pm (Ga1···Ga4) and 753.3.6(1) pm (Ga2···Ga3), so the cavity size of **11** is similar to that of the SiNSi-bridged paracyclophane **5** (N1···N2: 753.2(2) pm). The Ga–N bond distances are 204.4(2) pm for Ga1–N1 and 203.9(2) pm for N4–Ga1 in the expected range.[1] The Ga atoms exhibit a distorted tetrahedral environment with average angles ranging from 86.4(1)° (N–Ga–N) to 118.4(1)° (C–Ga–C).

After the analogous reaction of the primary silylphosphane **9** with GaEt$_3$, a similar structure motif to the above described compound **11** was found by X-ray diffraction. *p*-[C_6H_4{Si*i*Pr$_2$P(H)GaEt$_2$}$_2$]$_2$ (**12**) crystallises within 2 d in the form of colourless plates in the space group $P\bar{1}$ with two molecules per unit cell and one disordered toluene molecule. **12** can be described as a Ga and P bridged paracyclophane (Fig. 9). The two aryl

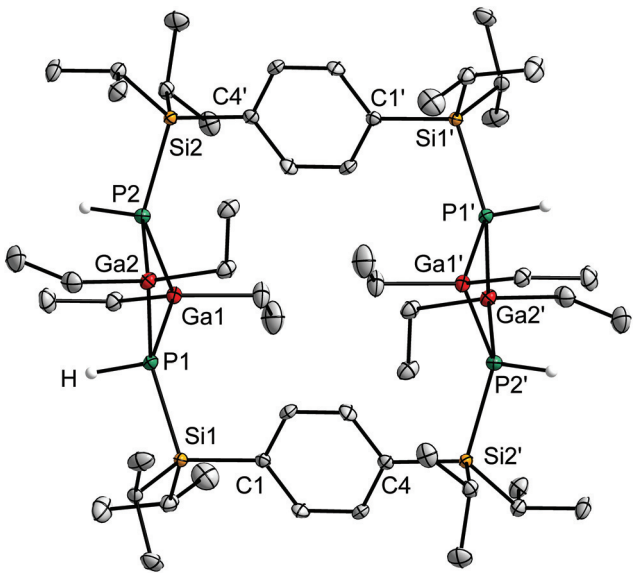

Fig. 9 Molecular structures of *p*-[C_6H_4{Si*i*Pr$_2$P(H)GaEt$_2$}$_2$]$_2$ (**12**) in the crystal. Thermal ellipsoids represent the 50% probability level. Disordered toluene and C bonded H atoms are not displayed. Selected bond lengths [pm], interatomic distances [pm] and angles [°]: Ga1–P1: 243.9(1), Ga1–P2 : 246.0(1), Ga2–P1: 247.2(1), Ga2–P2: 244.4(1), Si1–P1: 226.2(1), Si2–P2: 225.5(1), Si1–C1: 187.7(3), Si2–C4′: 187.9(3), Ga1···Ga2: 362.1(1), Ga1···Ga2′: 724.4(1), C1···C4′: 838.6(3), P1–Ga1–P2: 83.0(1), P1–Ga2–P2: 82.6(1), Ga1–P1–Ga2: 95.0(1), Ga1–P2–Ga2: 95.2(1), Si1–P1–Ga1: 126.3(1), Si1–P1–Ga2: 128.9(1), Si2–P2–Ga1: 126.3(1), Si2–P2–Ga2: 124.2(1), Si1–C1···C4: 176.5(1), Si2′–C4···C1: 178.2(1).

cycles are coplanar and oriented as observed in the SiPSi bridged [3.3]paracyclophane **10**. With values of 724.4(1) pm width (Ga1···Ga2′) and 838.6(3) pm height (C1···C4′), compound **12** has the largest dimensions of the herein presented paracyclophanes. The Ga–P bond lengths are between 243.9(1) pm and 247.2(1) pm, and are in agreement with the Ga–P–Ga angles of average 95.1(1)° in the range of similar compounds, while the P–Ga–P angle with 83.0(1)° and 82.6(1)° is slightly smaller.[26] The $(GaP)_2$-cycle shows, as in **11**, a butterfly conformation. The Ga atoms exhibit a distorted tetrahedral environment with average C–Ga–C angles of 118.4(1)°. The H atoms of the phosphorus show, together with the Si*i*Pr_2 group, a *cis* arrangement, which can be explained by the rigidity of the molecule. In solution, no isomerisation was observed as experimentally shown by means of NMR spectroscopy. In the ^{31}P NMR spectrum, one multiplet of the AA′XX′ spin systems was detected at δ = −247.4 ppm, whereas the $^{31}P\{^1H\}$ NMR spectrum reveals one singlet. In the ^{1}H NMR spectrum, the P bonded H atoms give one multiplet representing the AA′ part. To our knowledge, compound **12** represents the first example of a stable *cis*-$(GaP)_2$ heterocycle, which can be related to the rigid framework of the paracyclophane, as was also described for **11**. In the IR spectrum, the weak P–H stretching vibration was found at 2314 cm^{-1}, and the purity was confirmed *via* CHN analysis.

The molecular structures of **11** and **12** show that an increased distance between two PnH_2 groups (Pn = N, P) by an aromatic ring system doesn't lead to larger PnGa-cycles by reaction with $GaEt_3$, as was the case for *i*$Pr_2Si(PH_2)_2$ and $O(Si$*i*$Pr_2PH_2)_2$ (Scheme 1: **II** and **III**). Instead, the reactivity of *p*-$C_6H_4(Si$*i*$Pr_2PH_2)_2$ shows similarities to molecules incorporating one PnH_2 group (**I**), which commonly gives four membered $(GaPn)_2$ cycles, as depicted in Scheme 1. The π-interaction between the aromatic rings leads to the observed ring closure by the formation of two $(GaPn)_2$ cycles, and the resulting preference of the *cis* isomer. *trans* isomerisation would give chain type, polymeric structures, though they were not observed by ^{31}P NMR spectroscopy of the reaction solution. In that case, the stabilising π-interactions would not take place, which may explain the present selectivity towards the *cis* isomer.

Experimental

General experimental techniques

Except for the synthesis of **7** and the working up of **1** and **3**, all procedures were conducted under rigorous exclusion of oxygen and moisture using a Schlenk line and a nitrogen atmosphere. Solvents were dried and freshly distilled before use. NMR spectra were recorded with a Bruker Avance HD 300, Bruker DRX 400 or Bruker Avance 500 and visualised with MestReNova.[27] IR vibrational spectra were gathered with the Bruker Alpha ATR-FT-IR, and MS spectra with the Accu TOF-GC (LIFDI) and the LTQ-FT (ESI, APCI). Elemental analysis was performed on a Vario Micro Cube. The starting materials 1,4-dibromobenzene (Sigma-Aldrich), PH_3 (Air Liquide), $GaEt_3$ (Billiton Precursors B. V.) and $SiMe_2HCl$ (Sigma-Aldrich) were commercially purchased. $LiAl(PH_2)_4$[17] and *i*Pr_2SiHCl[28] were prepared by reported methods.

Crystal structures

Data collection was performed on a Bruker D8 Quest or on an IPDS2 diffractometer at 100(2) K with Mo K_α radiation and graphite monochromatization. Structures were solved by direct methods, and refined by full-matrix-least-squares against F^2 using shelxs-2014, shelxl-2014, shelxt-2014 and olex2 software.[29,30] The presentation of crystal structures was done with Diamond 4.2.2.[31]

$C_6H_4(SiMe_2H)_2$ (1).[32] 69.4 g (0.29 mol, 1.1eq.) of 1,4-dibromobenzene was dissolved in 150 mL of THF. At room temperature, 8 mL of this solution was quickly added to a stirred suspension of 13.0 g (0.54 mol, 2eq.) of magnesium, 250 mL THF and a few drops of 1,2-dibromoethane. After 5 min the reaction mixture started to warm until reflux, and the remaining solution of 1,4-dibromobenzene and THF was slowly added to the suspension. After complete addition, the reaction mixture was stirred for an additional 2 h at room temperature. Subsequently, at 0 °C, 51.1 g (0.54 mol, 2eq.) of $HSiMe_2Cl$ in 100 mL THF was slowly added to the reaction mixture and stirred for 14 h at ambient temperature. The reaction was stopped by addition of 200 mL of H_2O, and the product was extracted with 200 mL of *n*-pentane. The aqueous phase was washed two times with 50 mL of *n*-pentane, and the combined organic phases were dried over $MgSO_4$. The suspension was filtered, and the solvent was removed under reduced pressure. The product was purified by distillation (15 mmHg, 49 °C) yielding 68% (35.7 g, 0.18 mol) of a colourless oil. ^{1}H NMR (300 MHz, C_6D_6): δ = 037–0.38 (d, $^3J_{HH}$ = 3.8 Hz, 12H, CH_3), 4.19 (m, 2H, Si*H*), 7.58 ppm (s, 4H, H_{ar}); $^{13}C\{^1H\}$ NMR (75 MHz, C_6D_6): δ = −3.7 (s, CH_3), 131.4 (s, C_{ar}), 133.8 ppm (s, C_{ar}); $^{29}Si\{^1H\}$ NMR (60 MHz, C_6D_6): δ = −17.5 ppm (s); ^{29}Si NMR (60 MHz, C_6D_6): δ = −17.5 ppm (d, $^1J_{SiH}$ = 189 Hz); IR/cm^{-1} 2943(w), 2893(w), 2863(w), 2101(m), 1461(w), 1377(w), 1238(w), 1132(w), 1070(w), 1000(w), 919(w), 880(w), 777(s), 729(w), 657(m), 618(w), 511(m), 455(w), 413(w); MS (EI): *m*/*z* [%] calcd: 306.22, found: 306.2199 $[M]^+$ (100).

$C_6H_4(SiMe_2Cl)_2$ (2). At −20 °C, 4.59 g (19.3 mmol, 2eq.) of TCCA was slowly added to a stirred solution of 5.59 g (28.9 mmol, 3eq.) of **1** in 120 mL of THF. After complete addition, the reaction mixture was allowed to warm to ambient temperature and was stirred for an additional 18 h. Subsequently, the solvent was removed *in vacuo* and the residue was dissolved in 100 mL of *n*-pentane and was subsequently filtered. The solvent was evaporated and 61% (4.67 g, 17.7 mmol) of **2** was obtained in the form of a colourless oil which crystallized at ambient temperature within 1 d. ^{1}H NMR (300 MHz, C_6D_6): δ = 0.44 (s, 12H, CH_3), 7.51 ppm (s, 4H, H_{ar}); $^{13}C\{^1H\}$ NMR (75 MHz, C_6D_6): δ = −1.86 (s, CH_3), 131.56 (s, C_{ar}), 132.96 ppm (s, C_{ar}); $^{29}Si\{^1H\}$ NMR (60 MHz, C_6D_6): δ = 19.86 ppm (s); elemental analysis [%] calcd: C 44.61, H 6.12, found: C 44.38, H 6.13.

$C_6H_4(SiiPr_2H)_2$ (3). The preparation is similar to that of **1**. (1,4-dibromobenzene: 35.0 g, 0.15 mol, 1.1eq.; Mg: 6.56 g, 0.27 mol, 2eq.; HSi*i*PrCl: 40.7 g, 0.27 mol, 2eq.). Distillative purification: 1×10^{-3} mbar, 65 °C. Yield: 90% (37.2 g, 0.12 mol) in the form of a colourless oil. ^{1}H NMR (300 MHz, C_6D_6): δ = 0.96–1.24 (m, 28H, $H_{i\mathrm{Pr}}$), 4.19 (t, $^3J_{HH}$ = 3.0 Hz, 2H, Si*H*), 7.57 ppm (s, 4H, H_{ar}); ^{13}C{^{1}H} NMR (C_6D_6): δ = 11.1 (s, *C*H(CH_3)$_2$), 18.8 (s, CH(*C*H$_3$)$_2$), 18.9 (s, CH(*C*H$_3$)$_2$), 135.2 (s, C_{ar}), 135.5 ppm (s, C_{ar}); ^{29}Si{^{1}H} NMR (60 MHz, C_6D_6): δ = 5.7 ppm (s); IR [cm^{-1}] 2943(w), 2893(w), 2863(w), 2101(m), 1461(w), 1377(w), 1238(w), 1132(w), 1070(w), 1000(w), 919(w), 880(w), 777(s), 729(w), 657(m), 618(w), 511(m), 455(w), 413(w); MS (EI): *m*/*z* [%] calcd: 306.22, found: 306.2199 $[M]^+$ (100).

$C_6H_4(SiiPr_2Cl)_2$ (4). The preparation is similar to that of **2**. (**3**: 37.2 g, 0.12 mol, 3eq.; TCCA: 18.8 g, 0.81 mol, 2 eq.). Yield: 98% (44.6 g, 0.12 mol) in the form of colourless crystals. ^{1}H NMR (300 MHz, C_6D_6): δ = 0.89–1.07 (m, 24H, CH(C*H*$_3$)$_2$), 1.31–1.14 (m, 4H, C*H*(CH$_3$)$_2$), 7.64 ppm (s, 4H, H_{ar}); ^{13}C{^{1}H} NMR (75 MHz, C_6D_6): δ = 14.1 (s, *C*H(CH$_3$)$_2$), 16.9 (s, CH(*C*H$_3$)$_2$), 17.2 (s, CH(*C*H$_3$)$_2$), 133.6 (s, C_{ar}), 134.5 ppm (s, *C*H$_3$); ^{29}Si{^{1}H} NMR (60 MHz, C_6D_6): δ = 27.1 ppm (s); IR [cm^{-1}]: 2949(s), 2867(m), 2848(m), 1461(m), 1385(w), 1366(w), 1260(w), 1240(w), 1131(s), 1064(m), 989(s), 923(w), 878(s), 807(s), 739(w), 699(w), 671(s), 648(vs), 555(vs), 517(vs), 444(s); CHN [%] calcd: C 57.57, H 8.59, found: C 57.58, H 8.466; MS (EI): *m*/*z* [%] calcd: 374.14196, found: 374.14002[*M*] (7).

$[C_6H_4(SiMe_2NH)_2]_2$ (5). A stirred solution of 6.54 g (24.8 mmol, 1eq.) of **2** in 100 mL of toluene was purged with ammonia for 3.5 h. The completion of the reaction was controlled *via* a ^{29}Si{^{1}H} NMR experiment of the solution using a glass capillary with D_2O as the standard. The white precipitate was separated by filtration, and the solvent was removed *in vacuo*. The raw product was purified by recrystallization from toluene and dichloromethane (2 : 1) at −25 °C within 4 d. 74% (3.8 g, 9.2 mmol) of **5** was obtained in the form of colourless plates. ^{1}H NMR (300 MHz, C_6D_6): δ = 0.34 (s, 24H, C*H*$_3$), 0.50 (s, 2H, N*H*$_2$), 7.68 ppm (s, 8H, C_6H_4); ^{13}C{^{1}H} NMR (75 MHz, C_6D_6): δ = 1.4 (s, *C*H$_3$), 131.2 (s, C_{ar}), 133.2 (s, C_{ar}), 135.4 (s, C_{ar}), 142.3 ppm (s, C_{ar}); ^{29}Si{^{1}H} NMR (60 MHz, C_6D_6): δ = −3.9 ppm (s); IR [cm^{-1}]: 3342(w, *N-H*), 3040(w), 2952(w), 1377(w), 1246(m), 1190(m), 1129(s), 930(s), 849(m), 821(s), 782(vs), 661(s), 603(m), 496(s), 4412(w); elemental analysis [%] calcd: N 6.75, C 57.91, H 8.26, found: N 6.01, C 56.19, H 7.900; MS (+p APCI): *m*/*z* [%] calcd: 414.1870 $[MH]^+$, found: 414.1872 $[MH]^+$ (70).

$C_6H_4(SiiPr_2NH_2)_2$ (6). The preparation is similar to that of **5**. (**4**: 3.26 g, 8.7 mmol). 86% (2.5 g, 7.5 mmol) yield was obtained after recrystallization from toluene and dichloromethane within 2 d at −25 °C in the form of colourless blocks. ^{1}H NMR (300 MHz, C_6D_6): δ = 0.20 (s, 4H, N*H*$_2$), 0.97 (d, $^3J_{HH}$ = 6.5 Hz, 12H, C*H*$_3$), 1.03 (d, $^3J_{HH}$ = 6.3 Hz, 12H, C*H*$_3$), 1.00–1.16 (m, 4H, $H_{i\mathrm{Pr}}$), 7.68 ppm (s, 4H, H_{ar}); ^{13}C{^{1}H} NMR (75 MHz, C_6D_6): δ = 12.4 (s, *C*H(CH$_3$)$_2$), 17.6 (s, CH(*C*H$_3$)$_2$), 17.8 (s, CH(*C*H$_3$)$_2$), 134.0 (s, C_{ar}), 137.9 ppm (s, C_{ar}); ^{29}Si{^{1}H} NMR (60 MHz, C_6D_6): δ = 0.0 (s); IR [cm^{-1}]: 3376(w, *N-H*), 3043(w), 2948(m), 2891(w), 2862(s), 1546(m), 1460(m), 1382(w), 1365(w), 1236(m), 1161(w), 1129(s), 1064(m), 989(s), 920(w), 880(s), 817(s), 780 (vs), 739(w), 723(w), 650(s), 622(vs), 546(m), 517(s), 499(s); elemental analysis [%] calcd: N 8.32, C 64.22, H 10.78, found: N 7.62, C 63.51, H 10.498; MS (+p APCI): *m*/*z* [%] calcd: 361.2466, found: 361.2490 $[M\mathrm{Na}]^+$ (100).

$C_6H_4(SiiPr_2OH)_2$ (7). To a stirred solution of 0.80 g (2.4 mmol, 1eq.) of $C_6H_4(SiiPr_2NH_2)_2$ in 50 mL diethylether was added 0.20 mL (9.5 mmol, 4eq.) of H_2O. The reaction mixture was stirred for 18 h, followed by removal of the aqueous phase. The solvent was removed and 86% (0.71 g, 2.0 mmol) of **7** was obtained in the form of a colourless powder. **7** was recrystallized from diethylether at −35 °C within 4 d. ^{1}H NMR (300 MHz, C_6D_6): δ = 0.89 (d, 7.3 Hz, 12H, CH(C*H*$_3$)$_2$), 10.96(d, 7.2 Hz, 12H, CH(C*H*$_3$)$_2$), 1.08–1.18 (m, 4H, C*H*(CH$_3$)$_2$), 7.44 ppm (s, 4H, H_{ar}); ^{13}C{^{1}H} NMR (75 MHz, C_6D_6): δ = 13.0 (s, *C*H(CH$_3$)$_2$), 17.2 (s, CH(*C*H$_3$)$_2$), 17.5 (s, CH(*C*H$_3$)$_2$), 133.7 (s, C_{ar}), 136.1 ppm (s, C_{ar}); ^{29}Si{^{1}H} NMR (60 MHz, C_6D_6): δ = 7.1 ppm (s); IR [cm^{-1}]: 3299(w, *O-H*), 2941(m), 2863(m), 1462(m), 1382(w), 1367(w), 1242(w), 1135(m), 1064(m), 992(w), 920(w), 881(s), 817(vs), 801(vs), 748(w), 670(vs), 628(vs), 603(s), 523(vs), 502(s), 445(w), 420(w); elemental analysis [%] calcd: C 63.84, H 10.12, found: C 64.58, H 10.354; MS (ESI−): *m*/*z* [%] calcd: 337.2025, found: 337.2014 $[M]^-$ − H (100).

$C_6H_4(SiMe_2PH_2)_2$ (8). At −50 °C, 10.5 g (39.9 mmol, 2eq.) of **2** in 100 mL of dimethoxyethane (DME) was slowly added to a stirred solution of 60 mL (24.0 mmol, 0.4 M in DME, 1.1eq.) of $[LiAl(PH_2)_4]$. The resulting suspension was allowed to warm to ambient temperature and was stirred for additional 14 h. Subsequently, the solvent was removed under reduced pressure, and the residue was suspended in 150 mL of *n*-pentane. The suspension was filtered, and the white precipitate was washed two times with 50 mL of *n*-pentane. The solvent of the filtrate was removed under reduced pressure, and 97% (10.0 g, 38.8 mmol) of the pure product was obtained in the form of a colourless solid. **8** was recrystallized at 6 °C from benzene and yielded colourless blocks within 2 d.

^{1}H NMR (300 MHz, C_6D_6): δ = 0.38 (d, $^3J_{PH}$ = 3.8 Hz, 12H, C*H*$_3$), 1.42 (d, $^1J_{PH}$ = 183.7 Hz, 4H, P*H*$_2$), 7.48 ppm (s, 4H, C_6H_4); ^{13}C{^{1}H} NMR (75 MHz, C_6D_6): δ = 1.38 (d, $^2J_{PC}$ = 9.1 Hz, *C*H$_3$), 132.00 (s, C_{ar}), 133.76 ppm (d, $^3J_{PC}$ = 2.16, C_{ar}); ^{29}Si{^{1}H} NMR (75 MHz, C_6D_6): δ = −1.40 ppm (d, $^1J_{PSi}$ = 17.6 Hz); ^{31}P{H} NMR (102 MHz, C_6D_6): δ = −237.46 ppm (s); ^{31}P NMR (102 MHz, C_6D_6): δ = −237.45 ppm (t, $^1J_{PH}$ = 183.7 Hz); IR [cm^{-1}]: 3043(vw), 2952(w), 2287(m, *P-H*), 1569(vw), 1404(w), 1375(m), 1246(s), 1127(s), 1052(m), 1012(m), 834(s), 775(vs), 648(s), 616(m), 486(vs), 446(m), 410(vw); elemental analysis [%] calcd: C 46.48, H 7.80, found: C 46.330, H 7.829; MS (+p APCI): *m*/*z* [%] calcd: 258.06, found: 259.0667 $[MH]^+$ (100).

$C_6H_4(SiiPr_2PH_2)_2$ (9). At −25 °C, PH_3 was slowly passed into a solution of 7.0 g (18.72 mmol, 1eq.) of **4** and 300 mL of Et_2O. After 10 min, 14.98 mL (37.44 mmol, 2eq., 2.5 M in hexane) of *n*-BuLi in 100 mL of *n*-heptane was slowly dropped into the stirred solution under continuous flow of PH_3. After complete addition of *n*-BuLi, the PH_3 flow was maintained for an additional 10 min. Subsequently, the reaction vessel was

purged with N_2 for at least 10 min. The reaction mixture was allowed to slowly warm to ambient temperature and was stirred for 16 h. The solvent was separated under reduced pressure, and to the residue was added 150 mL of *n*-pentane. The white precipitate was removed by filtration and was washed two times with 100 mL of *n*-pentane followed by filtration. The solvent was removed *in vacuo* and **9** was obtained in the form of a colourless solid. By distillation (1×10^{-3} mbar, 85 °C) 64% (4.4 g, 11.9 mmol) of **9** was obtained in the form of a white solid. Single crystals were obtained from benzene within 2 d at 6 °C. ^{1}H NMR (300 MHz, C_6D_6): δ = 0.94 (d, $^3J_{HH}$ = 7.3 Hz, 12H, CH(CH_3)$_2$), 1.00 (d, $^3J_{HH}$ = 7.3 Hz, 12H, CH(CH_3)$_2$), 1.15–1.28 (m, 4H, CH(CH$_3$)$_2$), 1.29 (d, $^1J_{PH}$ = 185.9 Hz, 4H, PH_2), 7.55 ppm (s, 4H, H_{ar}); ^{13}C{^{1}H} NMR (75 MHz, C_6D_6): δ = 13.2 (d, $^2J_{PC}$ = 6.2 Hz, CH(CH$_3$)$_2$), 18.2 (d, $^3J_{PC}$ = 2.0 Hz, CH(CH$_3$)$_2$), 18.4 (d, $^3J_{PC}$ = 1.8 Hz, CH(CH_3)$_2$), 134.7 (d, $^2J_{CP}$ = 4.0 Hz, C_{ar}), 136.4 ppm (d, $^3J_{CP}$ = 7.9 Hz, C_{ar}); ^{29}Si{^{1}H} NMR (75 MHz, C_6D_6): δ = 14.3 ppm (d, $^1J_{PSi}$ = 27.0 Hz); ^{31}P{H} NMR (102 MHz, C_6D_6): δ = −275.71 ppm (s); ^{31}P NMR (102 MHz, C_6D_6): δ = −275.71 ppm (t, $^1J_{PH}$ = 185.9 Hz); IR [cm^{-1}]: 3044(w), 2941(s), 2861(s), 2289(m, *P-H*), 1461(m), 1377(w), 1364(w), 1259(w), 1234(w), 1124(m), 1054(m), 987(s), 920(w), 878(s), 803(m), 700(m), 665(m), 643(s), 611(s), 536(vs), 505(s), 419(w); elemental analysis [%] calcd: C 58.34, H 9.79, found: C 58.12, H 9.607; MS (−p APCI): *m*/*z* [%] calcd: 369.1747, found: 369.1768 [*M*]$^-$ − H (10).

[C$_6$H$_4$(Si*i*Pr$_2$PH)$_2$]$_2$ (10). To 0.24 g (0.7 mmol, 1eq.) of **9** in 30 mL of THF was slowly added 0.22 g (1.3 mmol, 2eq.) of Li(HMDS) at −20 °C. The reaction mixture was warmed to ambient temperature and stirred for an additional 12 h. Subsequently, the reaction mixture was again cooled to −20 °C and 0.24 g (0.65 mmol, 1eq.) of **4** in 10 mL of THF was dropped into the solution. The reaction mixture was stirred for 12 h at ambient temperature and the solvent was removed under reduced pressure. To the residue was added 20 mL of toluene, and the white precipitate was removed by filtration. The precipitate was washed two times with 10 mL of toluene, followed by filtration. The filtrate was reduced until saturation and was recrystallized at −25 °C. After 2 d 54% (0.24 g, 0.04 mmol) of **10** was obtained in the form of colourless needles. ^{1}H NMR (100 MHz, C_6D_6): δ = 0.99 (d, $^1J_{PH}$ = 196.9 Hz, 2H, PH_2), 1.18 (d, $^3J_{HH}$ = 7.2 Hz, 12H, CH(CH_3)$_2$), 1.28 (d, $^3J_{HH}$ = 7.2 Hz, 12H, CH(CH_3)$_2$), 1.37–1.49 (m, 8H, CH(CH$_3$)$_2$), 7.04 ppm (s, 8H, C$_6H_4$); ^{13}C{^{1}H} NMR (75 MHz, C_6D_6): δ = 14.9 (d, $^2J_{PC}$ = 12.6 Hz, CH(CH$_3$)$_2$), 19.3 (d, $^3J_{PC}$ = 3.3 Hz, CH(CH$_3$)$_2$), 19.5 (d, $^3J_{PC}$ = 5.0 Hz, CH(CH$_3$)$_2$), 134.0 (s, C_{ar}), 134.7 ppm (s, C_{ar}); ^{29}Si{^{1}H} NMR (60 MHz, C_6D_6): δ = 8.4 ppm (d, $^1J_{PSi}$ = 38.5 Hz); ^{31}P{H} NMR (102 MHz, C_6D_6): δ = −273.5 ppm (s, $^1J_{SiP}$ = 38.8 Hz); ^{31}P NMR (102 MHz, C_6D_6): δ = −273.5 ppm (d, $^1J_{PH}$ = 196.9 Hz); IR [cm^{-1}]: 2941(m), 2886(m), 2862(s), 2283(w, *P-H*), 1629(w), 1461(m), 1382(w), 1367(w), 1260(w), 1237(w), 1175(w), 1125(m), 1096(w), 1067(w), 1040(w), 1013(m), 945(m), 879(s), 799(m), 756(w), 666(s), 650(m), 920(s), 519(vs), 434(m), 419(w); elemental analysis [%] calcd: C 64.23, H 9.88, found: C 62.88, H 9.815; MS(ESI+): *m*/*z* [%] calcd: 673.801, found: 673.3790 [*M*H]$^+$ (100).

[C$_6$H$_4$(Si*i*Pr$_2$NHGaEt$_2$)$_2$]$_2$ (11). To 100 mg (0.3 mmol, 1eq.) of **6** in 10 mL of toluene was added 0.1 mL (0.6 mmol, 2eq.) of $GaEt_3$ at −10 °C. The reaction mixture was stirred for 4 h at ambient temperature and was subsequently reduced until saturation. After 4 d at −35 °C, 26% (45 mg, 3.9×10^{-5} mol) of **11** was obtained in the form of colourless blocks. ^{1}H NMR (300 MHz, C_6D_6): δ = 0.59 (q, $^1J_{HH}$ = 8.1 Hz, 16H, CH_2CH$_3$), 0.91 (d, $^1J_{HH}$ = 7.3 Hz, 24H, CH(CH_3)$_2$), 0.97 (d, $^1J_{HH}$ = 7.2 Hz, 24H, CH(CH_3)$_2$), 1.05–1.12 (m, 8H, CH(CH$_3$)$_2$), 1.40 (t, $^1J_{HH}$ = 8.1 Hz, 24H, CH$_2$CH_3), 7.50 ppm (s, 8H, H_{ar}); ^{13}C{^{1}H} NMR (75 MHz, C_6D_6): δ = 5.5 (s, CH$_2$CH$_3$), 11.4 (s, CH$_2$CH$_3$), 12.2 (s, CH(CH$_3$)$_2$), 17.5 (s, CH(CH$_3$)$_2$), 17.6 (s, CH(CH$_3$)$_2$), 134.0 (s, C_{ar}), 136.4 ppm (s, C_{ar}); ^{29}Si{^{1}H} NMR: (300 MHz, C_6D_6): δ = 4.1 ppm; IR [cm^{-1}]: 3481(w), 3403(w), 3339(w), 3281(w), 2940(s), 2892(m), 2862(s), 1543(w), 1519(w), 1462(m), 1418(w), 1383(w), 1368(w), 1240(w), 1133(s), 1064(w), 993(s), 954(m), 919(m), 880(s), 829(s), 801(s), 731(s), 669(s), 645(s), 618(vs), 518(vs), 439(m), 413(m); elemental analysis [%] calcd: N 4.75, C 52.90, H 9.22, found: N 4.40, C 52.57, H 9.015.

[C$_6$H$_4$(Si*i*Pr$_2$PHGaEt$_2$)$_2$]$_2$ (12). The preparation is similar to that of **11**. (**9**: 205 mg, 0.6 mmol, 1eq.; $GaEt_3$: 0.16 mL, 1.1 mmol, 2eq.). Yield: 45% (155 mg, 0.12 mmol) in the form of colourless plates after 2 d at −35 °C. ^{1}H NMR (300 MHz, C_6D_6): δ = 0.98–1.03 (m, 8H, CH(CH$_3$)$_2$), 1.05 (d, $^1J_{HH}$ = 7.3 Hz, 24H, CH(CH_3)$_2$), 1.08 (d, $^1J_{HH}$ = 7.3 Hz, 24H, CH(CH_3)$_2$), 1.18 (br, 12H, CH$_2$CH_3), 1.24–1.30 (m, 12H, CH$_2$CH_3), 1.55 (t, $^1J_{HH}$ = 8.0 Hz, 12H, CH$_2$CH_3), 1.79–2.30 (m, 4H, PH), 7.78 ppm (s, 8H, H_{ar}); ^{13}C{^{1}H} NMR (75 MHz, C_6D_6): δ = 8.4 (t, $^2J_{CP}$ = 14.1 Hz, CH$_2$CH$_3$), 9.5 (t, $^2J_{CP}$ = 6.9 Hz, CH$_2$CH$_3$), 11.1 (t, $^3J_{CP}$ = 3.6 Hz, CH$_2$CH$_3$), 11.9 (br, CH$_2$CH$_3$), 15.0 (br, CH(CH$_3$)$_2$), 18.6 (s, CH(CH$_3$)$_2$), 18.9 (s, CH(CH$_3$)$_2$), 134.8 (br, C_{ar}), 135.8 ppm (t, $^2J_{CP}$ = 7.6 Hz, C_{ar}). ^{29}Si{^{1}H} NMR: (300 MHz, C_6D_6): δ = 17.6–18.2 ppm (m, *Si*-P); ^{31}P{^{1}H} NMR (102 MHz, C_6D_6): δ = −247.4 ppm (s, *P*-H); ^{31}P NMR (300 MHz, C_6D_6): δ = −247.4 ppm (m, *P*-H); IR [cm^{-1}]: 2939(m), 2890(m), 2861(m), 2314(w, *P-H*), 1460(m), 1414(w), 1381(w), 1371(w), 1130(m), 1078(w), 1063(w), 996(m), 990(m), 959(w), 934(w), 920(m), 880(m), 800(m), 753(m), 733(w), 651(s), 608(s), 547(vs), 525(s), 503(s), 484(vs), 434(m), 410(m); elemental analysis [%] calcd: C 50.02, H 8.72, found: C 49.81, H 8.759.

Conclusions

Within this paper, we have shown that aryl bridged 1,4-bis(silanes) provide access to heteroatomic bridged paracyclophanes. One synthetic method consists of the reaction of NH_3 with the aryl bridged chlorosilanes **2** and **4**. The SiNSi bridged paracyclophane **5** was obtained after the *in situ* condensation due to the smaller steric hindrance of the Me-groups. In the case of larger substituents at the Si atoms as present in **4**, the analogous reaction yielded the primary amine **6**. The functionalisation of the chlorosilanes **2** and **4** with PH_2 was accomplished by using [LiAl(PH$_2$)$_4$] and [LiPH$_2$(dme)] which respectively yielded the primary silylphosphanes **8** and **9**. The *i*Pr sub-

stituted species **9** serves as a suitable precursor for the synthesis of the SiPSi bridged [3.3]paracyclophane **10**, which was accomplished by lithiation and subsequent salt metathesis with **4**. The obtained paracyclophanes **5** and **10** possess two coordination sites as they incorporate π-aromatic systems as well as the group 15 elements N and P. Their reactivity towards Lewis acids is matter of current investigation.

The second approach towards heteroatomic bridged paracyclophanes was the reaction of the primary silylamine **6** and -phosphane **9** with $GaEt_3$. Due to the large distance between the two $SiPnH_2$ units, they react in a similar way to compounds incorporating only one $SiPnH_2$ group, so that the twofold $Si_2(GaPn)_2$ bridged paracyclophanes **11** and **12** were obtained. They both show *cis* conformation in the solid state and in solution owing to the rigid structure of the aryl bridged framework.

Acknowledgements

The authors thank the Deutsche Forschungsgemeinschaft (DFG) for financial support.

Notes and references

1 G. He, O. Shynkaruk, M. W. Lui and W. Rivard, *Chem. Rev.*, 2014, **114**, 7815.
2 B.-J. Bae, J. E. Park, Y. Kim, J. T. Park and I.-H. Suh, *Organometallics*, 1999, **18**, 2513; C. von Hänisch and B. Rolli, *Phosphorus, Sulfur Silicon Relat. Elem.*, 2004, **179**, 749.
3 C. von Hänisch, *Eur. J. Inorg. Chem.*, 2003, 2955.
4 C. von Hänisch and S. Stahl, *Angew. Chem., Int. Ed.*, 2006, **45**, 2302.
5 S. J. Geier and D. W. Stephan, *Chem. Commun.*, 2010, **46**, 1026.
6 R. Gleiter and H. Hopf, *Modern Cyclophane Chemistry*, Wiley-VCH, Weinheim, 2004; H. Sakurai, S. Hoshi, A. Kamiya, A. Hosomi and C. Kabuto, *Chem. Lett.*, 1986, **15**, 1781.
7 G. Meyer-Eppler, E. Vogelsang, C. Benkhäuser, A. Schneider, G. Schnakenburg and A. Lützen, *Eur. J. Org. Chem.*, 2013, 4523; M. Austeri, M. Enders, M. Nieger and S. Bräse, *Eur. J. Org. Chem.*, 2013, 1667; G. J. Rowlands, *Isr. J. Chem.*, 2012, **52**, 60.
8 C. O. Ulloa, M. Ponce-Vargas, R. de Mattos Piccoli, G. F. Caramori, G. Frenking and A. Muñoz-Castro, *RSC Adv.*, 2015, **5**, 7803; C. Elschenbroich, B. Kanellakopulos, F. H. Köhler, B. Metz, R. Lescouëzec, N. W. Mitzel and W. Strauß, *Chem. – Eur. J.*, 2007, **13**, 1191; C. Elschenbroich, J. Hurley, W. Massa and G. Baum, *Angew. Chem., Int. Ed. Engl.*, 1988, **5**, 684; H. Schmidbaur, W. Bublak, B. Huber and G. Müller, *Organometallics*, 1986, **5**, 1647.
9 J. Beckmann, A. Duthie, G. Reeske and M. Schürmann, *Organometallics*, 2005, **24**, 3629; S. Shirai, S. Iwata, Y. Maegawa, T. Tani and S. Inagaki, *J. Phys. Chem. A*, 2012, **116**, 10194; C. Dutan, S. Choua, T. Berclaz, M. Geoffroy, N. Mézailles, A. Moores, L. Ricard and P. Le Floch, *J. Am. Chem. Soc.*, 2003, **125**, 4487.
10 H. J. Emeléus and M. Onyszchuk, *J. Am. Chem. Soc.*, 1958, 604; R. West, L. S. Whatley and K. J. Lake, *J. Am. Chem. Soc.*, 1961, **83**, 761; B. D. Shepherd, *J. Am. Chem. Soc.*, 1991, **113**, 5581.
11 A. Decken, J. Passmore and X. Wang, *Angew. Chem., Int. Ed.*, 2006, **118**, 2839; J. S. Ritch and T. Chivers, *Angew. Chem., Int. Ed.*, 2007, **46**, 4610.
12 A. Decken, F. A. LeBlanc, J. Passmore and X. Wang, *Eur. J. Inorg. Chem.*, 2006, 4033; T. S. Cameron, A. Decken, I. Krossing, J. Passmore, J. M. Rautiainen, X. Wang and X. Zeng, *Inorg. Chem.*, 2013, **52**, 4441; K. Reuter, M. R. Buchner, G. Thiele and C. von Hänisch, *Inorg. Chem.*, 2016, **55**, 4441; K. Reuter, G. Thiele, T. Hafner, F. Uhlig and C. von Hänisch, *Chem. Commun.*, 2016, **52**, 13265.
13 R. L. Merker and M. J. Scott, *J. Polym. Sci., A*, 1964, **2**, 15.
14 S. Varaprath and D. H. Stutts, *J. Organomet. Chem.*, 2007, **692**, 1892.
15 T. Kottke, U. Klingebiel, M. Noltemeyer, U. Pieper, S. Walter and D. Stalke, *Chem. Ber.*, 1991, **124**, 1941.
16 J. Beckmann and S. L. Jänicke, *Eur. J. Inorg. Chem.*, 2006, 3351; T. Steiner, *Angew. Chem., Int. Ed.*, 2002, **41**, 48; T. Steiner, *Angew. Chem., Int. Ed.*, 2002, **114**, 50; R. West and R. H. Baney, *J. Am. Chem. Soc.*, 1959, **81**, 6145.
17 M. Baudler, G. Scholz, K.-F. Tebbe and M. Fehér, *Angew. Chem., Int. Ed. Engl.*, 1989, **28**, 339; M. Baudler, G. Scholz and W. Oehlert, *Z. Naturforsch., B: Chem. Sci.*, 1989, **44**, 627; C. von Hänisch and E. Matern, *Z. Anorg. Allg. Chem.*, 2005, **631**, 1655.
18 H. Schäfer, G. Fritz and W. Hölderich, *Z. Anorg. Allg. Chem.*, 1977, **438**, 222; G. Fritz and P. Scheer, *Chem. Rev.*, 2000, **100**, 3341.
19 The condensed species $[p\text{-}C_6H_4\{SiMe_2P(H)\}_2]_2$ (**10**) occurred as the by-product, when solid $[LiPH_2(dme)]$ was used. This can be referred to the presence of small amounts of Li_2PH, which is a typical impurity in neat $[LiPH_2(dme)]$. The presence of Li_2PH can be avoided by the *in situ* reaction of $[LiPH_2(dme)]$ and the corresponding chlorosilane.
20 K. Reuter and C. von Hänisch, *Chem. Commun.*, 2014, **50**, 7709.
21 Y. Zhai, J. Li, H. Gu, D. Wei, Y.-C. Xu, W. Fu and Z. Yu, *Interdiscipl. Sci. Comput. Life Sci.*, 2015, **7**, 211.
22 M. O. Sinnokrot, E. F. Valeev and C. D. Sherrill, *J. Am. Chem. Soc.*, 2002, **124**, 10887.
23 Y. Soneta, T. Moritaka and K. Miyamura, *Inorg. Chim. Acta*, 2007, **360**, 3123; Y. Yoshitake, H. Nakagawa, M. Eto and K. Harano, *Tetrahedron*, 2000, **56**, 6015.
24 W. Uhl and C. H. Emden, *J. Organomet. Chem.*, 2004, **690**, 1529; C. J. Carmalt, J. D. Mileham, A. J. P. White and D. J. Williams, *Dalton Trans.*, 2003, 4255.

25 B. Ringler and C. von Hänisch, *Z. Anorg. Allg. Chem.*, 2016, **642**, 294.
26 M. Westerhausen, T. Rotter, C. Pfaller, A. N. Kneifel and A. Schulz, *Inorg. Chim. Acta*, 2005, **358**, 4253.
27 M. R. Willcott, *J. Am. Chem. Soc.*, 2009, **131**, 13180.
28 S. Anwar and P. A. Davis, *Tetrahedron*, 1988, **44**, 3761.
29 G. M. Sheldrick, *SHELXL14, Program for the Refinement of Crystal Structures*, Universität Göttingen, 2014.
30 O. V. Dolomanov, L. J. Bourhis, R. J. Hildea, J. A. K. Howard and H. Puschmann, *J. Appl. Crystallogr.*, 2009, **42**, 339.
31 H. Putz and K. Brandenburg, *Diamond – Crystal and Molecular Structure Visualization, Crystal Impact*, Kreuzherrenstr. 102, 53227 Bonn, Germany.
32 Modified synthesis pathway of. H. Chen, J. Kong and X. D. Fan, *Macromol.*, 2012, **45**, 6185.